2013

Evaluating chalcogen heteroatoms in conjugated polymers for organic electronics

Brandon Michael Kobilka
Iowa State University

Evaluating chalcogen heteroatoms in conjugated polymers for organic electronics

by

Brandon M. Kobilka

A dissertation submitted to the graduate faculty

in partial fulfillment of the requirements for the degree of

DOCTOR OF PHILOSOPHY

Major: Organic Chemistry

Program of Study Committee:

Malika Jeffries-EL, Major Professor

William Jenks

Aaron Sadow

Jason Chen

Sumit Chaudhary

Iowa State University
Ames, Iowa
2013

TABLE OF CONTENTS

CHAPTER 1

General Introduction

1.1 DISSERTATION OVERVIEW

This dissertation discusses and details the research performed by the author in the Jeffries-EL research group from 2007-2013. The work presented herein is centrally focused around the design, synthesis, and characterization of conjugated polymers for tunable organic semiconductors. This was accomplished by studying how various structural modifications affect the properties of these materials and the subsequent performance in organic semiconductors. Chapter 1 begins with a general introduction to the physical and electronic properties of conjugated polymers for use in organic semiconducting applications and how they can be altered through structural modifications. An overview of the physics and molecular engineering of organic photovoltaic devices and a discussion of the properties requirement for the fabrication of successful organic electronics follows. Lastly, the background and significance of the primary organic heterocycles studied in this dissertation, benzo[1,2-*b*:4,5-*b*']dichalcogenophenes, is discussed.

Chapter 2 is a paper published in *Chemical Communications* in 2012 that discusses the synthesis, characterization and some theoretical analysis of two thiophene-flanked benzodifuran molecules and their subsequent copolymers with isoindigo. The copolymers were then studied as the active layer in organic photovoltaic devices. The author of this dissertation performed the synthesis and characterization of both polymers and the (5,5'-(3,7-didecylbenzo[1,2-b:4,5-b']difuran-2,6-diyl)bis(3-decylthiophene-5,2-diyl))bis(trimethyl-stannane) and also wrote the experimental section in the supporting information. The synthesis of the isoindigo monomer as well as the device fabrication and testing was performed by Monique D. Ewan. The theoretical evaluation was performed by Dr. Aimée L. Tomlinson. The majority of the paper was written by Dr. Malika Jeffries-EL with contributions from the author of this dissertation.

Chapter 3 is a paper published in *Polymer Chemistry* in 2013 that discusses the effects of structure versus function of the copolymers of one of the benzodifuran monomers (synthesized in Chapter 2 of this dissertation) and various diketopyrrolopyrrole on organic photovoltaic device performance. The synthesis and characterization of the copolymers was carried out by the author of this dissertation. All of the diketopyrrolopyrrole monomer synthesis was performed by Benjamin J. Hale, except for the synthesis of bis(thiophen-2-yl)-2,5-bis(tetradecyl)pyrrolo[3,4-c]pyrrole-1,4(2H,5H)-dione which was synthesized by Dr. Toby D. Nelson. The final bromination step for the synthesis of 3,6-di(5-bromo-2-thienyl)-2,5-bis(2-ethylhexyl)pyrrolo[3,4-*c*]pyrrole-1,4(2*H*,5*H*)-dione**,** and bis(5-bromothiophen-2-yl)-2,5-bis(tetradecyl)pyrrolo[3,4-c]pyrrole-1,4(2H,5H)-dione was performed by the author of this dissertation. The device fabrication and testing was performed by Monique D. Ewan with the assistance of Dr. Volodimyr Duzhko. The results and discussion, experimental section, and the supporting information were written by the author of this dissertation, except for the synthesis of the diketopyrrolopyrrole monomers which was written by Benjamin J. Hale. The introduction section was written by Dr. Malika Jeffries-EL.

Chapter 4 is a manuscript that is in preparation for *Macromolecules* and reports on the synthesis of an analogous series of benzodichalcogenophene monomers and their incorporation into donor-acceptor copolymers with furanyl-diketopyrrolopyrrole for organic solar cells. The majority of the synthetic work was done by the author. Benjamin J. Hale synthesized 3,6-bis(5-bromofuran-2-yl)-2,5-bis(2-ethylhexyl)pyrrolo[3,4-c]pyrrole-1,4(2H,-5H)-dione. The device fabrication and testing was performed by Monique D. Ewan. The manuscript was written by the author of this dissertation.

Chapter 5 is a manuscript that is in preparation for the *Journal of Polymer Science: A* and expands on the series of benzodichalcogenophene monomers synthesized in Chapter 4, by substituting the aliphatic side-chains on the benzodichalcogenophene core for 5-alkylthiophen-2-yl side-chains to study the effect of 2-dimensional conjugation on organic solar cell performance in donor-acceptor copolymers with furanyl-diketopyrrolopyrrole. Benjamin J. Hale and Dr. Balaji Ganapathy each contributed to the synthesis 3,6-bis(5-bromofuran-2-yl)-2,5-bis(2-ethylhexyl)pyrrolo[3,4-c]pyrrole-1,4(2H,5H)-dione, and 3,6-bis-(5-bromofuran-2-yl)-2,5-bis(tetradecyl)pyrrolo[3,4-c]pyrrole-1,4(2H,5H)-dione. The device

fabrication and testing was performed by Monique D. Ewan. The manuscript was written by the author of this dissertation.

Chapter 6 draws some conclusions from the work presented in this dissertation and discusses some future and ongoing research. This future work is related to improving upon the conjugated systems presented in this dissertation by proposing new strategies and molecular designs for reducing steric hinderdance within the molecules. Also, this section includes a brief discussion on the potential for the benzodifurans in this dissertation to be used in conjugated polymers for OLED devices. The author's acknowledgments are also included at the end of this chapter.

1.2 CONJUGATED POLYMERS: BACKGROUND

The first example of electrical conductivity in an organic polymer was reported over three decades ago in doped polyacetylene prepared by Shirakawa, McDiarmid, and Heeger, et al.[1, 2] Since that initial discovery, the field of organic-based semiconductors has taken significant strides forward and are moving toward the realm of commercial realization, including organic light-emitting diodes (OLEDs),[3-6] photovoltaics (OPVs),[7-11] field-effect transistors (OFETs),[12-15] electrochemical cells (polymer batteries),[16-18] non-linear optics,[19-21] and sensor devices.[22-24] Despite the overall excellent performance of their inorganic counterparts, organic semiconductors are being adopted as practical replacements. Inorganic semiconducting materials are most commonly based on silicon, germanium, gallium arsenide, metallic sulfides, etc., and they lack the ability to be processed cheaply on an industrial scale. For example, silicon-based devices are most common, but achieving higher performance requires the use of expensive processing techniques such as vapor deposition and lithographic printing as well as fabrication from costly high-purity silicon.[25-27] In attempt to reduce expenses, lower-cost amorphous silicon has been implemented in applications like solar cells, but these cells tend to suffer from relatively low efficiencies and can degrade quickly with use.[28]

Conversely, organic-based materials exhibit solubility in common organic solvents which allow materials to be cast using various cheap processing techniques like spin casting,[29] dip coating[30], ink jet printing,[31] and screen printing.[32] These techniques are highly desirable for scaled-up commercial use in roll-to-roll processing, as many of them can be extended to large area panels in addition to being processed onto flexible substrates.[33] Although recent progress has been made in the manufacturing of flexible silicon-based devices,[34] organic synthesis provides a larger palette of tunable properties used to manipulate the physical and electronic properties of the organic materials. Simple structural alterations made to an organic molecule can be used to control how it performs in semiconducting devices and for which applications it would be best suited.[35]

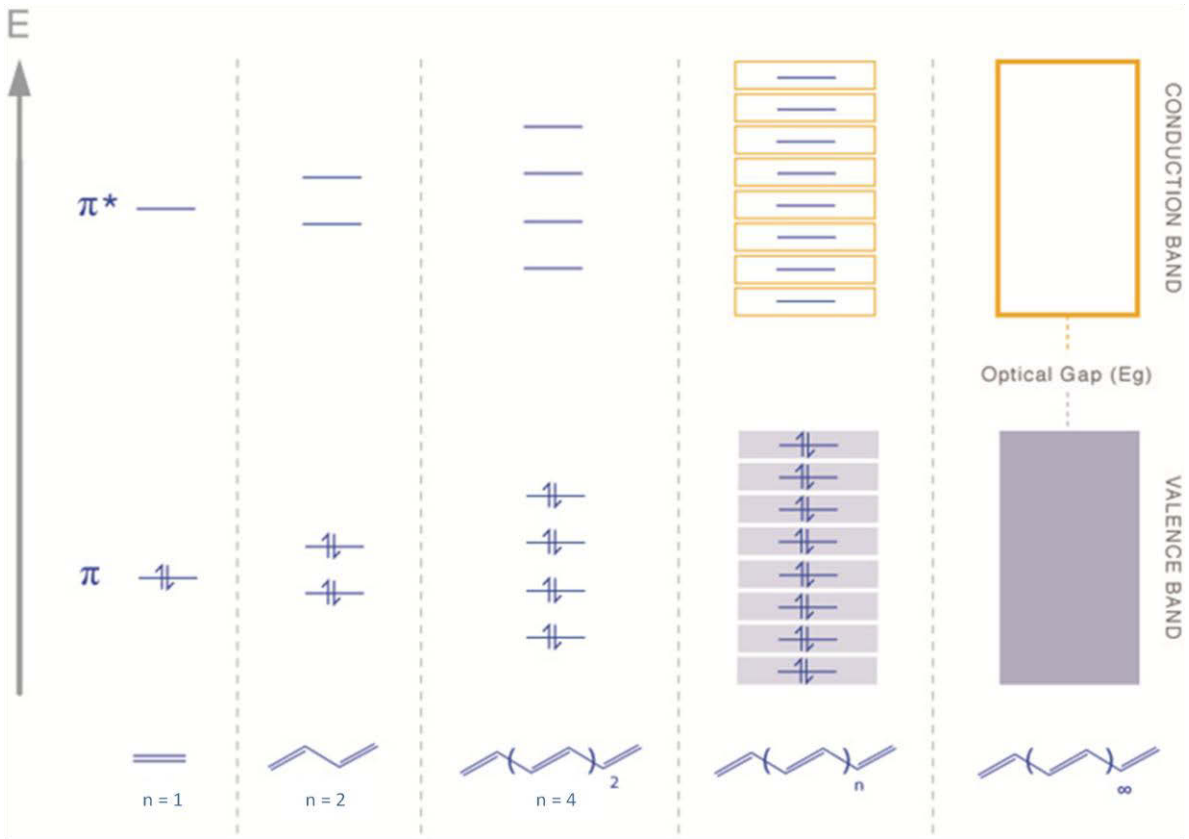

Figure 1.1. Evolution of conjugated polymer band structures from π molecular orbitals in finite to infinite polyenes.

The origin of conductivity in organic materials lies within the π-conjugated backbone, comprised of alternating single and double bonds which creates an extended π-molecular orbital that exists throughout the polymer chain. Conceptually, Figure 1.1 shows how as the π-conjugation is extended from ethylene, the number of π- and π*-molecular orbitals (MOs) increases from n = 1, to n = 2 in butadiene, to n = 4 in octatetraene and so on. As the number of MOs increases with each addition to the conjugation length, the set of MOs spans a wider range of energy. In this fashion, the energy of the highest occupied molecular orbital (HOMO) increases, while the energy of the lowest unoccupied molecular orbital (LUMO) decreases.[36] As the conjugation approaches infinity, the fully occupied π-MOs become very close in energy to one another. Likewise, the same phenomenon occurs in the unoccupied π*-MOs, resulting in two distinct bands of MOs, separated by a band gap (E_g). These two sets of overlapping orbitals resemble the traditional band structure of inorganic semiconductors where the π- and π*-MOs represent the conduction and valence bands, respectively.[2] It is this band structure which dictates the properties of organic semiconducting materials, but, as will be discussed later, this band structure can also be fined-tuned and tailored to make materials suitable for various semiconducting applications.

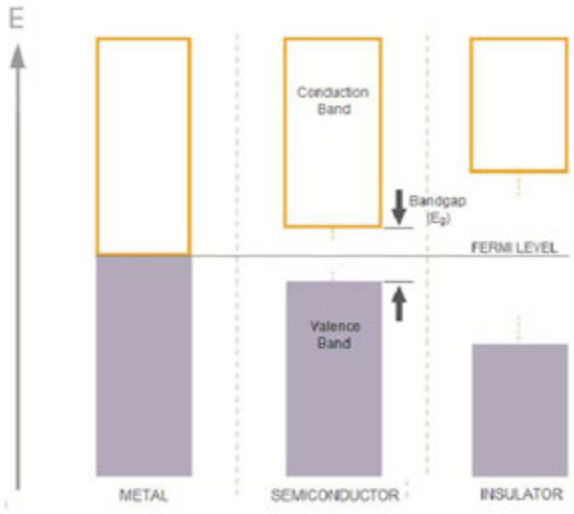

Figure 1.2. Band diagram of various materials.

Initially, it might not seem obvious that a band gap should exist at all in an extended conjugated system. In theory, as the conjugation increases, and the continuously increasing HOMO energy level is raised and decreasing LUMO energy level is lower until the two

converge, resulting in the elimination of the band gap. This situation, by definition, make polyacetylene an organic metal. As illustrated in Figure 1.2, metals possess no band gap, but rather a single, partially-filled band of electrons that allows for free conduction. Conversely, insulators have a band gap that is too large to promote conduction in any case, whereas semiconductors have a relatively small band gap that allows for conduction in some instances: typically when charge carriers are induced by either thermal, electrochemical, or optical means.[37] In reality, most conjugated polymers may include various defects or experience steric interactions that can cause backbone twisting. This can limit the delocalization of π-electrons to smaller segments of polymer which correspond to size of the band gap. This is called the effective conjugation of the polymer and will be discussed in greater detail later.

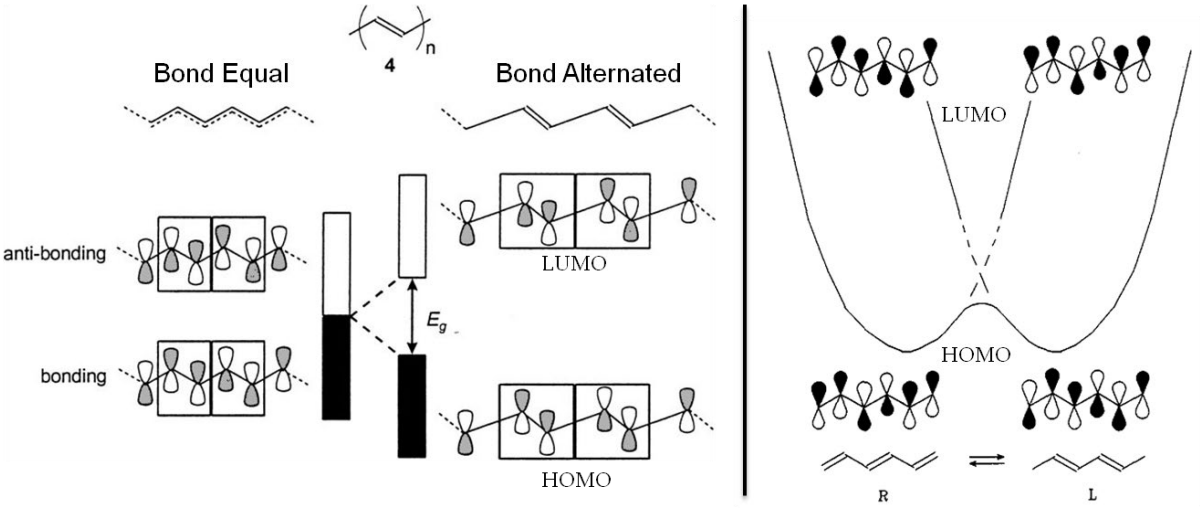

Figure 1.3. The degenerate forms of poly(acetylene) that result in a Peierls distortion.

Hypothetically, if polyacetylene existed as an organic metal, the effective conjugation length would extend across the entire polymer chain, enabling the free movement of electrons. In this scenario, there would be no differentiation between single or double bonds along the backbone and polyacetylene could be represented as $(-CH-)_n$, shown by the Bond-Equal Form in Figure 1.3. As a result, the π-electrons would be fully delocalized and able to freely move across the molecule and the material would exhibit the band structure of a metal. Of course, this situation does not occur, and polyacetylene experiences a geometric deformation that results in alternating short and long bonds also known as a Peierls

distortion. X-ray diffraction and nuclear magnetic resonance can be used to measure the difference in the bond lengths at approximately 1.35 Å and 1.45 Å.[38, 39] This effect is largely responsible for the splitting of the energy levels and causes the widening of the band gap.[40]

This discrepancy in the bond length arises from a forbidden transition between the two possible degenerate states of polyacetylene, labeled as R or L in Figure 1.3. Both forms differ in how the single and double bonds alternate in the structure, with the HOMOs having bonding interactions between the double bonds and anti-bonding interactions between the single bonds and the LUMOs experiencing the reverse scenario. At this point, the two states are energetically equivalent. Interestingly the symmetric HOMO of the R form actually corresponds to the LUMO of the L form, while the HOMO of the L form corresponds to the LUMO of the R form. This leads to a thermally forbidden transition between the R and L forms, resulting in a "dimerization" of the polymer and alternating bonds.[41] This difference in the two forms is what leads to the splitting of the two bands and gives polyacetylene a finite band gap of 1.5 eV, which makes it an organic semiconductor.[42]

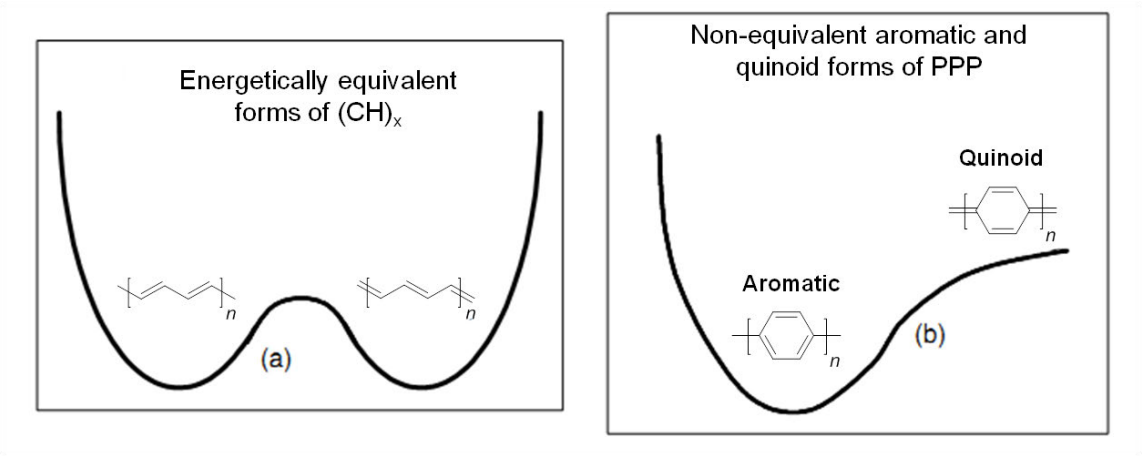

Figure 1.4. Relative energy potential diagram of (a) the degenerate forms of polyacetylene and (b) nondegenerate forms of poly(*p*-phenylene) (PPP).

However, most conjugated polymers are more complex than polyacetylene and have two possible nondegenerate ground state resonance forms, called the aromatic and quinoid. A representative example of this is shown in poly(*p*-phenylene) (PPP) in Figure 1.4.[43] The aromatic form is lower in energy and is characterized by carbocyclic or heterocyclic units separated by a single bond. This form maintains aromaticity by having its π-electrons

localized primarily within each cycle. The other possible resonance structure is the quinoid form, where the single bonds and double bonds swap places and the π-electrons become delocalized between each cycle, leading to a less stable but highly planar backbone. The difference between these two forms can be seen geometrically in the difference between the bond lengths of the single and double bonds. This parameter, called bond length alternation (BLA), is defined as the average of the differences between adjacent carbon-carbon bonds. Larger BLA values correspond to the aromatic form being more prevalent in the ground state, whereas smaller BLA values indicate increased contribution from the quinoid form.[44] Most importantly, band gaps tend to decrease with increasing quinoidal character and smaller differences in BLA.[45]

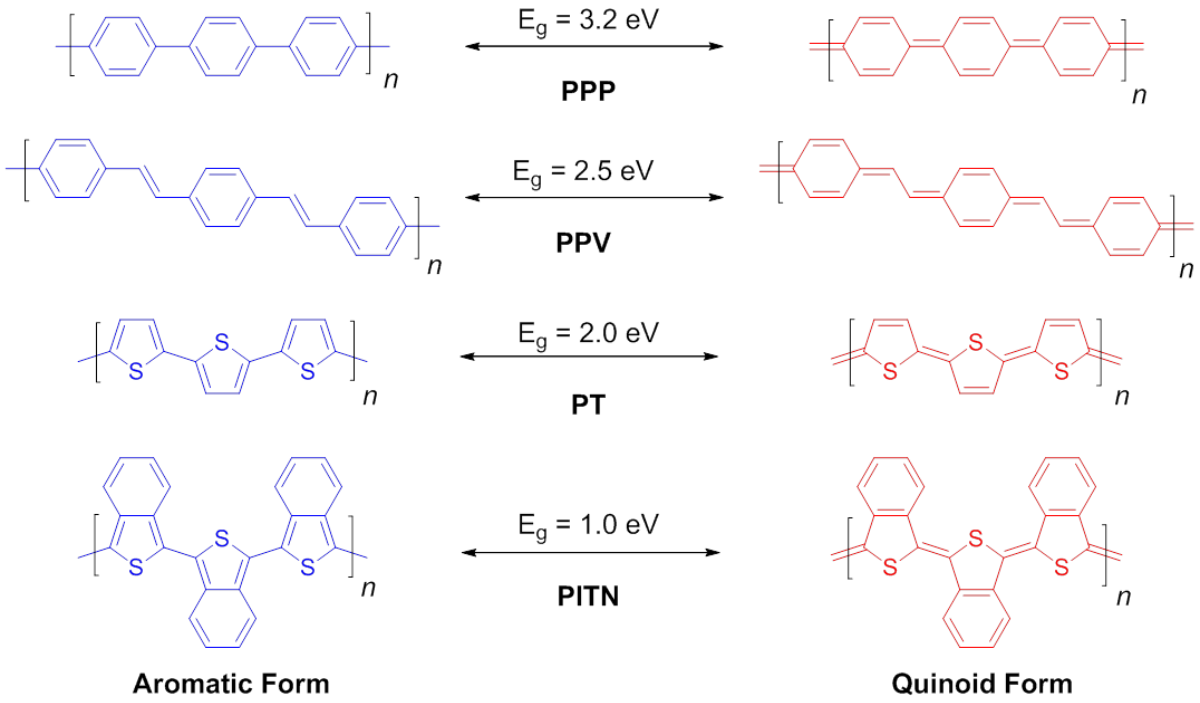

Figure 1.5. Resulting band gap of the aromatic and quinoid forms for poly(*p*-phenylene) (PPP), poly(*p*-phenylenevinylene) (PPV), polythiophene (PT), and polyisothianaphthene (PITN).

Strategic structural modifications can be introduced along the conjugated backbone to control the size of the band gap by favoring either the aromatic or quinoid forms. Benzene has an inherent, high-degree of aromaticity, primarily due to twisting of the phenyl-phenyl bond, so it is expected that poly(*p*-phenylene) (PPP) displays a wide band gap of 3.2 eV (Figure 1.5). This band gap can be reduced simply by introducing vinyl groups within the

backbone. The result is a lower band gap in poly(*p*-phenylenevinylene) (PPV), which is likely a result of the potential for the vinyl groups to reduce twisting and stabilize the quinoid form. Replacing benzene with various heterocycles also has a significant impact on the band gap. For example, thiophene has a much higher preference for the quinoid form than benzene, thus, polythiophene (PT) has a significantly reduced band gap of 2.0 eV.[46] Other strategies can be employed to promote the stability of the quinoid form, such as ring annulation exemplified by poly(isothianaphthene) (PITN).[47] The quinoid form of PITN breaks the aromaticity of the thiophene ring and simultaneously creates the more favorable aromatic form of benzene, leading to a significant 1.0 eV reduction in the band gap when compared with polythiophene.[48]

Another approach to reducing the band gap involves increasing the planarity of the conjugated backbone by minimizing various steric interactions between aromatic units. As mentioned previously, steric interactions tend to cause backbone twisting that result in a π-electron conjugation that is only effective over shorter, segmented distances. This distance is affected by the structure of different compounds and inherently varies between different materials.[49-52] To reiterate, as the conjugation length is increased, the band gap will decrease continually; however, conjugated organic materials will reach a point at which additional conjugated units will no longer result in any significant band gap decrease. In this way, increasing conjugation length quickly approaches an asymptotic value for the band gap.

A representative example the relationship between effective conjugation length and band gap size can be seen in a study by Otsubo, *et al*, wherein the band gaps of varying lengths of functionalized oligothiophenes were measured.[52] Shown in Figure 1.6, as the chain length is increased from the dimer (n = 2) up to a repeat unit of n = 12, the band gap decreases by 1.51 eV from -3.96 eV to -2.45 eV. This change is substantial, but each additional repeat unit results in a smaller change in the band gap than the previous one. As such, going from the 12-mer to the 18-mer only results in a band gap that is 0.05 eV smaller. To see another decrease of just under 0.05 eV, it takes a sizeable 76 additional repeat units. Several studies have claimed that the effective conjugation length is achieved between 11 – 20 repeat units, and sometimes with as few as 8.[53-55] The authors of this study make the claim that continuous red-shifting of the absorption is seen up to the 96-mer; however, the point at which no significant decrease in band gap is achieved is up for debate. While significantly

increasing polymer chain length may result in very small changes in band gap, it does affect other important properties such as film-formation and charge transport mobility which will be discussed later.[56, 57] Regardless, increasing the effective conjugation is a useful way to modify the band gap.

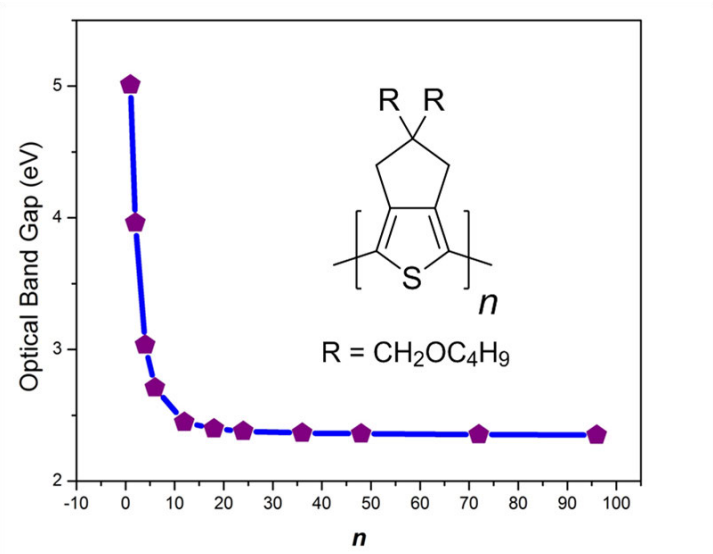

Figure 1.6. Correlation between chain length and optical band gap in functionalized oligothiophene.

Clever synthetic strategies exist that utilize steric effects between aromatic units to modify the effective conjugation. Interactions between alkyl chains on adjacent molecules can cause significant twisting of the conjugated backbone reducing the effective conjugation length. Similarly, hydrogen-hydrogen interactions can cause backbone twisting, although to a lesser degree than in the case of polythiophene. Chemical rigidification can also be used to reduce backbone twisting. This is typically done by bridging two or more adjacent

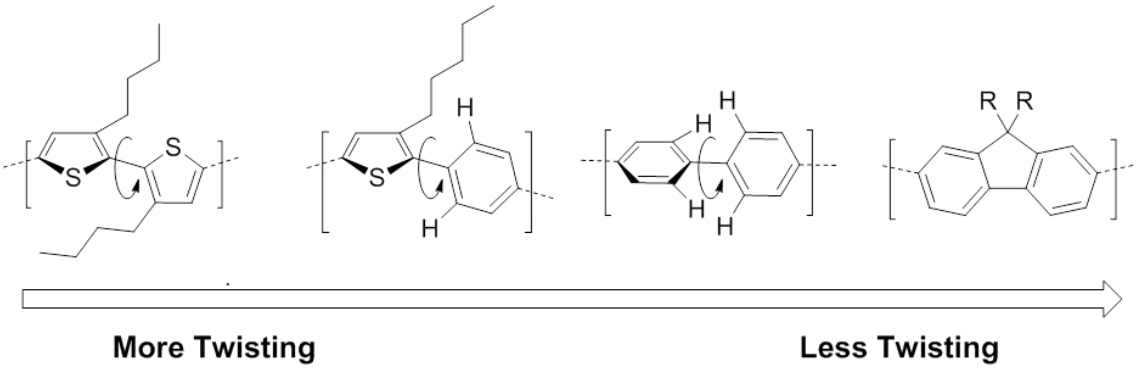

Figure 1.7. Examples of steric interactions between aromatic rings that can lead to twisting of the conjugated backbone.

aromatic rings into a rigid, ladder-like structure. Representative examples include molecules such as fluorine and cyclopentatdithiophene. By extending the bridging of the ladder structure, the effective conjugation can be increased further, resulting in the simultaneous reduction of the band gap.[58, 59]

Band gap tuning of conjugated polymers is not limited to the control of the planarity of the system. Another synthetic strategy exists that takes advantage of either inductive or resonance effects by the introduction of electron-donating and electron-withdrawing heteroatoms and functional groups along the polymer backbone.[60] Some examples of common electron-donating and electron-withdrawing aromatic molecules are shown in Figure 1.8. Typically, the incorporation of electron-donating substituents such as alkyls, alkoxyls, amines, or electron rich chalcogens increase the ionization potential and raise the HOMO level of aromatic molecules. Conversely, electron-withdrawing substituents like fluorines, imines, nitriles, nitro groups, ketones, esters, or amides increase the electron affinity and result in lower LUMO levels.[61] By far the most widely-used approach to engineer narrow band gaps while controlling the relative energy of the HOMO and LUMO levels is through the synthesis of conjugated polymers with a backbone comprised of alternating electron-rich donor (D) and electron-deficient (A) molecules.[62-65]

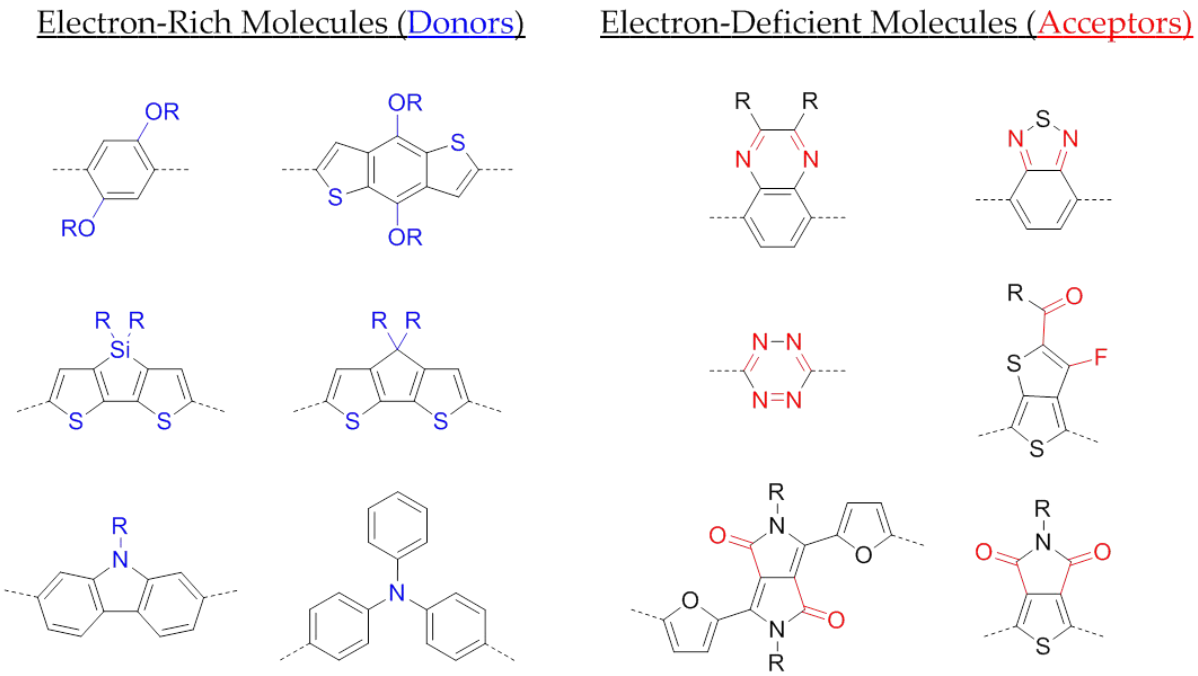

Figure 1.8. Examples of some common donor (n-type) and acceptor (p-type) molecules.

These donor-acceptor (D-A) frameworks produce copolymers with reduced BLAs which arise from their push-pull nature associated with the formation quinoid structures with mesomeric character (D−A → D^{+}=A^{-}).[61] However, perhaps the most straightforward explanation of the reduced D-A polymer band gaps is through orbital mixing, which results in hybridization of the donor and acceptor MOs.[66] Illustrated in Figure 1.9, the interaction of the HOMO levels of the donor and acceptor generates a new higher-lying HOMO, while a new, lower-lying LUMO results from the interaction of the donor and acceptor LUMOs. Due to the relative similarity in the energy of the donor HOMO and the HOMO of the D-A copolymer, the donor typically has a much stronger influence on the HOMO of D-A copolymer. Similarly, the LUMO of the acceptor strongly influences the LUMO of the D-A copolymer.[46] In this way, by careful selection of both the donor and the acceptor, one can tune both the size and the relative position of the band gap.

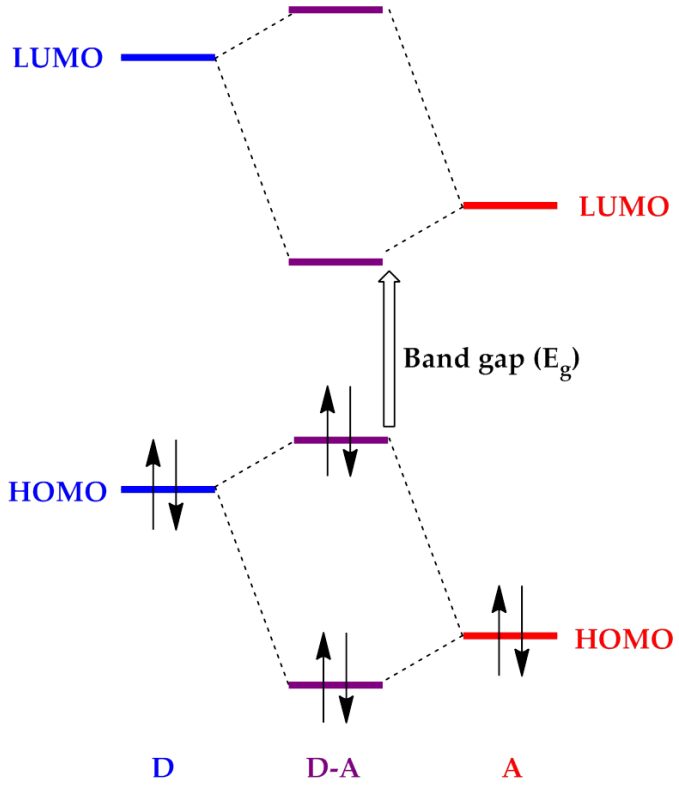

Figure 1.9. Reduction of band gap resulting from orbital interactions of donor (D) and acceptor (A) molecules.

To employ conjugated polymers in industrially viable organic electronics, the materials must be crystalline enough to maintain good charge transport capabilities, but still remain soluble in common organic solvents to make use of solution processing techniques. Numerous factors inherent to the polymer structure are responsible for the solubility of a given polymer. One determining factor is the degree of polymerization, or the molecular weight of a polymer.[67] Another significant factor governing polymer solubility are intermolecular interactions.[68, 69] These interactions are heavily influenced by backbone rigidity within the chain and π-π stacking between chains. Unsurprisingly, solubility decreases with both increasing polymer chain length and increasing intermolecular interactions. This is unfortunate, as high molecular weight polymers can result in more ordered films and yield higher charge carrier mobility.

Perhaps the most common method of controlling solubility is by attaching flexible, aliphatic side-chains to the polymer backbone. In the vast majority of conjugated polymers, these alkyl side-chains are a necessity in obtaining solution-processable material. The judicious choice alkyl chains can have a large impact on the performance of organic semiconductors by not only imparting varying degrees of order in polymer thin films, but also modifying the energy levels as well.[70] Generally, polymers with short or linear alkyl chains tend to suffer from poorer solubility.[71] The use of longer, or long and branched alkyl chains is commonly employed on the most insoluble conjugated materials, but this technique is not without consequence. Bulky alkyl chains break up interchain interactions and have a negative effect on photoconductivity in OPVs, but they can be useful in OLEDs as they tend to limit fluorescence quenching through excimer formation.[72] In some cases, a compromise can be made by means of short, branched alkyl chains that can greatly improve solubility while attempting to minimize interference with polymer order and π-stacking.[73] Additionally, alkyl chains can reduce a polymer's thermal stability,[74] although, the thermal decomposition temperature of most typical conjugated polymers still remains above the operating temperature of the average organic electronic device.

Success in organic semiconductors is also tied to ability of a given conjugated polymer to transport charges in the solid state.[75] Charge transport in organic semiconductors occurs via a charge-hopping mechanism, where the electrons and holes travel through the polymer film by "hopping" from one polymer chain to the next.[76, 77] This charge hopping mechanism

contributes to the lower mobilities that conjugated polymers tend to suffer from and is affected by randomness in molecular positions or "kinks" in the polymer, grain and phase segregation boundaries, charge traps formed by polymer defects, functional end-groups, and impurities such as residual metal catalysts.[57, 78-80] Conjugated polymers also tend to have imbalanced charge transport in that they typically have better hole mobilities than electron mobilities due to their electron-rich nature.[81, 82] Work is being done to synthesize polymers with high electron mobilities but it has proven difficult to obtain n-type materials that still perform well in electronic devices.[83]

As mentioned previously, many of the factors that affect solubility also impact charge transport and mobility. Charge carrier mobility is dependent upon the ability of the molecules to order themselves and the extent of π-π stacking they display.[78] After solution-processing, the strong inter-chain interactions of the material allow it to self-assemble into well-ordered regions of π-stacked polymer chains.[84] Careful use of solution processing time and techniques can also have a large impact on film morphology and charge mobility.[85] Some of the investigated properties that have been shown to influence mobility include polymer shape,[86] regioregularity,[87] solubilizing alkyl chains,[88] and molecule weight.[67] Also, mobility measurements between devices can be difficult to compare accurately. For example, in OPVs and OLEDS, charge propagates perpendicular to the polymer film whereas in OFETs, (commonly used to measure mobility of new polymers) charge moves parallel to the film. This can lead to discrepancies in comparing charge transport measurements, as charge hopping between polymer chains can differ from charge transport along polymer chains.[89] Due to the number of variables that effect mobility and its measurement, it can be difficult to draw conclusions between mobility and device performance.

1.3 ORGANIC PHOTVOLTAICS

Focus on scaling up infrastructure in the wind, water, and sunlight-based energy systems has led to a number of proposed implementations.[90-92] Among these, solar energy has the potential to outshine all other energy production, both renewable and nonrenewable combined, due to the large excess of sunlight the planet receives every day.[93] In spite of this, photovoltaic technology still remains a largely untapped resource because certain barriers

still exist to large-scale implementation of solar technology. As mentioned previously, high fabrication costs of silicon-based inorganic cells, which constitute the vast majority of current light-harvesting technology, result in a high cost of each kilowatt of energy produced.

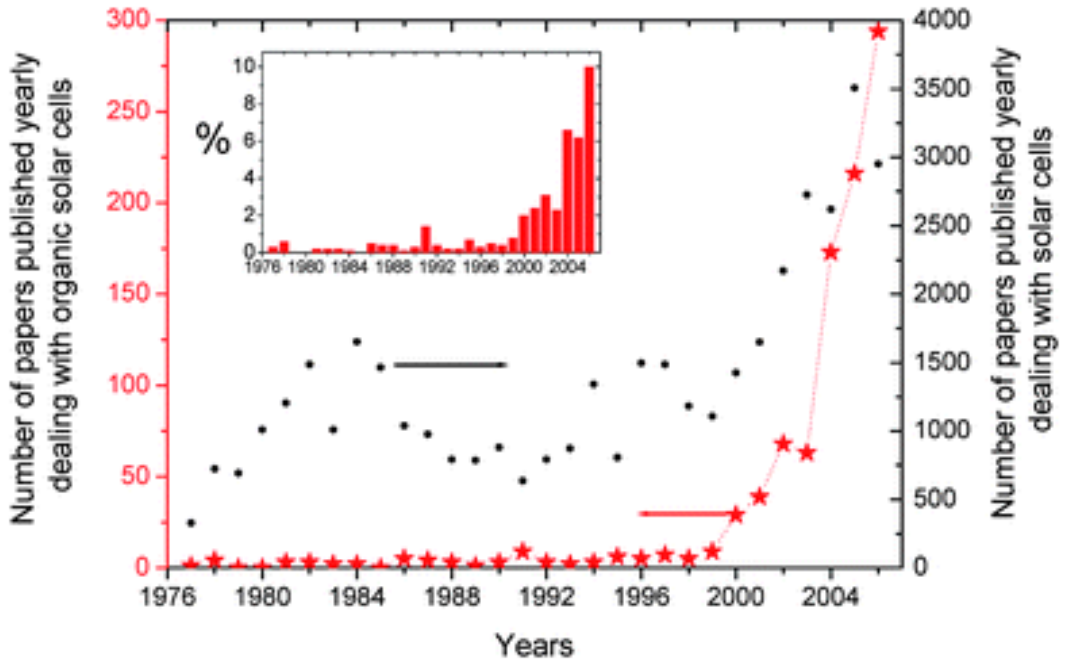

Figure 1.10. Number of scientific papers published on semiconductors and organic semiconductors since 1976.

Organic photovoltaic cell (OPV) technology has become an attractive alternative to these problems as it offers the potential of being made from cheap, renewable materials, the ability to be fabricated at low-cost and high volumes, and the capacity for use in flexible, light-weight devices.[11, 94, 95] Interest in this technology is evident from the incredible spike in the amount of research focused on solar cells during the last 10 years, with the increases in publications concerning OPVs exploding from only a handful to hundreds per year (Figure 1.10).[96] Currently, there are multiple examples of optimized polymer-based OPVs with power conversion efficiencies (PCEs) of 8 to 9%,[97-99] with some of the latest breakthroughs being reported above 10%.[100, 101] Despite these large gains in efficiency, further development is still requirement to promote commercial viability.

Early OPVs represented a class of basic device architectures based on a single organic component sandwiched between two electrodes. For example, one OPV was fabricated by spin-coating and thermally annealing a PPV active layer on top of a transparent indium-tin oxide (ITO) anode.[102] This is followed by the evaporation of a low-work function cathode contact layer, typically aluminum, calcium, or magnesium. A schematic representation of this single-layer device is shown in Figure 1.11 and can be used to illustrate the fundamental principles of OPVs. The differing values of the work functions results in band bending and creation of an electric field in the active layer. Electrical power in the device is generated by photoexcitation of the organic polymer due to the absorption of photons of light, which generates a coulombically bound electron-hole pair, called an exciton. Under the driving force of the electric field, the electrons and holes separate with the result that electrons travel towards the cathode and holes travel towards the anode. This process produces the photocurrent and photovoltage that can be taken advantage of for energy applications.[103]

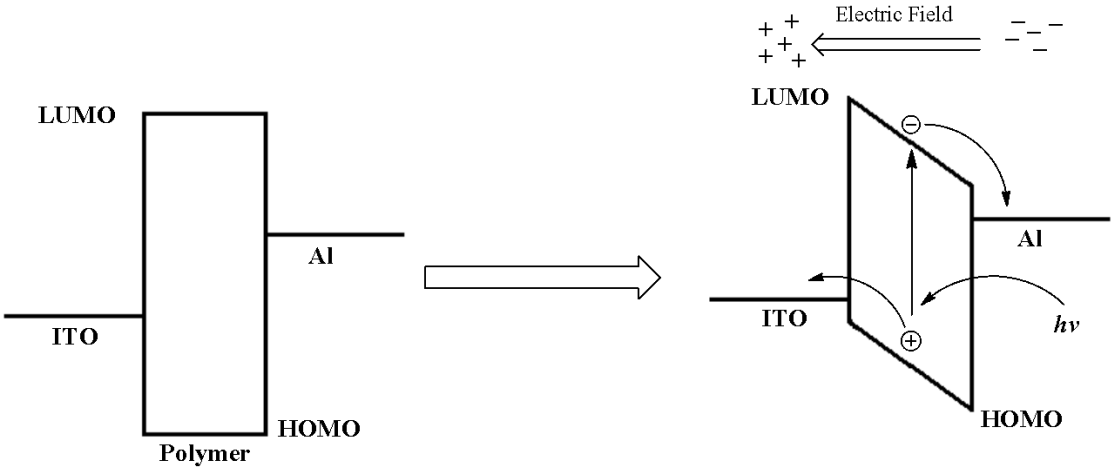

Figure 1.11. Relative energy level diagram of a single layer OPV device including light induced excitation , exciton dissociation and band bending.

The success of a photovoltaic (PV) cell is primarily evaluated by the generated power conversion efficiency (PCE); however, the quantity of the PCE is not measured as a direct output variable of the cell. Instead several other crucial parameters in PV performance are measured and used to obtain the device efficiency. These parameters, shown in Figure 1.12,

are the short circuit current density (J_{sc}), the open circuit voltage (V_{oc}), and the fill factor (FF) are defined as:[104]

$\boldsymbol{J_{sc}}$ – The short circuit current (I_{sc}) per area of cell surface (perpendicular to charge transport). The I_{sc} is the current that flows because of the drifting of charges due to the internal field when no external field is applied. I_{sc} is governed by the quantum efficiency for charge separation, charge-carrier transport through the material, and loss of carriers due to recombination.

$\boldsymbol{V_{oc}}$ – The maximum possible voltage obtained from a cell. This voltage is measured at zero current and governed by the inherent energy levels of the various PV materials.

FF – The ratio of areas B to A as shown in Figure 1.12. B is determined by the actual maximum obtainable voltage (V_m) and current density (J_m), and A is determined by J_{sc} and V_{oc}. The FF is governed by the series resistance and the shunt resistance and can be expressed by the following equation:

$$FF = V_m \cdot J_m / V_{oc} \cdot J_{sc}$$

PCE – power conversion efficiency, also represented by η, is the ratio of electrical power generated by the cell (P_{out}) over the light power into the cell (P_{in}). It can be determined by the following equation:

$$\eta = P_{out}/P_{in} = J_{sc} \cdot V_{oc} \cdot FF/P_{in}$$

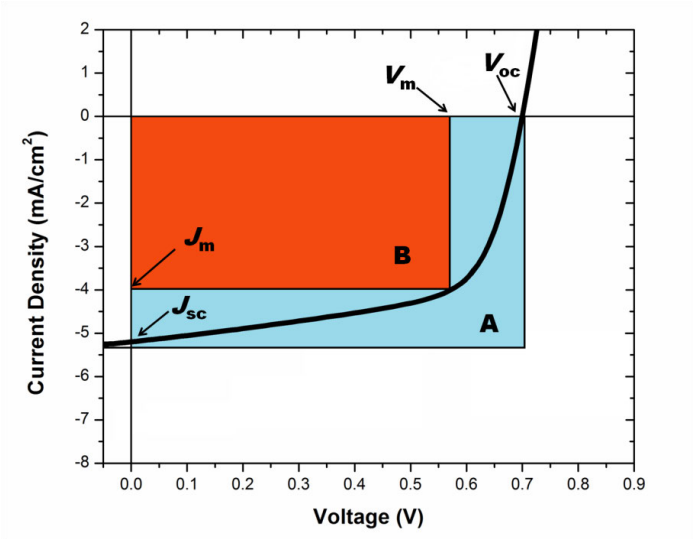

Figure 1.12. Current density versus voltage (J vs. V) of a solar cell and the relevant parameters for determining fill factor (FF).

While useful for demonstrating some basic operating principles and sometimes producing a respectable V_{oc}, the single layer architecture makes for poor performing OPVs owing to a set of significant shortcomings. The most detrimental problem is poor exciton dissociation in the active later. Excitons predominantly favor remaining bound together and decay, primarily via recombination, rather than dissociate at room temperature.[105] Other factors such as imbalanced charge transport and the disordered nature of organic polymers also contribute.[106] These drawbacks ultimately results in rather low PCEs of ~0.1-1%.[102] To overcome the problems of exciton dissociation and imbalanced charge transport, devices comprised of two different semiconducting organic materials that form a heterojunction have been employed.[107-109] This bilayer-based strategy (Figure 1.13) combines an electron-rich or p-type material with a higher-lying HOMO used as a donor layer and an electron-deficient or n-type material with a lower-lying LUMO used as an acceptor layer in tandem. This time, when an exciton is generated in either layer it can diffuse to the donor-acceptor (D-A) interface and dissociate. The dissociation occurs by the transfer of an electron from the LUMO of donor to the LUMO acceptor, accompanied by the concomitant transfer of a hole from the HOMOs of the acceptor to the donor. The D-A interface provides a driving force for exciton dissociation as long as the energy difference between the LUMOs is greater than ~0.2 eV, the dissociation energy of an exciton.[110] The separated electrons and holes can now transport through the donor or acceptor materials to the respective electrodes, resulting in the generation of photocurrent.

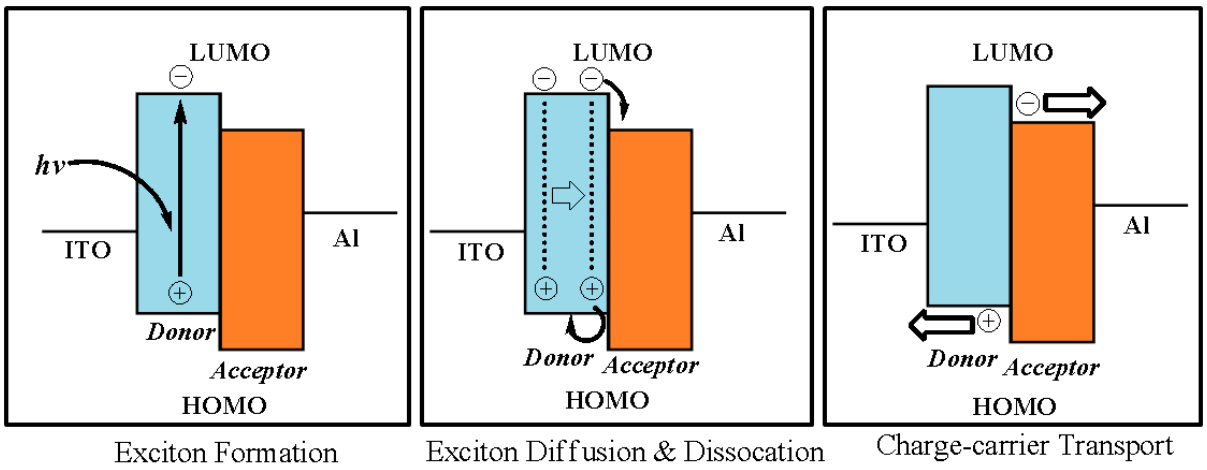

Figure 1.13. Working mechanism of a bilayer OPV device involving exciton formation, diffusion to D-A interface, and dissociation into charge carriers ready to transport.

Although bilayered devices represent a step forward in OPV design by demonstrating the necessity of a D-A interface, they still suffer from several fundamental flaws leading to reduced PCEs. Chief among these issues is that the active layer in OPVs should be thick, around 100 nm, to efficiently absorb incident photons while excitons have short diffusion lengths, approximately 10 nm, due to their limited lifetimes.[109, 111, 112] This means that only excitons generated near the D-A interface will be able to dissociate and those created too far away will decay and be wasted. To overcome this, the ideal scenario is a device possessing a highly-ordered heterojunction with 10-20 nm thick layers of interdigitated donor and acceptor material domains (Figure 1.14). This would allow a majority of the excitons to reach the D-A interface while maintaining a direct corridor for the dissociated electrons and holes to travel to their respective electrodes. Although it has been theorized, this device architecture has yet to be realized owing to a high degree of difficulty in fabrication and the issue of efficient charge separation remains perhaps the single biggest problem for OPVs.

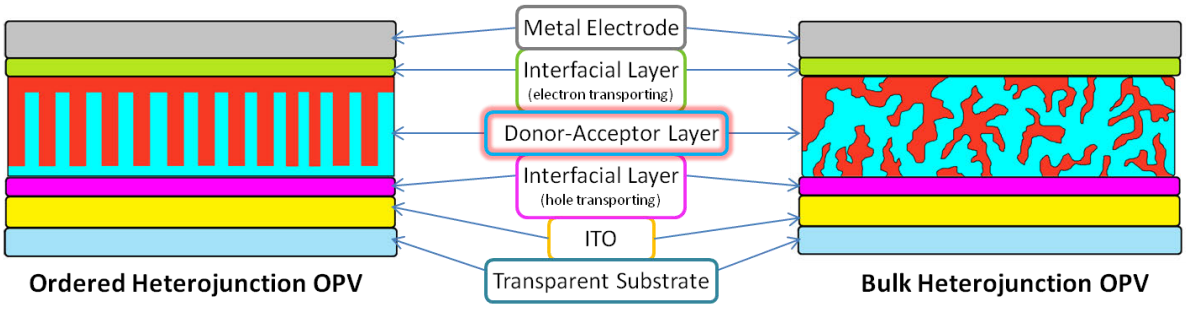

Figure 1.14. Device architecture of idealized ordered heterojunction and the more practical bulk heterojunction solar cells (including highlighted isolated domain of material).

As a more realistic compromise between bilayer and highly-ordered devices, the concept of a bulk-heterojunction (BHJ) device was introduced by Yu and Halls.[113, 114] The active layer in BHJs is formed by blending the donor and acceptor materials into an interpenetrating, single active layer, which allows for the formation of a D-A interface with a very large surface area (Figure 1.14). With the proper control of the phase separation, domain sizes, and film morphology, most of the exciton formation could occur near the interface while still allowing channels for charge transport to the electrodes. Since BHJ cells only require a single active layer, problems related processing two adjacent layers with potentially similar solubility profiles can be avoided. Initial attempts at BHJ devices

involved intermixing two polymers with offset energy levels, which led to PCEs up to 1.9% after optimization.[115]

Perhaps the most important advance in OPV research came when Sariciftci *et al* observed the photoinduced electron transfer in blends of conjugated polymer and buckminsterfullerene.[116] C_{60} fullerenes possess many unique qualities that make them ideal candidates for acceptor materials. Fullerenes are excellent for accepting electrons from p-type materials due to a comparatively low-lying LUMO.[117] They are also well-suited at stabilizing negative charges as the LUMO is triply-degenerate and can accept up to six electrons at a time. Fullerenes also provide a kinetic driving force for highly efficient charge separation, as electron transfer takes place at around 45 fs, significantly faster than back electron transfer or radiative decay through photoluminescence.[118] While p-type polymers can suffer from photooxidation of their excited states, fullerene can help mitigate this problem by quickly quenching the excited state.[119, 120] Lastly, fullerenes also display high electron mobilities in OFETs, a quality required for good n-type materials.[121]

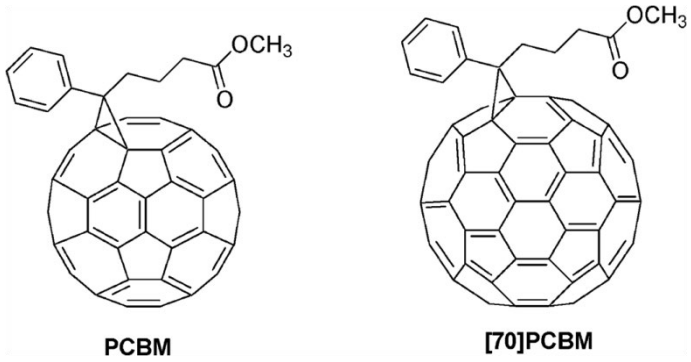

Figure 1.15. Molecular structures of [6,6']-phenyl-C_{61}-butyric acid methyl ester (PCBM) and [6,6']-phenyl-C_{71}-butyric acid methyl ester $PC_{71}BM$.

Unfortunately, C_{60} lacks solubility in organic solvents. This problem has been overcome by the functionalization of C_{60}, most notably in the case of [6,6']-phenyl-C_{61}-butyric acid methyl ester (PCBM) (Figure 1.15).[122] PCBM does not absorb particularly well in the visible region and is sometimes replaced by the C_{70} version of PCBM, $PC_{71}BM$, which is less symmetric and has more low-energy transitions (Figure 1.15).[123-125] Nevertheless, BHJ cells are not perfect and typically have problems related to maintaining good segregation of

PCBM and polymer phases. If domains form of either polymer or PCBM that are much larger than the average exciton diffusion distance, there will be less excitons reaching the D-A interface and less dissociation into charge carriers. Also, during the solution processing of the active layer, it is possible for domains of either polymer or PCBM to become isolated from the electrode (Figure 1.14). Any excitons that form charge carriers within this isolated domain are cut-off from any transport pathways. Both of these issues have become a major focus of the OPV community, as they lead to reduced PCE in devices. Accordingly, there has been a plethora of research done in attempt to address them.[126] Some of the many examples include varying process conditions and post-production treatment to control self-assembly,[127-129] introducing small amounts of solvent additives like 1,8-diidooctane and 1-chloronapthalene during film processing,[130, 131] the synthesis of block copolymers,[132-134] the use of nanostructures to influence morphology,[135-137] and even covalently attaching PCBM to the conjugated polymer itself.[138-141] Nevertheless, the PCBM-conjugated polymer systems are currently the best performing polymer OPVs.

Not only does control of the polymer:PCBM morphology affect the percolation pathways for charge carries, it also plays an important role in enhancing fill factors (FF) and open circuit current densities (J_{sc}).[142-144] This has been accomplished by the aforementioned incorporation of a solvent additive[145] as well as controlling the film growth rate,[84] optimizing film thickness and the use of thermal annealing.[146] As discussed in the previous section, the use of solubilizing side-chains is an impactful way to control the film forming capabilities of the polymer. Another performance-determining set of polymeric parameters that is interrelated with solubility is the molecular weight (M_w) and polydispersity index (PDI) of the polymer. Although higher molecular weights tend to improve performance, respective M_w and PDI Respective values of around 20-30 kDa and 1.2-2.0 are typical minimum benchmarks. These aspects affect a multitude of other morphology-influencing properties, including solubility, thermal stability solution and film aggregation, and formulation rheology.[147] These morphological considerations are heavily influence by the structure of the polymer.

One example of how structure plays a role in morphology is that of poly(3-hexylthiophene) (P3HT). The short linear side-chains in P3HT interdigitate and form a herringbone-like pattern.[148] This introduces improved crystallinity by the formation of 3-dimensional packing of the polymer chains, leading to highly-ordered lamellar structures in films (Figure 1.16).[149] Although the use of long or branched alkyl chains to increase solubility typically disrupts good film forming ability, there are examples of polymers that exhibit enhanced OPV performance when branched chains are used instead of linear ones.[70] Unfortunately, predicting which side-chains will perform best with a specific polymer system is very difficult and determining the best performing structure typically arises from synthesizing many different iterations.[150, 151] Alkyl chains can also affect the phase segregation of BHJ cells by affecting how well the polymer aggregates with PCBM.[152]

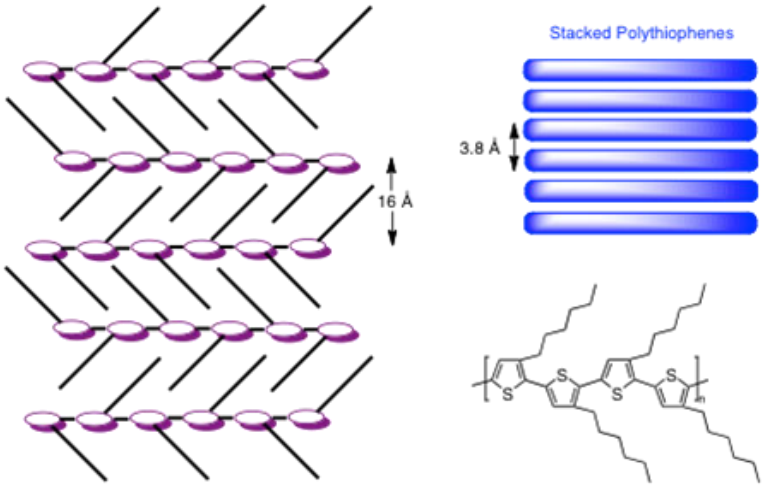

Figure 1.16. Illustration of how the regioregularity of poly(3-hexylthiophene) leads to interdigitated alkyl side-chains and well-order crystalline packing of the polymer chains.

Since the main function of any solar cell is convert sunlight to electrical energy, it is necessary to design materials suitable for absorbing as much of the solar spectrum as possible. As shown in Figure 1.17, the maximum amount of solar radiation occurs from 500 nm up to approximately 700 nm, with a significant amount tailing off into the near IR region. To take advantage of this, an absorbing material with a band gap of about 1.6-1.7 eV is required. Coincidentally, narrower band gaps lead to increases in open circuit current densities (J_{sc}) as this variable is directly proportional to the number of excitons generated.

This leads to the generation of more potential charge carries and, thus, more current.[142] Given that PCBM, as an acceptor, has a much wider band gap and only absorbs high energy radiation, it falls onto the conjugated polymer to absorb this broad swath of lower energy. As discussed in the previous section, many techniques and strategies have been employed to manipulate the band gap of conjugated polymers to give very broad absorbance.[46, 153] Ultimately, these techniques involve raising and lowering the HOMO and LUMO levels in the polymer either individually or simultaneously.

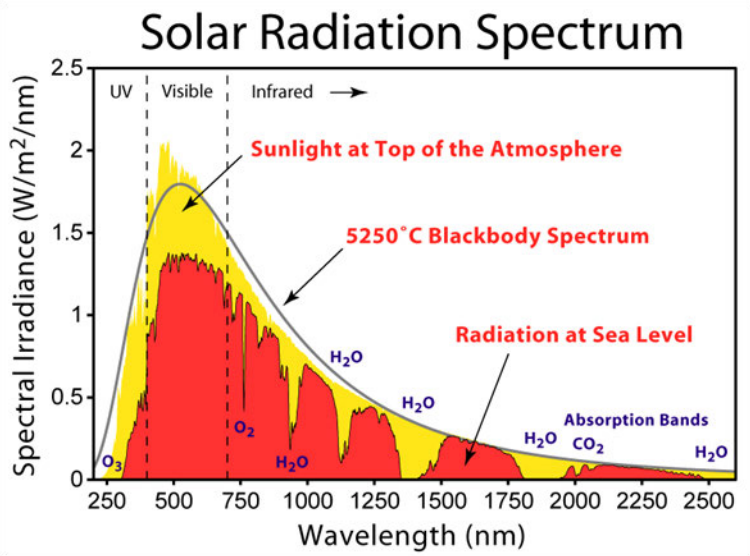

Figure 1.17. Solar irradiation spectrum of sunlight at the top of the atmosphere and at sea level.

The position of the energy levels and resulting size of the band gap affect more than just the amount of light absorbed; other properties of BHJ cells are attributed to the optoelectronic characteristics of the materials in the active layer. One of these properties, previously discussed, was that the LUMO of the acceptor must be at least 0.2-0.3 eV higher than that of the conjugated polymer to drive electron transfer between the two materials. Another critical property determined by the relative energy levels of the active layer materials is the open circuit voltage (V_{oc}). The value of the V_{oc} is linearly proportional to the energy difference between the LUMO of the acceptor and the HOMO of the donor as described in Figure 1.18.[154, 155] Since the V_{oc} is also directly proportional to the PCE, optimizing this parameter is of great importance. Within the conjugated polymer, the V_{oc} can

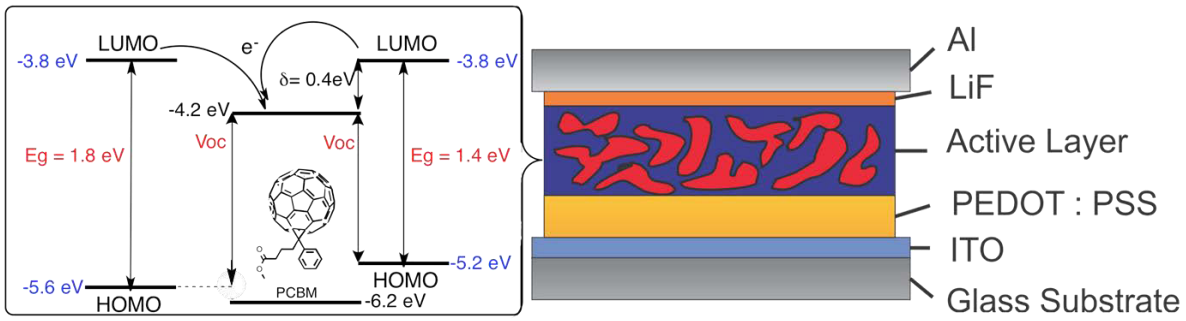

Figure 1.18. Illustration of the optimal energy levels of a conjugated polymer-based donor material used with PCBM in a BHJ-OPV. The important factors are the difference in the LUMOs for effective charge separation, narrow band gaps for optimal solar absorbance, and maximizing the V_{oc} by stabilizing the HOMO of the donor.

be maximized by lowering the HOMO and raising the LUMO levels, but not to an extreme where the band gap becomes so large that not enough solar radiation is absorbed. It becomes apparent that a balance between good absorbance (narrow band gap), favorable exciton dissociation (difference in LUMOs), and high V_{oc} (~ $LUMO_{acceptor}$ - $HOMO_{donor}$) is needed. Taking these factors into account, the ideal PCBM-based OPV has a LUMO of around -3.7 to -4.0 eV and a HOMO between -5.2 and -5.7.[156, 157] It is worth noting that attempts to optimize these parameters by synthetically tuning the energy levels of fullerene-based acceptors, most specifically the LUMO, have also been attempted.[158, 159]

1.4 A BRIEF INTRODUCTION TO BENZODICHALCOGENOPHENES

Among fused-ring building blocks for organic semiconducting materials, benzo[1,2-*b*:4,5-*b'*]dithiophene (BDT), shown in Figure 1.19, is one of the most widely used for electron-donating molecules.[160] The fused-ring structure allows for increased planarity while its symmetric nature allows for regioregularity desired for many D-A copolymers. These promising properties led to one of the highest reported hole mobility of 0.25 $cm^2V^{-1}s^{-1}$ in OFETS back in 2007.[161] The first report of BDT in OPVs was in 2008 by Hou *et al* resulting in a moderate 2% PCE.[162] Since then, BDT has been incorporated into many successful BHJ OPVs with PCEs of over 7% in standard architecture solar cells and 9.2% in inverted cells.[98, 163-165] Much this success can be related to the fact that most BDT-containing D-A copolymers maintain a good balance between narrow band gaps and deep HOMO

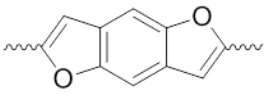

Benzo[1,2-b:4,5-b']difuran (**BDF**)

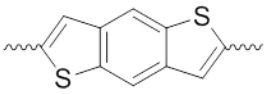

Benzo[1,2-b:4,5-b']dithiophene (**BDT**)

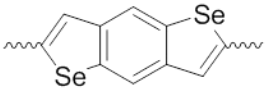

Benzo[1,2-b:4,5-b']diselenophene (**BDSe**)

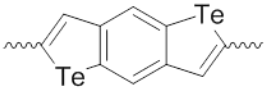

Benzo[1,2-b:4,5-b']ditellurophene (**BDTe**)

Figure 1.19. Molecular structures of aromatic cores for the known benzo[1,2-*b*:4,5-*b'*]dichalcogenoophenes (BDCs).

levels. Also, advantageous synthetic routes to BDT allow for tunable properties through easy side-chain modification.

While there are multiple syntheses reported for BDT,[166-168] the most commonly used route was reported first by Beimling and Kossmehl in1986.[169] This synthetic pathway is highlighted in Scheme 1.19. The key step involves the cyclization of diethyl-3-thiophene carboxylic acid amide **2** to give the 4,8-substituted dione **3**. The main advantage of this route is that the dione **3** can be functionalized with a variety of side-chains to tune the electronics of BDT. The standard alkyl-chain can be replaced by alkoxy chains to increase the donor strength of the molecules. Additionally, 2-alkylthiophenes have been affixed to the BDT core as an attempt to modify the electronic through 2-dimensional conjugation and enhance the film forming properties by increasing planarity.[170, 171]

Recently, there has been an interest in exploring how the incorporation of various heteroatoms will affect conjugated materials and the devices made from them. One approach to this has been through the synthesizing BDT analogues that take advantage of the other members of the chalcogen family: oxygen, selenium, and even tellurium (Figure 1.19). These other benzo[1,2-*b*:4,5-*b'*]dichalcogenophenes are isoelectronic to BDT, but may possess other unique properties beneficial to organic electronics. Furan, for example, is an attractive alternative to thiophene as that it is less aromatic and, thus, could stabilize the quinoid form better leading to narrower band gaps.[172] Furan also has a diatomic radius that is approximately 60% as large as that of thiophene. As a result, bifuran is a highly planar molecular whereas bithiophene experiences more steric interactions and is twisted out of

plane by about 20°.[173] Despite this, oligofurans maintain better solubility in common organic solvents than do oligothiophenes. However, furan has some significant drawbacks as well, including being more electron-rich than thiophene resulting in a higher-lying HOMO that is more easily oxidized.[174] In addition to be more unstable, oligofurans also suffer from reduced hole mobility when compared to thiophene. In spite of all this, recent research has suggested that conjugated polymers that judiciously incorporate furan into the backbone can experience increases in overall performance.

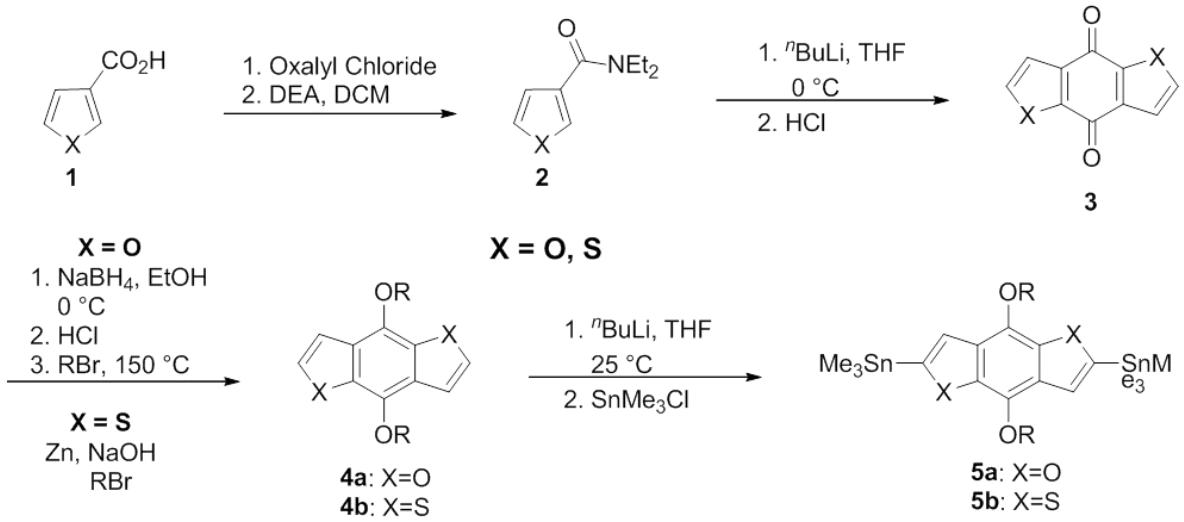

Scheme 1.1. The most widely used synthetic pathway to BDT and the analogous synthesis of BDF.

To take advantage of these qualities, there has been a recent uptick in the number of OPV-related papers published on benzo[1,2-*b*:4,5-*b'*]difuran (BDF). Until recently, the general lack of synthetic routes to functional BDF has prevented its widespread use.[175-177] One of these syntheses produces BDF in a manner analogously to BDT (Scheme 1.1), only differing in the conditions of the alkylation step to give **4a**. The incorporation of these BDF monomers into copolymers with benzothiadiazole gave good efficiencies of up to 5%.[178] Another novel route, which will be discussed in more detail in the latter chapters of this thesis, was first reported by Larock *et al* in 2005.[179] This chemistry involved the electrophilic cyclizations of various heterocyclic annulenes, specifically the reaction of iodine with *o*-alkynylanisoles (Scheme 1.2). During a synthesis this library of benzofurans with the goal of providing new synthetic pathways toward the total synthesis of natural products, one attempt was made at synthesizing a BDF molecule. Unfortunately, the

resulting product was almost completely insoluble. In the work described in the following chapters, the author of this thesis has taken steps to address these solubility issues.[180]

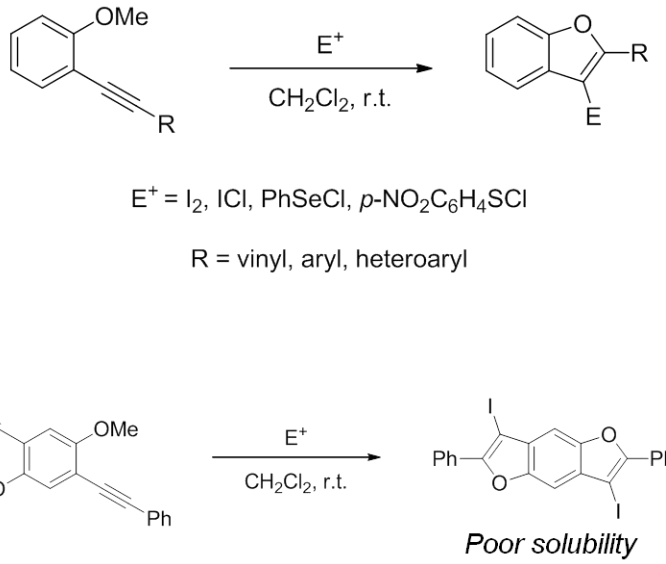

Scheme 1.2. Larock electrophilic cyclization resulting in functionalized benzofurans (top) and synthesis of bisphenylbenzodifuran reported by Larock (bottom).

There are even fewer examples of benzo[1,2-*b*:4,5-*b'*]diselenophenes (BDSe) in the literature, with a few examples of the synthesis of the BDSe core.[181-183] It is proposed that a selenium-based conjugated heterocycle should have narrower band gaps and enhanced interchain interactions, due to the greater polarizability, which should lead to higher hole mobility. One report compares BDSe to BDT-based polymers in OFETs and finds a negligible difference in electronics and only a slight increase in hole mobility from BDT to BDSe. There is only one account of BDSe being used in OPVs, with promising results.[184] The BDSe-based polymers had higher PCEs in both examples when compared with the analogous BDT-based polymers by 5% in one case and an impressive 20% in another.[185] These improvements were attributed to the synergistic effects of a more optimal band gap, charge carrier mobility, and absorbance of the solar spectrum.

To date, there have only been two reports on the synthesis of benzo[1,2-*b*:4,5-*b'*]ditellurophene (BDTe): one as evaluation of its optoelectronic properties along with BDT and BDSe, and one incorporating these molecules into OFETS.[186, 187] BDTe has a smaller band gap due to the destabilization of its HOMO level and, as a result, it has a significantly

red-shifted absorbance; however, it did not perform as well as the analogous BDSe compound in OFETs. The only other significant report of the use of covalently-bonded tellurium in organic semiconductors was a report of a D-A copolymer of tellurophene and diketopyrrolopyrrole (DPP) that was used in OFETs.[188] The tellurophene-based polymer had a higher hole mobility by an order of magnitude when compared to the thiophene-based polymer. Despite the potential benefits of tellurium heterocycles, the synthetic difficulties and rarity of tellurium in the earth's crust limit its widespread adoption into semiconducting materials.[189]

1.5 CONCLUSIONS

From a design standpoint, synthesizing the ideal p-type conjugated polymers for use in OPVs must take the following considerations into account:

- Suitable Energy (HOMO and LUMO) levels
  - Good overlap of absorbance with solar spectrum
    - Reasonably narrow band gaps (1.5-1.8 eV)
      - Tuned by controlling effective conjugation length
        - Stabilizing/destabilizing the aromatic form
        - Minimizing undesirable steric interactions
      - Tuned by using donor/acceptor copolymers
        - Increasing relative donor/acceptor strength leads to narrow band gaps
    - Good absorbance improves short circuit current density (J_{sc})
  - Determines charge separation/dissociation of excitons
    - $LUMO_{donor} - LUMO_{acceptor} \geq 0.25\text{-}0.4$ eV – effect separation
      - $HOMO_{donor}$ primarily influenced by electron-rich monomer
      - $LUMO_{acceptor}$ determined by the acceptor/n-type material (typically PCBM)
  - Determines open circuit voltage (V_{oc})
    - $LUMO_{acceptor}$ - $HOMO_{donor} \approx V_{oc}$ - which should be maximized (within reason)
      - $HOMO_{donor}$ primarily influenced by electron-rich monomer

- ➢ $LUMO_{acceptor}$ determined by the acceptor/n-type material (typically PCBM)

- Determines oxidative stability (V_{oc})
  - ♦ Higher-lying $HOMO_{donor}$ decreases oxidative stability

❖ Good thin film morphologies

- Higher molecular weights tend to improve performance in OPVs
  - Longer polymer chains increase crystallinity and higher charge carrier mobilities
  - ♦ Appropriate Choice of Alkyl Chains
    - Short, linear alkyl chains that are interdigitated can increase crystallinity but decrease solubility (example: P3HT)
    - Long and/or branched chains can disrupt π-stacking, but increase solubility
- Narrow PDIs lead to more consistent film-forming properties
- Judicious choice of structure of conjugated polymer backbone
  - ♦ More planar molecules tend to experience better π-stacking
  - ♦ Certain heteroatoms, heterocycles, and other functionalities influence π-stacking

The factors influencing the performance of conjugated polymers in OPVs are numerous and are highly interrelated. Changing one design aspect of a material can lead to various effects in other areas, either desirable or undesirable, and can be rather frustrating at times. While there are many of examples of well-performing organic semiconductors there still exists a great need to synthesize and explore new materials for both p-type and n-type applications. Only through the exploration of structure-function relationships and the development of new, elegant synthetic pathways can the field of organic semiconductors move towards widespread commercial implementation.

1.6 REFERENCES

1. Chiang, C. K.; Fincher, C. R.; Park, Y. W.; Heeger, A. J.; Shirakawa, H.; Louis, E. J.; Gau, S. C.; MacDiarmid, A. G., *Phys. Rev. Lett.* **1977,** *39* (17), 1098.
2. Shirakawa, H.; Louis, E. J.; MacDiarmid, A. G.; Chiang, C. K.; Heeger, A. J., *J. Chem. Soc., Chem. Commun.* **1977,** *0* (16), 578-580.
3. Intemann, J. J.; Mike, J. F.; Cai, M.; Barnes, C. A.; Xiao, T.; Roggers, R. A.; Shinar, J.; Shinar, R.; Jeffries-El, M., *J. Poly. Sci. A.* **2013,** *51* (4), 916-923.
4. Friend, R. H.; Gymer, R. W.; Holmes, A. B.; Burroughes, J. H.; Marks, R. N.; Taliani, C.; Bradley, D. D. C.; Dos Santos, D. A.; Bredas, J. L.; Logdlund, M.; Salaneck, W. R., *Nature* **1999,** *397* (6715), 121-128.
5. Ego, C.; Marsitzky, D.; Becker, S.; Zhang, J.; Grimsdale, A. C.; Muellen, K.; MacKenzie, J. D.; Silva, C.; Friend, R. H., *J. Am. Chem. Soc.* **2003,** *125* (2), 437-443.
6. Shinar, J.; Shinar, R., 1.04 - An Overview of Organic Light-Emitting Diodes and their Applications. In *Comprehensive Nanoscience and Technology*, Editors-in-Chief: David, L. A.; Gregory, D. S.; Gary, P. W., Eds. Academic Press: Amsterdam, 2011; pp 73-107.
7. Bhuwalka, A.; Mike, J. F.; He, M.; Intemann, J. J.; Nelson, T.; Ewan, M. D.; Roggers, R. A.; Lin, Z.; Jeffries-El, M., *Macromolecules* **2011,** *44* (24), 9611-9617.
8. Wu, Y.; Li, Z.; Ma, W.; Huang, Y.; Huo, L.; Guo, X.; Zhang, M.; Ade, H.; Hou, J., *Adv. Mater.* **2013,** *25* (25), 3449-3455.
9. Kobilka, B. M.; Hale, B. J.; Ewan, M. D.; Dubrovskiy, A. V.; Nelson, T. L.; Duzhko, V.; Jeffries-El, M., *Polym. Chem.* **2013,** *4* (20), 5329-5336.
10. Beaujuge, P. M.; Fréchet, J. M. J., *J. Am. Chem. Soc.* **2011,** *133* (50), 20009-20029.
11. Brabec, C. J.; Sariciftci, N. S.; Hummelen, J. C., *Adv. Funct. Mater.* **2001,** *11* (1), 15-26.
12. Chua, L. L.; Zaumseil, J.; Chang, J. F.; Ou, E. C. W.; Ho, P. K. H.; Sirringhaus, H.; Friend, R. H., *Nature* **2005,** *434*, 194.
13. Horowitz, G., *Adv. Mater.* **1998,** *10* (5), 365-377.
14. Facchetti, A., *Materials Today* **2007,** *10* (3), 28-37.
15. Li, J.; Zhao, Y.; Tan, H. S.; Guo, Y.; Di, C.-A.; Yu, G.; Liu, Y.; Lin, M.; Lim, S. H.; Zhou, Y.; Su, H.; Ong, B. S., *Sci. Rep.* **2012,** *2*.
16. Novak, P.; Muller, K.; Santhanam, K. S. V.; Haas, O., *Chem. Rev.* **1997,** *97* (1), 76.
17. Mike, J. F.; Lutkenhaus, J. L., *J. Polym. Sci. Part B* **2013,** *51* (7), 468-480.
18. Wegner, G., *Polym. Adv. Technol.* **2006,** *17* (9-10), 705-708.
19. Ellinger, S.; Graham, K. R.; Shi, P.; Farley, R. T.; Steckler, T. T.; Brookins, R. N.; Taranekar, P.; Mei, J.; Padilha, L. A.; Ensley, T. R.; Hu, H.; Webster, S.; Hagan, D. J.; Van Stryland, E. W.; Schanze, K. S.; Reynolds, J. R., *Chem. Mater.* **2011,** *23* (17), 3805-3817.
20. Wolfe, J. F., *Proceedings of SPIE-The International Society for Optical Engineering* **1987,** *682* (Mol. Polym. Optoelectron. Mater.: Fundam. Appl.), 70-76.
21. May, J. C.; Biaggio, I.; Bures, F.; Diederich, F., *Appl. Phys. Lett.* **2007,** *90* (25), 251106-3.
22. Yoon, J.; Chae, S. K.; Kim, J. M., *J. Am. Chem. Soc.* **2007,** *129* (11), 3038-3039.

23. Goldenberg, L. M.; Bryce, M. R.; Petty, M. C., *J. Mater. Chem.* **1999,** *9* (9), 1957-1974.
24. McQuade, D. T.; Pullen, A. E.; Swager, T. M., *Chem. Rev.* **2000,** *100* (7), 2537-2574.
25. Spear, W. E.; Willeke, G.; Le Comber, P. G.; Fitzgerald, A. G., *J. Phys. Colloques* **1981,** *42* (C4), C4-257-C4-260.
26. Sarti, D.; Einhaus, R., *Sol. Energy Mater. Sol. Cells* **2002,** *72* (1–4), 27-40.
27. Gribov, B. G.; Zinov'ev, K. V., *Inorg. Mater.* **2003,** *39* (7), 653-662.
28. Klaver, A.; van Swaaij, R. A. C. M. M., *Sol. Energy Mater. Sol. Cells* **2008,** *92* (1), 50-60.
29. Woo, H. Y.; Shim, H.-K.; Lee, K.-S., *Polymer Journal* **2000,** *32* (1), 8-14.
30. Guangming Wang, J. S., Daniel Moses, Alan J. Heeger, *J. Appl. Phys.* **2003,** *93* (10).
31. Li, B.; Santhanam, S.; Schultz, L.; Jeffries-El, M.; Iovu, M. C.; Sauve, G.; Cooper, J.; Zhang, R.; Revelli, J. C.; Kusne, A. G.; Snyder, J. L.; Kowalewski, T.; Weiss, L. E.; McCullough, R. D.; Fedder, G. K.; Lambeth, D. N., *Sens. Actuators, B* **2007,** *123* (2), 651-660.
32. Shaheen, S. E.; Radspinner, R.; Peyghambarian, N.; Jabbour, G. E., *Appl. Phys. Lett.* **2001,** *79* (18), 2996-2998.
33. Coakley, K. M.; McGehee, M. D., *Chem. Mater.* **2004,** *16* (23), 4533-4542.
34. He, R.; Day, T. D.; Krishnamurthi, M.; Sparks, J. R.; Sazio, P. J. A.; Gopalan, V.; Badding, J. V., *Adv. Mater.* **2013,** *25* (10), 1460-1460.
35. Hilberer, A.; Moroni, M.; Gill, R. E.; Brouwer, H. J.; Krasnikov, V. V.; Pham, T. A.; Malliaras, G. G.; Veenstra, S.; Werts, M. P. L.; Van Hutten, P. F.; Hadziioannou, G., *Macromol. Symp.* **1998,** *125* (Organic Light-Emitting Materials and Devices), 99-109.
36. Moliton, A.; Hiorns, R. C., *Polym. Int.* **2004,** *53* (10), 1397-1412.
37. Harrison, W. A., *Elementary Electronic Structure*. Revised Ed. ed.; World Scientific Publishing Company: 2004; p 806.
38. Peierls, R. E., *Quantum Theory of Solids*. Oxford University Press: 2001; p 240.
39. Yannoni, C. S.; Clarke, T. C., *Phys. Rev. Lett.* **1983,** *51* (13), 1191-1193.
40. A. R. Blythe, D. B., *Electrical Poperties of Polymers*. 2nd ed.; Cambridge University Press: New York, NY, 2005.
41. Tolbert, L. M., *Acc. Chem. Res.* **1992,** *25* (12), 561-568.
42. Anslyn, E. V.; Dougherty, D. A., *Modern Physical Organic Chemistry*. University Sciences: Sausalito, CA, 2006; p 1095.
43. Bredas, J. L.; Silbey, R.; Boudreaux, D. S.; Chance, R. R., *J. Am. Chem. Soc.* **1983,** *105* (22), 6555-6559.
44. Bredas, J. L., *J. Chem. Phys.* **1985,** *82* (8), 3808-3811.
45. Lee, Y.-S.; Kertesz, M., *J. Chem. Phys.* **1988,** *88* (4), 2609-2617.
46. Cheng, Y.-J.; Yang, S.-H.; Hsu, C.-S., *Chem. Rev.* **2009,** *109* (11), 5868-5923.
47. Hoogmartens, I.; Adriaensens, P.; Vanderzande, D.; Gelan, J.; Quattrocchi, C.; Lazzaroni, R.; Bredas, J. L., *Macromolecules* **1992,** *25* (26), 7347-7356.
48. Bredas, J. L.; Heeger, A. J.; Wudl, F., *J. Chem. Phys.* **1986,** *85* (8), 4673-4678.
49. Wohlgenannt, M.; Jiang, X. M.; Vardeny, Z. V., *Phys. Rev. B* **2004,** *69* (24), 241204/1-241204/4.
50. Elandaloussi, E. H.; Frere, P.; Richomme, P.; Orduna, J.; Garin, J.; Roncali, J., *J. Am. Chem. Soc.* **1997,** *119* (44), 10774-10784.
51. Klaerner, G.; Miller, R. D., *Macromolecules* **1998,** *31* (6), 2007-2009.

52. Izumi, T.; Kobashi, S.; Takimiya, K.; Aso, Y.; Otsubo, T., *J. Am. Chem. Soc.* **2003,** *125* (18), 5286-5287.
53. Ten Hoeve, W.; Wynberg, H.; Havinga, E. E.; Meijer, E. W., *J. Am. Chem. Soc.* **1991,** *113* (15), 5887-5889.
54. Havinga, E. E.; Rotte, I.; Meijer, E. W.; Hoeve, W. T.; Wynberg, H., *Synth. Met.* **1991,** *41* (1–2), 473-478.
55. Meier, H.; Stalmach, U.; Kolshorn, H., *Acta Polymerica* **1997,** *48* (9), 379-384.
56. Kline, R. J.; McGehee, M. D.; Kadnikova, E. N.; Liu, J.; Frechet, J. M. J.; Toney, M. F., *Macromolecules* **2005,** *38* (8), 3312-3319.
57. Kline, J. R.; McGehee, M. D.; Kadnikova, E. N.; Liu, J.; Frechet, J. M. J., *Adv. Mater.* **2003,** *15* (18), 1519-1522.
58. Brisset, H.; Thobie-Gautier, C.; Jubault, M.; Gorgues, A.; Roncali, J., *J. Chem. Soc., Chem. Commun.* **1994,** *0* (15), 1765-1766.
59. Blanchard, P.; Verlhac, P.; Michaux, L.; Frere, P.; Roncali, J., *Chem. Eur. J.* **2006,** *12* (4), 1244-1255.
60. Brocks, G.; Tol, A., *Synth. Met.* **1996,** *76* (1–3), 213-216.
61. van Mullekom, H. A. M.; Vekemans, J. A. J. M.; Havinga, E. E.; Meijer, E. W., *Mater. Sci. Eng., R* **2001,** *32* (1), 1-40.
62. Kitamura, C.; Tanaka, S.; Yamashita, Y., *Chem. Mater.* **1996,** *8* (2), 570-8.
63. Yu, G.; Gao, J.; Hummelen, J. C.; Wudl, F.; Heeger, A. J., *Science* **1995,** *270* (5243), 1789-1791.
64. Colladet, K.; Fourier, S.; Cleij, T. J.; Lutsen, L.; Gelan, J.; Vanderzande, D.; Nguyen, L. H.; Neugebauer, H.; Sariciftci, S.; Aguirre, A.; Janssen, G.; Goovaerts, E., *Macromolecules* **2007,** *40* (1), 65-72.
65. Yamamoto, T.; Zhou, Z.-h.; Kanbara, T.; Shimura, M.; Kizu, K.; Maruyama, T.; Nakamura, Y.; Fukuda, T.; Lee, B.-L.; et al., *J. Am. Chem. Soc.* **1996,** *118* (43), 10389-10399.
66. Brocks, G.; Tol, A., *J. Phys. Chem.* **1996,** *100* (5), 1838-1846.
67. Kline, R. J.; McGehee, M. D.; Kadnikova, E. N.; Liu, J.; Fréchet, J. M. J., *Adv. Mater.* **2003,** *15* (18), 1519-1522.
68. Kim, J., *Pure Appl. Chem.* **2002,** *74* (11), 2031-2044.
69. Janaki, N. L.; Priyanka, B.; Thomas, A.; Bhanuprakash, K., *J. Phys. Chem. C* **2012**.
70. Yang, L.; Zhou, H.; You, W., *J. Phys. Chem. C* **2010,** *114* (39), 16793-16800.
71. Gadisa, A.; Mammo, W.; Andersson, L. M.; Admassie, S.; Zhang, F.; Andersson, M. R.; Inganäs, O., *Adv. Funct. Mater.* **2007,** *17* (18), 3836-3842.
72. Egbe, D. A. M.; Roll, C. P.; Birckner, E.; Grummt, U.-W.; Stockmann, R.; Klemm, E., *Macromolecules* **2002,** *35* (10), 3825-3837.
73. Szarko, J. M.; Guo, J.; Liang, Y.; Lee, B.; Rolczynski, B. S.; Strzalka, J.; Xu, T.; Loser, S.; Marks, T. J.; Yu, L.; Chen, L. X., *Adv. Mater.* **2010,** *22* (48), 5468-5472.
74. Mike, J. F.; Makowski, A. J.; Mauldin, T. C.; Jeffries-El, M., *J. Poly. Sci. A.* **2010,** *48* (6), 1456-1460.
75. Tsao, H. N.; Cho, D. M.; Park, I.; Hansen, M. R.; Mavrinskiy, A.; Yoon, D. Y.; Graf, R.; Pisula, W.; Spiess, H. W.; Müllen, K., *J. Am. Chem. Soc.* **2011,** *133* (8), 2605-2612.
76. Rakhmanova, S. V.; Conwell, E. M., *Appl. Phys. Lett.* **2000,** *76* (25), 3822-3824.

77. Zuppiroli, L.; Bussac, M. N.; Paschen, S.; Chauvet, O.; Forro, L., *Phys. Rev. B* **1994,** *50* (8), 5196-203.
78. Malliaras, G.; Friend, R., *Physics Today* **2005,** *58* (5), 53-58.
79. Cheng, H.-L.; Lin, W.-Q.; Wu, F.-C., *Appl. Phys. Lett.* **2009,** *94* (22), 223302-3.
80. Krebs, F. C.; Nyberg, R. B.; Jørgensen, M., *Chem. Mater.* **2004,** *16* (7), 1313-1318.
81. Mihailetchi, V. D.; Wildeman, J.; Blom, P. W. M., *Phys. Rev. Lett.* **2005,** *94* (12), 126602.
82. Bernius, M. T.; Inbasekaran, M.; O'Brien, J.; Wu, W., *Adv. Mater.* **2000,** *12* (23), 1737-1750.
83. Yan, H.; Chen, Z.; Zheng, Y.; Newman, C.; Quinn, J. R.; Dotz, F.; Kastler, M.; Facchetti, A., *Nature* **2009,** *457* (7230), 679-686.
84. Li, G.; Shrotriya, V.; Huang, J.; Yao, Y.; Moriarty, T.; Emery, K.; Yang, Y., *Nature Mater.* **2005,** *4* (11), 864-868.
85. Park, Y. D.; Park, J. K.; Seo, J. H.; Yuen, J. D.; Lee, W. H.; Cho, K.; Bazan, G. C., *Adv. Energy Mater.* **2011,** *1* (1), 63-67.
86. Ponomarenko, S. A.; Kirchmeyer, S.; Elschner, A.; Huisman, B. H.; Karbach, A.; Drechsler, D., *Adv. Funct. Mater.* **2003,** *13* (8), 591-596.
87. Wang, G.; Swensen, J.; Moses, D.; Heeger, A. J., *J. Appl. Phys.* **2003,** *93* (10), 6137-6141.
88. Saeki, A.; Ohsaki, S.-i.; Koizumi, Y.; Seki, S.; Tagawa, S., *Synth. Met.* **2009,** *159* (17-18), 1800-1803.
89. Siddiqui, A. S.; Wilson, E. G., *J. Phys. C.* **1979,** *12* (20), 4237.
90. Jacobson, M. Z.; Masters, G. M., *Science* **2001,** *293* (5534), 1438-1438.
91. Pacala, S.; Socolow, R., *Science* **2004,** *305* (5686), 968-972.
92. Fthenakis, V.; Mason, J. E.; Zweibel, K., *Energy Policy* **2009,** *37* (2), 387-399.
93. Perez, R.; Perez, M., *The IEA SHC Solar Update* **2009,** *50*, 2.
94. Hung, M.-C.; Liao, J.-L.; Chen, S.-A.; Chen, S.-H.; Su, A.-C., *J. Am. Chem. Soc.* **2005,** *127* (42), 14576-14577.
95. Gunes, S.; Neugebauer, H.; Sariciftci, N. S., *Chem. Rev.* **2007,** *107* (4), 1324-1338.
96. Ameri, T.; Dennler, G.; Lungenschmied, C.; Brabec, C. J., *Energy Environ. Sci.* **2009,** *2* (4), 347-363.
97. Yang, T.; Wang, M.; Duan, C.; Hu, X.; Huang, L.; Peng, J.; Huang, F.; Gong, X., *Energy Environ. Sci.* **2012,** *5* (8), 8208-8214.
98. He, Z.; Zhong, C.; Su, S.; Xu, M.; Wu, H.; Cao, Y., *Nature Photon.* **2012,** *6* (9), 591-595.
99. Chen, H.-C.; Chen, Y.-H.; Liu, C.-C.; Chien, Y.-C.; Chou, S.-W.; Chou, P.-T., *Chem. Mater.* **2012,** *24* (24), 4766-4772.
100. Green, M. A.; Emery, K.; Hishikawa, Y.; Warta, W.; Dunlop, E. D., *Progress in Photovoltaics: Research and Applications* **2012,** *20* (5), 606-614.
101. http://www.heliatek.com/wp-content/uploads/2013/01/130116_PR_Heliatek_achieves_record_cell_effiency_for_OPV.pdf.
102. Marks, R. N.; Halls, J. J. M.; Bradley, D. D. C.; Friend, R. H.; Holmes, A. B., *J. Phys.: Condes. Matter* **1994,** *6* (7), 1379.
103. Hoppe, H.; Sariciftci, N. S., *J. Mater. Res.* **2004,** *19* (07), 1924-1945.

104. Heeger, A. J.; Sariciftci, N. S.; Namdas, E. B., *Semiconducting and Metallic Polymers*. Oxford University Press: 2010; p 278.
105. Gregg, B. A., *J. Phys. Chem. B* **2003,** *107* (20), 4688-4698.
106. Wöhrle, D.; Meissner, D., *Adv. Mater.* **1991,** *3* (3), 129-138.
107. Tang, C. W., *Appl. Phys. Lett.* **1986,** *48* (2), 183-185.
108. Peumans, P.; Yakimov, A.; Forrest, S. R., *J. Appl. Phys.* **2003,** *93* (7), 3693-3723.
109. Halls, J. J. M.; Pichler, K.; Friend, R. H.; Moratti, S. C.; Holmes, A. B., *Appl. Phys. Lett.* **1996,** *68* (22), 3120-3122.
110. Halls, J. J. M.; Cornil, J.; dos Santos, D. A.; Silbey, R.; Hwang, D. H.; Holmes, A. B.; BrÈdas, J. L.; Friend, R. H., *Phys. Rev. B* **1999,** *60* (8), 5721.
111. Haugeneder, A.; Neges, M.; Kallinger, C.; Spirkl, W.; Lemmer, U.; Feldmann, J.; Scherf, U.; Harth, E.; Gügel, A.; Müllen, K., *Phys. Rev. B* **1999,** *59* (23), 15346-15351.
112. Theander, M.; Yartsev, A.; Zigmantas, D.; Sundström, V.; Mammo, W.; Andersson, M. R.; Inganäs, O., *Phys. Rev. B* **2000,** *61* (19), 12957-12963.
113. Yu, G.; Heeger, A. J., *J. Appl. Phys.* **1995,** *78* (7), 4510-4515.
114. Halls, J. J. M.; Walsh, C. A.; Greenham, N. C.; Marseglia, E. A.; Friend, R. H.; Moratti, S. C.; Holmes, A. B., *Nature* **1995,** *376*, 498-500.
115. Granstrom, M.; Petritsch, K.; Arias, A. C.; Lux, A.; Andersson, M. R.; Friend, R. H., *Nature* **1998,** *395* (6699), 257-260.
116. Sariciftci, N. S.; Smilowitz, L.; Heeger, A. J.; Wudl, F., *Science* **1992,** *258* (5087), 1474-1476.
117. Allemand, P. M.; Koch, A.; Wudl, F.; Rubin, Y.; Diederich, F.; Alvarez, M. M.; Anz, S. J.; Whetten, R. L., *J. Am. Chem. Soc.* **1991,** *113* (3), 1050-1051.
118. Brabec, C. J.; Zerza, G.; Cerullo, G.; De Silvestri, S.; Luzzati, S.; Hummelen, J. C.; Sariciftci, S., *Chem. Phys. Lett.* **2001,** *340* (3–4), 232-236.
119. Neugebauer, H.; Brabec, C. J.; Hummelen, J. C.; Janssen, R. A. J.; Sariciftci, N. S., *Synth. Met.* **1999,** *102* (1–3), 1002-1003.
120. Neugebauer, H.; Brabec, C.; Hummelen, J. C.; Sariciftci, N. S., *Sol. Energy Mater. Sol. Cells* **2000,** *61* (1), 35-42.
121. Singh, T. B.; Marjanović, N.; Matt, G. J.; Günes, S.; Sariciftci, N. S.; Montaigne Ramil, A.; Andreev, A.; Sitter, H.; Schwödiauer, R.; Bauer, S., *Organic Electronics* **2005,** *6* (3), 105-110.
122. Hummelen, J. C.; Knight, B. W.; LePeq, F.; Wudl, F.; Yao, J.; Wilkins, C. L., *J. Org. Chem.* **1995,** *60* (3), 532-538.
123. Wienk, M. M.; Kroon, J. M.; Verhees, W. J. H.; Knol, J.; Hummelen, J. C.; van Hal, P. A.; Janssen, R. A. J., *Angew, Chem. Int. Ed.* **2003,** *42* (29), 3371-3375.
124. Arbogast, J. W.; Foote, C. S., *J. Am. Chem. Soc.* **1991,** *113* (23), 8886-8889.
125. Yao, Y.; Shi, C.; Li, G.; Shrotriya, V.; Pei, Q.; Yang, Y., *Appl. Phys. Lett.* **2006,** *89* (15), 153507-3.
126. Yang, X.; Loos, J., *Macromolecules* **2007,** *40* (5), 1353-1362.
127. van Duren, J. K. J.; Yang, X.; Loos, J.; Bulle-Lieuwma, C. W. T.; Sieval, A. B.; Hummelen, J. C.; Janssen, R. A. J., *Adv. Funct. Mater.* **2004,** *14* (5), 425-434.
128. Jonkheijm, P.; Van Duren, J. K. J.; Kemerink, M.; Janssen, R. A. J.; Schenning, A. P. H. J.; Meijer, E. W., *Macromolecules* **2006,** *39* (2), 784-788.

129. Byun, M.; Laskowski, R. L.; He, M.; Qiu, F.; Jeffries-El, M.; Lin, Z. Q., *Soft Matter* **2009,** *5* (8), 1583-1586.
130. Lee, J. K.; Ma, W. L.; Brabec, C. J.; Yuen, J.; Moon, J. S.; Kim, J. Y.; Lee, K.; Bazan, G. C.; Heeger, A. J., *J. Am. Chem. Soc.* **2008,** *130* (11), 3619-3623.
131. Hoven, C. V.; Dang, X.-D.; Coffin, R. C.; Peet, J.; Nguyen, T.-Q.; Bazan, G. C., *Adv. Mater.* **2010,** *22* (8), E63–E66.
132. Hammer, B. A. G.; Bokel, F. A.; Hayward, R. C.; Emrick, T., *Chem. Mater.* **2011,** *23* (18), 4250-4256.
133. Botiz, I.; Darling, S. B., *Macromolecules* **2009,** *42* (21), 8211-8217.
134. Lindner, S. M.; Hüttner, S.; Chiche, A.; Thelakkat, M.; Krausch, G., *Angew, Chem. Int. Ed.* **2006,** *45* (20), 3364-3368.
135. Al-Dmour, H.; Taylor, D. M.; Cambridge, J. A., *J. Phys. D.* **2007,** *40* (17), 5034-5038.
136. Stefopoulos, A. A.; Chochos, C. L.; Prato, M.; Pistolis, G.; Papagelis, K.; Petraki, F.; Kennou, S.; Kallitsis, J. K., *Chem. Eur. J.* **2008,** *14* (28), 8715-8724.
137. Goodman, M. D.; Xu, J.; Wang, J.; Lin, Z., *Chem. Mater.* **2009,** *21* (5), 934-938.
138. Yang, C.; Lee, J. K.; Heeger, A. J.; Wudl, F., *J. Mater. Chem.* **2009,** *19* (30), 5416-5423.
139. Lee, J. U.; Cirpan, A.; Emrick, T.; Russell, T. P.; Jo, W. H., *J. Mater. Chem.* **2009,** *19* (10), 1483-1489.
140. Lee, J. U.; Jung, J. W.; Emrick, T.; Russell, T. P.; Jo, W. H., *J. Mater. Chem.* **2010,** *20* (16), 3287-3294.
141. Kim, J. B.; Allen, K.; Oh, S. J.; Lee, S.; Toney, M. F.; Kim, Y. S.; Kagan, C. R.; Nuckolls, C.; Loo, Y.-L., *Chem. Mater.* **2010,** *22* (20), 5762-5773.
142. Zhou, H.; Yang, L.; Stoneking, S.; You, W., *ACS Appl. Mater. Interfaces* **2010,** *2* (5), 1377-1383.
143. He, Z.; Zhong, C.; Huang, X.; Wong, W.-Y.; Wu, H.; Chen, L.; Su, S.; Cao, Y., *Adv. Mater.* **2011,** *23* (40), 4636-4643.
144. Kim, M.-S.; Kim, B.-G.; Kim, J., *ACS Appl. Mater. Interfaces* **2009,** *1* (6), 1264-1269.
145. Peet, J.; Kim, J. Y.; Coates, N. E.; Ma, W. L.; Moses, D.; Heeger, A. J.; Bazan, G. C., *Nature Mater.* **2007,** *6* (7), 497-500.
146. Kim, Y.; Cook, S.; Tuladhar, S. M.; Choulis, S. A.; Nelson, J.; Durrant, J. R.; Bradley, D. D. C.; Giles, M.; McCulloch, I.; Ha, C.-S.; Ree, M., *Nature Mater.* **2006,** *5* (3), 197-203.
147. Facchetti, A., *Chem. Mater.* **2011,** *23* (3), 733-758.
148. Kline, R. J.; DeLongchamp, D. M.; Fischer, D. A.; Lin, E. K.; Richter, L. J.; Chabinyc, M. L.; Toney, M. F.; Heeney, M.; McCulloch, I., *Macromolecules* **2007,** *40* (22), 7960-7965.
149. McCullough, R. D.; Tristam-Nagle, S.; Williams, S. P.; Lowe, R. D.; Jayaraman, M., *J. Am. Chem. Soc.* **1993,** *115*, 4910-4911.
150. Shi, Q.; Fan, H.; Liu, Y.; Chen, J.; Ma, L.; Hu, W.; Shuai, Z.; Li, Y.; Zhan, X., *Macromolecules* **2011,** *44* (11), 4230-4240.
151. Yiu, A. T.; Beaujuge, P. M.; Lee, O. P.; Woo, C. H.; Toney, M. F.; Fréchet, J. M. J., *J. Am. Chem. Soc.* **2011,** *134* (4), 2180-2185.

152. Thompson, B. C.; Kim, B. J.; Kavulak, D. F.; Sivula, K.; Mauldin, C.; Frechet, J. M. J., *Macromolecules* **2007,** *40* (21), 7425-7428.
153. Roncali, J., *Chem. Rev.* **1997,** *97* (1), 173-205.
154. Brabec, C. J.; Cravino, A.; Meissne, D.; Sariciftci, N. S.; Fromherz, T.; Rispens, M. T.; Sanchez, L.; Hummelen, J. C., *Adv. Funct. Mater.* **2001,** *11* (5), 374-380.
155. Lenes, M.; Wetzelaer, G.-J. A. H.; Kooistra, F. B.; Veenstra, S. C.; Hummelen, J. C.; Blom, P. W. M., *Adv. Mater.* **2008,** *20* (11), 2116-2119.
156. Blouin, N.; Michaud, A.; Gendron, D.; Wakim, S.; Blair, E.; Neagu-Plesu, R.; Belletete, M.; Durocher, G.; Tao, Y.; Leclerc, M., *J. Am. Chem. Soc.* **2008,** *130* (2), 732-742.
157. Scharber, M.; Mühlbacher, D.; Koppe, M.; Denk, P.; Waldauf, C.; Heeger, A.; Brabec, C., *Adv. Mater.* **2006,** *18* (6), 789-794.
158. Kooistra, F. B.; Knol, J.; Kastenberg, F.; Popescu, L. M.; Verhees, W. J. H.; Kroon, J. M.; Hummelen, J. C., *Org. Lett.* **2007,** *9* (4), 551-554.
159. Meng, X.; Zhao, G.; Xu, Q.; Tan, Z. a.; Zhang, Z.; Jiang, L.; Shu, C.; Wang, C.; Li, Y., *Adv. Funct. Mater.* **2013**, 1-6.
160. Huo, L.; Hou, J., *Polym. Chem.* **2011,** *2* (11), 2453-2461.
161. Pan, H.; Li, Y.; Wu, Y.; Liu, P.; Ong, B. S.; Zhu, S.; Xu, G., *J. Am. Chem. Soc.* **2007,** *129* (14), 4112-4113.
162. Hou, J. H.; Park, M. H.; Zhang, S. Q.; Yao, Y.; Chen, L. M.; Li, J. H.; Yang, Y., *Macromolecules* **2008,** *41*, 6012.
163. Liang, Y.; Xu, Z.; Xia, J.; Tsai, S.-T.; Wu, Y.; Li, G.; Ray, C.; Yu, L., *Adv. Mater.* **2010,** *22* (20), E135-E138.
164. Chen, H.-Y.; Hou, J.; Zhang, S.; Liang, Y.; Yang, G.; Yang, Y.; Yu, L.; Wu, Y.; Li, G., *Nature Photon.* **2009,** *3* (11), 649-653.
165. Zhou, H.; Yang, L.; Stuart, A. C.; Price, S. C.; Liu, S.; You, W., *Angew, Chem. Int. Ed.* **2011,** *50* (13), 2995-2998.
166. Aggarwal, N.; MacDowell, D. W. H., *Organic Preparations and Procedures International* **1979,** *11* (5), 247-249.
167. Koßmehl, G.; Beimling, P.; Manecke, G., *Die Makromolekulare Chemie* **1983,** *184* (3), 627-650.
168. Citterio, A.; Sebastiano, R.; Maronati, A.; Viola, F.; Farina, A., *Tetrahedron* **1996,** *52* (41), 13227-13242.
169. Beimling, P.; Koßmehl, G., *Chemische Berichte* **1986,** *119* (10), 3198-3203.
170. Huo, L.; Zhang, S.; Guo, X.; Xu, F.; Li, Y.; Hou, J., *Angew, Chem. Int. Ed.* **2011,** *50* (41), 9697-9702.
171. Duan, R.; Ye, L.; Guo, X.; Huang, Y.; Wang, P.; Zhang, S.; Zhang, J.; Huo, L.; Hou, J., *Macromolecules* **2012,** *45* (7), 3032-3038.
172. Gidron, O.; Dadvand, A.; Sheynin, Y.; Bendikov, M.; Perepichka, D. F., *J. Mater. Chem. C* **2011,** *1* (28), 4358-4367.
173. Gidron, O.; Dadvand, A.; Sheynin, Y.; Bendikov, M.; Perepichka, D. F., *Chem. Commun.* **2011,** *47* (7), 1976-1978.
174. Gidron, O.; Diskin-Posner, Y.; Bendikov, M., *J. Am. Chem. Soc.* **2010,** *132* (7), 2148-2150.
175. Liang, Z.; Ma, S.; Yu, J.; Xu, R., *Tetrahedron* **2007,** *63* (52), 12877-12882.

176. Tsuji, H.; Mitsui, C.; Ilies, L.; Sato, Y.; Nakamura, E., *J. Am. Chem. Soc.* **2007,** *129* (39), 11902-11903.
177. Li, H.; Tang, P.; Zhao, Y.; Liu, S.-X.; Aeschi, Y.; Deng, L.; Braun, J.; Zhao, B.; Liu, Y.; Tan, S.; Meier, W.; Decurtins, S., *J. Poly. Sci. A.* **2012,** *50* (14), 2935–2943.
178. Huo, L.; Huang, Y.; Fan, B.; Guo, X.; Jing, Y.; Zhang, M.; Li, Y.; Hou, J., *Chem. Commun.* **2012,** *48* (27), 3318-3320.
179. Yue, D.; Yao, T.; Larock, R. C., *J. Org. Chem.* **2005,** *70* (25), 10292-10296.
180. Kobilka, B. M.; Dubrovskiy, A. V.; Ewan, M. D.; Tomlinson, A. L.; Larock, R. C.; Chaudhary, S.; Jeffries-EL, M., *Chem. Commun.* **2012,** *48* (71), 8919-8921.
181. Wang, Y.; Parkin, S. R.; Watson, M. D., *Org. Lett.* **2008,** *10* (20), 4421-4424.
182. Ebata, H.; Miyazaki, E.; Yamamoto, T.; Takimiya, K., *Org. Lett.* **2007,** *9* (22), 4499-4502.
183. Sashida, H.; Sadamori, K.; Tsuchiya, T., *Synth. Commun.* **1998,** *28* (4), 713-727.
184. Leenen, M. A. M.; Vian, F.; Cucinotta, F.; Pisula, W.; Thiem, H.; Anselmann, R.; De Cola, L., *Macromol. Chem. Phys.* **2010,** *211* (21), 2286-2291.
185. Saadeh, H. A.; Lu, L.; He, F.; Bullock, J. E.; Wang, W.; Carsten, B.; Yu, L., *ACS Macro Lett.* **2012,** *1* (3), 361-365.
186. Takimiya, K.; Kunugi, Y.; Konda, Y.; Niihara, N.; Otsubo, T., *J. Am. Chem. Soc.* **2004,** *126* (16), 5084-5085.
187. Takimiya, K.; Konda, Y.; Ebata, H.; Niihara, N.; Otsubo, T., *J. Org. Chem.* **2005,** *70* (25), 10569-10571.
188. Kaur, M.; Seul Yang, D.; Shin, J.; Wan Lee, T.; Choi, K.; Ju Cho, M.; Hoon Choi, D., *Chem. Commun.* **2013,** *49* (48), 5495-5497.
189. Suess, H. E.; Urey, H. C., *Reviews of Modern Physics* **1956,** *28* (1), 53-74.

CHAPTER 2

Synthesis of 3,7-Diiodo-2,6-di(thiophen-2-yl)benzo[1,2-*b*:4,5-*b*']difurans: Functional Building Blocks for the Design of New Conjugated Polymers.

Chemical Communications **2012**, 48, 8919.
DOI: 10.1039/C2CC34070D

Brandon M. Kobilka,[a] Anton V. Dubrovskiy,[a] Monique D. Ewan,[a] Aimée L. Tomlinson,[b] Richard C. Larock,[a] Sumit Chaudhary[c] and Malika Jeffries-EL[a]*

[a]Department of Chemistry, Iowa State University, Ames, IA 50011
[b] Department of Chemistry, North Georgia College & State University, Dalhonega, GA 30597
[c] Department of Electrical Engineering, Iowa State University, Ames, IA 50011

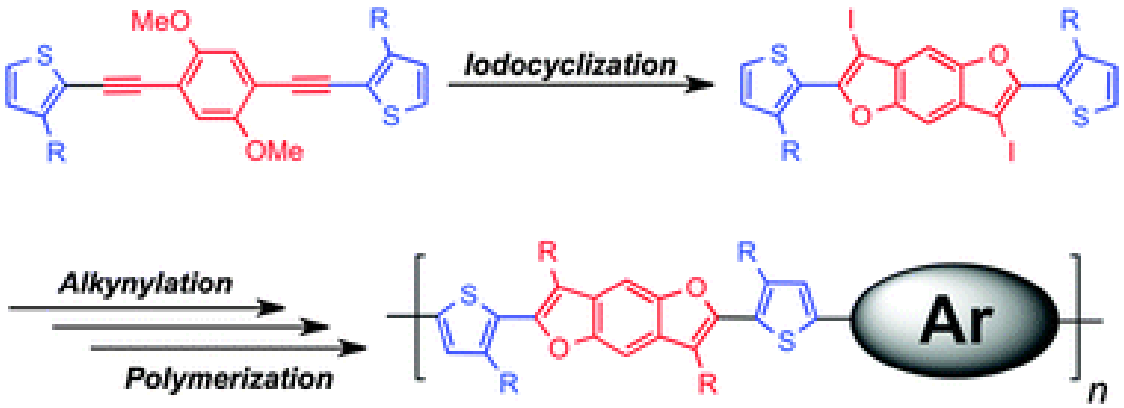

2.1 ABSTRACT

3,7-Diiodo-2,6-di(thiophen-2-yl)benzo[1,2-*b*:4,5-*b*']difurans are efficiently prepared by an iodine-promoted double cyclization. This new heterocyclic core is readily modified by the attachment of alkyl chains for improved solubility. The use of these compounds for the synthesis of new conjugated polymers is also reported.

2.2 INTRODUCTION

Organic semiconductors are finding widespread use as replacements for their inorganic counterparts in a range of applications, including field effect transistors (OFET)s, light-emitting diodes (OLED)s, and photovoltaic cells (OPVC)s.[1-3] These materials offer advantages in the form of facile device fabrication via solution-based techniques and energy levels that can be tuned by chemical synthesis. Tuning can be accomplished through the synthesis of materials with alternating electron-donating and electron-accepting moieties.[4, 5] Among electron-donating building blocks, benzo[1,2-*b*:4,5-*b*']dithiophene (BDT) is particularly promising, due to its planar conjugated structure that facilitates π–π stacking, leading to higher hole mobility.[6-9] Bulk heterojunction photovoltaic cells (BHJ-PVC)s using BDT copolymers as donors have achieved power-conversion efficiencies (PCE)s up to 7.4%.[8]

Recently, furan-containing molecules have been explored for the design of organic semiconductors.[10-13] Furan is an attractive alternative to thiophene, since it is isoelectronic, while possessing a Dewar resonance energy of 18.0 kJ mol^{-1}, which is less aromatic than that of thiophene (27.2 kJ mol^{-1}).[14] Thus, replacing thiophene with furan is expected to favor the formation of quinoid structures, leading to a reduction in the band gap of the resulting materials. Although benzo[1,2-*b*:4,5-*b*']difurans (BDF)s are known in the literature, the lack of methods for the synthesis of substituted derivatives has prevented their widespread use.[15-19] Encouraged by some of our earlier work on iodocyclization, we explored this approach for synthesizing BDFs.[20] Herein, we report the synthesis of functional BDFs and their polymerization with isoindigo, an electron-deficient moiety that has been used in several polymers with high PCE, when used as donor materials in BHJ-PVCs.[21, 22]

2.3 RESULTS AND DISCUSSION

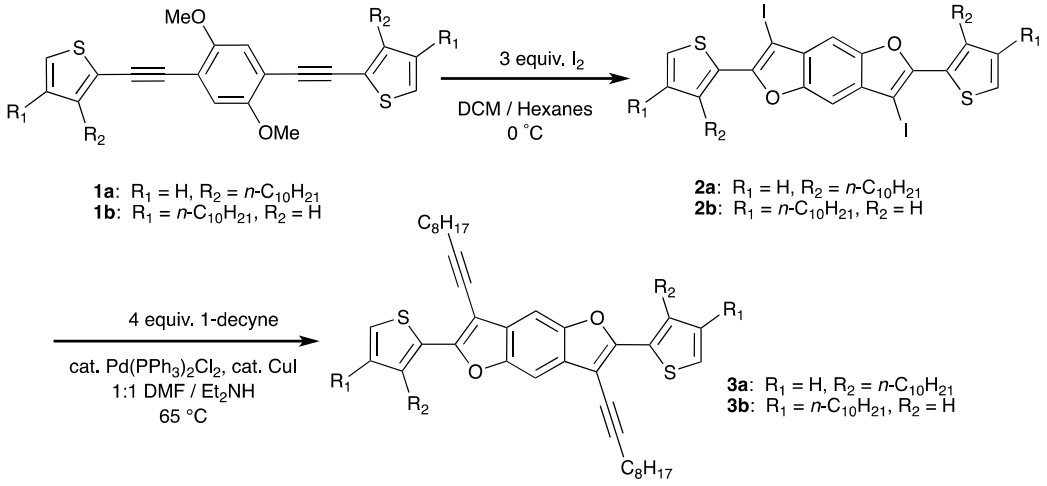

Scheme 2.1. Synthesis of 3,7-diiodo-2,6-di(thiophen-2-yl)benzo[1,2-*b*:4,5-*b*']difurans **2a** and **2b** and their subsequent alkynylation.

Our synthetic route to the BDFs is shown in Scheme 2.1. This approach offers several benefits, including: 1) the use of easily prepared starting materials and inexpensive catalysts; 2) the enhanced solubility afforded by the alkyl chains on the flanking thiophene rings; and 3) the opportunity to generate a variety of new substituted BDFs from a common intermediate via cross-coupling reactions. Compounds **1a** and **1b** have been prepared by the Sonogashira cross-coupling of 1,4-dibromo-2,5-dimethoxybenzene and either 2-ethynyl-3-decyl-thiophene or 2-bromo-3-decyl-5-ethynylthiophene (see Supplementary Information, SI). The iodine-induced double cyclization of compounds **1a** and **1b** afforded 3,7-diiodo-2,6-di(thiophen-2-yl)benzo[1,2-*b*:4,5-*b*']difurans **2a** and **2b** in yields of 70 and 82% respectively.[20] Both regioisomers are easily purified by recrystallization. The Sonogashira cross-coupling reactions of **2a** and **2b** with 1-decyne affords **3a** and **3b** in yields of 96% and 92% respectively. Crystals of **2a** suitable for X-Ray analysis were obtained by recrystallization. Detailed crystallographic data can be found in the SI. In addition to confirming the identity of this new compound, the X-ray analysis indicates that the BDF ring system is planar, which is beneficial to promoting efficient π-stacking and improving the charge transport of materials derived from this intermediate. The torsion angles between the BDF and thiophene rings are approximately 175.3°.

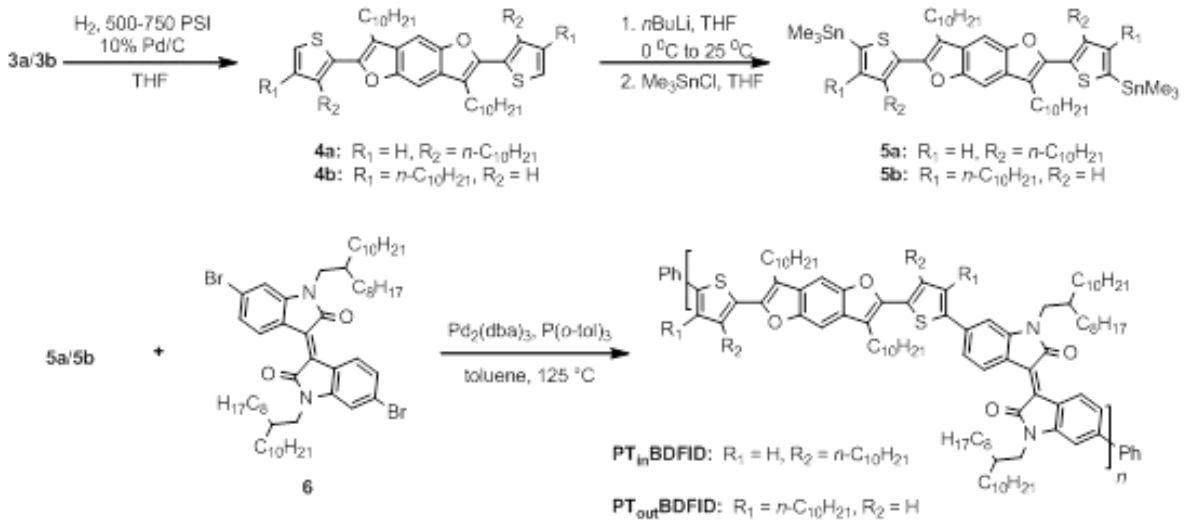

Scheme 2.2. Modification and polymerization of the 2,6-di(thiophen-2-yl)benzo[1,2-*b*:4,5-*b*']difurans.

The remaining synthetic steps to the desired polymers are shown in Scheme 2.2. The hydrogenation of the alkynyl BDFs **3a** and **3b** afforded the alkylated derivatives **4a** and **4b** in yields of ~95% each. Subsequent stannylation afforded **5a** and **5b** in yields of ~94% each. The Stille cross-coupling polymerization of **5a** or **5b** with 6,6'-dibromo-*N*,*N*'-(2-octyldodecanyl)-isoindigo **6**[23] afforded the polymers **PT$_{in}$BDFID** and **PT$_{out}$BDFID** in excellent yields after purification by Soxhlet extraction with methanol, followed by acetone, to remove residual catalyst and low molecular weight materials. Of the catalysts evaluated, $Pd_2(dba)_3$ gave the best results (Table 2.1). The polymers are soluble in standard organic solvents, such as THF and chloroform, at room temperature. Monomer **5a** consistently produced polymers with higher molecular weights. Presumably, this is due to the reduced steric hindrance at the 2- and 2'-positions of the BDF moiety.

We anticipated that the differences in the regiochemistry of the BDFs would result in differences in the optical spectra. Compounds **2b**, **3b**, and **4b**, with the alkyl substituents on the 4 and 4' positions of the thiophene rings, have less interaction with the pseudo-peri iodine, alkyne, or alkane substituents, and exhibit greater vibrational structure than analogs **2a**-**4a** (see SI). Arguably, this is due to the greater rigidity of the overall aromatic chromophore, *i.e.* reduction of out-of-plane rotation of the thiophene moieties. The dramatically different band shapes between the members of each pair mean that comparisons

of λ_{max} between "a" and "b" analogs is not particularly meaningful. However, the leading edge of the onset of strong S1 absorption for each "a-b" pair of compounds extrapolates to a very similar wavelength, with each pair distinct from the other two. This reflects the intrinsic electronic similarities between each pair of isomers.

Table 2.1. Reaction conditions and molecular weight data for PTBDFIDs.

Polymer[a]	Catalyst	Yield (%)[c]	M_w[b]	M_w/M_n	DPn
PT_{out}BDFID	$Pd(PPh_3)_4$	82	20,500	1.3	12
PT_{out}BDFID	$Pd_2(dba)_3$	86	33,100	1.9	19
PT_{in}BDFID	$Pd(PPh_3)_4$	79	35,000	1.9	21
PT_{in}BDFID	$Pd_2(dba)_3$	84	76,200	2.3	45

[a] [monomer] = 0.2 M in toluene, and Pd catalyst loading = 2 mol%. [b] Molecular weight data was obtained by GPC (see ESI). [c] Isolated yield.

As expected, the additional conjugation of the alkynyl groups of **3a** and **3b** produces a red shift in the onset of absorption and λ_{max} of the S1 absorption band. Compared to the alkyl substituents in compounds **4a** and **4b**, the iodo substituents in **2a** and **2b** induce a red-shift – albeit smaller than that of the alkyne – consistent with a reduction in conjugation length and orbital overlap (see SI). The UV–vis absorption spectra of **PT_{in}BDFID** and **PT_{out}BDFID** in solution and in thin films are shown in Figure 2.1 and the optical and electronic properties are summarized in Table 2.2. Both polymers exhibit two main absorption bands. The high energy bands can be attributed to the π-π* transition, whereas the low energy bands are due to intramolecular charge transfer between the donor and acceptor units. In solution, the λ_{max} of **PT_{in}BDFID**'s low energy band is red-shifted 18 nm relative to **PT_{out}BDFID**, whereas the λ_{max} of **PT_{in}BDFID's** high energy band is blue-shifted 21 nm relative to **PT_{out}BDFID**. In the solid state, the λ_{max} for the low energy band of **PT_{out}BDFID** is blue-shifted 41 nm relative to **PT_{in}BDFID** and the difference in the high energy band is only 12 nm. These results suggest that **PT_{out}BDFID** has a more twisted backbone than **PT_{in}BDFID**. The optimized geometries obtained for isoindigo/BDF oligomers calculated using density functional theory also support the notion that **PT_{out}BDFID** has a more twisted structure (see SI). The similarity

PT_{out}BDFID's solution and film spectra indicates the steric interaction between the out facing side chain and the isoindigo group inhibits planarization.

Table 2.2. Electronic and optical properties of PTBDFIDs.

Polymer	Media	λ_{max} (nm)	HOMO[a] (eV)	LUMO[b] (eV)	E_g^{opt} (eV)[c]	E_g^{EC} (eV)[d]
PT_{out}BDFID	THF	399, 582				
PT_{out}BDFID	Film	403, 612	-5.7	-3.8	1.7	1.9
PT_{in}BDFID	THF	378, 600				
PT_{in}BDFID	Film	415, 653	-5.7	-3.8	1.6	1.9

[a] HOMO= -(E_{onset}^{ox} + 5.1) (eV).. [b] LUMO = -(E_{onset}^{red} + 5.1) (eV). [c] Estimated from the optical absorption edge. [d] Onset of potentials (vs Fc).

The electrochemical properties of the polymers have been investigated by cyclic voltammetry (CV). Both polymers exhibit measureable and reproducible oxidation and reduction processes. The electrochemical band gaps are both approximately 0.3 eV higher than the optical band gaps (E_g^{opt}) determined via the tangent lines on the absorption spectra. This difference can be attributed to the electron injection barrier in the electrochemistry.[24, 25] The HOMO and LUMO values of both polymers are similar to those reported previously for **PBDT-OIO**, a related terpolymer of **6**, thiophene and BDT (LUMO -3.91 eV and HOMO -5.74 eV).[26] Unfortunately, we cannot arrive at a conclusion regarding the relative donor strength of BDF, as the BDT group had two electron-donating alkoxy groups on the central benzene ring. Although, the LUMO values are less than 0.3 eV lower than those of the $PC_{61}BM$ acceptor, impeding charge transfer the HOMO level of both polymers are deep enough to ensure air stability, while providing for good open-circuit voltage (V_{oc}).[27, 28]

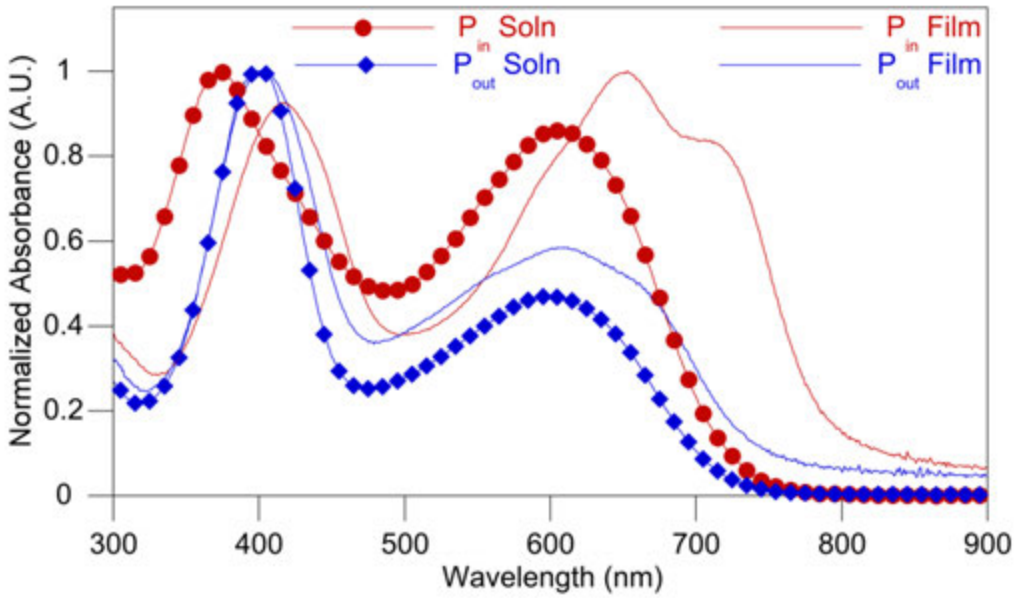

Fig. 2.1. UV-vis absorption of the polymers in solution and thin films.

The performance of both polymers in BHJ-PVCs was evaluated using $PC_{61}BM$ as the electron acceptor with a device configuration of indium tin oxide (ITO)/poly(3,4-ethylene dioxythiophene):polystyrene sulfonate (PEDOT:PSS)/polymer:$PC_{61}BM$(1:4, w/w)/LiF/Al. The active layer processing conditions were chosen to yield a layer thickness less than 100 nm. In general (for P3HT systems), thicker layers (~200 nm) are better, because they absorb more light. However, since new generation donor/acceptor polymer films do not have a long-range order like P3HT, thicker layers tend to have increased recombination due to hole traps, and thus lower efficiencies.[29] The fabrication conditions and PVC parameters (fill factor (FF), short-circuit current density (J_{sc}) and V_{oc}) are summarized in Table 2.3. The current-voltage (*I-V*) characteristics of our devices are shown in Figure 2.2.

Table 2.3. Photovoltaic performance of **P_{in}BDFID** and **P_{out}BDFID** with PCBM.

Polymer	V_{OC} (V)	I_{SC} (mA)	J_{SC} (mA/cm^2)	FF (%)	PCE (%)
P_{in}BDFID	0.7366	0.208	-1.66	48.6	0.590
P_{out}BDFID	0.6410	0.164	-1.306	36	0.301

Polymers films were prepared from solutions in *o*-DCB 10 mg/mL.

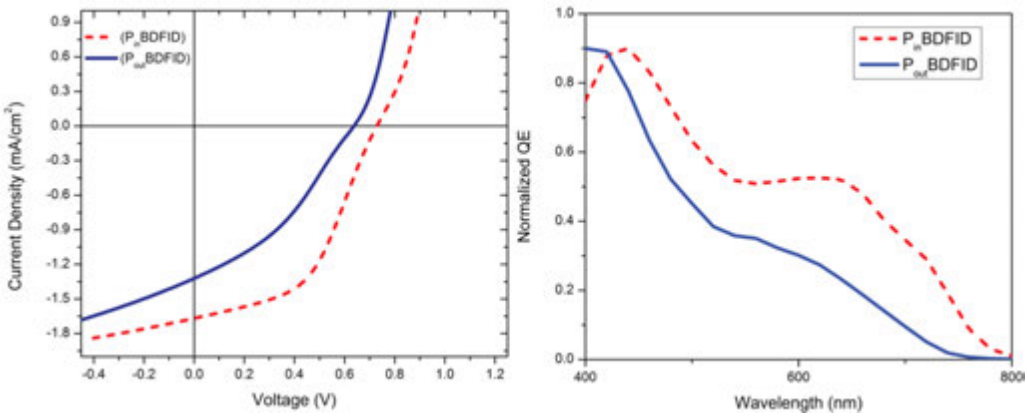

Fig. 2.2. Current-voltage characteristics of polymer PVCs (left). Normalized external quantum efficiency vs. wavelength curve of the PVCs (right).

Overall, **PT$_{in}$BDFID** PVCs performed better than **PT$_{out}$BDFID**-based devices in all categories. This is most likely an effect of the polymer's planarity on morphology, and is currently being evaluated further. Although the performance of these devices is lower than other conjugated polymers, this is our first attempt toward fabricating PVCs from these materials. We note that the performance of most new systems can be dramatically improved by the optimization of processing parameters.

2.4 CONCLUSIONS

In conclusion, we report the efficient synthesis of novel electron-rich building blocks based on 2,6-di(thiophen-2-yl)benzo[1,2-*b*:4,5-*b*']difurans and their use for the development of donor-acceptor copolymers. The highlights of this work are the overall high yields of the reactions and the versatility of the synthetic approach. The energy levels of the new polymers are suitable for use as donor materials in BHJ-PVCs. Preliminary device studies have shown good V_{oc} and FF, but low overall performance. We are currently working to optimize the device performance in addition to developing new materials based on BDFs.

2.5 EXPERIMENTAL

Detailed descriptions of the synthetic, analytical and device fabrication procedures and methods can be found in the supporting information section.

2.6 ACKNOWLEDGMENTS

Support for this work has been provided by Iowa State University (ISU) and the 3M Foundation. We thank Dr. Kamel Harrata and the ISU mass spectroscopy laboratory and Dr. Arkady Ellern and the ISU X-ray crystallography facility for analyses. The PVCs were fabricated at the ISU Institute for Physical Research and Technology's Microelectronics Research Center.

2.7 SUPPORTING INFORMATION

2.7.1 General Methods

All reactions were carried out at ambient atmosphere and temperature (18-25 °C) unless otherwise noted. Tetrahydrofuran and toluene were dried using an Innovative Technologies solvent purification system. Solvents used for Pd-catalyzed reactions were deoxygentated prior to use by bubbling a stream of argon through the stirred solvent for 30-60 minutes. Trimethylsilyl acetylene was purchased from GFS chemicals. Bis(triphenylphosphine)palladium(II) dichloride was purchased from Oakwood Products, Inc. All other chemicals were purchased from Sigma-Aldrich and used without further purification. 3-Decylthiophene[30], 2,5-diido-1,4-dimethoxybenzene[31] and 6,6'-dibromo-*N*,*N*'-(2-octyldodecanyl)isoindigo **6**[32, 33] were synthesized according to literature procedures. Nuclear magnetic resonance (NMR) spectra were carried out in $CDCl_3$ and recorded at either 400 MHz or 300 MHz (^{1}H NMR) and 150 MHz, 100 MHz or 75 MHz (^{13}C NMR) as noted. ^{1}H NMR spectra were internally referenced to the residual protonated solvent peak, and the ^{13}C NMR are referenced to the central carbon peak of the solvent. In all spectra, chemical shifts are given in δ relative to the solvent and coupling constants are reported in hertz (Hz). High-resolution mass spectra (HRMS) were recorded on a double-focusing magnetic sector mass spectrometer using ESI or APCI, as noted, at 70 eV. Melting points were obtained using a MELTEMP melting point apparatus with an upper temperature limit of 260 °C. Gel

permeation chromatography (GPC) measurements were performed on a separation module equipped with three 5 μm I-gel columns connected in series (guard, HMW, MMW and LMW) with a UV-vis detector. Analyses were performed at 35 °C using THF as the eluent with the flow rate at 1.0 mL/min. Calibration was based on polystyrene standards. Thermogravimetric analysis measurements were performed over an interval of 50-850 °C at a heating rate of 20 °C/min under a N_2 atmosphere. Differential scanning calorimetry was performed with a first scan heating rate of 15 °C/min to erase thermal history and a second scan to measure transitions between 0-330 °C under nitrogen. Transitions were also measured with cooling at 15 °C/min. Cyclic voltammetry was performed using a potentiostat with a scanning rate of 100 mV/s. The polymer solutions (1-2 mg/mL) were drop-cast on a platinum electrode and Ag/Ag^+ was used as the reference electrode. The reported values are referenced to Fc/Fc^+ (-5.1 versus vacuum). All electrochemistry experiments were performed in dry, degassed CH_3CN under an argon atmosphere using 0.1 M tetrabutylammonium hexafluorophosphate as the electrolyte. UV-visible spectroscopy was obtained on a Varian Cary Bio 50 using polymer solutions in THF and thin films spun from $CHCl_3$/*o*-dichlorobenzene solutions. The films were made by spin-coating 25 x 25 x 1 mm glass slides using 10 mg/mL polymer solutions at a spin rate of 1800 rpm on a spin-coater. X-ray crystal structure data for compound **2a** (CCDC 885622 was deposited with the Cambridge Crystallographic Data Centre, 12 Union Road, Cambridge CB2 1EZ, UK.

2.7.2 Device Fabrication and Characterization

All these devices were produced via a solution-based spin-casting fabrication process. All polymers were mixed with $PC_{60}BM$ (Sigma-Aldrich) (mixed 1:4 at 14 mg/mL for polymer and 56 mg/mL for $PC_{60}BM$) then dissolved in *o*-dichlorobenzene and magnetically stirred at 60 °C for 48 hours. ITO coated glass slides (Delta Technologies) were cleaned by consecutive 5 minute sonications in (i) isopropanol and acetone, (ii) precision cleaner detergent (dissolved in deionized water), (iii) ethanol and methanol, and then (iv) deionized water. The slides were then dried with nitrogen and cleaned with air plasma (Harrick Scientific plasma cleaner) for 10 minutes. Filtered (0.45μm) PEDOT:PSS (Clevios P^{TM}) was spin-coated onto the prepared substrates (9000 rpm/65 sec) after first being heated and stirred for one hour (80 °C, 1200 rpm). The casted PEDOT:PSS films were then annealed at

140 °C for 20 minutes. After cooling, the substrates were transferred to an argon-filled glovebox. After 48 hours of mixing, the Polymer:PCBM solutions were filtered (0.2 μm pore, VWR Scientific) and then stirred for an additional 5 hours at 60 °C . The solutions were heated up to 90 °C approximately 5 minutes prior to spin coating, after which the solutions were dropped onto the PEDOT:PSS-coated substrates by micropipette and spin-cast at 2000 rpm for 45 seconds. The active layer of the films was covered with a petri dish and annealed at 70 °C for 10 minutes. LiF (2 nm) and Al (120 nm) were successively thermally evaporated through a shadow mask under vacuum to complete the devices. *J-V* data was generated by illuminating the devices using an ETH quartzline lamp at 1 sun (calibrated using a crystalline silicon photodiode with a KG-5 filter).

2.7.3 Computation Methods

Electrostatic potential maps and frontier orbitals were generated using B3LYP/SVP density functional theory. All computations were performed using Gaussian09 [34343434] through the National Science Foundation's Extreme Science and Engineering Discovery Environment (XSEDE) on the San Diego Supercomputer Center's Gordon cluster. All side chains were truncated to methyl groups and only dimer-sized oligomers were examined.

2.7.4 Experimental Section

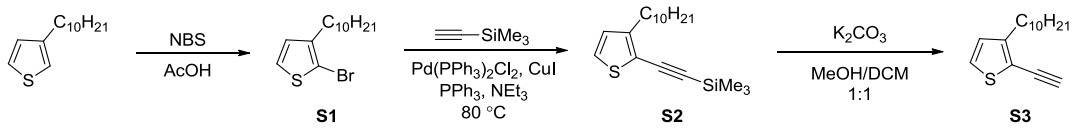

2-Bromo-3-decylthiophene (S1). To a stirred solution of 3-decylthiophene (21.10 g, 94 mmol) in 200 mL of glacial acetic acid was added *N*-bromosuccinimide (16.73 g, 94 mmol) in one portion. The reaction mixture was stirred for 5 hours and diluted with 300 mL of H_2O. The organic layer was extracted with hexane (x3) and the combined organic layers were washed subsequently with 1N NaOH, H_2O and brine, and then dried over $MgSO_4$. The solvents were removed *in vacuo* and the resulting crude product was purified by vacuum distillation to afford a pale yellow oil (27.0 g, 95 %). ^{1}H NMR (300 MHz; $CDCl_3$) δ 0.88

(3H, t, J = 6.6 Hz), 1.24-1.34 (14H, m), 1.57 (2H, p), 2.56 (2H, t, J =7.7 Hz), 6.79 (1H, d, J = 5.7 Hz), 7.18 (1H, d, J = 5.6 Hz).

3-Decyl-2-(trimethylsilylethynyl)thiophene (S2). To a stirred, deoxygenated solution of 2-bromo-3-decylthiophene (15.17 g, 50 mmol) dissolved in 75 mL of triethylamine was added 351 mg of $Pd(PPh_3)_2Cl_2$ (1 mol %), 191 mg of CuI (2 mol %) and 262 mg of PPh_3 (2 mol %). Finally, trimethylsilyl acetylene (6.38 g, 65 mmol) was added and the reaction mixture was heated to 80 °C, under argon, for 16 hours. The reaction mixture was then cooled to room temperature and most of the solvent was removed *in vacuo*. Water was added to the resulting slurry and the organic layer was extracted with CH_2Cl_2 (x3). The combined organic layers were washed with brine and dried over $MgSO_4$. The solvents were removed *in vacuo* and the crude mixture was purified by flash chromatography on silica gel with hexanes as the eluent to afford the product as a yellow oil (12.99 g, 81 %). ^{1}H NMR (400 MHz; $CDCl_3$) δ 0.26 (9H, s), 0.89 (3H, t, J = 6.8 Hz), 1.25-1.35 (14H, m), 1.62 (2H, m), 2.69 (2H, t, J = 7.8 Hz), 6.83 (1H, d, J = 5.1 Hz), 7.12 (1H, d, J = 5.1 Hz); ^{13}C NMR (100 MHz; $CDCl_3$) δ 0.21, 14.36, 22.92, 29.48, 29.58, 29.61, 29.67, 29.85, 29.94, 30.35, 32.15, 97.76, 100.85, 118.41, 126.06, 128.25, 149.03. HRMS (APCI) *m/z*: M^+ calcd for $C_{19}H_{32}SSi$, 321.2067; found, 321.2073, deviation 1.9 ppm.

3-Decyl-2-ethynylthiophene (S3). To a stirred solution of **S2** (10.69 g, 33.3 mmol) in 200 mL of CH_2Cl_2/MeOH (1:1) was added K_2CO_3 (5.07 g, 36.7 mmol) in one portion. The suspension was stirred at room temperature overnight (16 hours) and poured into H_2O. The layers were separated and the aqueous layer was extracted with CH_2Cl_2 (x3). The combined organic layers were rinsed with brine and dried over $MgSO_4$. The solvent was removed *in vacuo* and the crude product was purified on a silica plug with hexanes as the eluent to afford a yellow oil (7.20 g, 87 %). ^{1}H NMR (400 MHz; $CDCl_3$) δ 0.89 (3H, t, J = 6.7 Hz), 1.25-1.35 (14H, m), 1.62 (2H, p), 2.71 (2H, t, J = 7.7 Hz), 3.43 (1H, s), 6.85 (1H, d, J = 5.0 Hz), 7.15 (1H, d, J = 5.0 Hz); ^{13}C NMR (100 MHz; $CDCl_3$) δ 14.35, 22.92, 29.47, 29.57, 29.63, 29.80, 29.81, 29.85, 30.43, 32.14, 76.97, 83.33, 117.19, 126.36, 128.24, 149.27. HRMS (ESI) *m/z*: M^+ calcd for $C_{16}H_{24}S$, 249.1671; found, 249.1670, deviation 0.6 ppm.

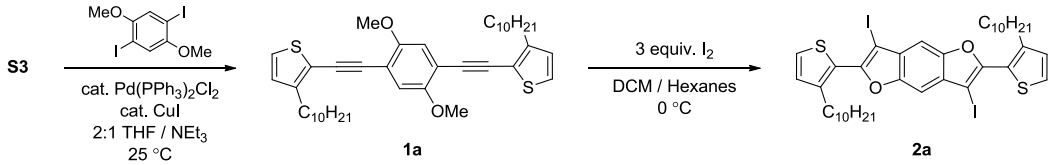

2,2'-((2,5-Dimethoxy-1,4-phenylene)bis(ethyne-2,1-diyl))bis(3-decylthiophene) (1a). To a stirred, deoxygenated solution of **S3** (5.302 g, 21.34 mmol) in 120 mL of THF/Et_3N (2:1) was added 1,4-dimethoxy-2,5-diidobenzene (4.04 g, 10.36 mmol). The solution was stirred at room temperature for 10 min (the 1,4-dimethoxy-2,5-diidobenzene does not dissolve completely at this point). Then $Pd(PPh_3)_2Cl_2$ (365 mg, 5 mol %) and CuI (198 mg, 10 mol %) were added to the reaction mixture and the flask was flushed with Ar for 10 min. The reaction mixture was stirred at room temperature for 2 days, until TLC indicated the disappearance of the dimethoxybenzene. Most of the solvent was then removed *in vacuo* and the resulting slurry was poured into water and extracted with CH_2Cl_2 (x3). The combined organic layers were dried over $MgSO_4$ and the solvent was removed *in vacuo*. The product was purified using column chromatography on silica using a gradient of hexane to hexane/ethyl acetate (99:1) to hexane/ethyl acetate (9:1) as the eluent. The resulting yellow solid was then purified further by recrystalization from hexane/ethanol. The product was collected by filtration and rinsed with cold ethanol to afford bright yellow crystals (5.81 g, 89 %), mp 84 °C. ^{1}H NMR (400 MHz; $CDCl_3$) δ 0.87 (6H, t, J = 6.8 Hz), 1.22-1.40 (28H, m), 1.68 (4H, p, J = 7.3 Hz), 2.80 (4H, t, J = 7.6 Hz), 3.89 (6H, s), 6.89 (2H, d, J = 5.1 Hz), 6.97 (2H, s), 7.19 (2H, d, J = 5.1 Hz); ^{13}C NMR (150 MHz; $CDCl_3$) δ 14.33, 22.88, 29.55, 29.59, 29.66, 29.77, 29.85, 29.87, 30.47, 32.10, 56.56, 88.44, 91.84, 113.53, 115.07, 118.43, 126.42, 128.45, 148.45, 153.89. HRMS (APCI) *m/z*: M^+ calcd for $C_{40}H_{54}O_2S_2$, 631.3638; found, 631.3653, deviation 2.4 ppm.

2,6-Bis(3-decylthiophen-2-yl)-3,7-diiodobenzo[1,2-*b*:4,5-*b*']difuran (2a). Compound **1a** (8.28 g, 13.1 mmol) was dissolved in 150 mL of CH_2Cl_2 and cooled to 0 °C. While stirring, a solution of 3 equiv of iodine (9.99 g, 39.3 mmol) in 200 mL of CH_2Cl_2/hexanes (3:1) was added dropwise over 10 minutes. Upon completion of the addition, the reaction mixture was stirred at 0 °C for 4 hours and was quenched by the addition of 50 mL of saturated aqueous sodium thiosulfate solution. The layers were separated and the aqueous layer was extracted

with CH_2Cl_2 (x2). The organic layers were combined, dried over $MgSO_4$ and the solvents were removed *in vacuo*. The crude product was purified by recrystalization from hexanes/ethanol and collected by filtration, followed by rinsing with cold ethanol to afford fine, yellow crystals (7.89 g, 70 %), mp 104 °C. ^{1}H NMR (300 MHz; $CDCl_3$) δ 0.88 (6H, t, *J* = 6.6 Hz), 1.22-1.40 (28H, m), 1.68 (4H, p, *J* = 7.2 Hz), 2.90 (4H, t, *J* =7.7 Hz), 7.05 (2H, d, *J* = 5.1 Hz), 7.42 (2H, d, *J* = 5.1 Hz), 7.47 (2H, s); ^{13}C NMR (75 MHz; $CDCl_3$) δ 14.38, 22.92, 29.59, 29.64, 29.72, 29.87, 29.94, 30.24, 31.03, 32.15, 64.63, 103.03, 124.67, 127.09, 129.92, 131.39, 145.42, 151.54, 152.43. HRMS (ESI) *m/z*: M^+ calcd for $C_{38}H_{48}I_2O_2S_2$, 855.1258; found, 855.1252, deviation 0.7 ppm. UV-Vis (THF) λ_{max} = 259 nm, 360 nm.

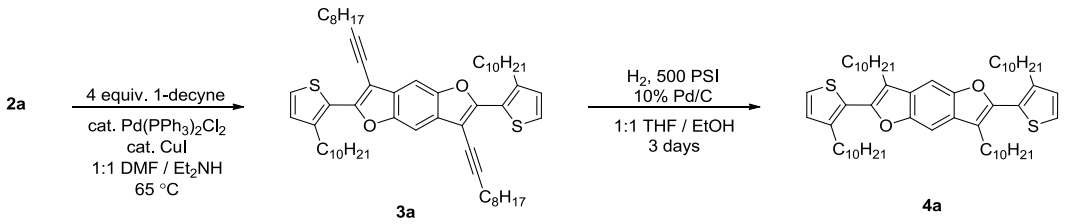

3,7-Di(dec-1-yn-1-yl)-2,6-bis(3-decylthiophen-2-yl)benzo[1,2-*b*:4,5-*b*']difuran (3a).[35] To a stirred, deoxygenated solution of **2a** (2.185 g, 2.6 mmol) and 1-decyne (1.41 g, 10.2 mmol) in 60 mL of DMF/Et_2NH (1:1) was added $Pd(PPh_3)_2Cl_2$ (107 mg, 6 mol %) and CuI (29 mg, 6 mol %). The solution was stirred under argon, heated to 65 °C and stirred for 8 hours. The reaction mixture was cooled to room temperature, poured into H_2O and extracted with CH_2Cl_2 (x3). The combined organic layers were washed with H_2O (x2), followed by brine (x1), dried over $MgSO_4$ and the solvent was removed *in vacuo*. The crude product was purified by chromatography on silica gel using a gradient of hexane to hexane/CH_2Cl_2 (98:2) to hexane/CH_2Cl_2 (95:5) as the eluent to afford light yellow crystals (2.14 g, 96 %), mp 56 °C. ^{1}H NMR (400 MHz; $CDCl_3$) δ 0.89 (12H, m), 1.22-1.45 (48H, m), 1.55 (4H, m), 1.72 (8H, m), 2.60 (4H, t, *J* = 7.1 Hz), 3.07 (4H, t, *J* = 7.8 Hz), 6.89 (2H, d, *J* = 5.1 Hz), 7.34 (2H, d, *J* = 5.1 Hz), 7.62 (2H, s); ^{13}C NMR (75 MHz; $CDCl_3$) δ 14.35, 20.34, 22.92, 28.93, 29.26, 29.32, 29.42, 29.52, 29.60, 29.76, 29.82, 29.88, 29.89, 30.35, 31.22, 32.12, 32.13, 78.14, 99.79, 100.64, 101.10, 126.13, 126.18, 128.47, 130.22, 143.73, 151.04, 154.14. HRMS (ESI) *m/z*: M^+ calcd for $C_{58}H_{82}O_2S_2$, 875.5829; found, 875.5814, deviation 1.7 ppm. UV-Vis (THF) λ_{max} = 235 nm, 386 nm.

3,7-Didecyl-2,6-bis(3-decylthiophen-2-yl)benzo[1,2-*b*:4,5-*b*']difuran (4a.) Dialkyne **3a** (3.40 g, 4.0 mmol) was dissolved in 20 mL of THF/ethanol (1:1) and Pd/C (10 %, 426 mg, 0.4 mmol) was added to the solution. The resulting mixture was placed in a Parr bomb apparatus, flushed twice with H_2 and stirred under pressurized H_2 (500 PSI) for 72 hours at room temperature. The reaction mixture was filtered through a pad of Celite to remove the Pd/C and rinsed with THF (x2). The solvent was removed *in vacuo* and the resulting solid was purified on a silica gel plug with hexane as the eluent to afford a pale yellow solid (3.35 g, 95 %), mp 57 °C. ^{1}H NMR (400 MHz; $CDCl_3$) δ 0.86 (12H, m), 1.20-1.42 (56H, m), 1.63 (4H, p, J = 7.2 Hz), 1.72 (4H, p, J =7.5 Hz), 2.80 (8H, m), 7.02 (2H, d, J = 5.1 Hz), 7.36 (2H, d, J = 5.1 Hz), 7.53 (2H, s); ^{13}C NMR (150 MHz; $CDCl_3$) δ 14.34, 22.92, 24.69, 29.58, 29.65, 29.66, 29.70, 29.78, 29.85, 29.86, 29.93, 31.01, 32.13, 32.14, 100.48, 118.92, 126.00, 126.02, 127.94, 129.63, 143.62, 146.73, 151.39. HRMS (ESI) *m/z*: M^+ calcd for $C_{58}H_{90}O_2S_2$, 883.6455; found, 883.6450, deviation 0.6 ppm. UV-Vis (THF) λ_{max} = 248 nm, 346 nm.

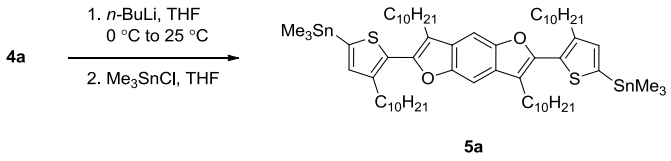

5a

(5,5'-(3,7-Didecylbenzo[1,2-*b*:4,5-*b*']difuran-2,6-diyl)bis(4-decylthiophene-5,2-diyl))bis(trimethylstannane) (5a). To a stirred solution of **4a** (884 mg, 1.0 mmol) in 20 mL of anhydrous THF, under argon, at 0 °C was added *n*-BuLi in hexanes (2.5 M, 1.0 mL, 2.5 mmol) dropwise. The reaction mixture was warmed to room temperature and stirred for 2 hours. A solution of trimethylstannyl chloride in THF (1.0 M, 2.75 mL, 2.75 mmol) was then added to the reaction at 0 °C and the reaction was warmed to room temperature, stirred overnight and poured into H_2O. The layers were separated and the aqueous layer was extracted with ether (x3). The combined organic layers were dried over $MgSO_4$ and the solvent was removed *in vacuo*. The resulting reddish oil was heated at 50 °C under vacuum to remove residual Me_3SnCl (1.14 g, 94 %). ^{1}H NMR (400 MHz; $CDCl_3$) δ 0.41 (81H, s), 0.87 (12H, m), 1.20-1.42 (56H, m), 1.64 (4H, p, J = 7.3 Hz), 1.73 (4H, p, J = 7.6 Hz), 2.82 (8H, m), 7.07 (2H, s), 7.51 (2H, s); ^{13}C NMR (100 MHz; $CDCl_3$) δ -7.98, 14.36, 22.93, 24.73, 29.56, 29.60, 29.67, 29.70, 29.79, 29.83, 29.88, 29.90, 29.92, 31.23, 32.15, 32.17,

100.32, 118.50, 127.97, 131.85, 137.89, 138.83, 144.58, 147.12, 151.37. HRMS (APCI) *m/z*: M^+ calcd for $C_{64}H_{106}O_2S_2Sn_2$, 1209.5765; found, 1209.5747, deviation 1.5 ppm.

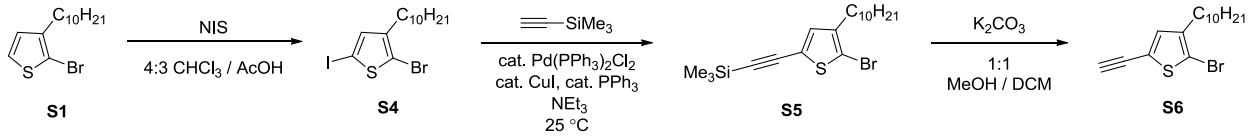

2-Bromo-3-decyl-5-iodothiophene (S4).[36] To a stirred solution of 2-bromo-3-decylthiophene (5.70 g, 18.8 mmol) in 35 mL of $CHCl_3$/AcOH (4:3) was added *N*-iodosuccinimide (5.92 g, 26.3 mmol) in one portion. The reaction was stirred in the absence of light for 16 hours and poured into H_2O. The layers were separated and the aqueous layer was extracted with hexanes (x3). The combined organic layers were then neutralized with 1 M KOH, washed subsequently with H_2O and brine, and dried over $MgSO_4$. The solvent was removed *in vacuo* and the crude oil was purified by column chromatography on silica with hexanes as the eluent to afford a pale pink oil (7.80 g, 97 %). ^{1}H NMR (400 MHz; $CDCl_3$) δ 0.88 (3H, t, J = 6.6 Hz), 1.24-1.34 (14H, m), 1.53 (2H, m), 2.52 (2H, t, J = 7.7 Hz), 6.96 (1H, s); ^{13}C NMR (100 MHz; $CDCl_3$) δ 14.38, 22.93, 29.36, 29.41, 29.56, 29.60, 29.77, 29.83, 29.87, 32.13, 71.27, 111.90, 138.16, 144.43. HRMS (APCI) *m/z*: M^+ calcd for $C_{14}H_{22}BrIS_2$, 428.9743; found, 428.9751, deviation 1.9 ppm.

((5-Bromo-4-decylthiophen-2-yl)ethynyl)trimethylsilane (S5). To a stirred deoxygenated solution of 2-bromo-3-decyl-5-iodothiophene (7.80 g, 18.2 mmol) in 50 mL of THF/NEt_3 (1:1) was added $Pd(PPh_3)_2Cl_2$ (319 mg, 2.5 mol %) and CuI (173 mg, 5 mol %). The resulting suspension was stirred for 10 minutes under argon before trimethylsilyl acetylene (1.88 g, 19.1 mmol) was added dropwise and the reaction mixture was stirred at room temperature under argon. After 18 hours, TLC analysis indicated complete consumption of the starting material and most of the solvent was removed *in vacuo*. The resulting dark slurry was then filtered and rinsed with hexanes. The solvent was removed *in vacuo* and the crude oil was purified on a silica gel plug with hexanes as the eluent to afford a yellow oil (7.04 g, 97 %). ^{1}H NMR (400 MHz; $CDCl_3$) δ 0.23 (9H, s), 0.88 (3H, t, J = 6.8 Hz), 1.24-1.34 (14H, m), 1.53 (2H, p, J = 7.2 Hz), 2.49 (2H, t, J = 7.6 Hz), 6.92 (1H, s); ^{13}C NMR (100 MHz;

$CDCl_3$) δ 0.02, 14.34, 22.92, 29.31, 29.55, 29.58, 29.61, 29.76, 29.77, 29.82, 32.13, 97.16, 99.93, 110.22, 123.15, 133.77, 142.36. HRMS (APCI) *m/z*: M^+ calcd for $C_{19}H_{31}BrSSi$, 399.1172; found, 399.1171, deviation 0.2 ppm.

2-Bromo-3-decyl-5-ethynylthiophene (S6). To a stirred solution of **S5** (7.04 g, 17.6 mmol) in 100 mL of CH_2Cl_2/MeOH (1:1) was added K_2CO_3 (2.68 g, 19.4 mmol) in one portion. The suspension was stirred at room temperature for 8 hours and poured into H_2O. The organic layer was separated and the aqueous layer was extracted with CH_2Cl_2 (x3). The combined organic layers were rinsed with brine and dried over $MgSO_4$. The solvent was removed *in vacuo* and the crude product was purified on a silica gel plug with hexanes as the eluent to afford an orange oil (5.52 g, 96 %). ^{1}H NMR (400 MHz; $CDCl_3$) δ 0.88 (3H, t, *J* = 6.7 Hz), 1.24-1.34 (14H, m), 1.55 (2H, p, *J* = 7.0 Hz), 2.51 (2H, t, *J* =7.6 Hz), 3.35 (1H, s), 6.96 (1H, s); ^{13}C NMR (75 MHz; $CDCl_3$) δ 14.35, 22.92, 29.34, 29.56, 29.56, 29.60, 29.77, 29.82, 29.94, 32.12, 76.69, 82.19, 110.50, 121.94, 134.21, 142.39. HRMS (APCI) *m/z*: M^+ calcd for $C_{16}H_{23}BrS$, 327.0777; found, 327.0768, deviation 2.9 ppm.

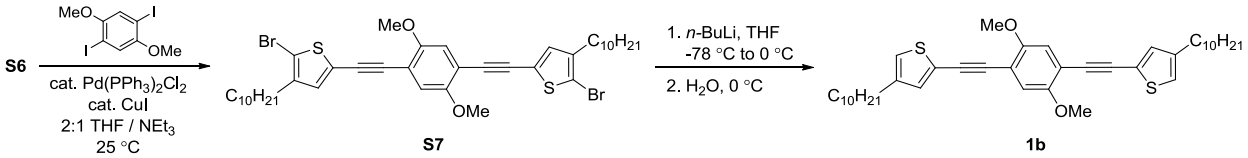

Note: the iodocyclization reaction was performed on compound **S7** and the resulting benzodifuran was insoluble in organic solvents at room temperature. Attempts were made to attach 1-decyne through Sonogashira chemistry; however, the elevated temperatures required lead to a loss of selectivity of the aryl iodide over the aryl bromide in the cross-coupling reaction. Consequently, the product was obtained in low yields along with multiple side-products. The bromines on compound **S7** were thus removed to facilitate alkynylation at the appropriate site on the molecule.

5,5'-((2,5-Dimethoxy-1,4-phenylene)bis(ethyne-2,1-diyl))bis(2-bromo-3-decylthiophene) (S7). To a stirred, deoxygenated solution of **S6** (12.75 g, 39.0 mmol) in 200 mL of THF/Et_3N (2:1) was added 1,4-dimethoxy-2,5-diidobenzene (6.76 g, 17.3 mmol). The

solution was stirred at room temperature for 10 minutes (the 1,4-dimethoxy-2,5-diidobenzene does not dissolve completely at this point). Then $Pd(PPh_3)_2Cl_2$ (364 mg, 3 mol %), CuI (198 mg, 6 mol %) and PPh_3 (273 mg, 6 mol %) were added to the reaction mixture and the flask was flushed with Ar for 10 minutes. The reaction mixture was stirred at room temperature, under argon, for 2 days. Most of the solvent was then removed *in vacuo* and the resulting slurry was poured into water and extracted with CH_2Cl_2 (x3). The combined organic layers were dried over $MgSO_4$ and the solvent was removed *in vacuo*. The product was purified using column chromatography on silica using hexane/CH_2Cl_2 (3:1) to afford a yellow, flaky solid (11.17 g, 82 %), mp 72 °C. ^{1}H NMR (400 MHz; $CDCl_3$) δ 0.88 (6H, t, J = 6.8 Hz), 1.23-1.35 (28H, m), 1.57 (4H, m), 2.53 (4H, t, J = 7.6 Hz), 3.88 (6H, s), 6.96 (2H, s), 7.01 (2H, s); ^{13}C NMR (100 MHz; $CDCl_3$) δ 14.35, 22.91, 29.33, 29.54, 29.62, 29.77, 29.79, 29.82, 29.86, 32.12. HRMS (APCI) *m/z*: M^+ calcd for $C_{40}H_{52}Br_2O_2S_2$, 787.1848; found, 787.1835, deviation 1.7 ppm.

5,5'-((2,5-Dimethoxy-1,4-phenylene)bis(ethyne-2,1-diyl))bis(3-decylthiophene) (1b). To a stirred solution of **S7** (11.17 g, 14.2 mmol) in 125 ml of dry THF at -78 °C, under argon, was added *n*-BuLi in hexanes (2.5 M, 12.5 mL, 31.2 mmol) dropwise. The reaction mixture was stirred at -78 °C for 1 hour, warmed to room temperature and then quenched with 50 mL of H_2O. The layers were separated and the aqueous layer was extracted with diethyl ether. The combined organic layers were washed with brine and dried over $MgSO_4$. The solvent was removed *in vacuo* and the resulting yellow solid was passed through a short pad of silica gel with hexane/CH_2Cl_2 (2:1) as the eluent to afford a flaky yellow solid (8.94 g, 99 %), mp 51 °C. ^{1}H NMR (400 MHz; $CDCl_3$) δ 0.88 (6H, t, J = 6.8), 1.23-1.35 (28H, m), 1.60 (4H, p, J = 7.4 Hz), 2.57 (4H, t, J =7.6 Hz), 3.88 (6H, s), 6.89 (2H, d), 6.98 (2H, s), 7.16 (2H, d); ^{13}C NMR (100 MHz; $CDCl_3$) δ 14.31, 22.87, 29.38, 29.52, 29.63, 29.77, 29.80, 30.45, 30.57, 32.08, 56.50, 88.90, 89.18, 113.32, 115.37, 122.65, 122.84, 133.60, 143.47, 153.85. HRMS (ESI) *m/z*: M^+ calcd for $C_{40}H_{54}O_2S_2$, 631.3638; found, 631.3623, deviation 2.4 ppm.

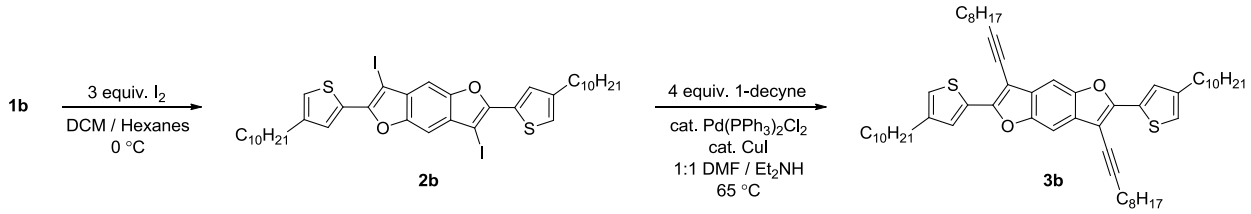

2,6-Bis(4-decylthiophen-2-yl)-3,7-diiodobenzo[1,2-*b*:4,5-*b*']difuran (2b). Compound **1b** (8.94 g, 14.1 mmol) was dissolved in 150 mL of CH_2Cl_2 and cooled to 0 °C. While stirring, a solution of 3 equiv of iodine (10.74 g, 42.3 mmol) in 200 mL of CH_2Cl_2/hexanes (3:1) was added dropwise over 10 minutes. Upon completion of the addition, the reaction mixture was stirred at 0 °C for 4 hours and was quenched by the addition of 50 mL of saturated aqueous sodium thiosulfate solution. The layers were separated and the aqueous layer was extracted with CH_2Cl_2 (x2). The organic layers were combined, dried over $MgSO_4$ and the solvent was removed *in vacuo*. The resulting crude product was recrystalized from ethanol/$CHCl_3$ and collected by filtration, followed by rinsing with cold ethanol, to afford fine, yellow crystals (9.88 g, 82 %), mp 146 °C. ^{1}H NMR (400 MHz; $CDCl_3$) δ 0.88 (6H, t, J = 6.7 Hz), 1.23-1.40 (28H, m), 1.68 (4H, p, J = 7.4 Hz), 2.67 (4H, t, J = 7.7 Hz), 7.07 (2H, s), 7.42 (2H, s), 7.78 (2H, s); ^{13}C NMR (150 MHz; $CDCl_3$) δ 14.31, 22.92, 29.54, 29.57, 29.71, 29.85, 29.87, 30.65, 30.71, 32.16, 60.38, 102.73, 122.63, 128.85, 131.71, 132.09, 144.26, 151.27, 151.87. HRMS (APCI) *m/z*: M^+ calcd for $C_{38}H_{48}I_2O_2S_2$, 855.1258; found, 855.1254, deviation 0.5 ppm. UV-Vis (THF) λ_{max} = 256 nm, 360 nm, 379 nm, 401 nm.

3,7-Di(dec-1-yn-1-yl)-2,6-bis(4-decylthiophen-2-yl)benzo[1,2-*b*:4,5-*b*']difuran (3b). To a stirred, deoxygenated solution of **2b** (4.27 g, 5.0 mmol) and 1-decyne (2.77 g, 20.0 mmol) in 110 mL of DMF/Et_2NH (1:1) was added $Pd(PPh_3)_2Cl_2$ (175 mg, 5 mol %) and CuI (48 mg, 5 mol %). The solution was stirred under argon, heated to 80 °C and stirred overnight. The reaction mixture was cooled to room temperature, poured into H_2O and extracted with CH_2Cl_2 (x3). The combined organic layers were washed with H_2O (x2), followed by brine (x1), dried over $MgSO_4$ and the solvent was removed *in vacuo*. The crude product was purified by chromatography on silica gel using a gradient of hexane to hexane/CH_2Cl_2 (95:5) as the eluent to afford bright yellow crystals (4.02 g, 92 %), mp 95 °C. ^{1}H NMR (400 MHz;

$CDCl_3$) δ 0.92 (12H, m), 1.26-1.45 (48H, m), 1.59 (4H, p, J = 7.0 Hz), 1.65-1.80 (8H, m), 2.65 (8H, m), 7.00 (2H, s), 7.57 (2H, s), 7.69 (2H, s); ^{13}C NMR (100 MHz; $CDCl_3$) δ 14.36, 20.34, 22.95, 29.04, 29.33, 29.47, 29.53, 29.59, 29.61, 29.76, 29.88, 29.89, 30.64, 30.67, 32.16, 71.74, 99.01, 100.03, 101.10, 121.74, 127.19, 128.84, 132.32, 144.00, 150.91, 153.59. HRMS (APCI) *m/z*: M^+ calcd for $C_{58}H_{82}O_2S_2$, 875.5829; found, 875.5814, deviation 1.7 ppm. UV-Vis (THF) λ_{max} = 231nm, 366 nm, 386 nm, 410 nm.

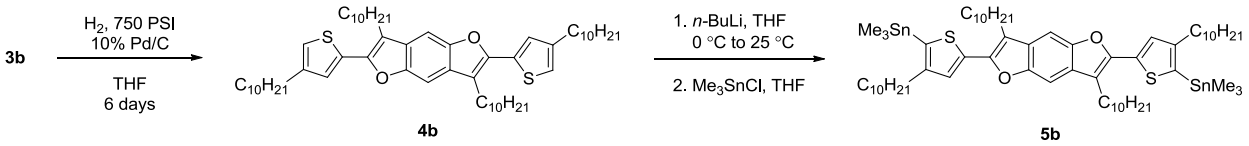

3,7-Didecyl-2,6-bis(4-decylthiophen-2-yl)benzo[1,2-*b*:4,5-*b*']difuran (4b). Dialkyne **3b** (3.55 g, 4.2 mmol) was dissolved in 30 mL of THF and Pd/C (10 %, 4 47mg, 0.4 mmol) was added to the solution. The resulting mixture was placed in a Parr bomb apparatus, flushed twice with H_2 and stirred under pressurized H_2 (750 PSI) for 6 days at room temperature. The reaction mixture was filtered through a pad of Celite to remove the Pd/C and rinsed with THF (x2). The solvent was removed *in vacuo* and the resulting solid was purified on a silica gel plug with hexane as the eluent to afford a bright yellow solid (3.96 g, 95 %), mp 75 °C. ^{1}H NMR (400 MHz; $CDCl_3$) δ 0.88 (12H, m), 1.23-1.40 (56H, m), 1.48 (4H, m), 1.68 (4H, m), 1.75 (4H, m), 2.66 (4H, t, J = 7.6 Hz), 2.93 (4H, t, J = 7.7 Hz), 6.96 (2H, d, J = 1.3 Hz), 7.32 (2H, d, J = 1.4 Hz), 7.48 (2H, s); ^{13}C NMR (150 MHz; $CDCl_3$) δ 14.34, 22.93, 24.67, 29.45, 29.57, 29.59, 29.73, 29.79, 29.85, 29.86, 29.88, 30.08, 30.69, 32.14, 32.15, 100.08, 116.33, 120.45, 126.22, 128.93, 133.20, 147.47, 151.04. HRMS (APCI) *m/z*: M^+ calcd for $C_{58}H_{90}O_2S_2$, 883.6455; found, 883.6467, deviation 1.4 ppm. UV-Vis (THF) λ_{max} = 239 nm, 376 nm, 397 nm.

(5,5'-(3,7-Didecylbenzo[1,2-*b*:4,5-*b*']difuran-2,6-diyl)bis(3-decylthiophene-5,2-diyl))bis(trimethylstannane) (5b). To a stirred solution of **4b** (221 mg, 0.25 mmol) in 10 mL of anhydrous THF, under argon, at 0 °C was added *n*-BuLi in hexanes (2.5 M, 0.25 mL, 0.625 mmol) dropwise. The reaction mixture was warmed to room temperature and stirred

for 2 hours. A solution of trimethylstannyl chloride in THF (1.0 M, 0.69 mL, 0.69 mmol) was then added to the reaction at 0 °C and the reaction was warmed to room temperature, stirred overnight and poured into H_2O. The layers were separated and the aqueous layer was extracted with ether (x3). The combined organic layers were dried over $MgSO_4$ and the solvent was removed *in vacuo*. The resulting yellow oil was heated at 50 °C under a vacuum to remove residual Me_3SnCl (284 mg, 94 %). ^{1}H NMR (400 MHz; $CDCl_3$) δ 0.43 (18H, s), 0.88 (12H, m), 1.23-1.40 (56H, m), 1.49 (4H, m), 1.65 (4H, p, J = 7.6 Hz), 1.76 (4H, p, J = 7.5 Hz), 2.64 (4H, t, J = 7.8 Hz), 2.94 (4H, t, J = 7.7 Hz), 7.45 (2H, s), 7.48 (2H, s); ^{13}C NMR (100 MHz; $CDCl_3$) δ -7.64, 14.37, 22.94, 24.70, 29.43, 29.61, 29.80, 29.85, 29.87, 29.90, 29.92, 30.07, 32.17, 32.31, 32.99, 99.97, 116.12, 127.16, 128.91, 132.91, 138.57, 147.62, 151.03, 151.50. HRMS (APCI) *m/z*: M^+ calcd for $C_{64}H_{106}O_2S_2Sn_2$, 1209.5765; found, 1209.5744, deviation 1.7 ppm.

General Polymerization Procedure (PT_{in}BDFID and PT_{out}BDFID) with $Pd_2(dba)_3$. To a stirred, deoxygenated solution of bisstannane (**5a** or **5b)** and isoindigo **6** in 10 mL of toluene was added $Pd_2(dba)_3$ (2 mol %) and tri(*o*-tolyl)phosphine (8 mol %). The reaction mixture was heated to reflux, under argon, and stirred for 4 hours. A few drops of trimethyl(phenyl)tin was added and the mixture was stirred for 4 hours at reflux. A few drops of iodobenzene were added and the mixture was stirred overnight at reflux. After cooling to room temperature, the polymer was precipitated in methanol. The precipitated polymer was filtered through a cellulose extraction thimble, placed into a Soxhlet extractor and washed with methanol, acetone, and $CHCl_3$. The polymer was recovered from the $CHCl_3$ extract by evaporation of the solvent.

Polymer PT_{in}BDFID: synthesized from bisstannane **5a** (479 mg, 94 %). ^{1}H NMR (400 MHz; $CDCl_3$) δ. 0.88, 1.15-1.50, 1.73, 1.80, 2.02, 2.88, 2.93, 3.77, 7.04, 7.35, 7.58, 9.26. UV-Vis ($CHCl_3$) λ_{max} = 373 nm, 605 nm; UV-Vis (film) λ_{max} = 415 nm, 653 nm. GPC M_n = 32664, M_w = 76253, PDI = 2.33. TGA T_d = 397 °C. T_g = not observed.

Polymer PT_{out}BDFID: synthesized from bisstannane **5b** (365 mg, 86 %). ^{1}H NMR (400 MHz; $CDCl_3$) δ 0.88, 1.10-1.55, 1.76, 2.68, 2.83, 3.00, 3.76, 6.97, 7.23, 7.42, 7.53, 9.29.

UV-Vis ($CHCl_3$) λ_{max} = 400 nm, 599 nm; UV-Vis (film) λ_{max} = 403 nm, 612 nm. GPC M_n = 17384, M_w = 33085, PDI = 1.90. TGA T_d = 407 °C. T_g = not observed.

General Polymerization Procedure ($PT_{in}BDFID$ and $PT_{out}BDFID$) with $Pd(PPh_3)_4$. To a stirred, deoxygenated solution of bisstannane (**5a** or **5b)** and isoindigo **6** in 10 mL of toluene was added $Pd(PPh_3)_4$ (5 mol %). The reaction mixture was heated to reflux, under argon, and stirred for 48 hours. A few drops of trimethyl(phenyl)tin was added and the mixture was stirred for 4 hours at reflux. A few drops of iodobenzene were added and the mixture was stirred overnight at reflux. After cooling to room temperature, the polymer was precipitated in methanol. The precipitated polymer was filtered through a cellulose extraction thimble, placed into a Soxhlet extractor and washed with methanol, acetone, and $CHCl_3$. The polymer was recovered from the $CHCl_3$ extract by evaporation of the solvent.

Polymer $PT_{in}BDFID$: synthesized from bisstannane **5a** (671 mg, 79 %). UV-Vis ($CHCl_3$) λ_{max} = 397 nm, 596 nm; UV-Vis (film) λ_{max} = 401 nm, 617 nm. GPC M_n = 35081, M_w = 18848, PDI = 1.86.

Polymer $PT_{out}BDFID$: synthesized from bisstannane **5b** (710 mg, 82 %). UV-Vis ($CHCl_3$) λ_{max} = 379 nm, 594 nm; UV-Vis (film) λ_{max} = 404 nm, 611 nm. GPC M_n = 20528, M_w = 15662, PDI = 1.31.

2.7.5. Spectral and Analytic Data

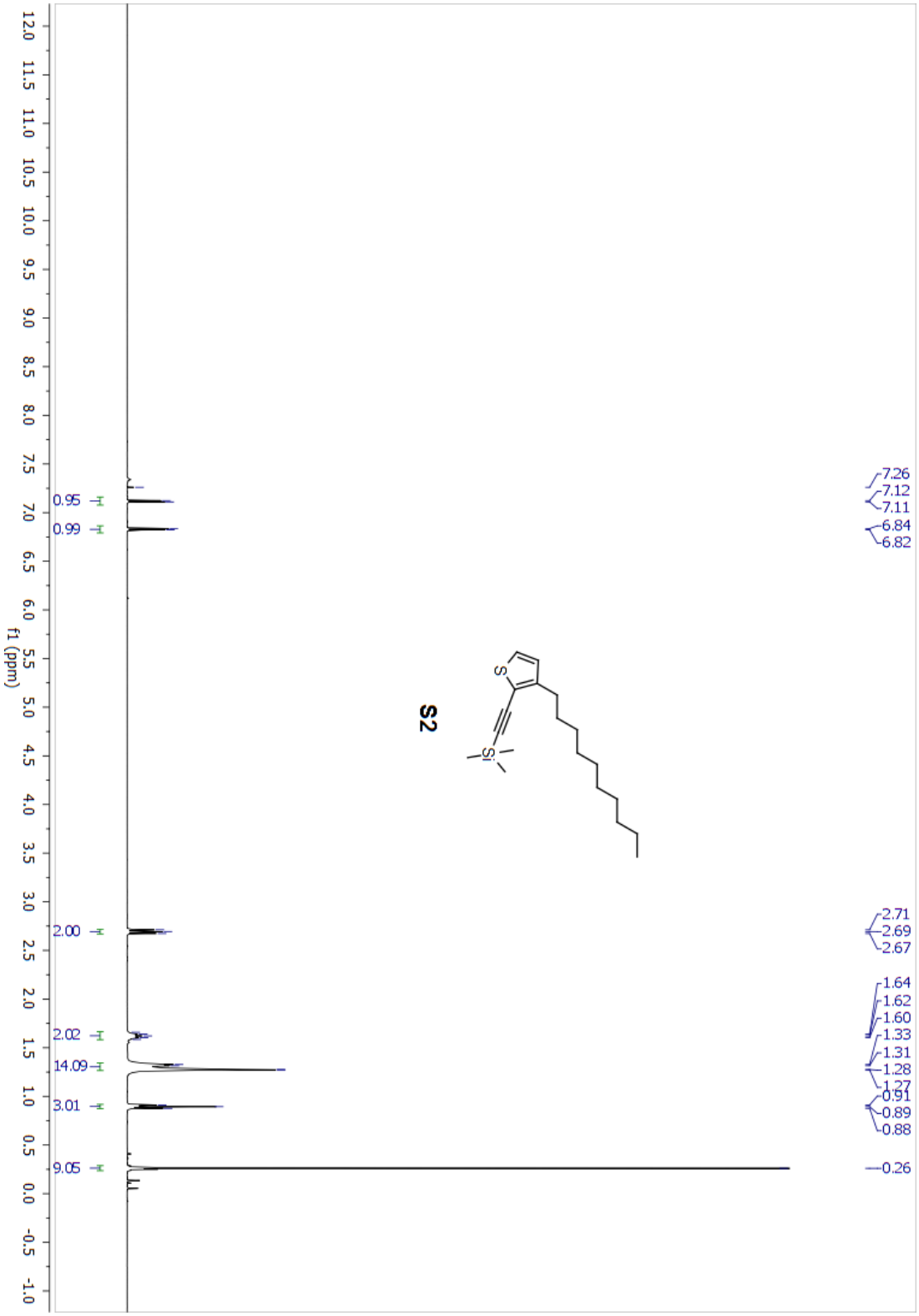

Figure S2.1. ^{1}H NMR of 3-decyl-2-(trimethylsilylethynyl)-thiophene (**S2**).

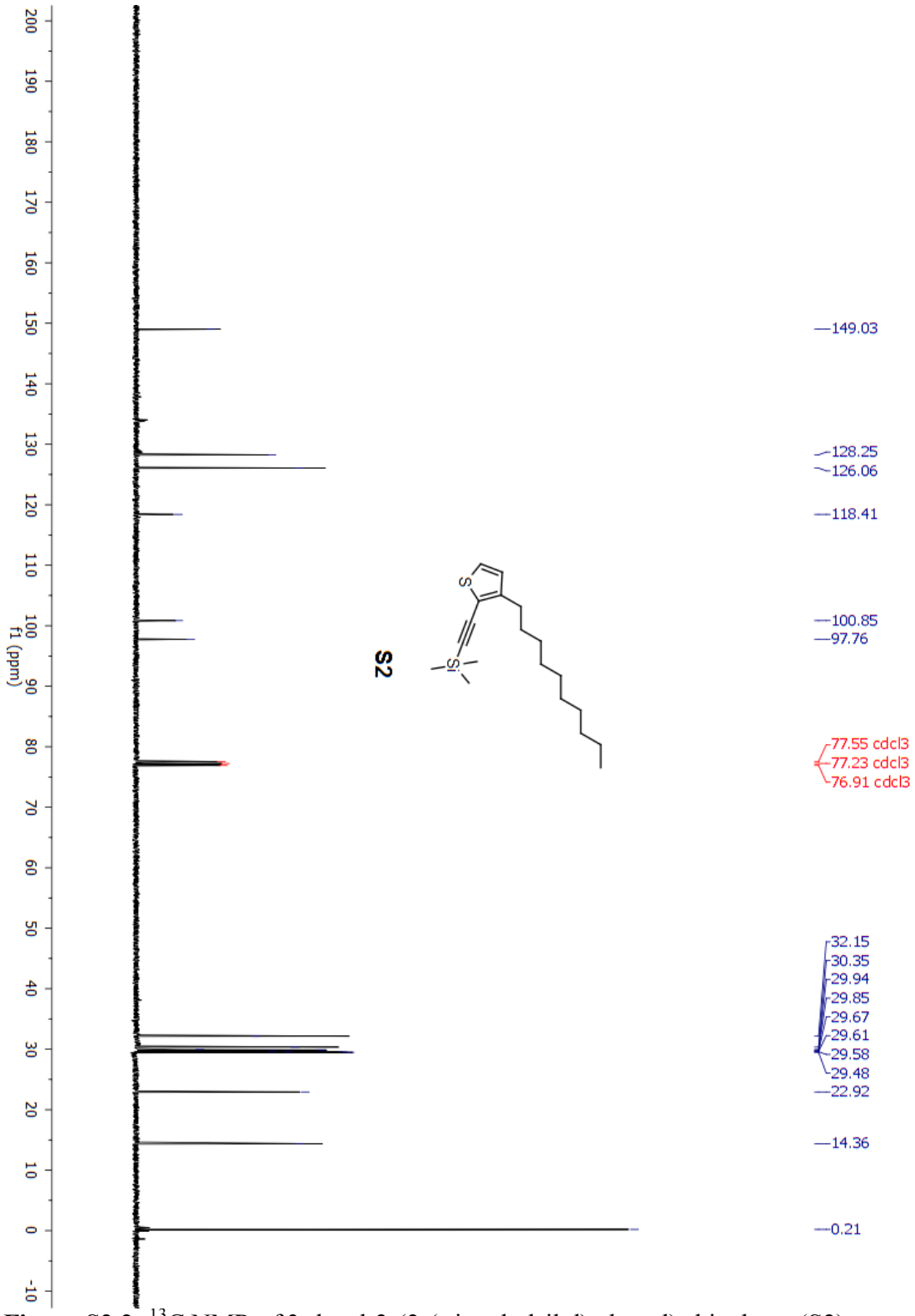

Figure S2.2. ^{13}C NMR of 3-decyl-2-(2-(trimethylsilyl)ethynyl)-thiophene (**S2**).

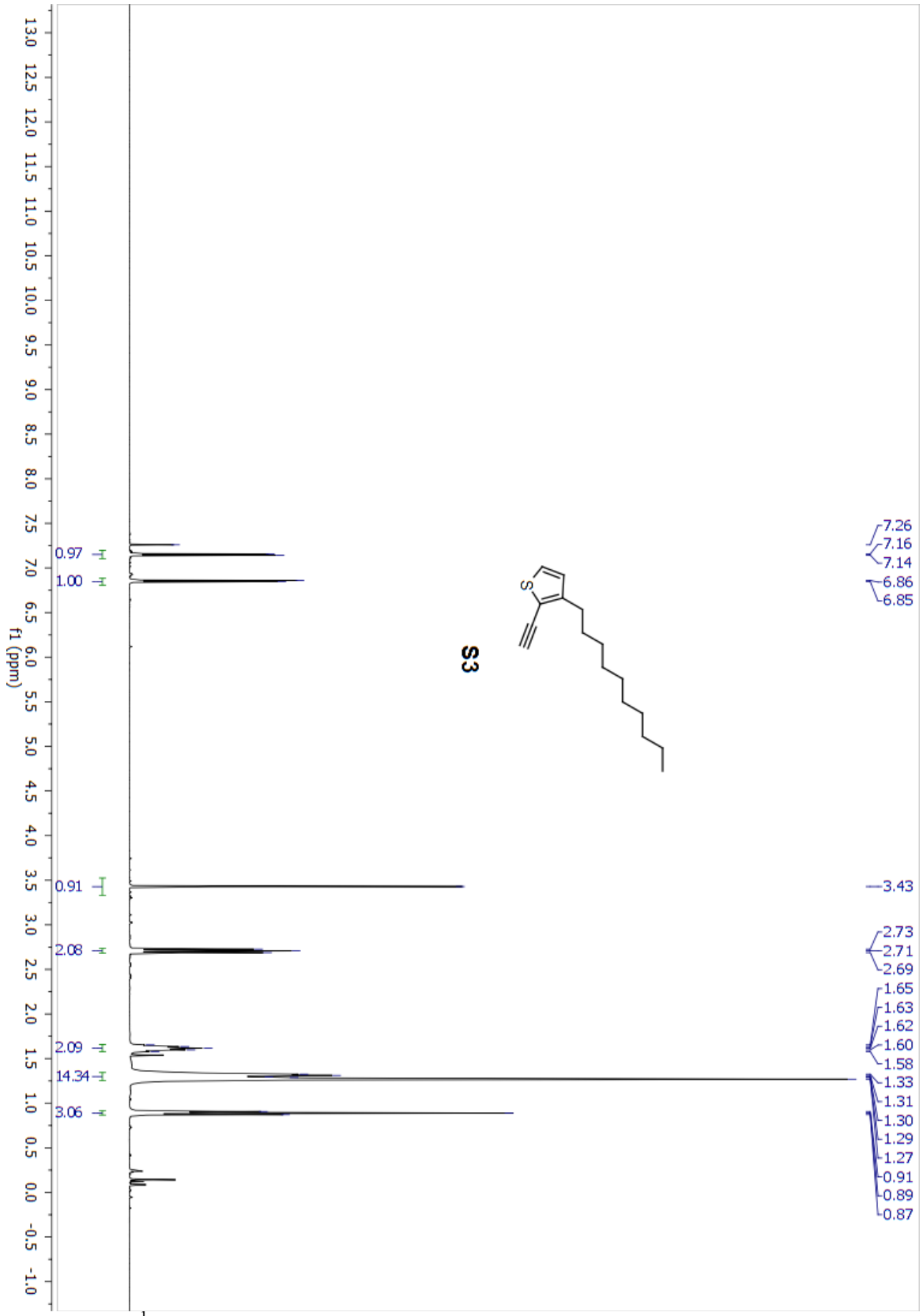

Figure S2.3. ^{1}H NMR of 3-decyl-2-ethynylthiophene (**S3**).

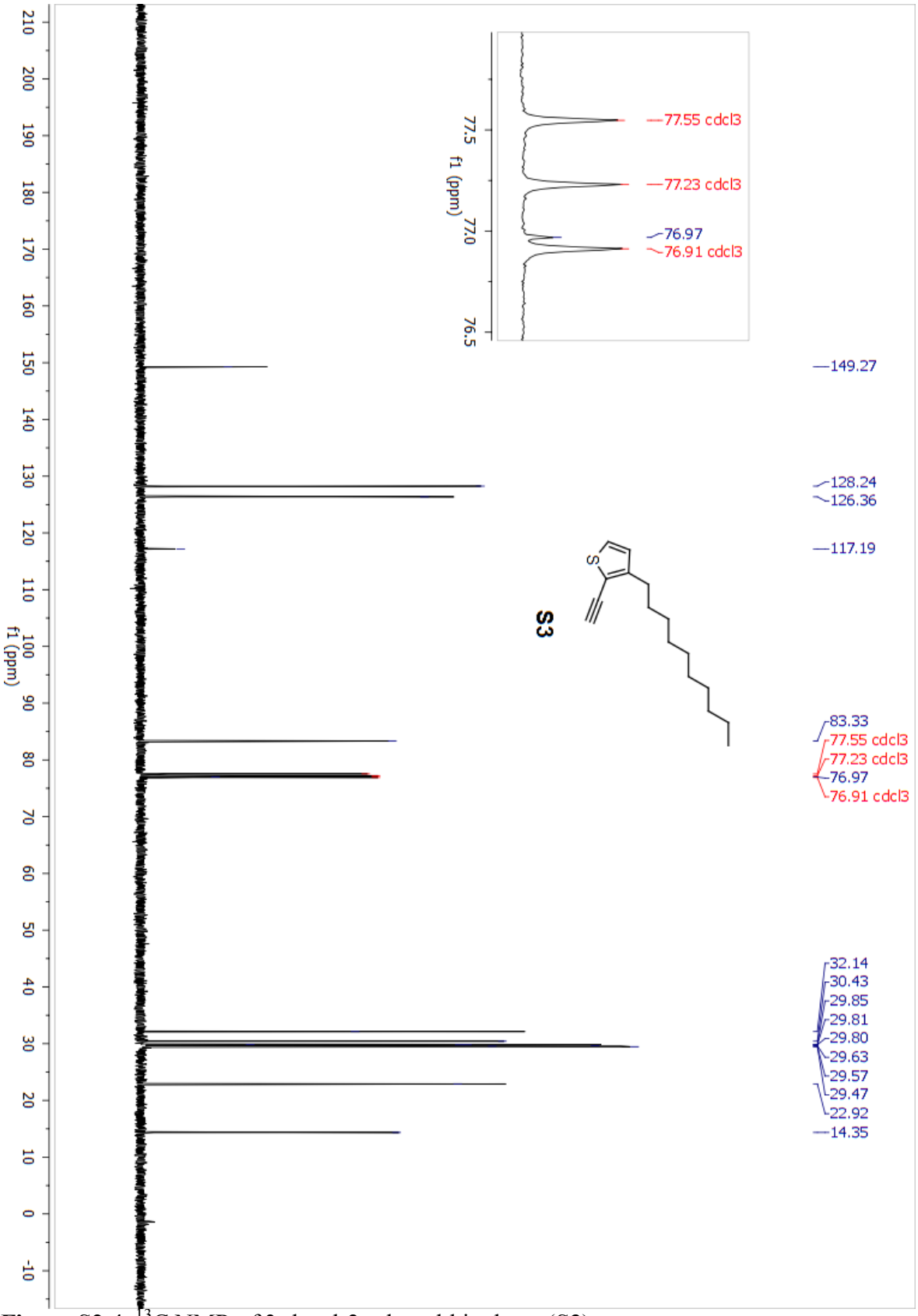

Figure S2.4. ^{13}C NMR of 3-decyl-2-ethynylthiophene (**S3**).

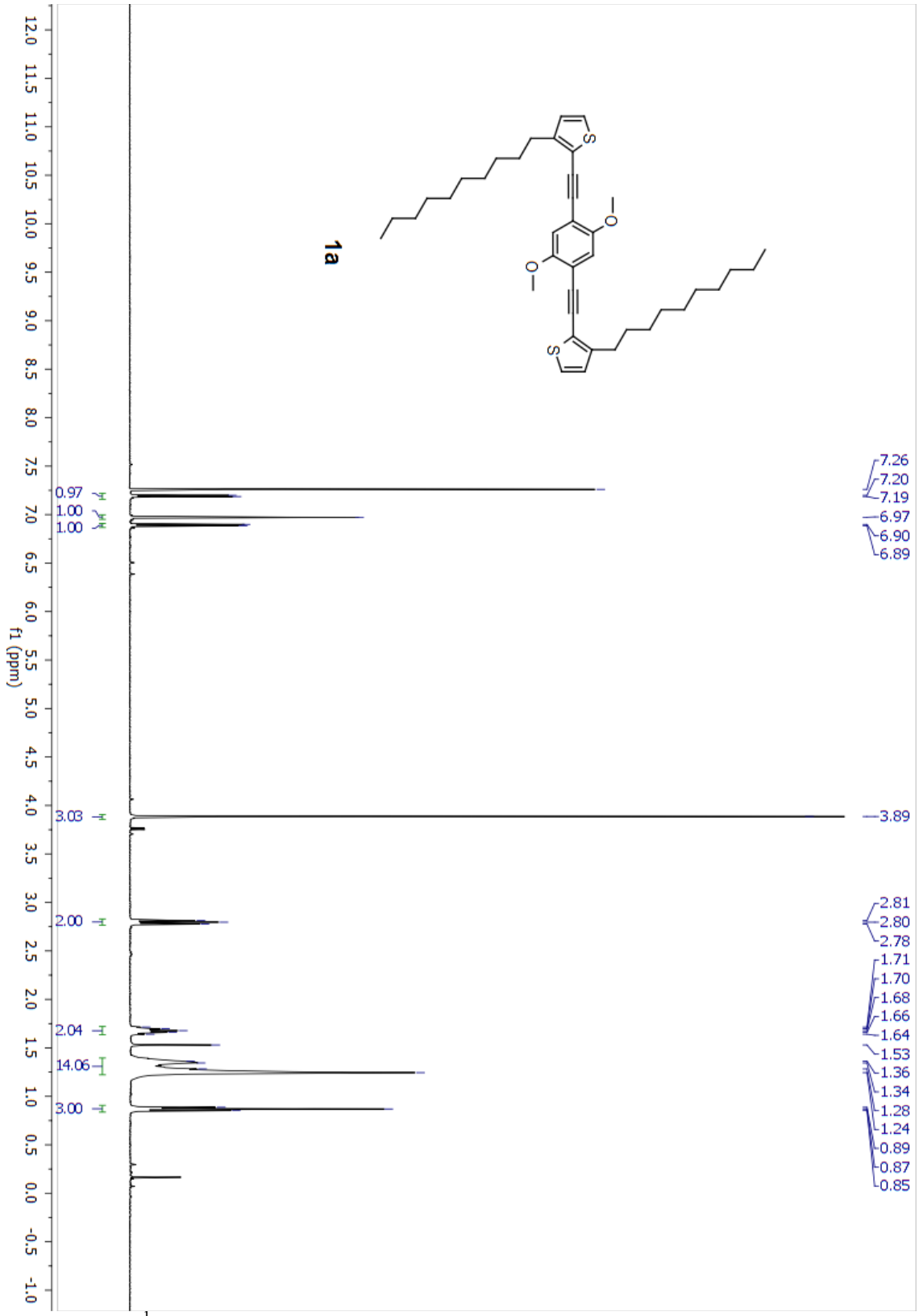

Figure S2.5. ^{1}H NMR of 2,2'-((2,5-dimethoxy-1,4-phenylene)bis(ethyne-2,1-diyl))bis(3-decylthiophene) (**1a**).

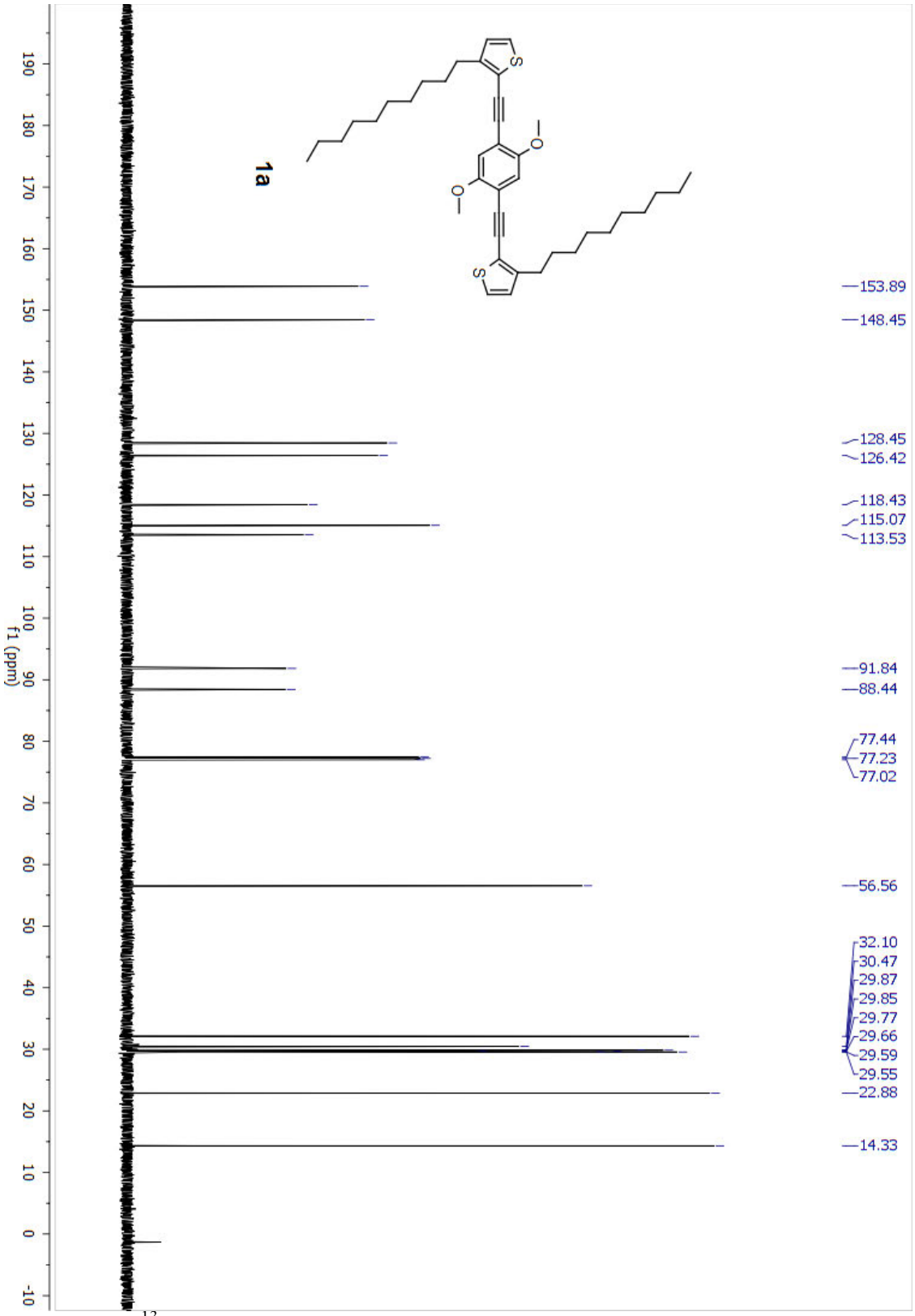

Figure S2.6. ^{13}C NMR of 2,2'-((2,5-dimethoxy-1,4-phenylene)bis(ethyne-2,1-diyl))bis(3-decylthiophene) (**1a**).

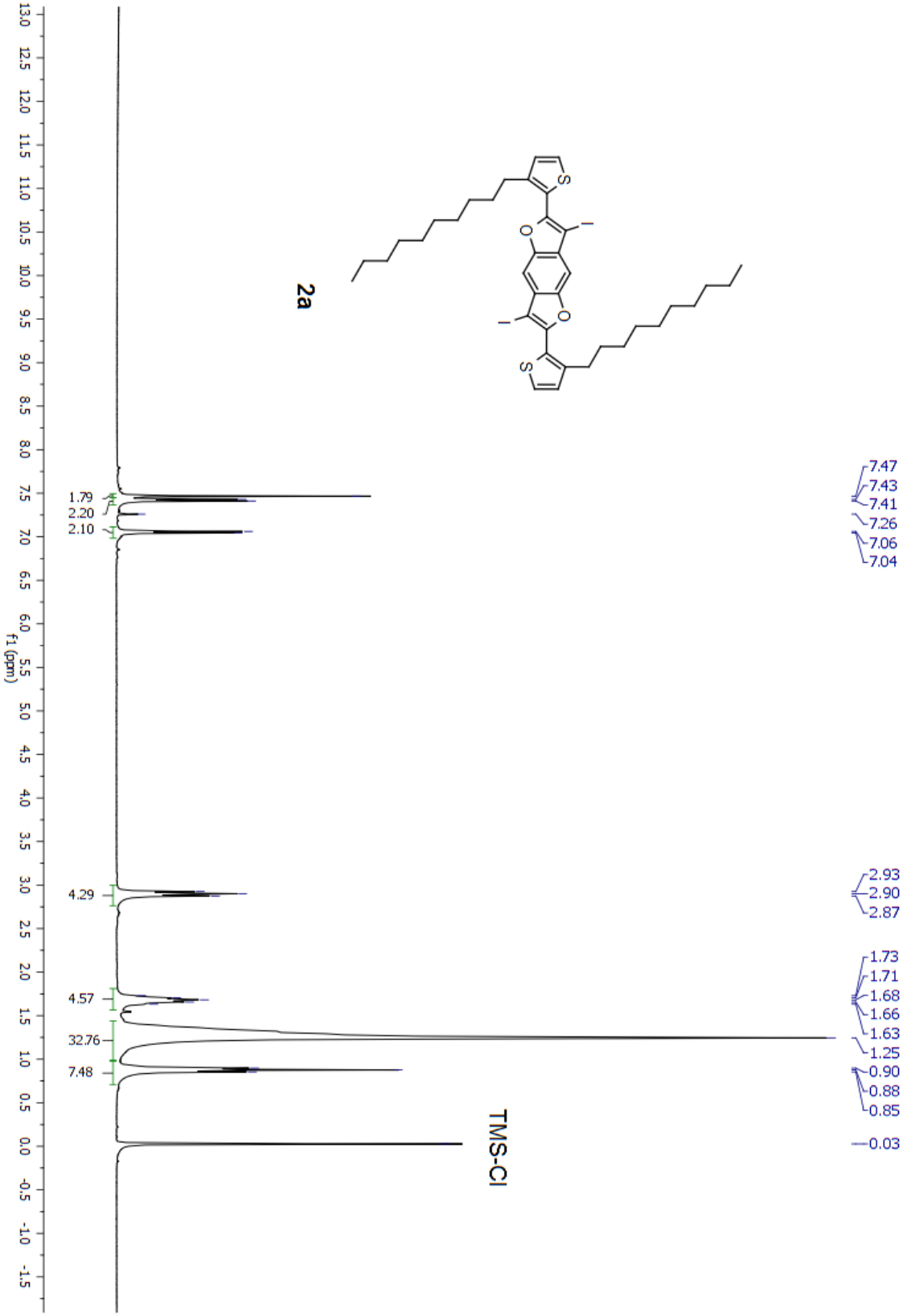

Figure S2.7. ^{1}H NMR of 2,6-bis(3-decylthiophen-2-yl)-3,7-diiodobenzo[1,2-*b*:4,5-*b*']difuran (**2a**).

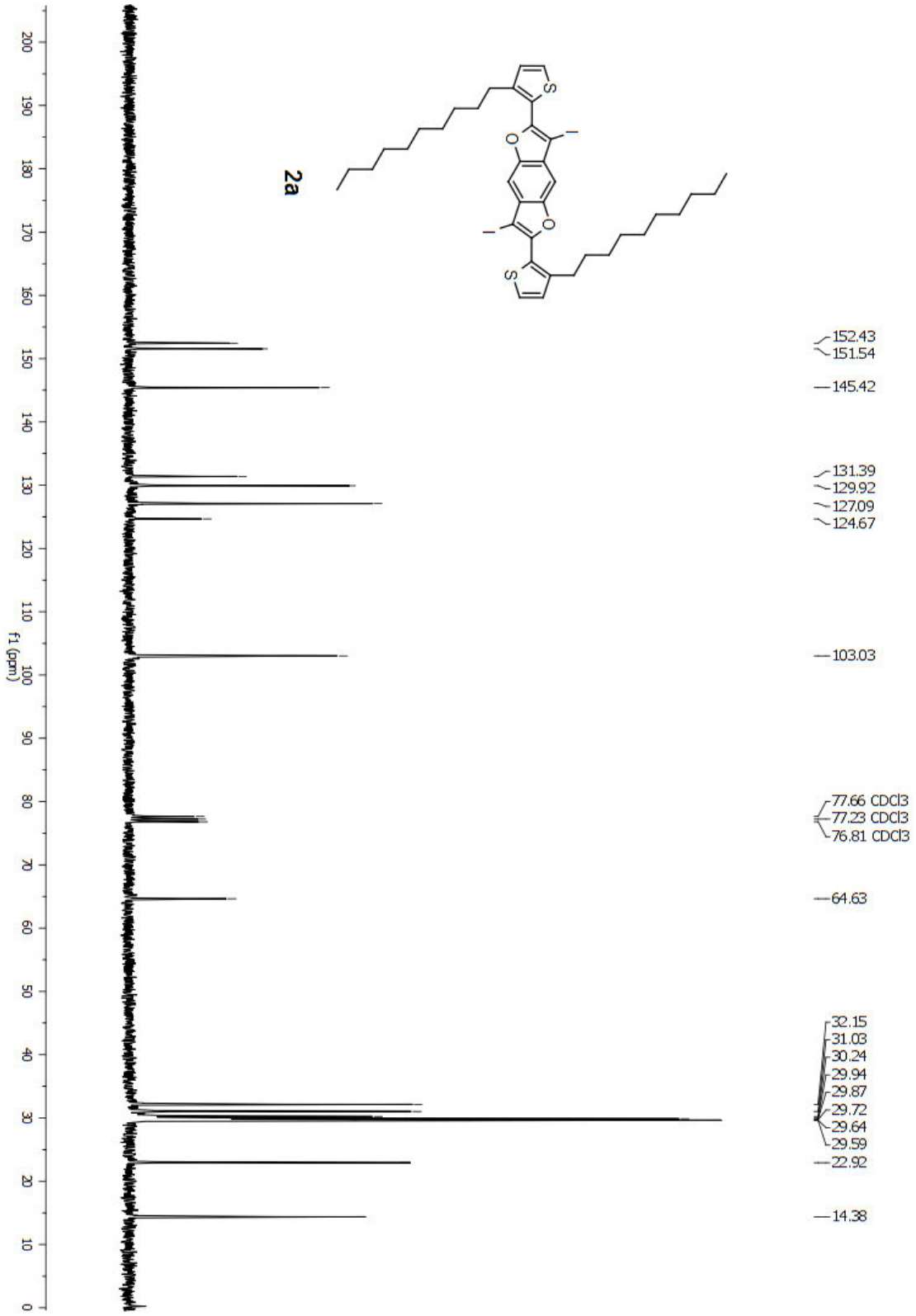

Figure S2.8. ^{13}C NMR of 2,6-bis(3-decylthiophen-2-yl)-3,7-diiodobenzo[1,2-*b*:4,5-*b*']difuran (**2a**).

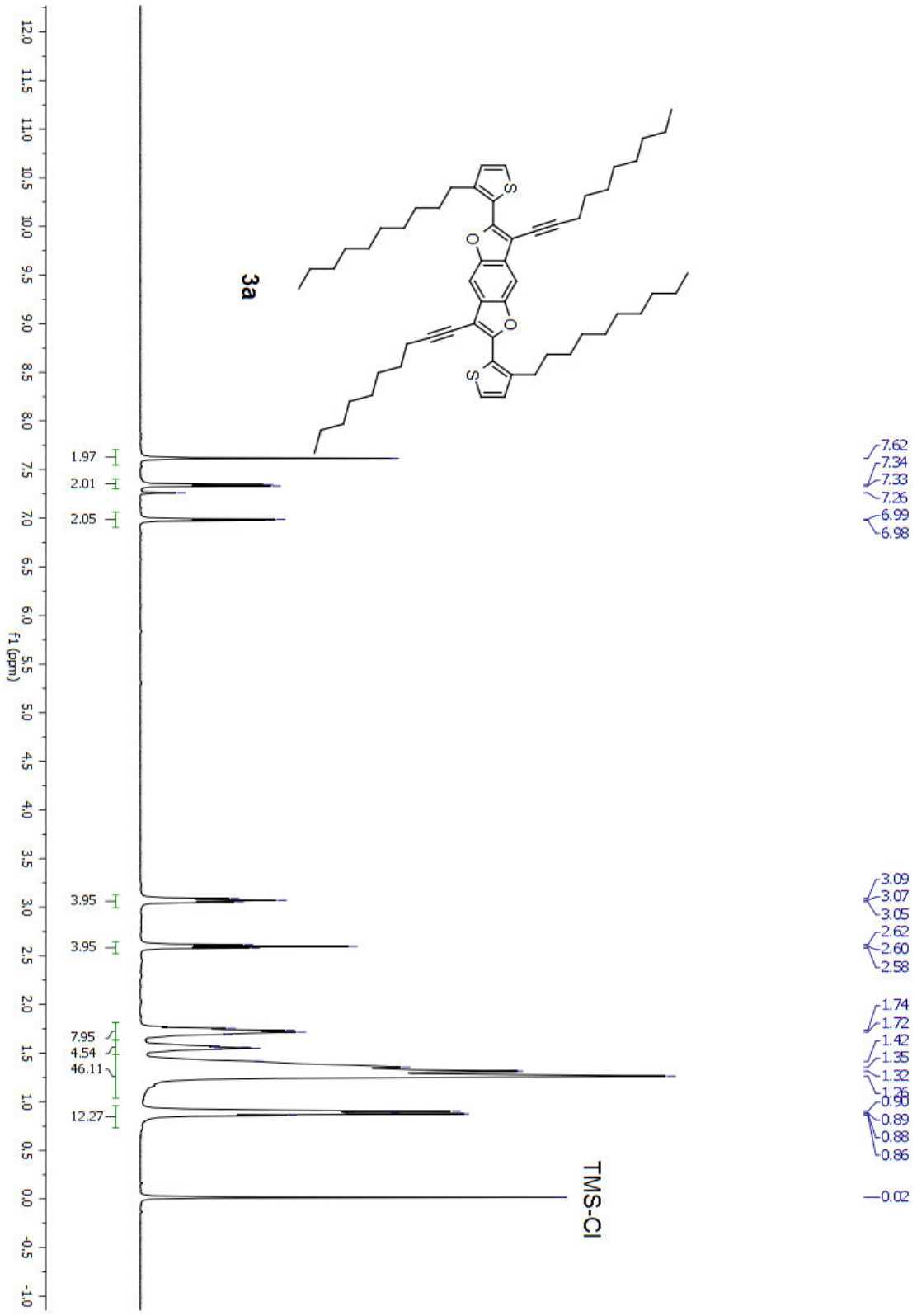

Figure S2.9. ^{1}H NMR of 3,7-di(dec-1-yn-1-yl)-2,6-bis(3-decylthiophen-2-yl)benzo[1,2-*b*:4,5-*b*']difuran (**3a**).

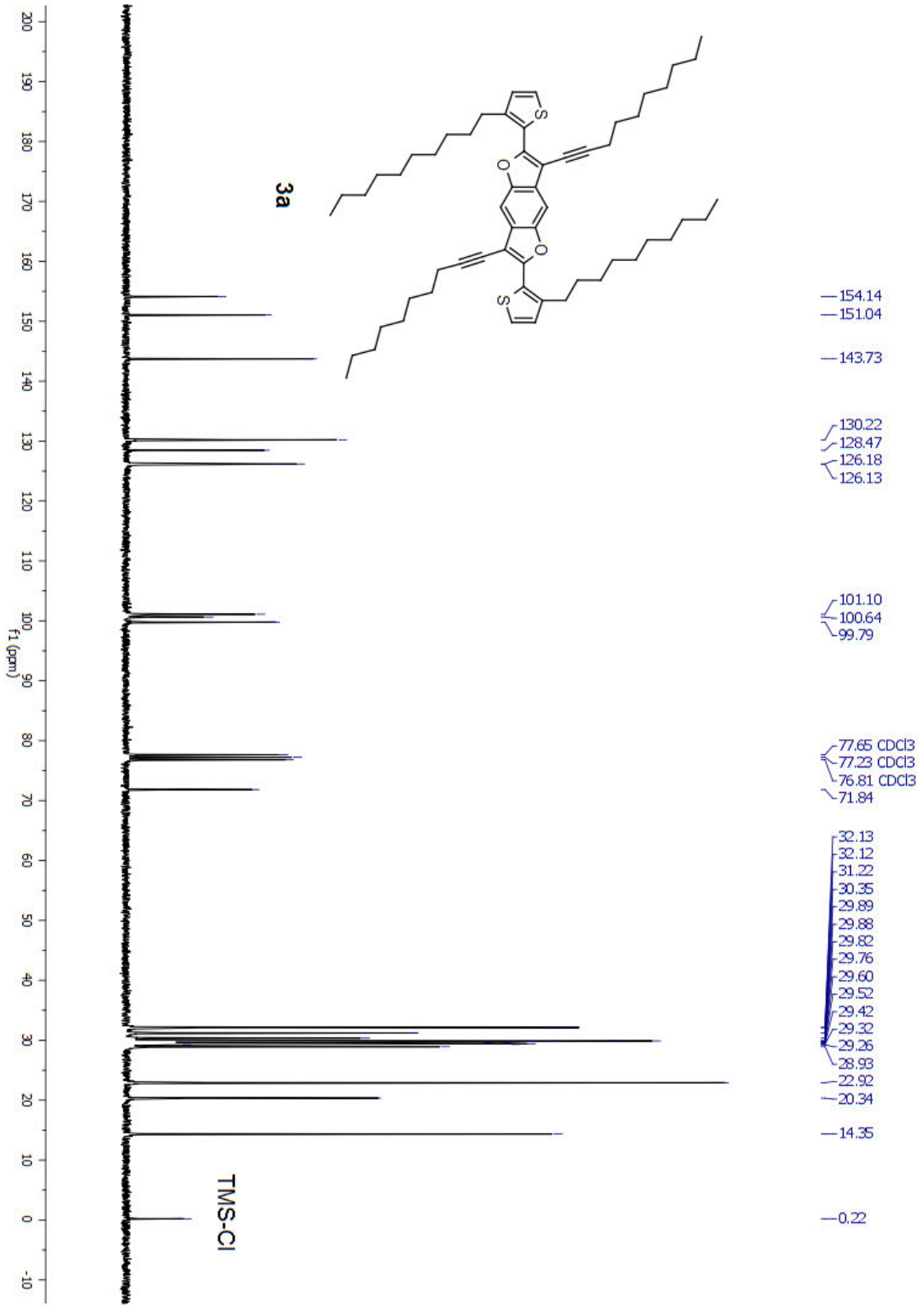

Figure S2.10. ^{13}C NMR of 3,7-di(dec-1-yn-1-yl)-2,6-bis(3-decylthiophen-2-yl)benzo[1,2-*b*:4,5-*b*']difuran (**3a**).

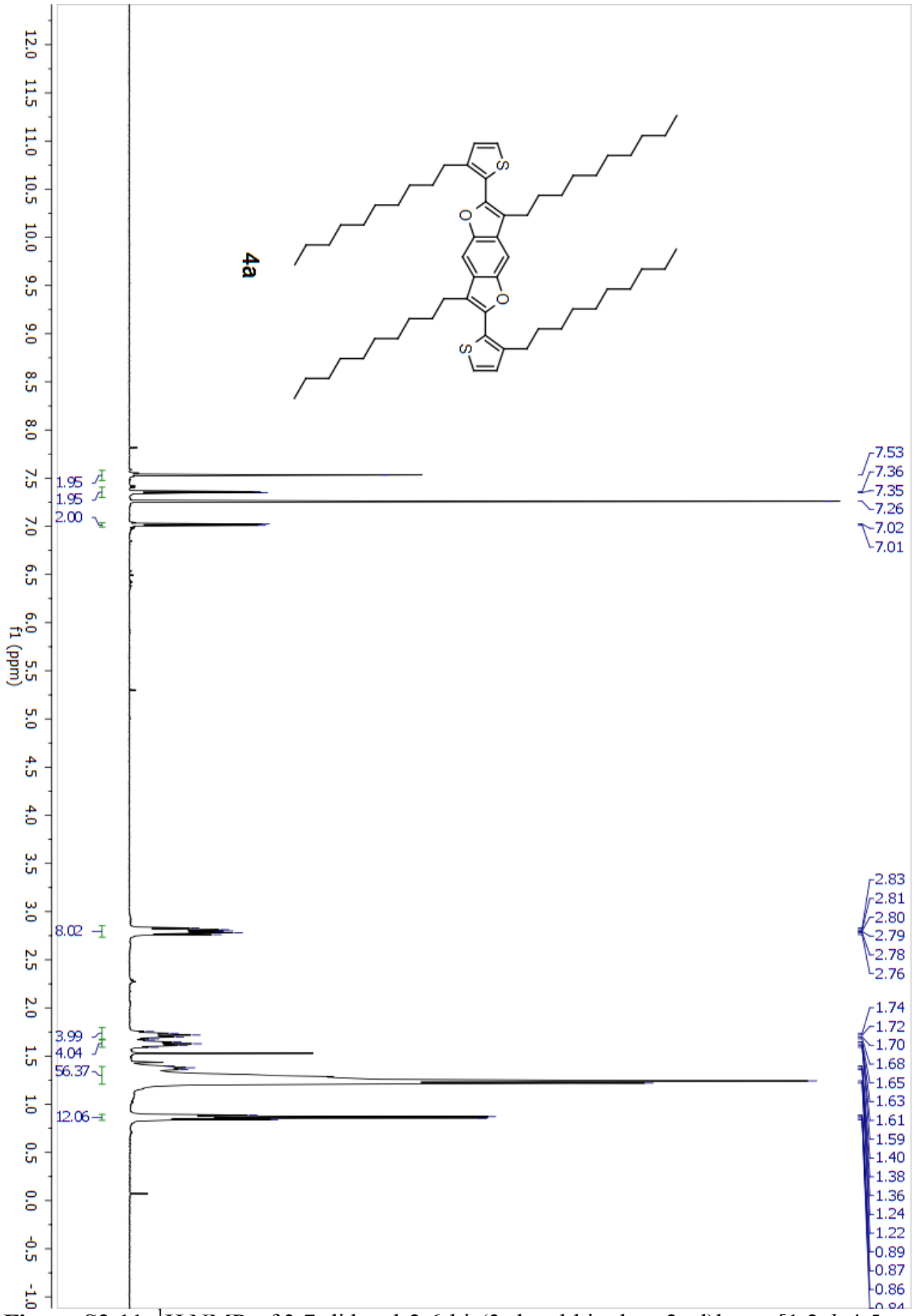

Figure S2.11. ^{1}H NMR of 3,7-didecyl-2,6-bis(3-decylthiophen-2-yl)benzo[1,2-*b*:4,5-*b*']difuran (**4a**).

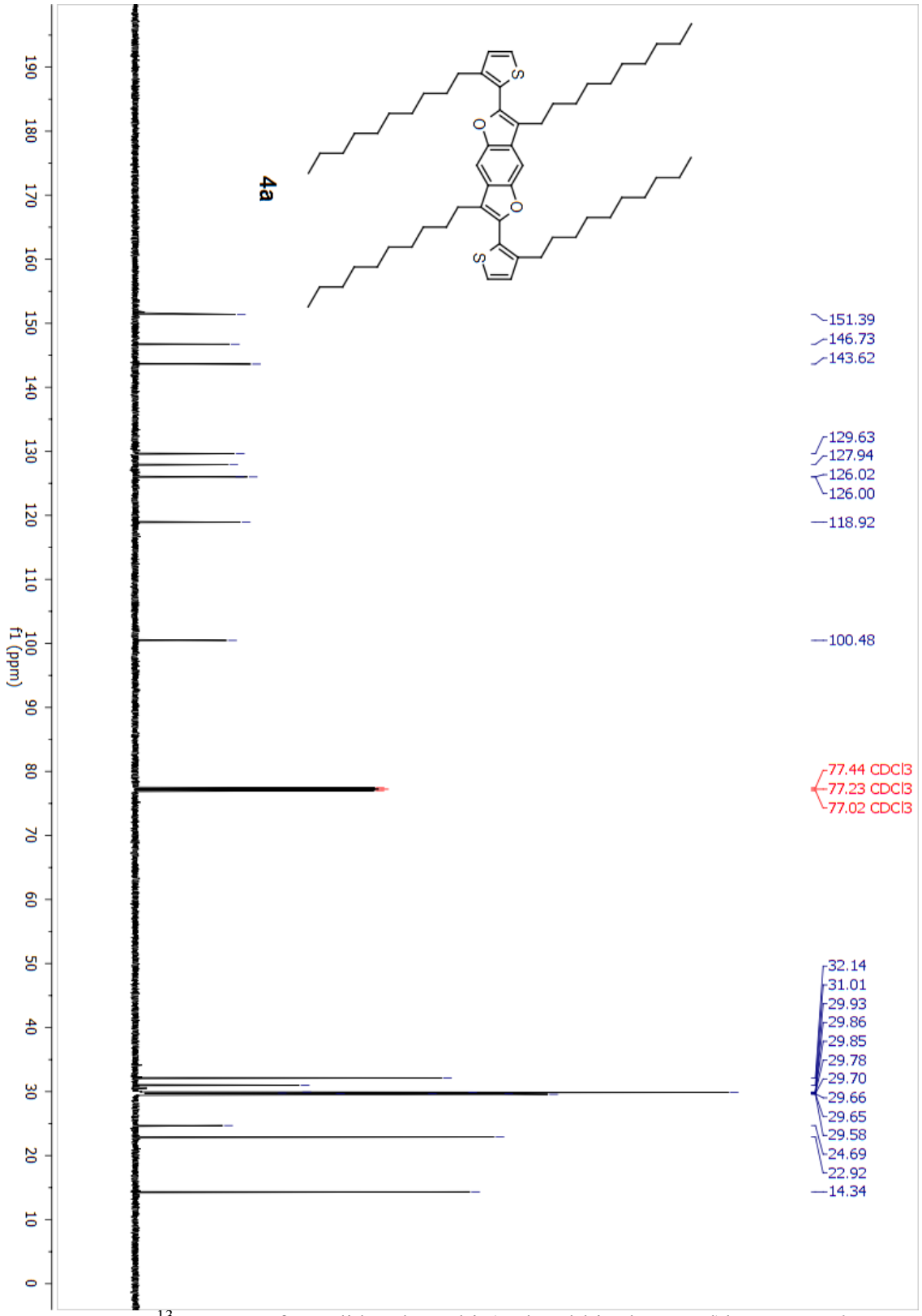

Figure S2.12. ^{13}C NMR of 3,7-didecyl-2,6-bis(3-decylthiophen-2-yl)benzo[1,2-*b*:4,5-*b*']difuran (**4a**).

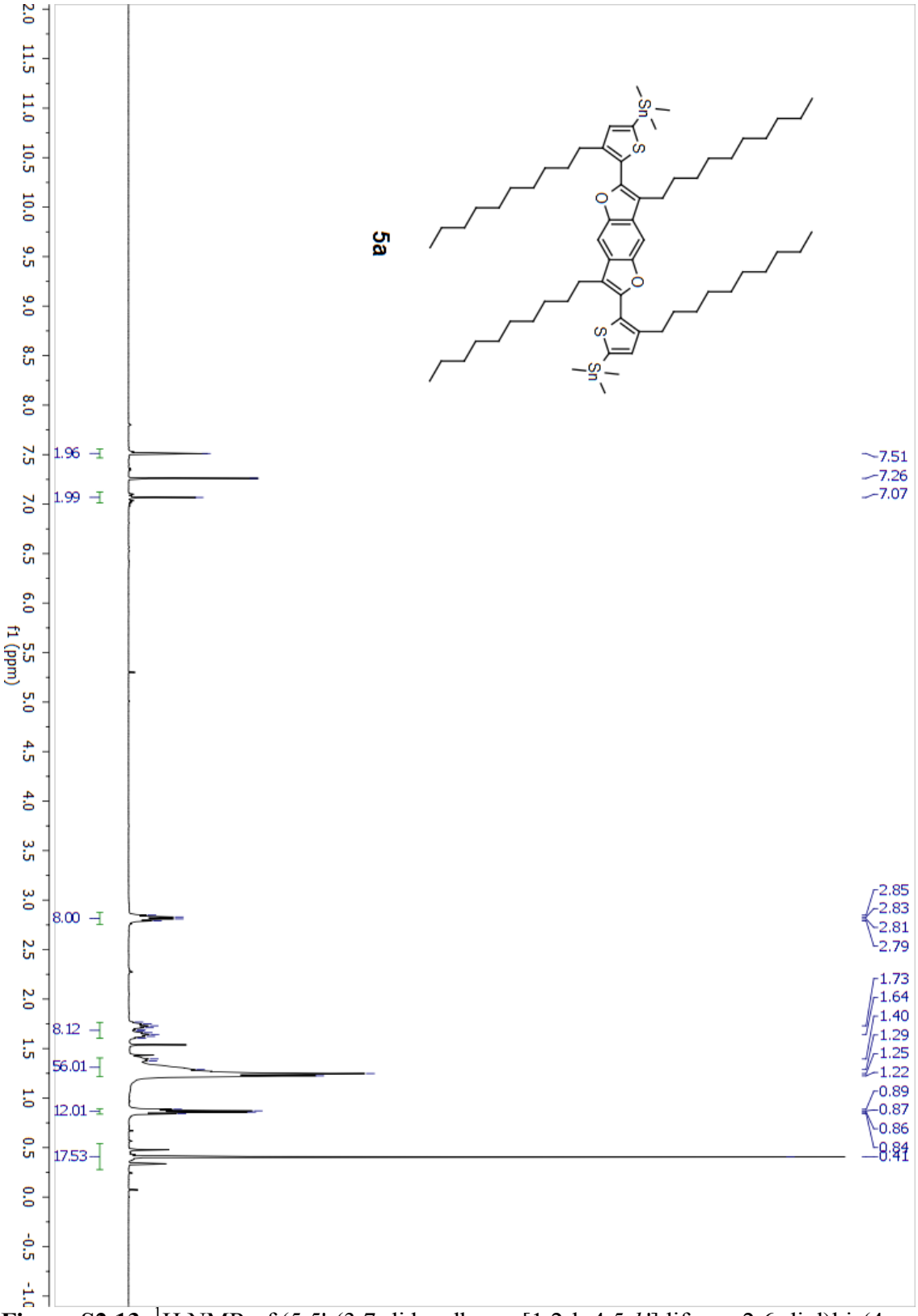

Figure S2.13. ^{1}H NMR of (5,5'-(3,7-didecylbenzo[1,2-b:4,5-*b*']difuran-2,6-diyl)bis(4-decylthiophene-5,2-diyl))bis(trimethylstannane) (**5a**).

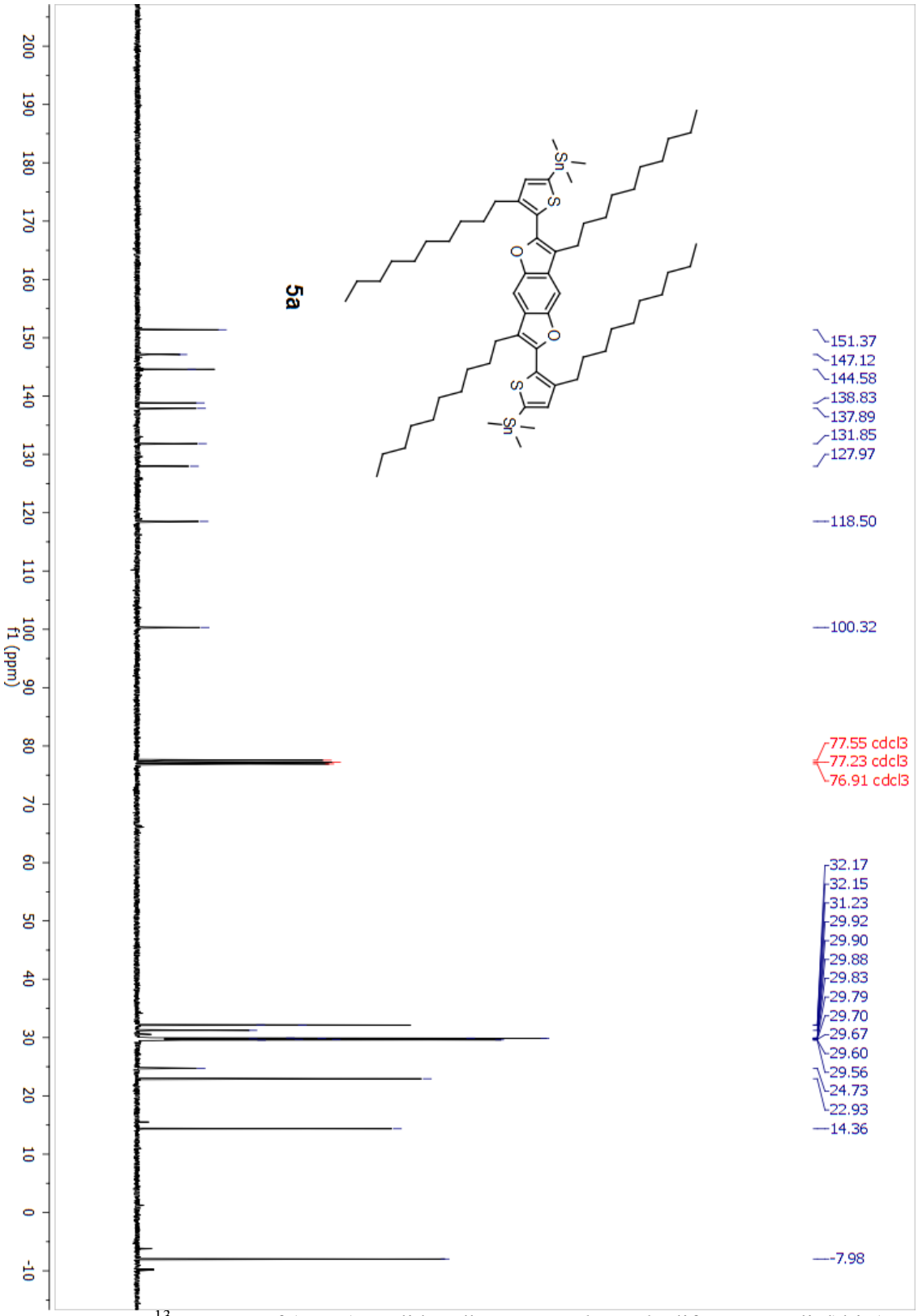

Figure S2.14. ^{13}C NMR of (5,5'-(3,7-didecylbenzo[1,2-*b*:4,5-*b*']difuran-2,6-diyl)bis(4-decylthiophene-5,2-diyl))bis(trimethylstannane) (**5a**).

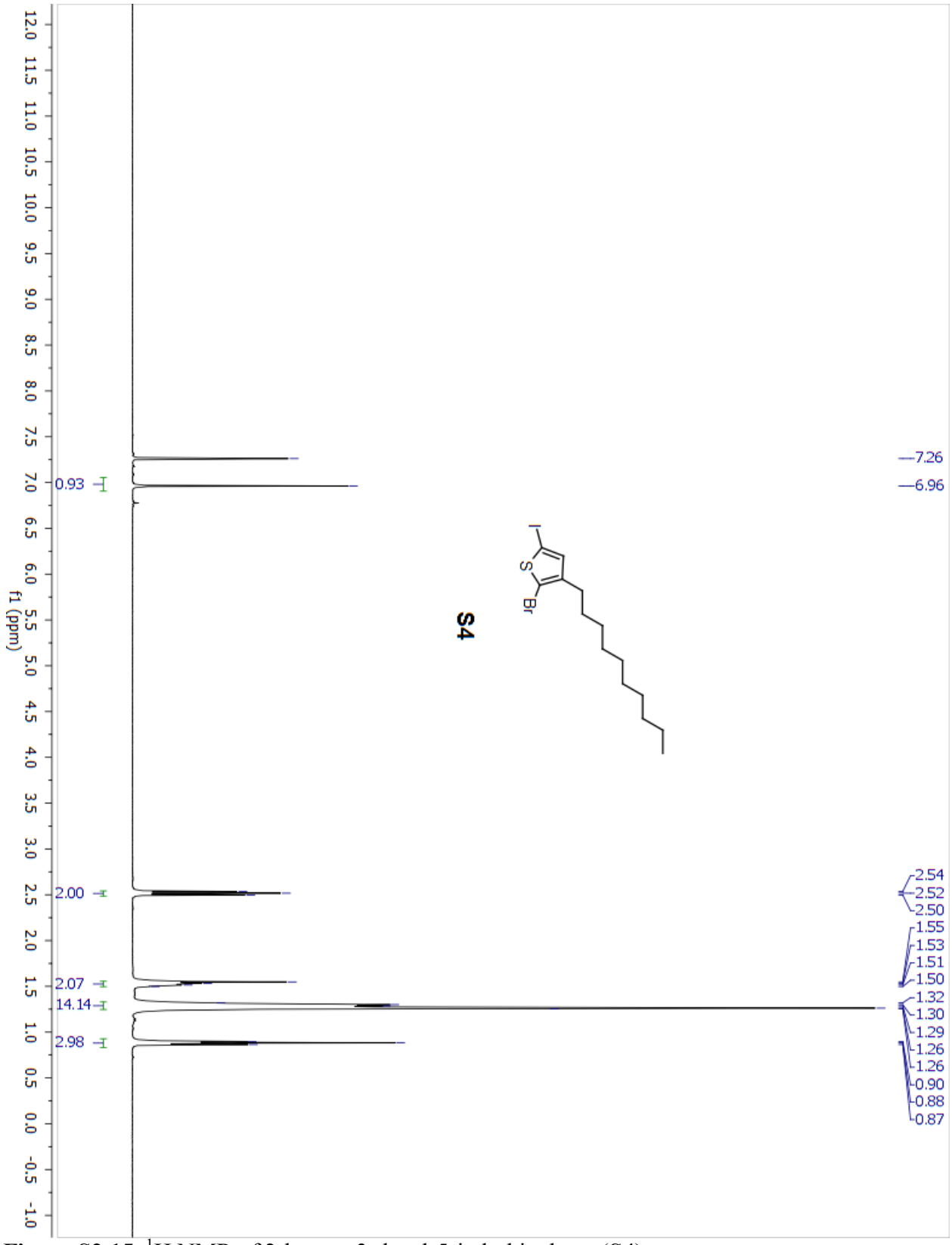

Figure S2.15. ^{1}H NMR of 2-bromo-3-decyl-5-iodothiophene (**S4**).

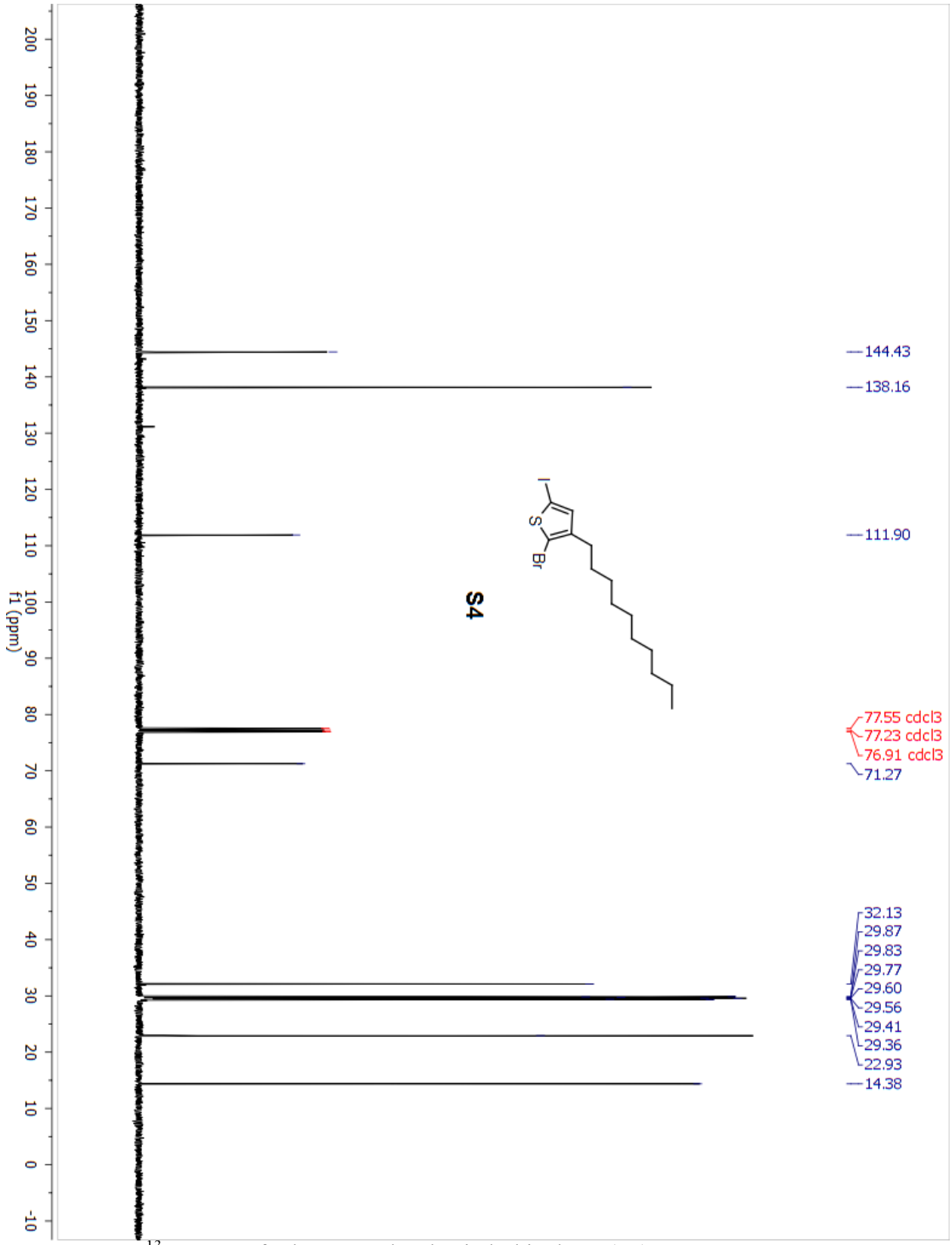

Figure S2.16. ^{13}C NMR of 2-bromo-3-decyl-5-iodothiophene (**S4**).

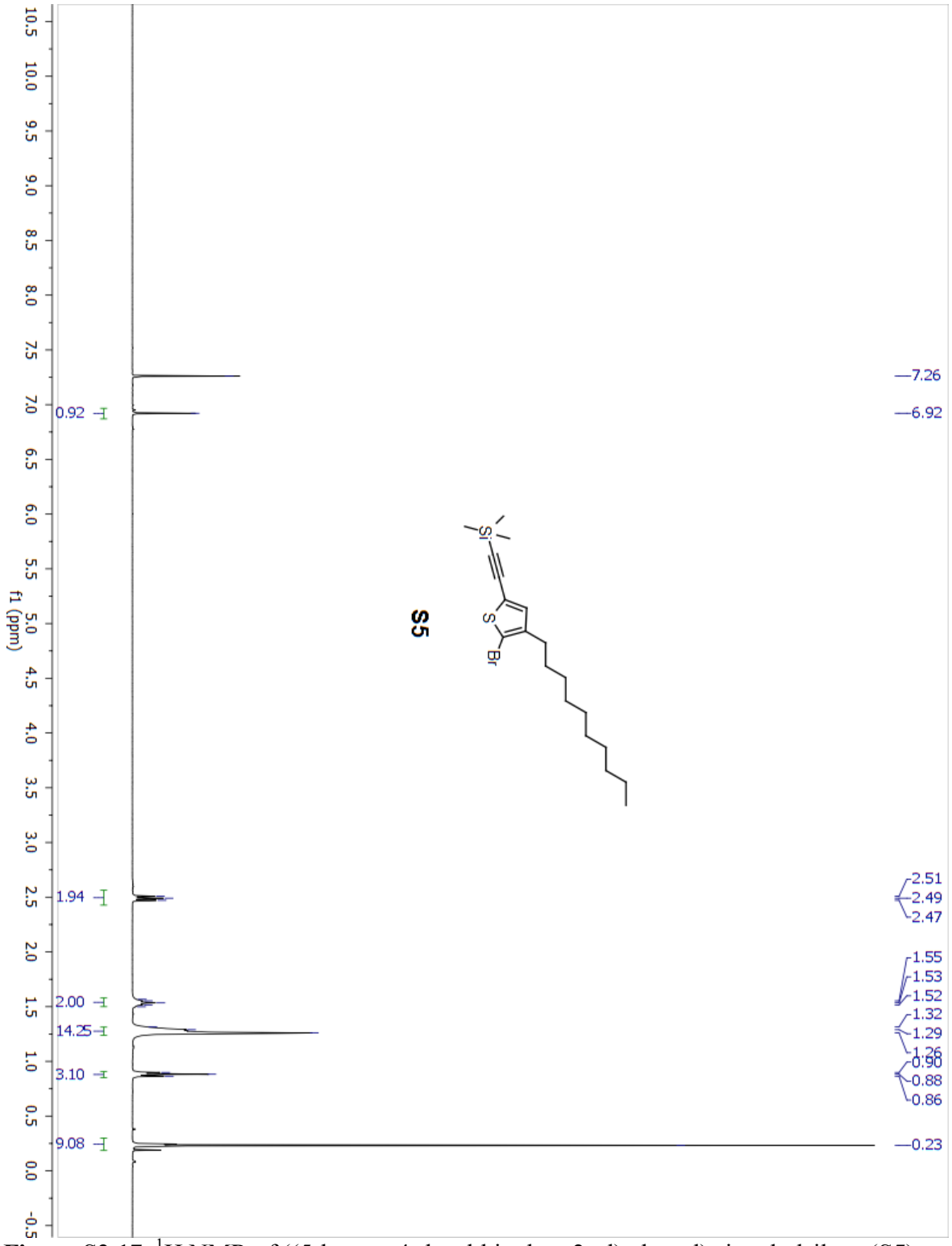

Figure S2.17. ^{1}H NMR of ((5-bromo-4-decylthiophen-2-yl)ethynyl)trimethylsilane (**S5**).

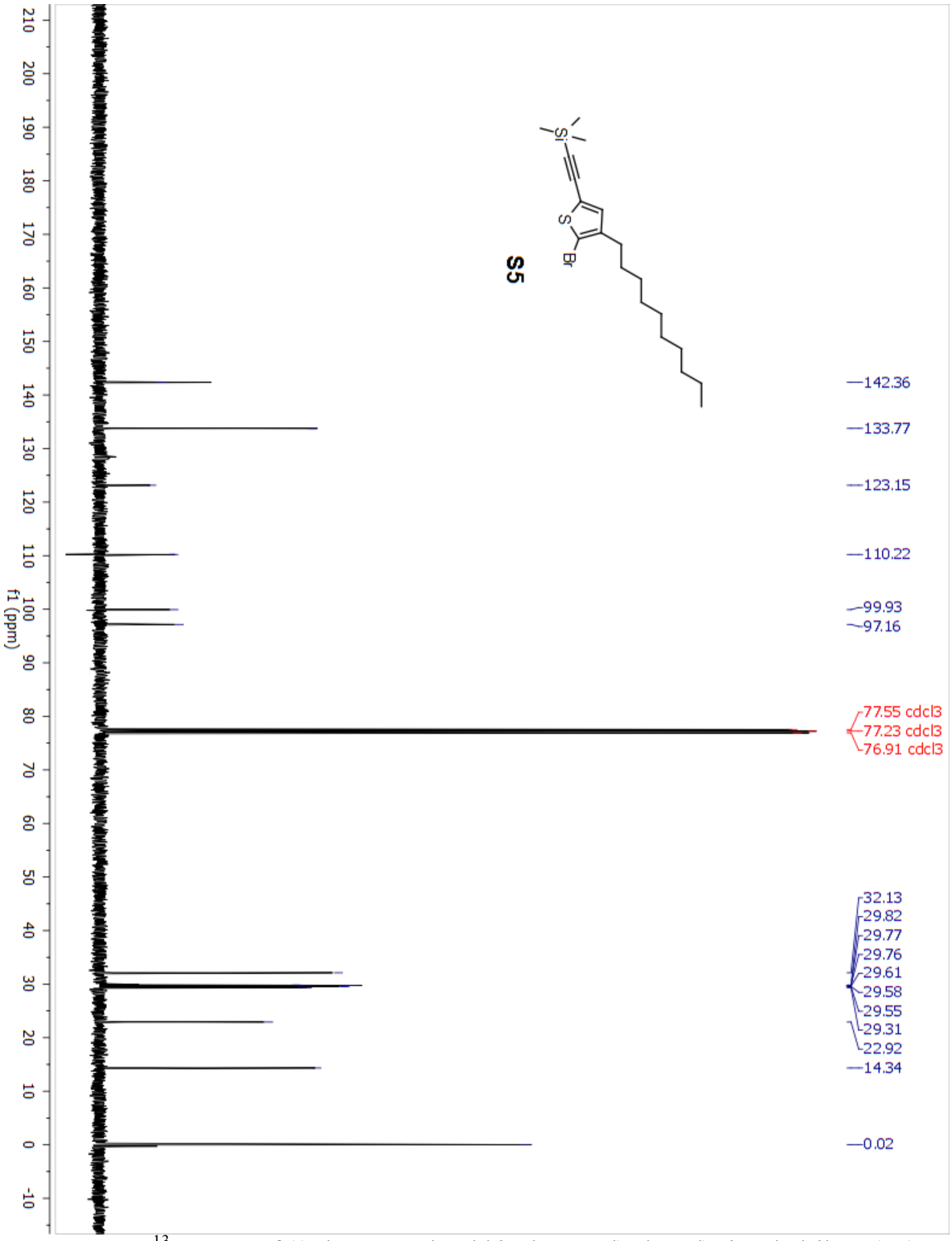

Figure S2.18. ^{13}C NMR of ((5-bromo-4-decylthiophen-2-yl)ethynyl)trimethylsilane (**S5**).

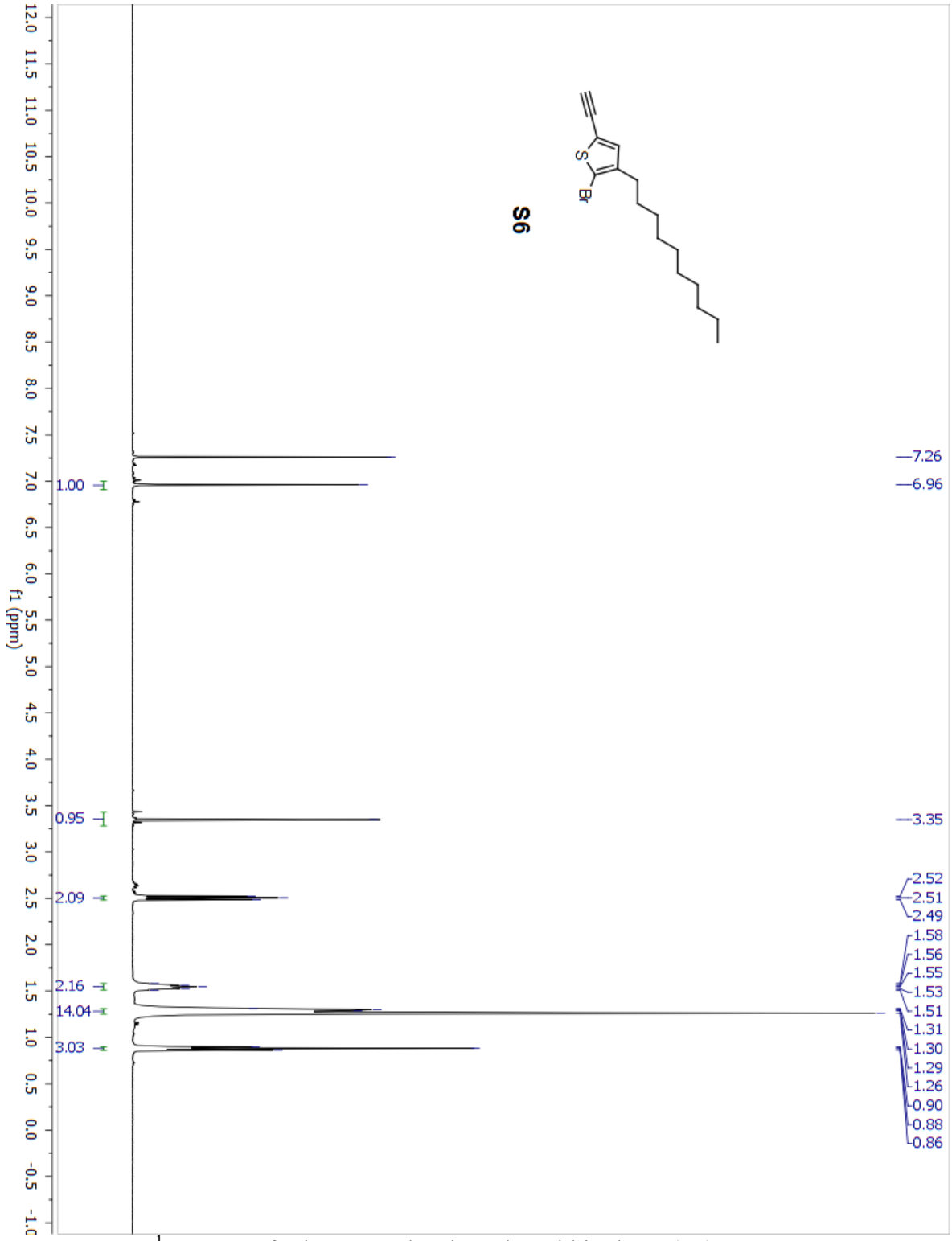

Figure S2.19. ^{1}H NMR of 2-bromo-3-decyl-5-ethynylthiophene (**S6**).

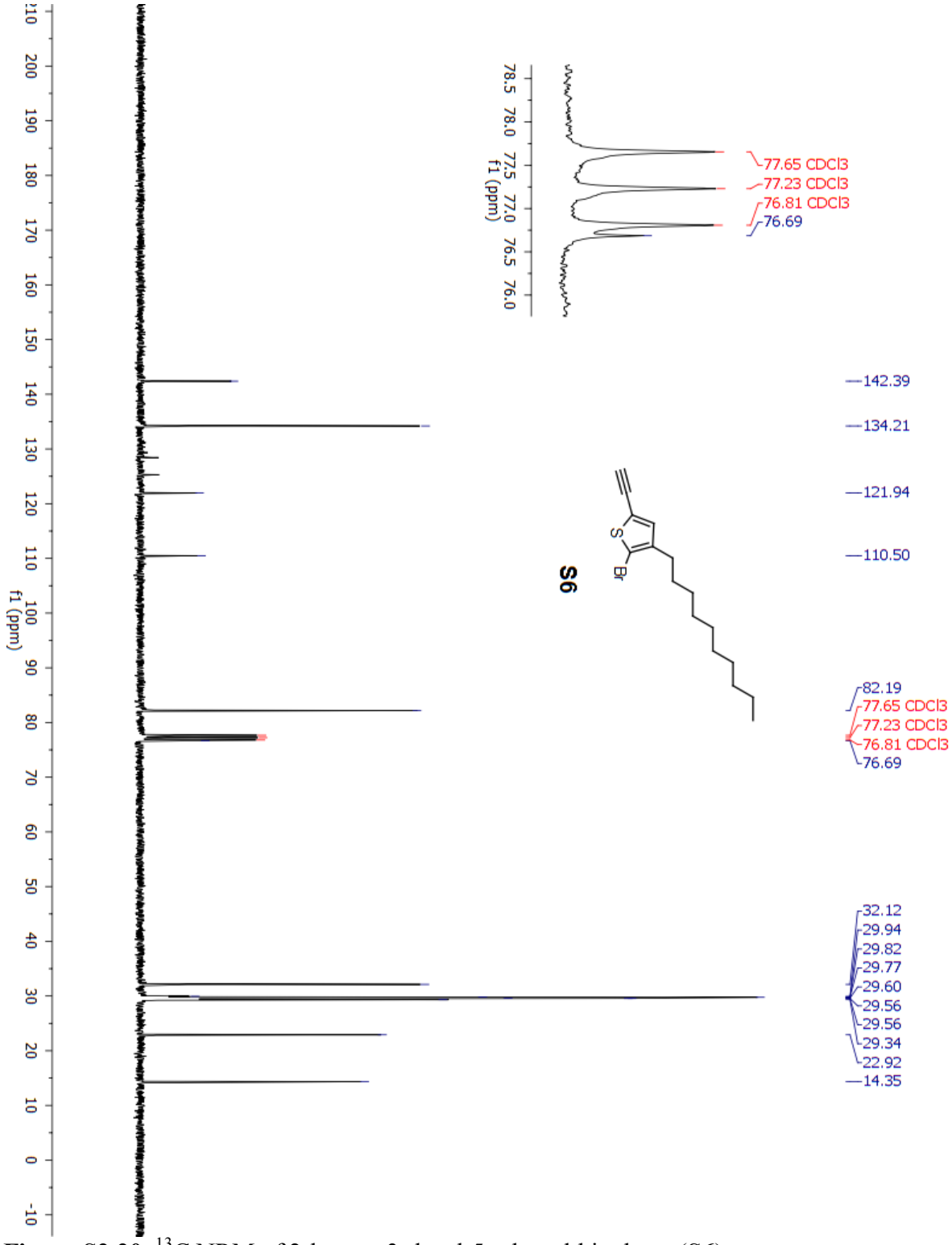

Figure S2.20. ^{13}C NRM of 2-bromo-3-decyl-5-ethynylthiophene (**S6**).

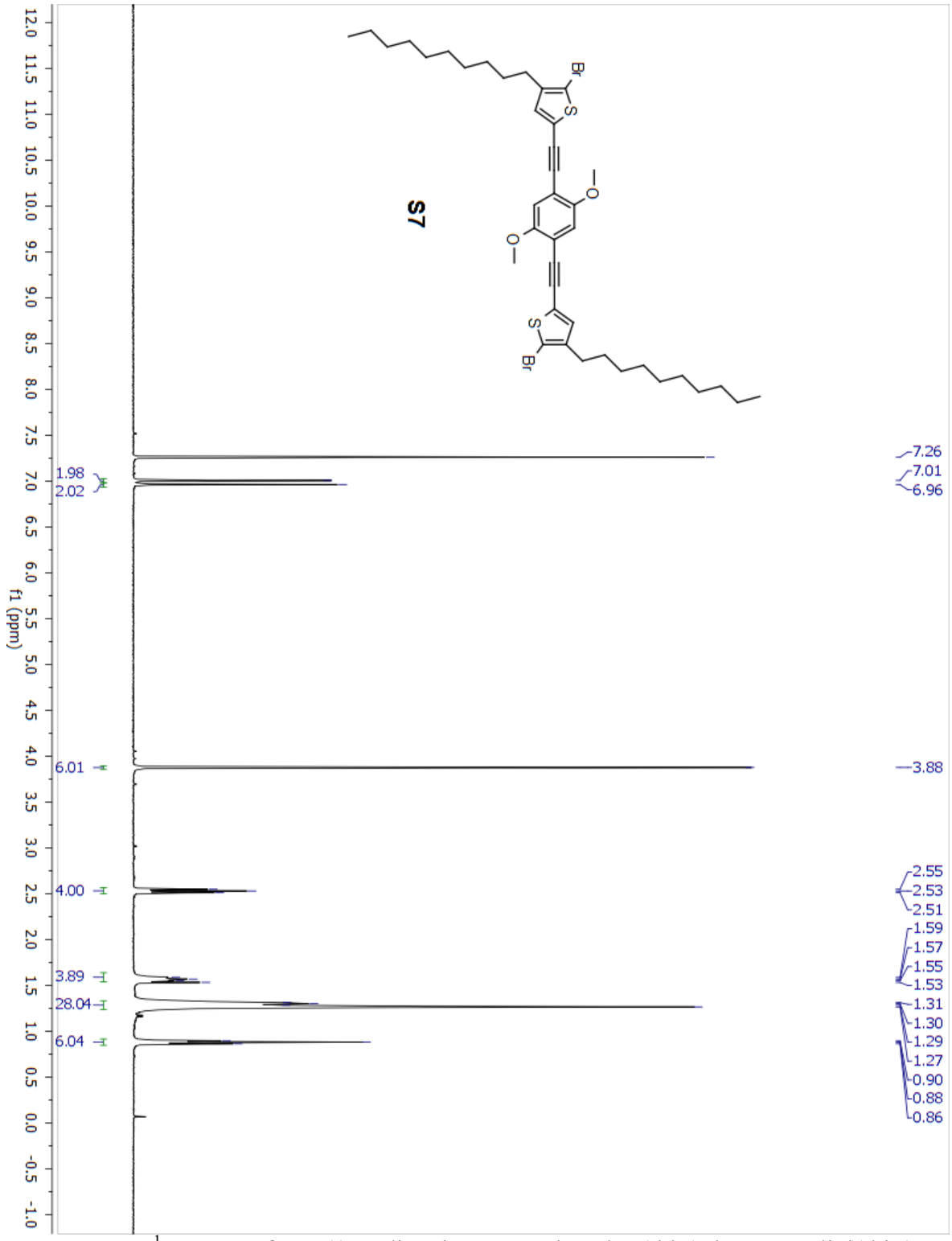

Figure S2.21. ^{1}H NMR of 5,5'-((2,5-dimethoxy-1,4-phenylene)bis(ethyne-2,1-diyl))bis(2-bromo-3-decylthiophene) (**S7**).

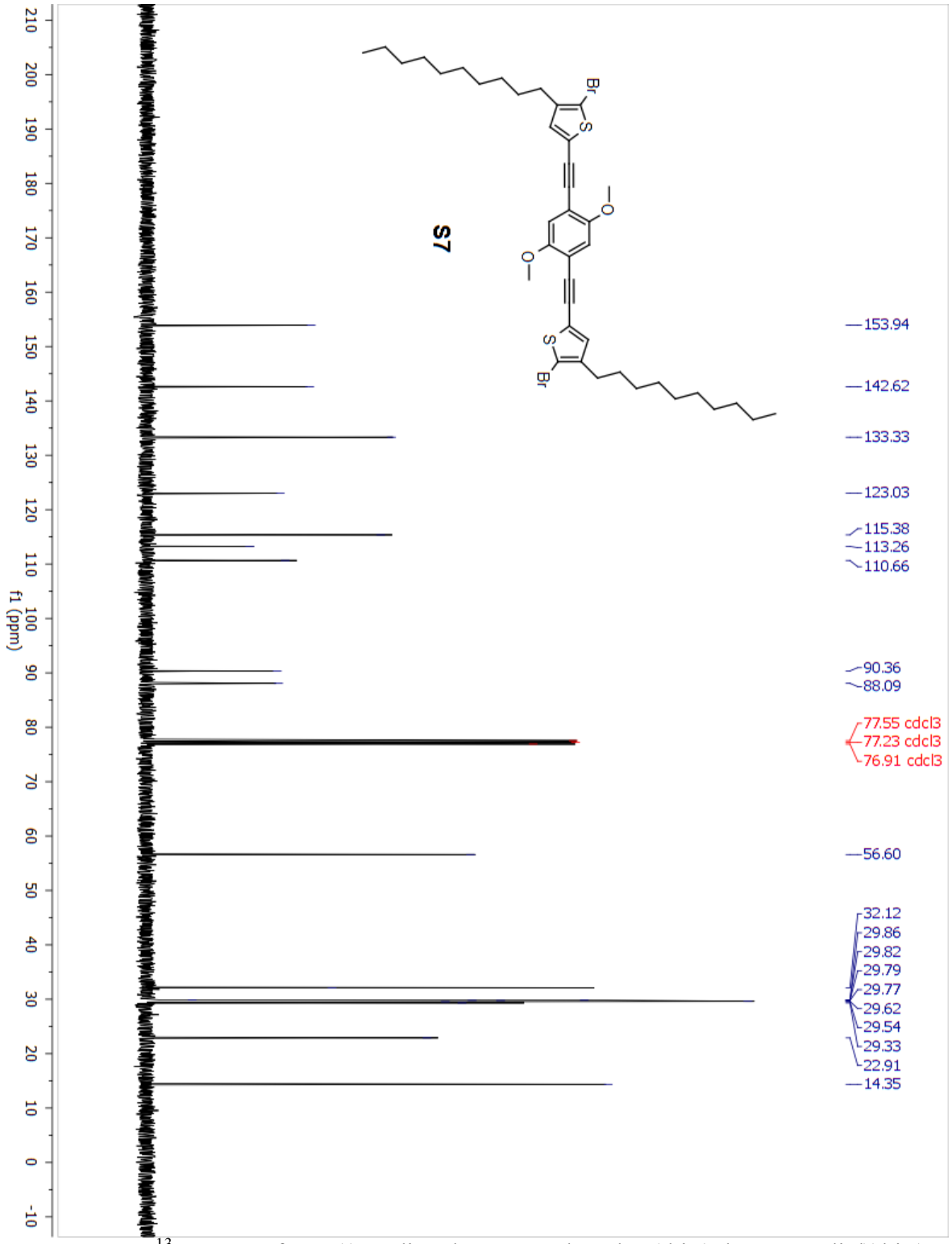

Figure S2.22. ^{13}C NMR of 5,5'-((2,5-dimethoxy-1,4-phenylene)bis(ethyne-2,1-diyl))bis(2-bromo-3-decylthiophene) (**S7**).

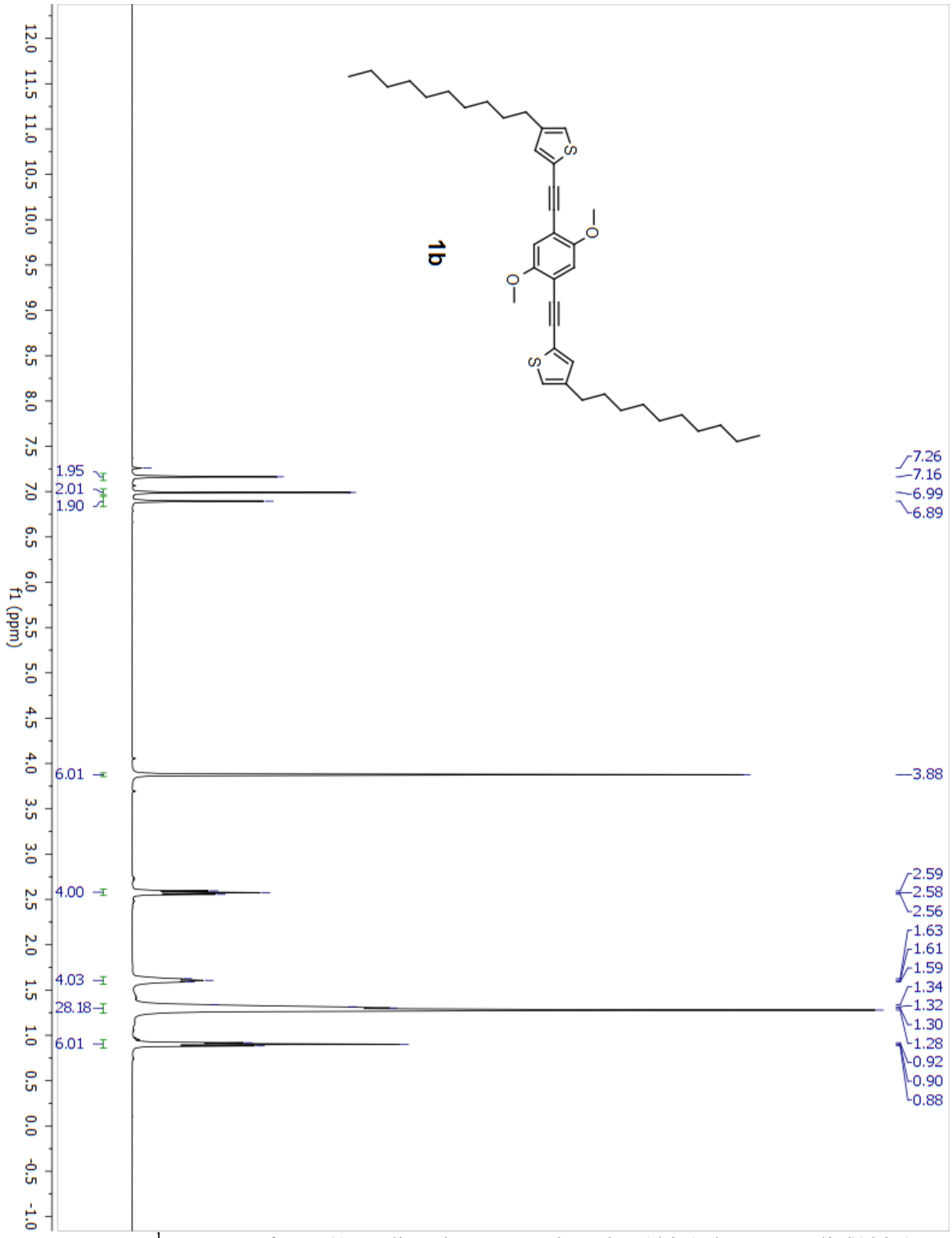

Figure S2.23. ^{1}H NMR of 5,5'-((2,5-dimethoxy-1,4-phenylene)bis(ethyne-2,1-diyl))bis(3-decylthiophene) (**1b**).

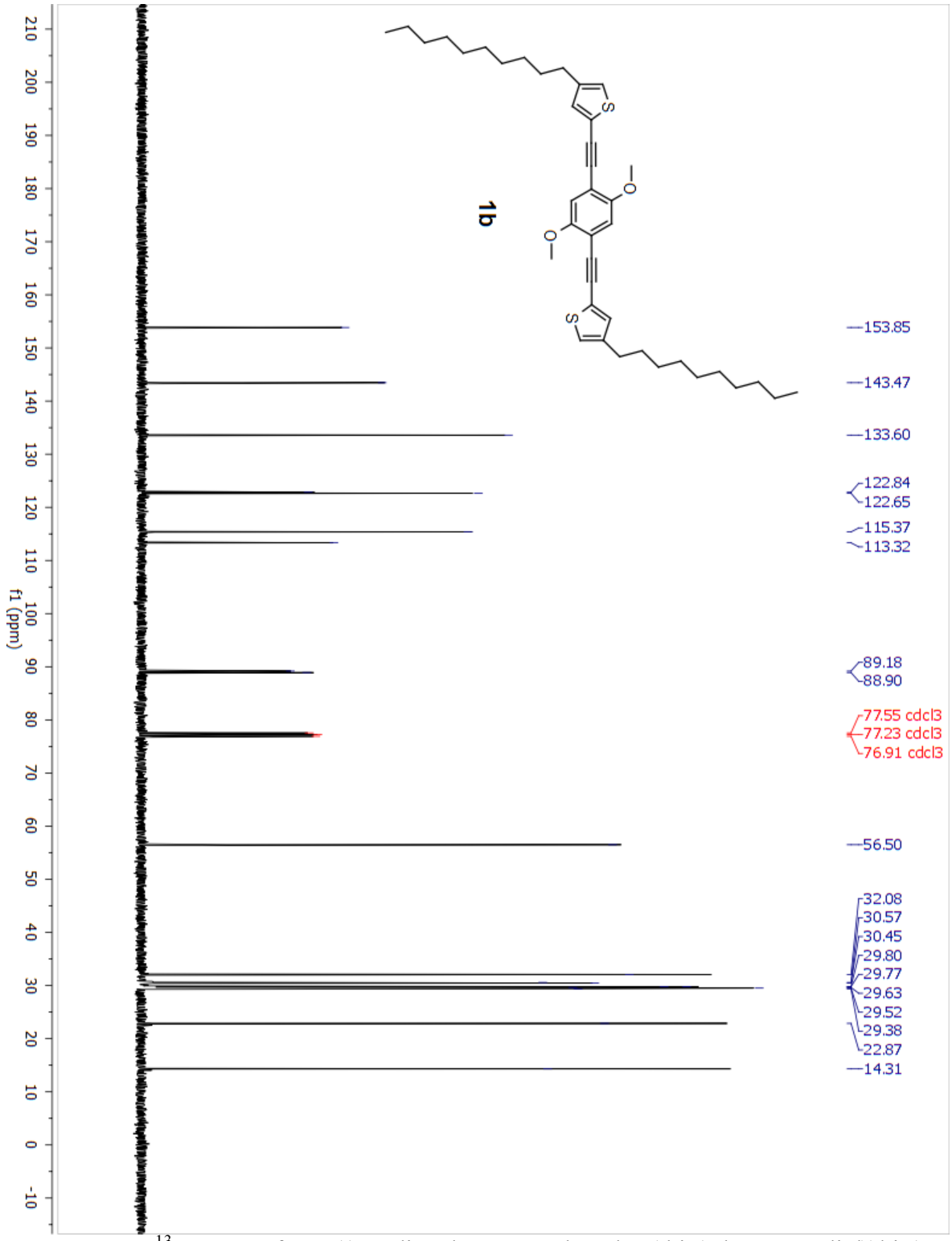

Figure S2.24. ^{13}C NMR of 5,5'-((2,5-dimethoxy-1,4-phenylene)bis(ethyne-2,1-diyl))bis(3-decylthiophene) (**1b**).

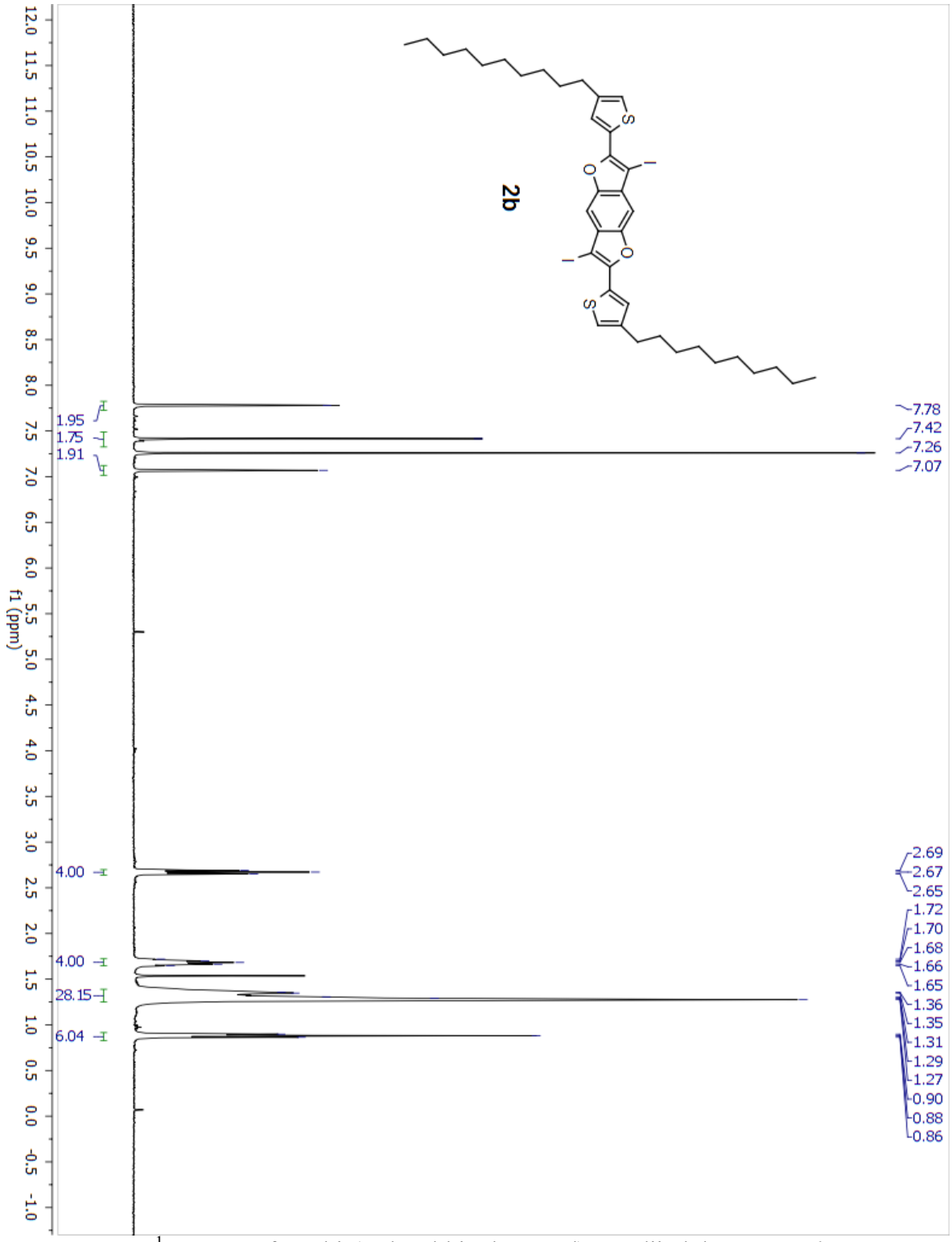

Figure S2.25. ^{1}H NMR of 2,6-bis(4-decylthiophen-2-yl)-3,7-diiodobenzo[1,2-*b*:4,5-*b*']difuran (**2b**).

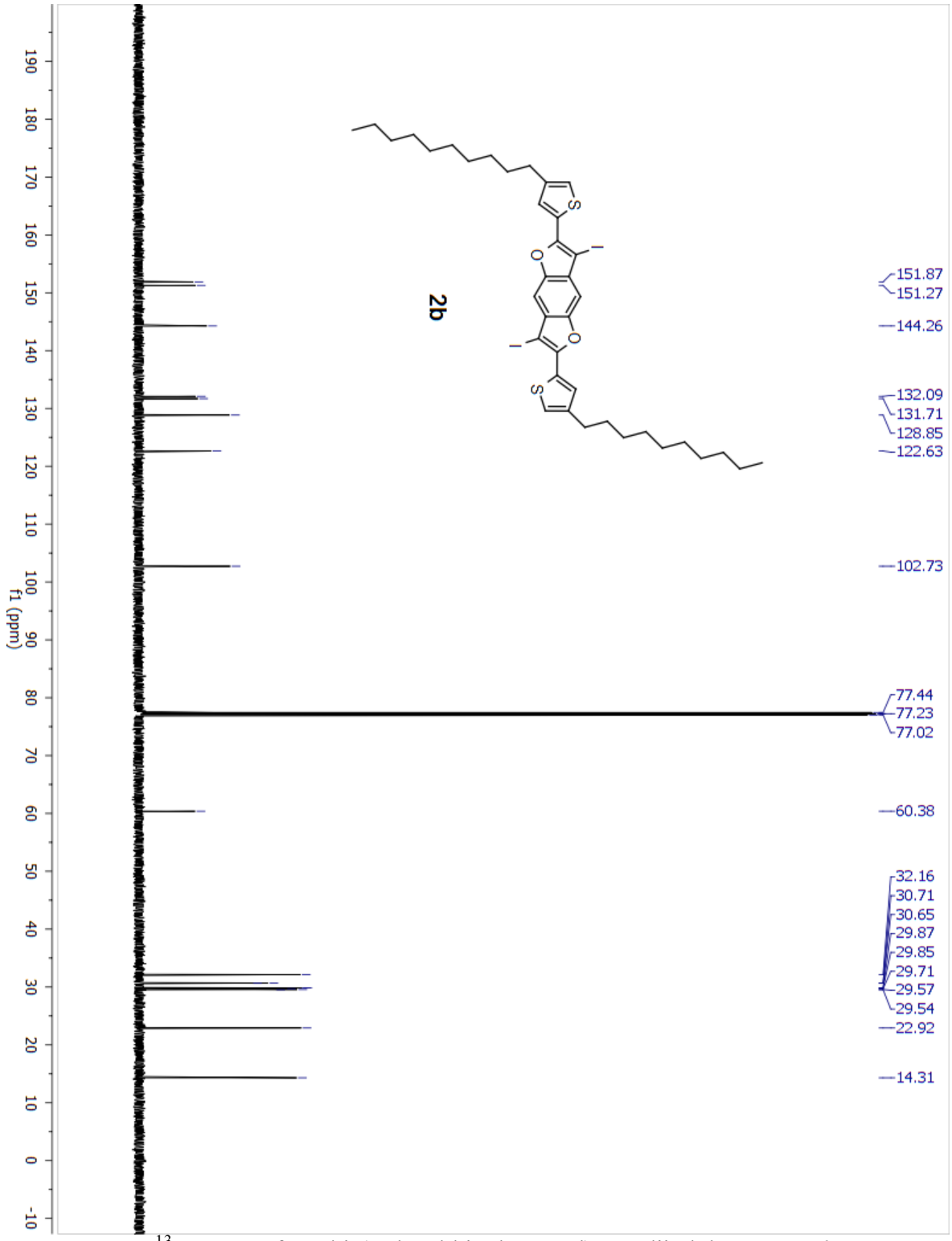

Figure S2.26. ^{13}C NMR of 2,6-bis(4-decylthiophen-2-yl)-3,7-diiodobenzo[1,2-*b*:4,5-*b*']difuran (**2b**).

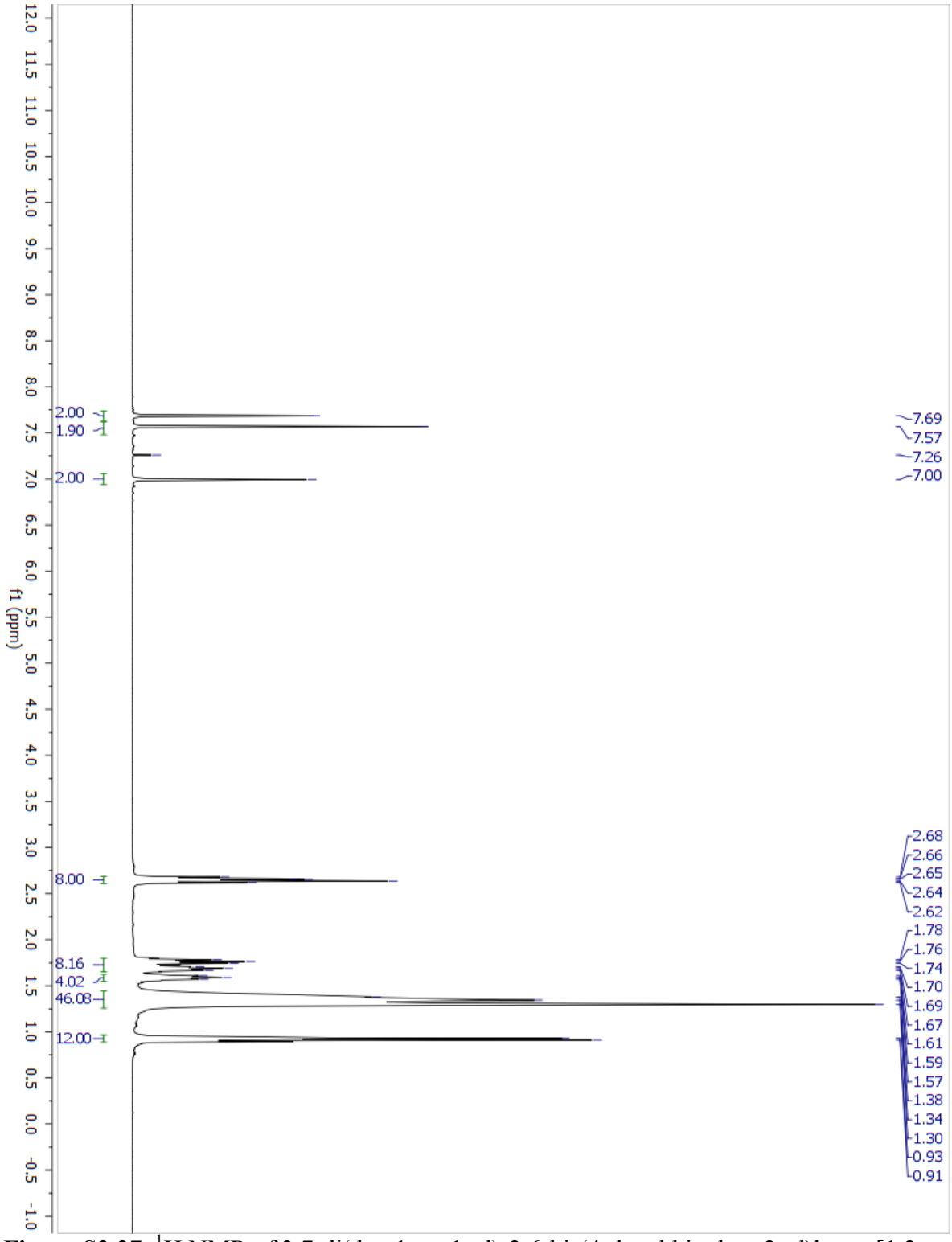

Figure S2.27. ^{1}H NMR of 3,7-di(dec-1-yn-1-yl)-2,6-bis(4-decylthiophen-2-yl)benzo[1,2-*b*:4,5-*b*']difuran (**3b**).

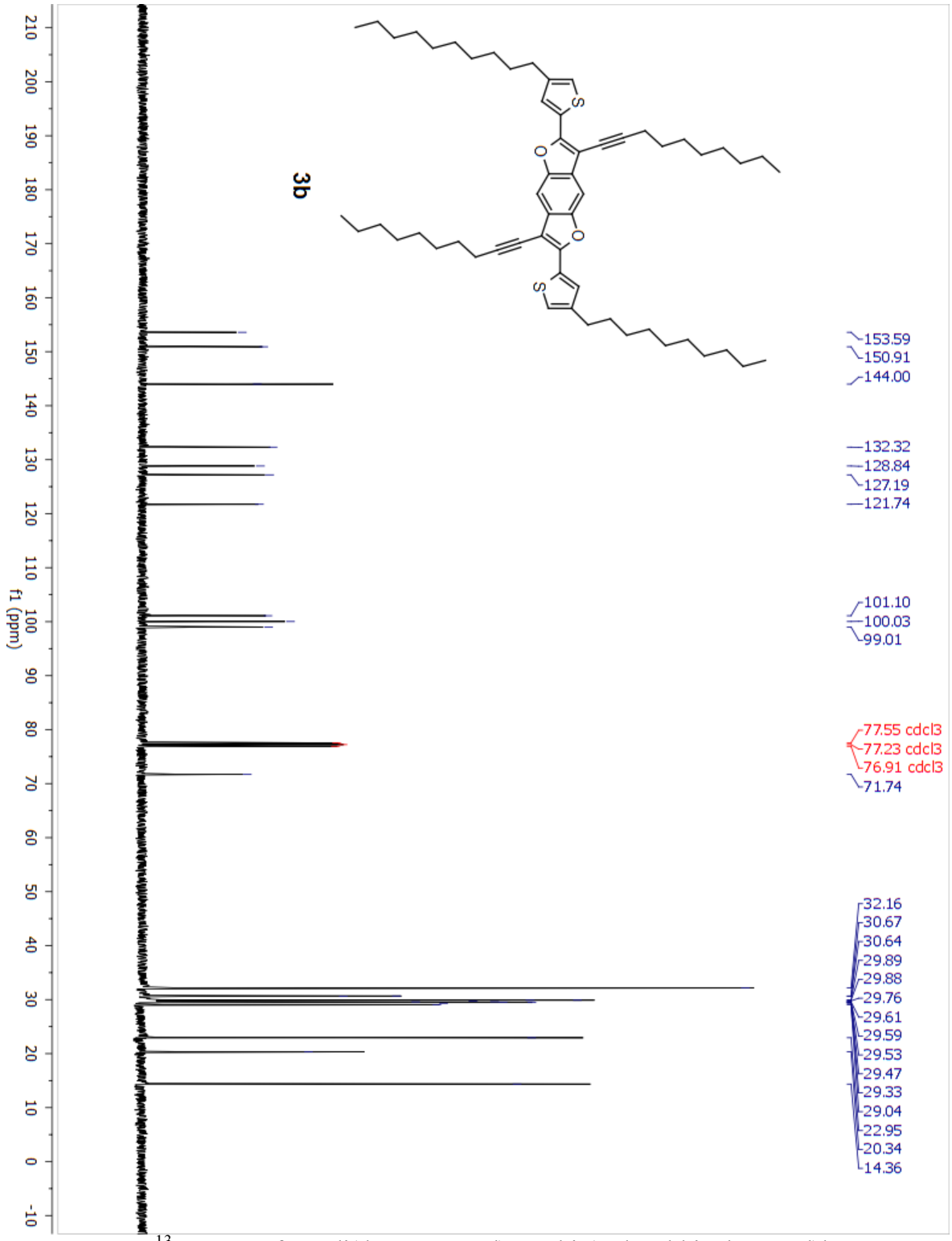

Figure S2.28. ^{13}C NMR of 3,7-di(dec-1-yn-1-yl)-2,6-bis(4-decylthiophen-2-yl)benzo[1,2-*b*:4,5-*b*']difuran (**3b**).

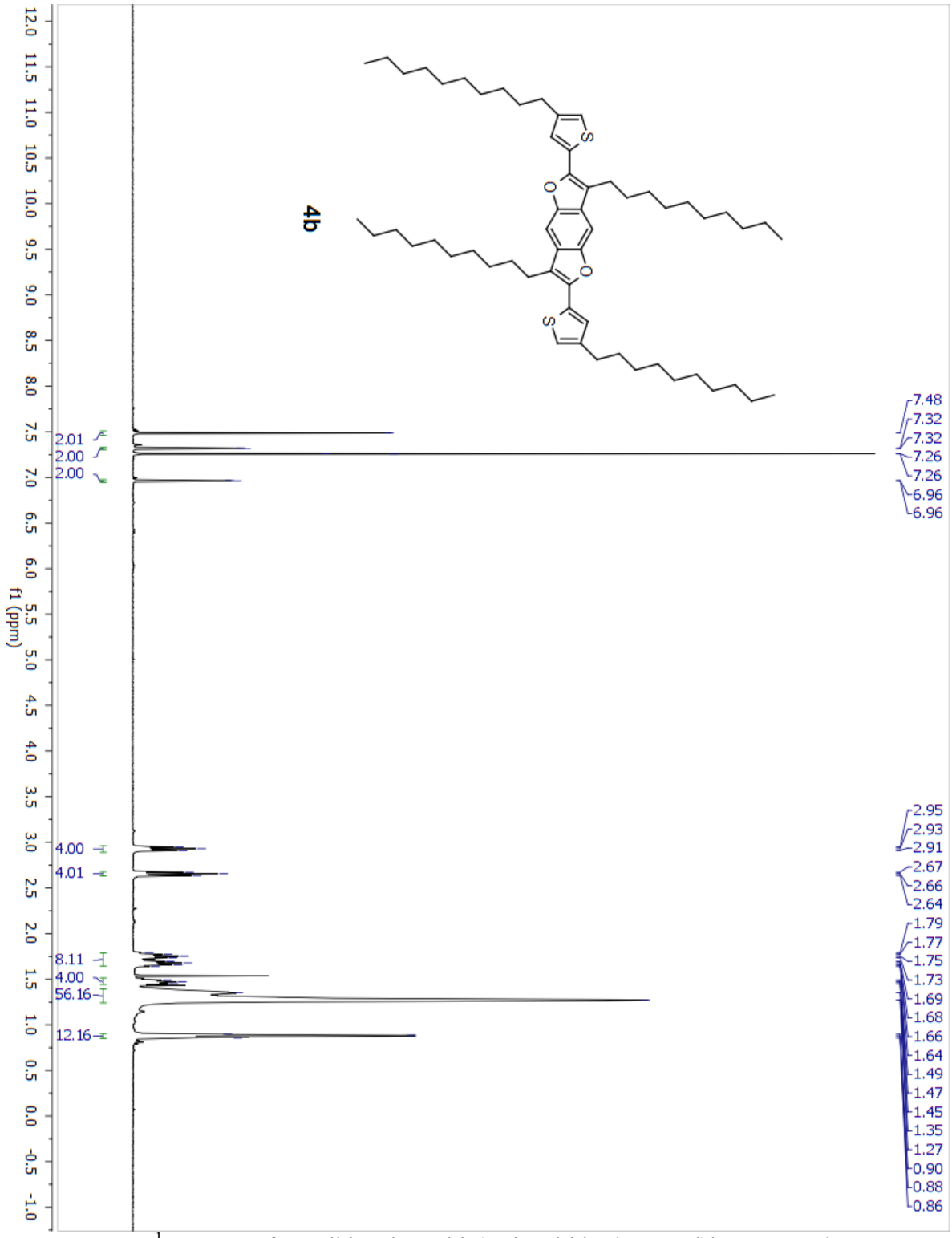

Figure S2.29. ^{1}H NMR of 3,7-didecyl-2,6-bis(4-decylthiophen-2-yl)benzo[1,2-*b*:4,5-*b*']difuran (**4b**).

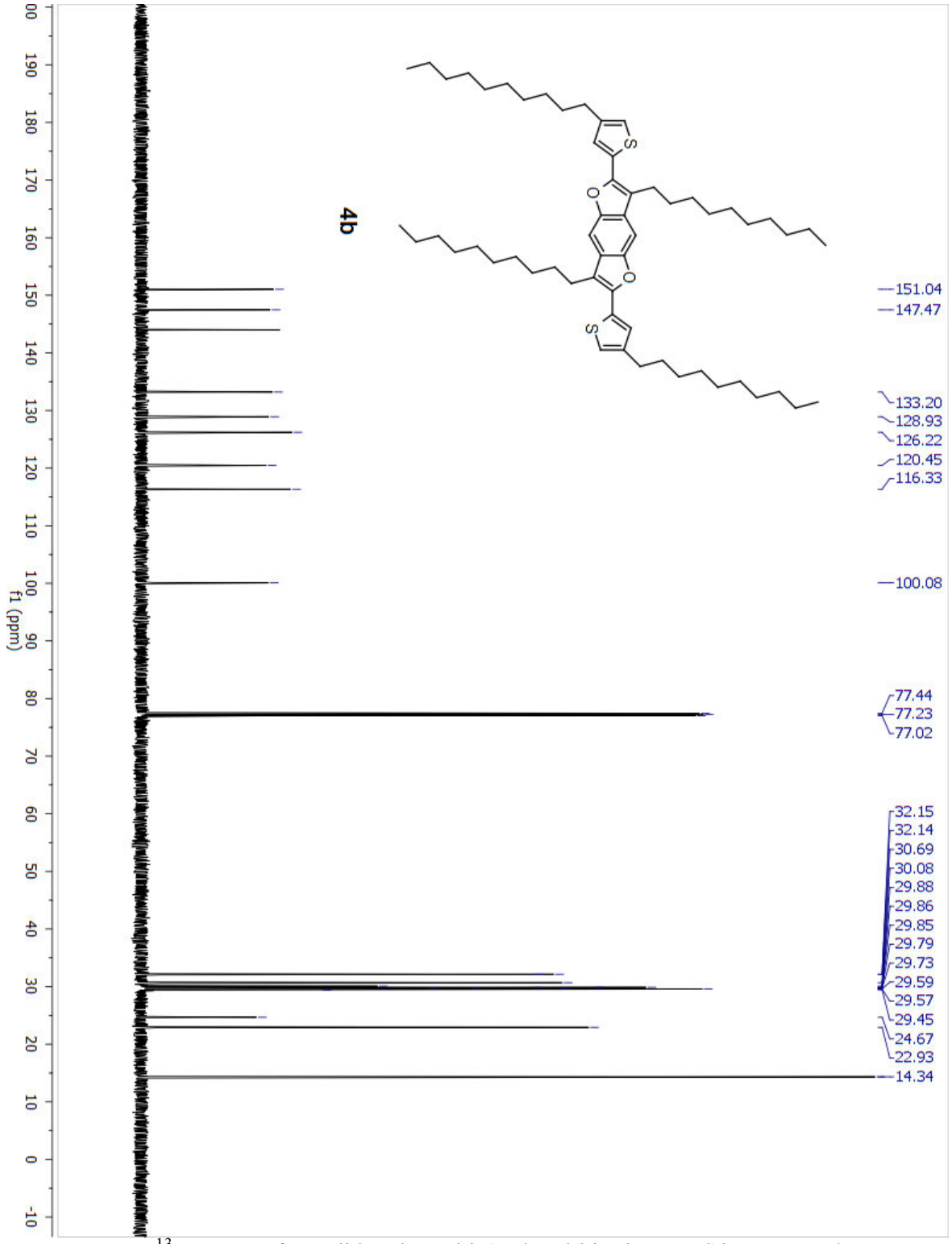

Figure S2.30. ^{13}C NMR of 3,7-didecyl-2,6-bis(4-decylthiophen-2-yl)benzo[1,2-*b*:4,5-*b*']difuran (**4b**).

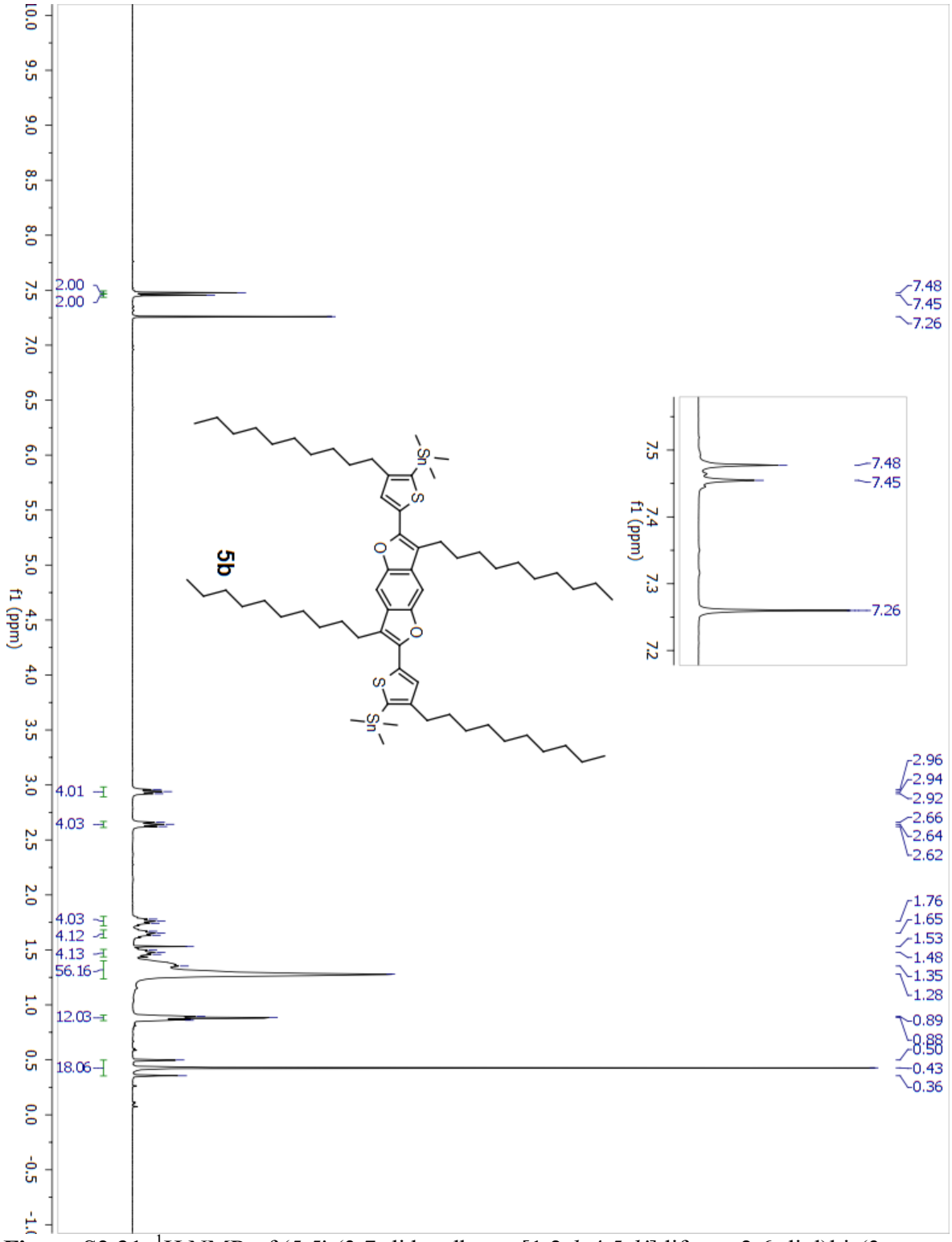

Figure S2.31. ^{1}H NMR of (5,5'-(3,7-didecylbenzo[1,2-*b*:4,5-*b*']difuran-2,6-diyl)bis(3-decylthiophene-5,2-diyl))bis(trimethylstannane) (**5b**).

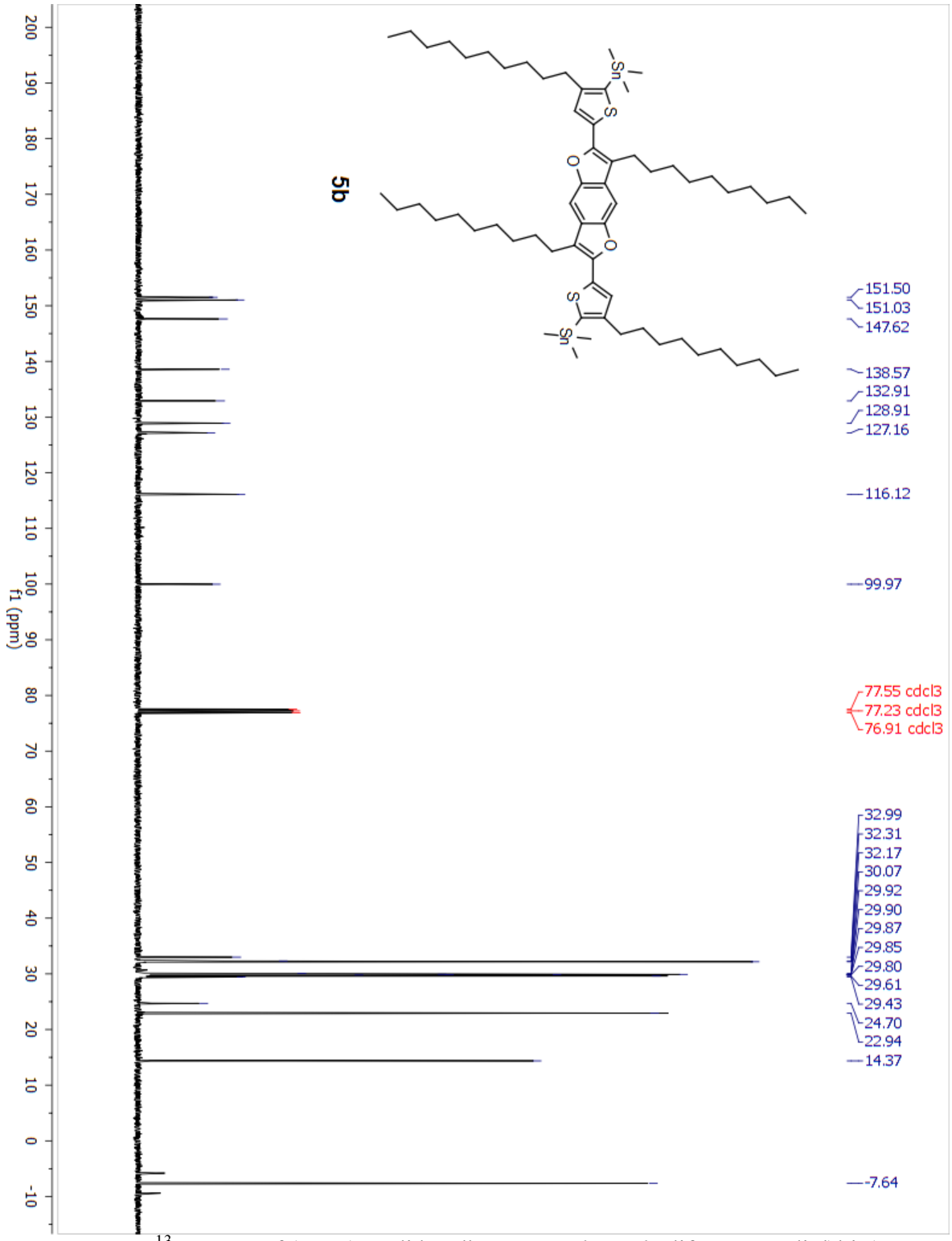

Figure S2.32. ^{13}C NMR of (5,5'-(3,7-didecylbenzo[1,2-*b*:4,5-*b*']difuran-2,6-diyl)bis(3-decylthiophene-5,2-diyl))bis(trimethylstannane) **(5b).**

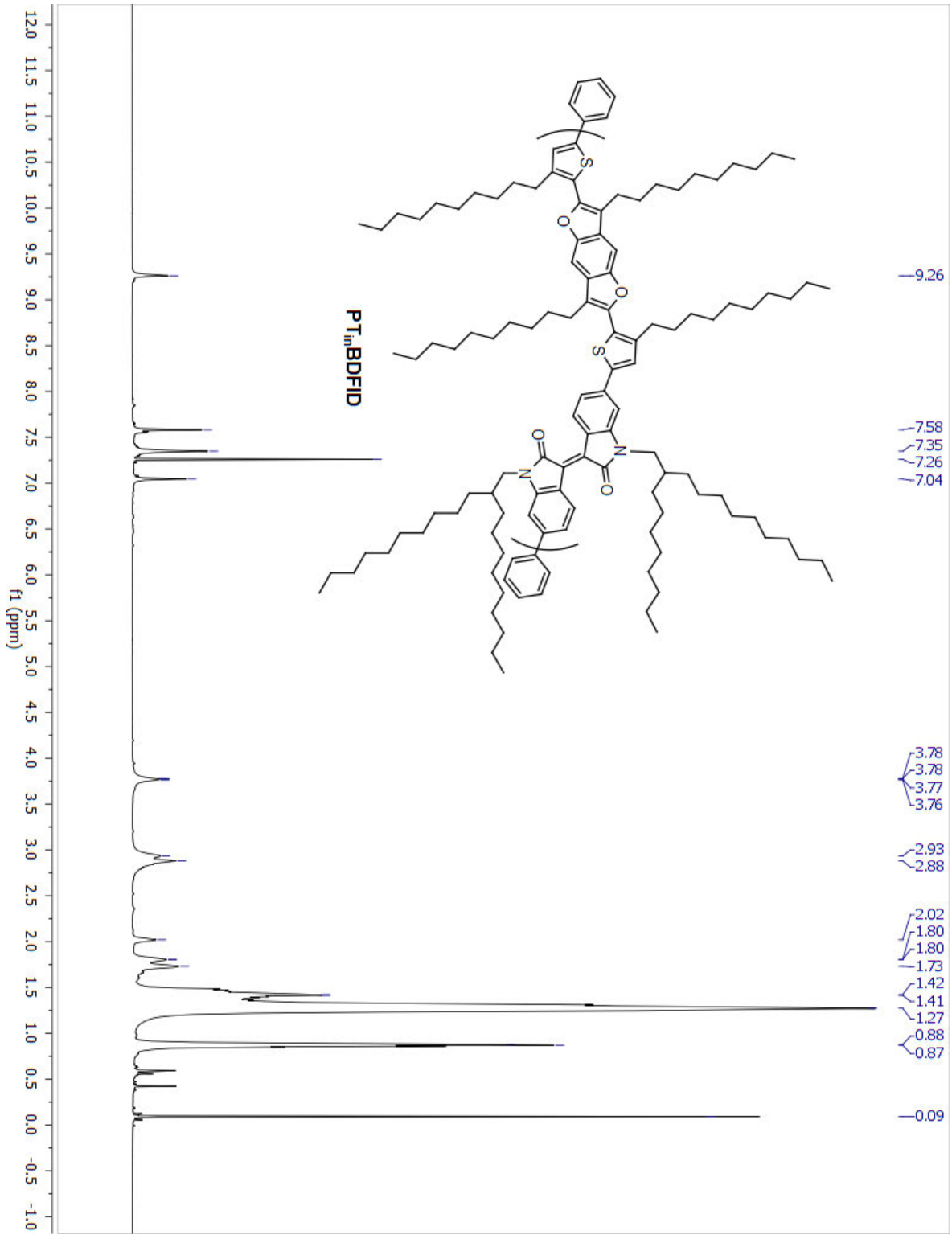

Figure S2.33. ^{1}H NMR of **PT_{out}BDFID**.

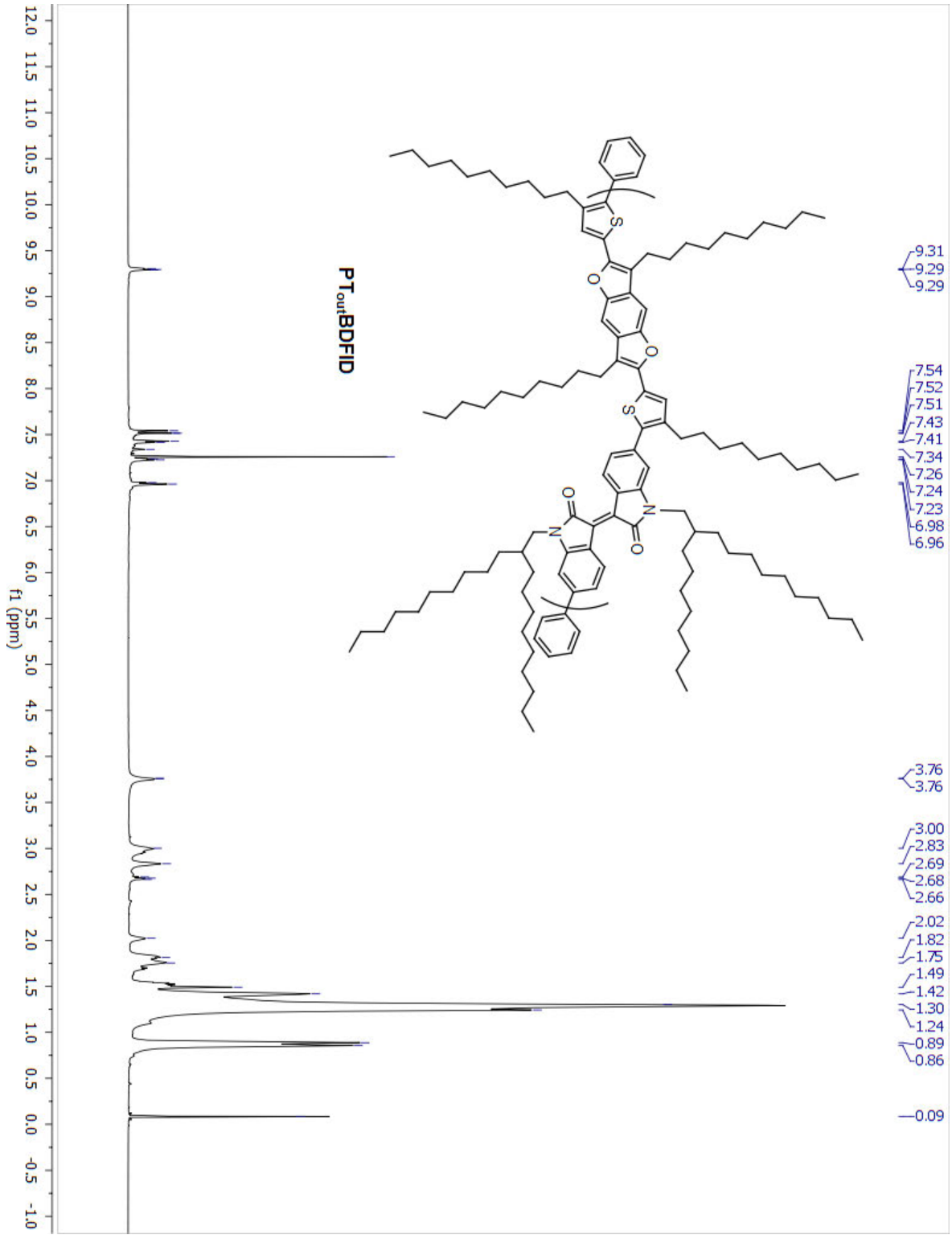

Figure S2.34. ^{1}H NMR of **PT_{out}BDFID**.

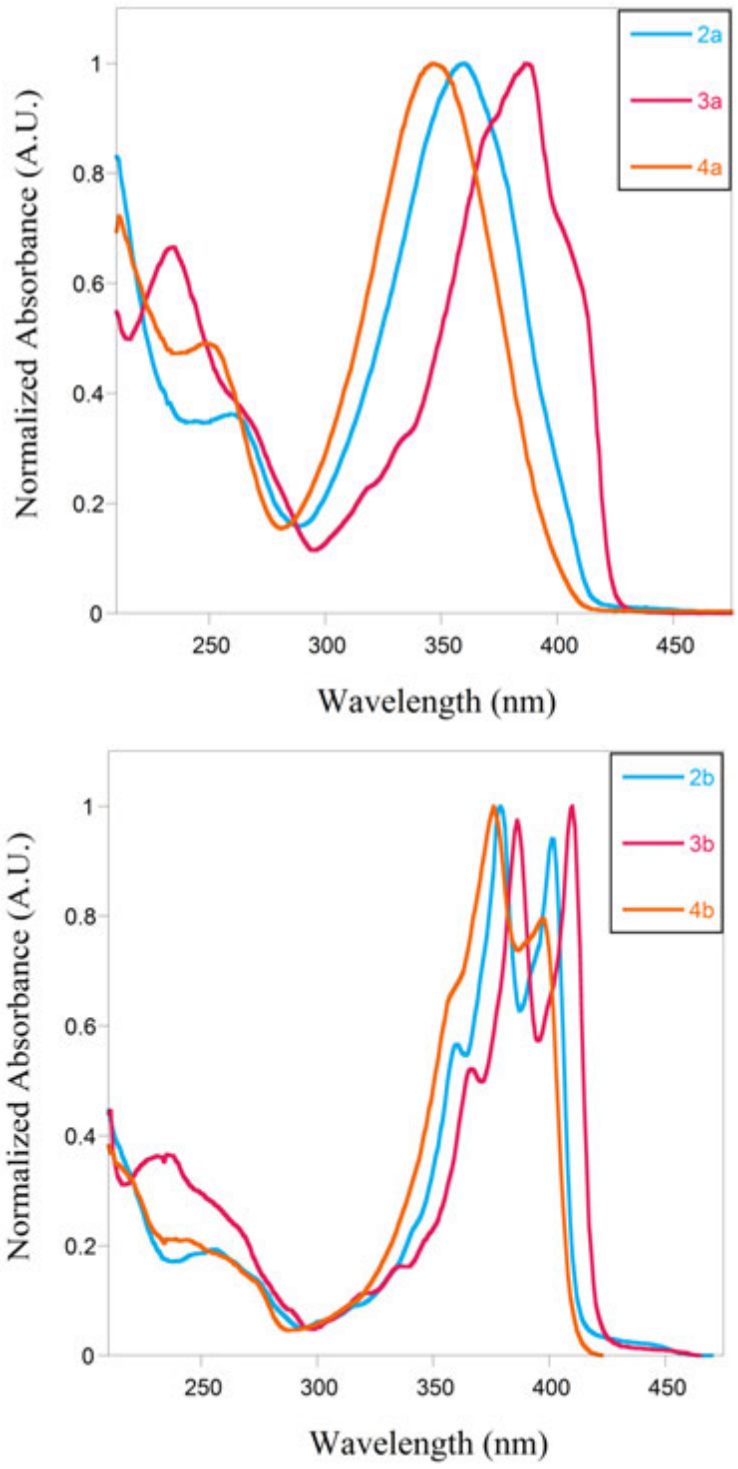

Figure S2.35. Normalized UV-vis absorption spectra of **2a**, **3a**, **4a**, **2b**, **3b**, and **4b** solutions in THF.

Table S2.1. Optical properties of Compounds **2a**, **3a**, **4a**, **2b**, **3b**, and **4b**.

Compound	**2a**	**3a**	**4a**	**2b**	**3b**	**4b**
λ_{max} (nm)	360	386	346	379, 401	386, 410	376, 397

Table S2. Electronic and optical properties of PTBDFID.

Polymer	E^{ox}_{onset} (eV)	E^{red}_{onset} (eV)	HOMO[a] (eV)	LUMO[b] (eV)	E_g^{opt} (eV)[c]	E_g^{EC} (eV)[d]
$PT_{out}BDFID$	0.56	-1.35	-5.66	-3.75	1.67	1.91
$PT_{in}BDFID$	0.60	-1.32	-5.70	-3.78	1.58	1.88

[a] HOMO= -(E^{ox}_{onset} + 5.1) (eV). [b] LUMO = -(E^{red}_{onset} + 5.1) (eV).
[c] Estimated from the optical absorption edge. [d] Onset of potentials (vs Fc).

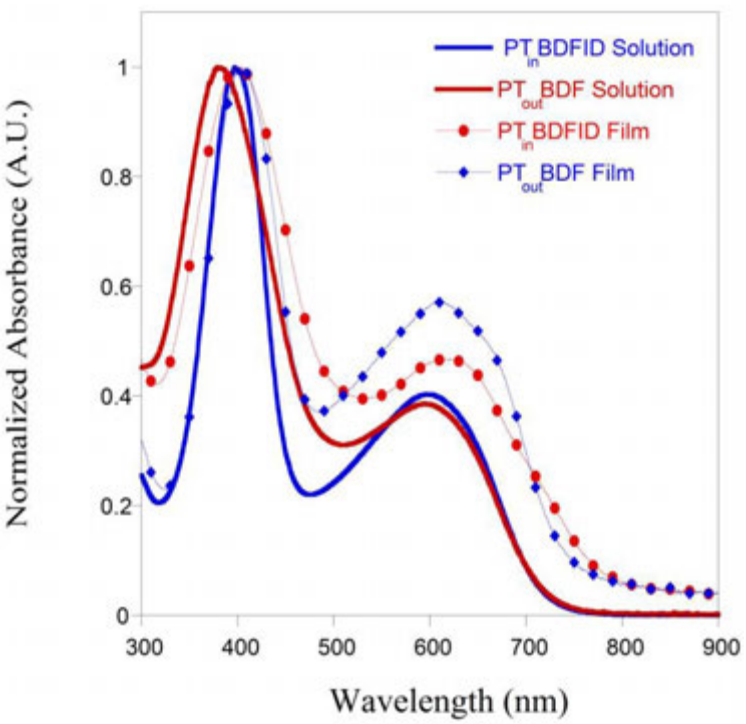

Figure S2.36. Normalized UV-vis absorption spectra of solutions ($CHCl_3$) and thin films of **PT_{in}BDFID** and **PT_{in}BDFID** polymerized using $Pd(PPh_3)_4$.

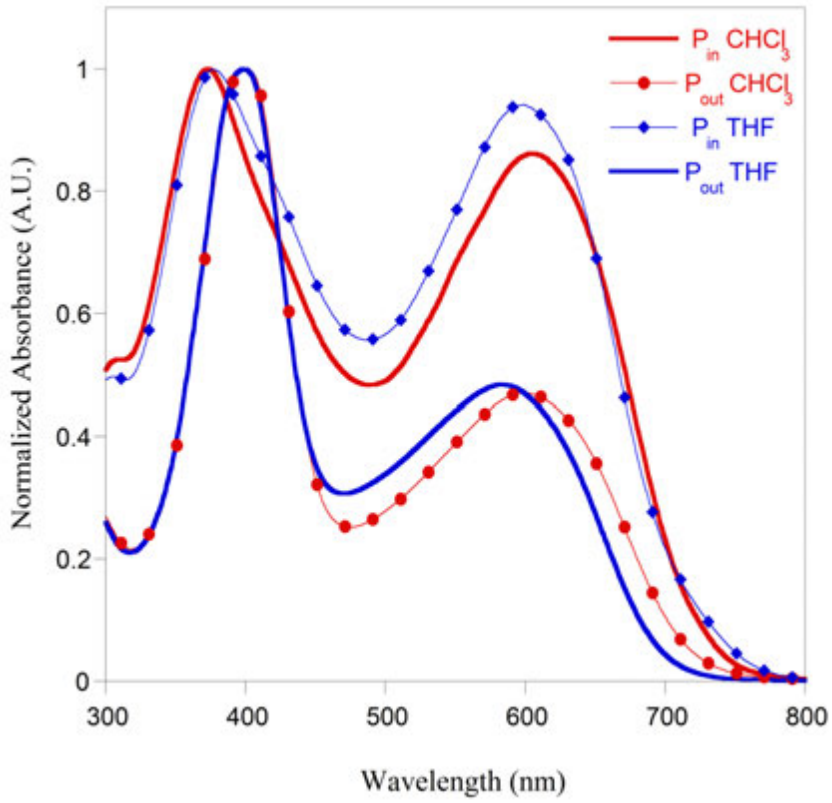

Figure S2.37. Normalized UV-vis absorption spectra of solutions of **PT_{in}BDFID** and **PT_{in}BDFID** polymers (polymerized using $Pd_2(dba)_3$/P(*o*-tol)$_3$) in THF and $CHCl_3$.

Table S3. Optical properties of PT_{out}BDFID and PT_{in}BDFID.

Polymer	Solvent	λ_{max} high-energy (nm)	λ_{max} low-energy (nm)
PT_{out}BDFID	THF	398	599
PT_{out}BDFID	$CHCl_3$	373	608
PT_{in}BDFID	THF	398	582
PT_{in}BDFID	$CHCl_3$	400	598

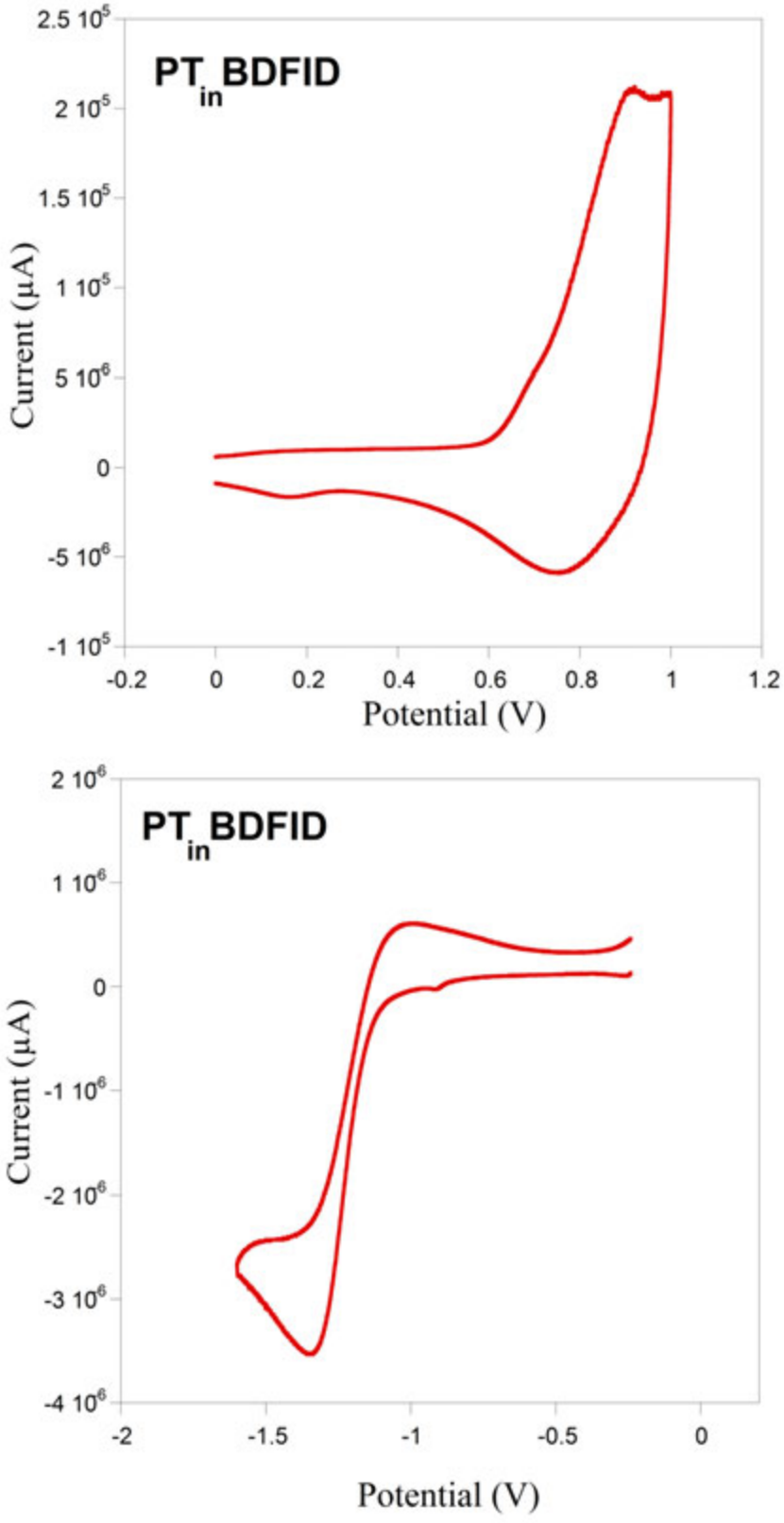

Figure S2.38. Cyclic voltammetry traces of **PT_{in}BDFID.**

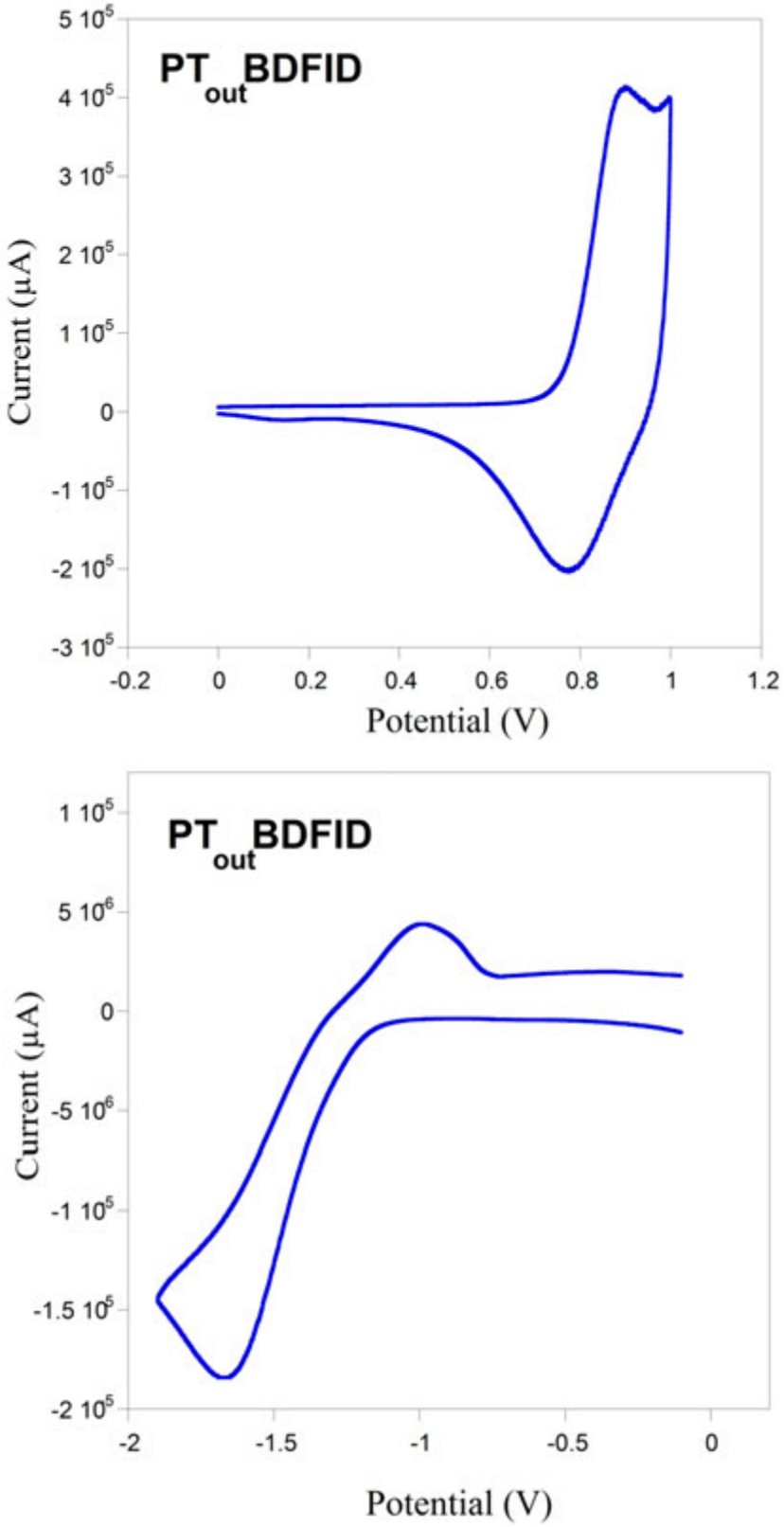

Figure S2.39. Cyclic voltammetry traces of **PT_{out}BDFID.**

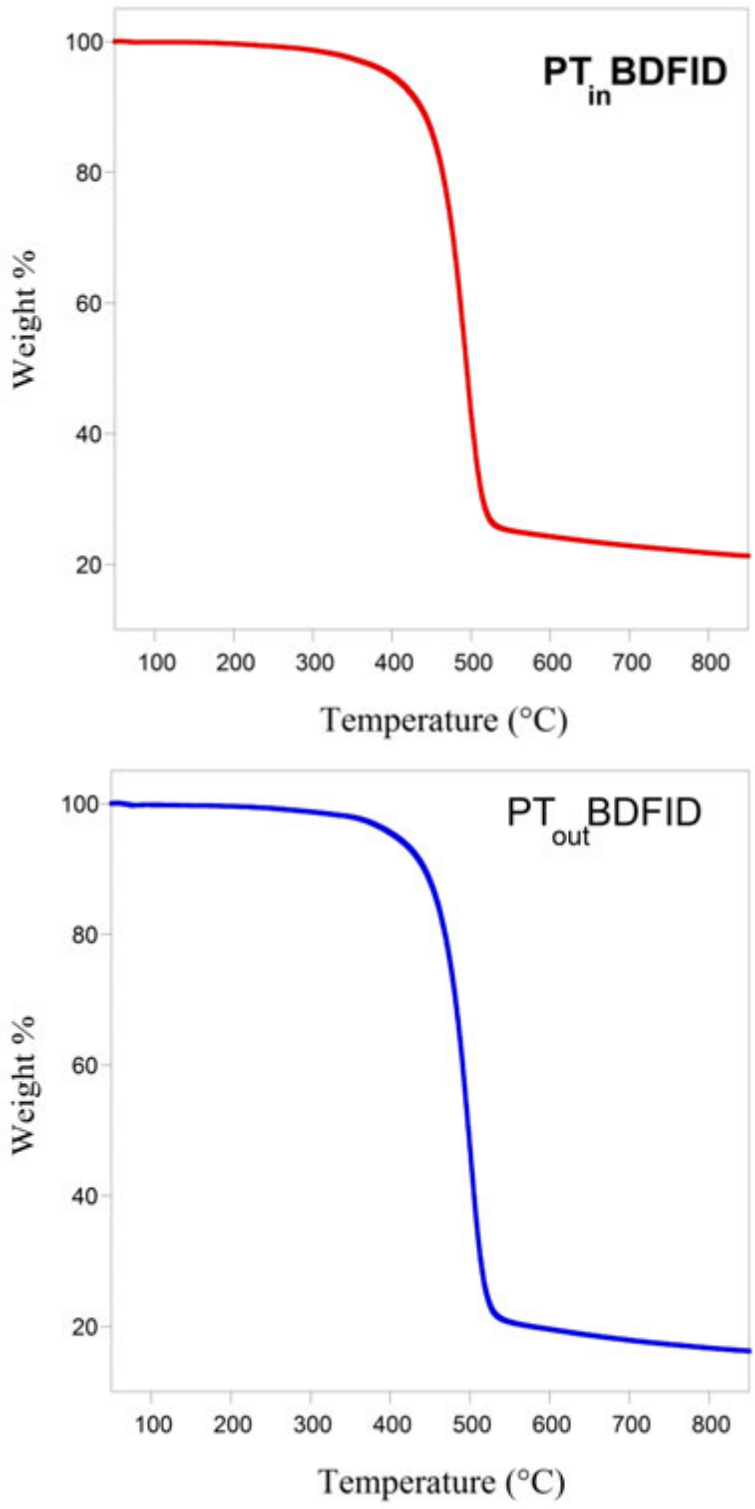

Figure S2.40. Thermal Gravometric Analysis of **PT_{in}BDFID** (top) and **PT_{out}BDFID** (bottom).

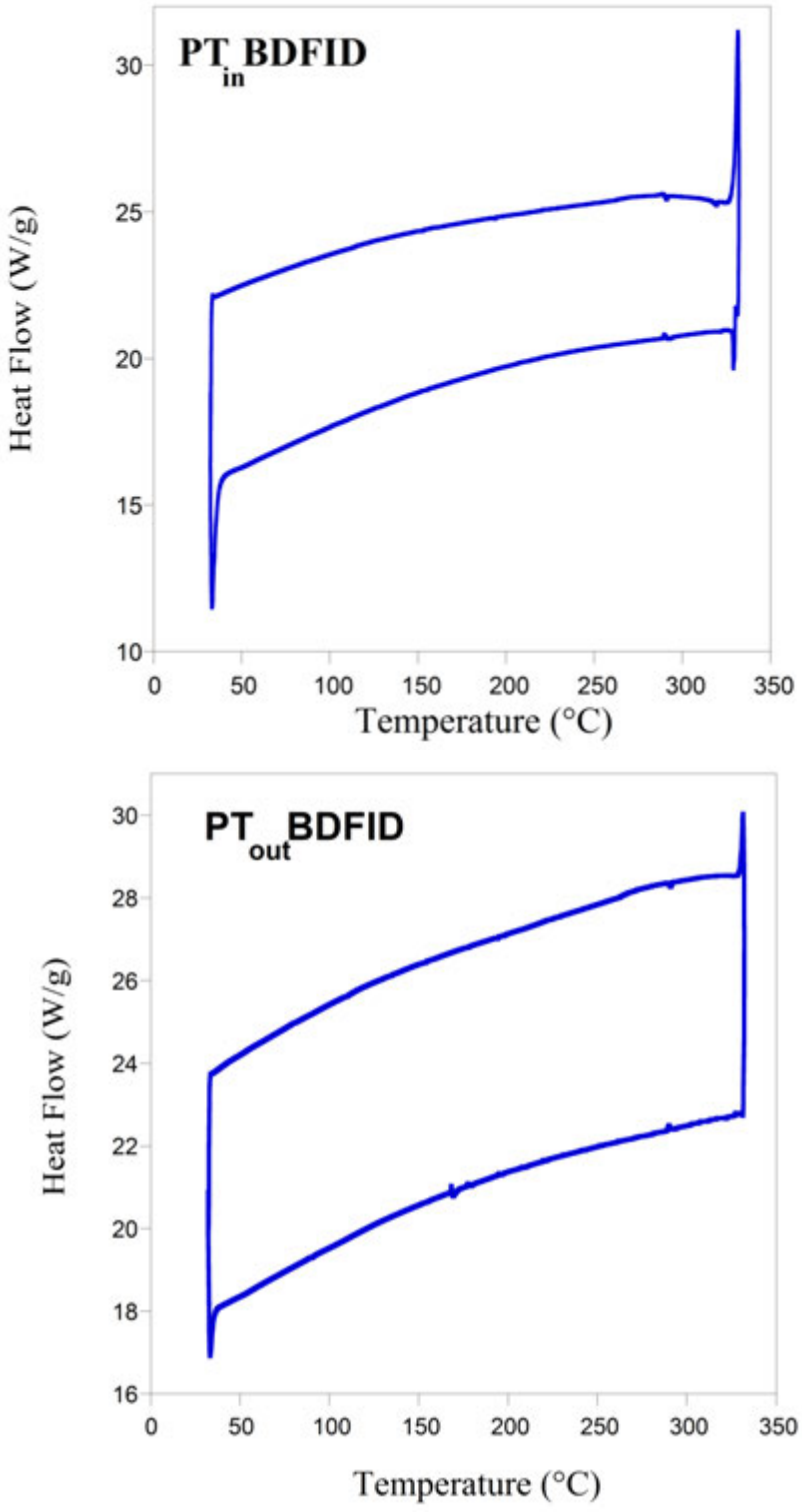

Figure S2.41. Differential Scanning Calorimetry of **PT_{in}BDFID** (top) and **PT_{out}BDFID** (bottom).

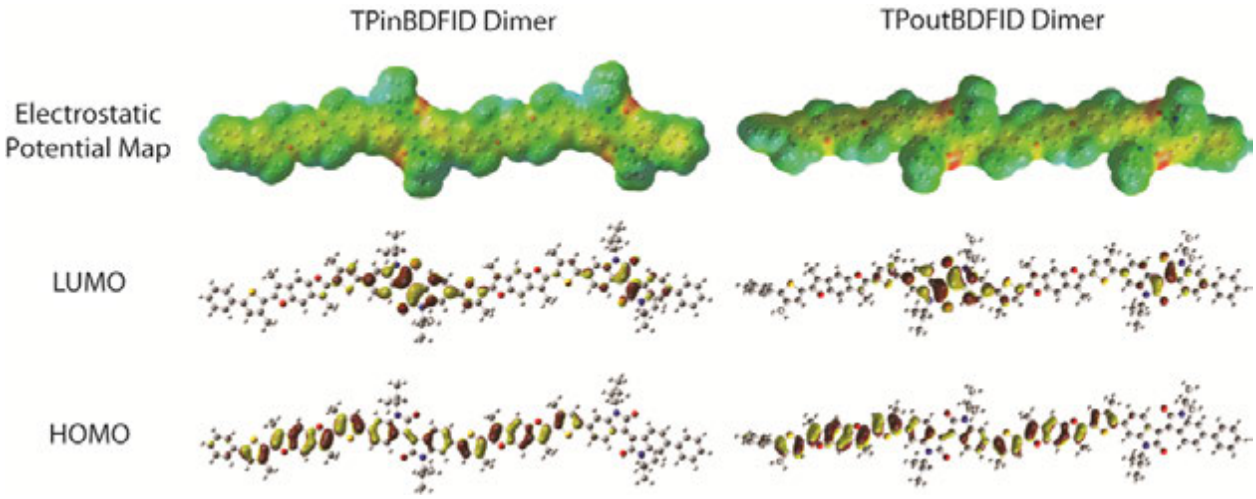

Figure S2.42. The electrostatic potential maps and frontier orbitals for TPinBDFID and TPoutBDFID dimers.

2.8 REFERENCES

1. Facchetti, A., *Chem. Mater.* **2011,** *23* (3), 733-758.
2. Grimsdale, A. C.; Leok Chan, K.; Martin, R. E.; Jokisz, P. G.; Holmes, A. B., *Chem. Rev.* **2009,** *109* (3), 897-1091.
3. Cheng, Y.-J.; Yang, S.-H.; Hsu, C.-S., *Chem. Rev.* **2009,** *109* (11), 5868-5923.
4. Havinga, E. E.; ten Hoeve, W.; Wynberg, H., *Polym. Bull.* **1992,** *29* (1), 119-126.
5. Havinga, E. E.; ten Hoeve, W.; Wynberg, H., *Synth. Met.* **1993,** *55* (1), 299-306.
6. Hou, J.; Park, M.-H.; Zhang, S.; Yao, Y.; Chen, L.-M.; Li, J.-H.; Yang, Y., *Macromolecules* **2008,** *41* (16), 6012-6018.
7. Sista, P.; Biewer, M. C.; Stefan, M. C., *Macromol. Rapid Comm.* **2012,** *33* (1), 9-20.
8. Liang, Y.; Xu, Z.; Xia, J.; Tsai, S.-T.; Wu, Y.; Li, G.; Ray, C.; Yu, L., *Adv. Mater.* **2010,** *22* (20), E135-E138.
9. Najari, A.; Beaupré, S.; Berrouard, P.; Zou, Y.; Pouliot, J.-R.; Lepage-Pérusse, C.; Leclerc, M., *Adv. Funct. Mater.* **2011,** *21* (4), 718-728.
10. Woo, C. H. Beau uge, P. M. Holcombe, T. . ee, . P. Fr chet, J. M. J., *J. Am. Chem. Soc.* **2010,** *132* (44), 15547-15549.
11. Peart, P. A.; Tovar, J. D., *Macromolecules* **2009,** *42* (13), 4449-4455.
12. Li, H.; Tang, P.; Zhao, Y.; Liu, S.-X.; Aeschi, Y.; Deng, L.; Braun, J.; Zhao, B.; Liu, Y.; Tan, S.; Meier, W.; Decurtins, S., *J. Poly. Sci. A.* **2012,** *50* (14), 2935–2943.
13. Bijleveld, J. C.; Karsten, B. P.; Mathijssen, S. G. J.; Wienk, M. M.; de Leeuw, D. M.; Janssen, R. A. J., *J. Mater. Chem.* **2011,** *21* (5), 1600-1606.
14. Hosmane, R. S.; Liebman, J. F., *Tetrahedron Lett.* **1992,** *33* (17), 2303-2306.

15. Liang, Z.; Ma, S.; Yu, J.; Xu, R., *J. Org. Chem.* **2007,** *72* (24), 9219-9224.
16. Huo, L.; Huang, Y.; Fan, B.; Guo, X.; Jing, Y.; Zhang, M.; Li, Y.; Hou, J., *Chem. Commun.* **2012,** *48* (27), 3318-3320.
17. Yi, C.; Blum, C.; Lehmann, M.; Keller, S.; Liu, S.-X.; Frei, G.; Neels, A.; Hauser, J.; Schürch, S.; Decurtins, S., *J. Org. Chem.* **2010,** *75* (10), 3350-3357.
18. Tsuji, H.; Mitsui, C.; Ilies, L.; Sato, Y.; Nakamura, E., *J. Am. Chem. Soc.* **2007,** *129* (39), 11902-11903.
19. Keller, S.; Yi, C.; Li, C.; Liu, S.-X.; Blum, C.; Frei, G.; Sereda, O.; Neels, A.; Wandlowski, T.; Decurtins, S., *Org. Biomol. Chem.* **2011,** *9* (18), 6410-6416.
20. Yue, D.; Yao, T.; Larock, R. C., *J. Org. Chem.* **2005,** *70* (25), 10292-10296.
21. Stalder, R.; Mei, J.; Reynolds, J. R., *Macromolecules* **2010,** *43* (20), 8348-8352.
22. Wang, E.; Ma, Z.; Zhang, Z.; Vandewal, K.; Henriksson, P.; Inganàs, O.; Zhang, F.; Andersson, M. R., *J. Am. Chem. Soc.* **2011,** *133* (36), 14244-14247.
23. Lei, T.; Cao, Y.; Fan, Y.; Liu, C.-J.; Yuan, S.-C.; Pei, J., *J. Am. Chem. Soc.* **2011,** *133* (16), 6099-6101.
24. Cardona, C. M.; Li, W.; Kaifer, A. E.; Stockdale, D.; Bazan, G. C., *Adv. Mater.* **2011,** *23* (20), 2367-2371.
25. Zhu, Y.; Champion, R. D.; Jenekhe, S. A., *Macromolecules* **2006,** *39* (25), 8712-8719.
26. Ma, Z.; Wang, E.; Jarvid, M. E.; Henriksson, P.; Inganas, O.; Zhang, F.; Andersson, M. R., *J. Mater. Chem.* **2012,** *22* (5), 2306-2314.
27. Thompson, B. C.; Kim, Y.-G.; Reynolds, J. R., *Macromolecules* **2005,** *38* (13), 5359-5362.
28. Scharber, M.; Mühlbacher, D.; Koppe, M.; Denk, P.; Waldauf, C.; Heeger, A.; Brabec, C., *Adv. Mater.* **2006,** *18* (6), 789-794.
29. Beiley, Z. M.; Hoke, E. T.; Noriega, R.; Dacuña, J.; Burkhard, G. F.; Bartelt, J. A.; Salleo, A.; Toney, M. F.; McGehee, M. D., *Adv. Energy Mater.* **2011,** *1* (5), 954-962.
30. Wang, B.; Tsang, S.-W.; Zhang, W.; Tao, Y.; Wong, M. S., *Chem. Commun.* **2011,** *47* (33), 9471-9473.
31. Wariishi, K.; Morishima, S.-i.; Inagaki, Y., *Org. Process Res. Dev.* **2003,** *7* (1), 98-100.
32. Cao, J.; Gao, H.; Bemis, G.; Salituro, F.; Ledeboer, M.; Harrington, E.; Wilke, S.; Taslimi, P.; Pazhanisamy, S.; Xie, X.; Jacobs, M.; Green, J., *Bioorg. Med. Chem. Lett.* **2009,** *19* (10), 2891-2895.
33. Mei, J.; Graham, K. R.; Stalder, R.; Reynolds, J. R., *Org. Lett.* **2010,** *12* (4), 660-663.
34. asanovas, . anuy, D. Alem n, C., *Macromolecules* **2008,** *41* (11), 3919-3924.
35. Cho, C.-H.; Neuenswander, B.; Lushington, G. H.; Larock, R. C., *J. Comb. Chem.* **2008,** *10* (6), 941-947.
36. Smeets, A.; Van den Bergh, K.; De Winter, J.; Gerbaux, P.; Verbiest, T.; Koeckelberghs, G., *Macromolecules* **2009,** *42* (20), 7638-7641.

CHAPTER 3

Influence of heteroatoms on photovoltaic performance of donor-acceptor copolymers based on 2,6-di(thiophen-2-yl)benzo[1,2-*b*:4,5-*b*']difurans and diketopyrrolopyrrole.

Polymer Chemistry, **2013**, 4, 5329.
DOI: 10.1039/C3PY00138E

Brandon M. Kobilka,[a] Benjamin J. Hale,[a§] Monique D. Ewan[a§], Anton V. Dubrovskiy,[a] Toby L. Nelson,[b] Volodimyr Duzhko[c] and Malika Jeffries-EL[a]*

[a] Department of Chemistry, Iowa State University, Ames, IA 50011
[b] Department of Chemistry, Oklahoma State University, 107 Physical Science I, Stillwater, OK
[c] Department of Polymer Science and Engineering, University of Massachusetts – Amherst, 120 Governors Drive, Conte A529, Amherst, MA 01003-9263, USA
[§]Both authors contributed equally to this work.

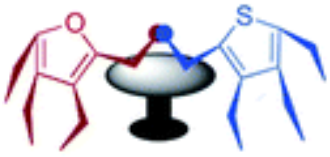

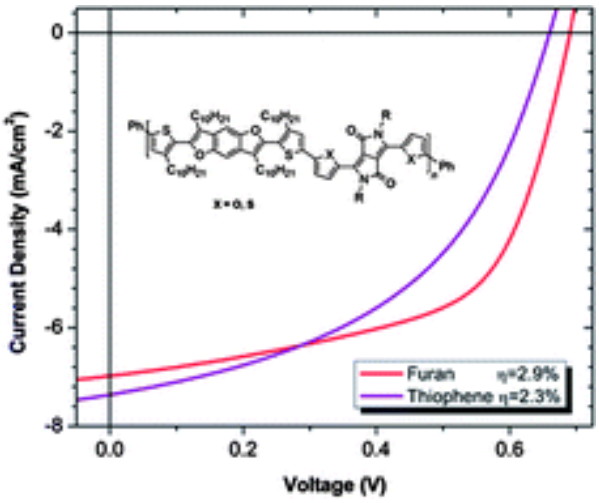

3.1 ABSTRACT

Donor–acceptor conjugated polymers based on the novel donor 3,7-didodecyl-2,6-di(thiophen-2-yl)benzo[1,2-*b*:4,5-*b'*]difuran, and 1,4-diketopyrrolo[3,4-*c*]pyrrole as the acceptor were synthesized via the Stille cross-coupling reaction. The alkyl chains on the diketopyrrolopyrrole monomers were varied to engineer the solubility and morphology of the materials. Thiophene and furan moieties were used to flank the DPP group and the impact of these heterocycles on the polymers' properties evaluated. All of the polymers have similar optoelectronic properties with optical band-gaps of 1.3-1.4 eV, LUMO levels of -3.7 to -3.8 eV and HOMO levels of -5.5 to -5.6 eV. The furan-containing polymers have better solubility than the all-thiophene polymers, as significantly higher molecular weight materials of the former were readily dissolved. When the polymers were used as donor materials along with $PC_{71}BM$ as the electron-acceptor in bulk-heterojunction photovoltaic cells, power conversion efficiencies of up to 2.9% were obtained, with the furan-containing polymers giving the best results.

3.2 INTRODUCTION

Since their discovery over 35 years ago, conjugated polymers have evolved from being mere academic curiosities into a booming global enterprise in both academic and industrial labs.[1, 2] These organic semiconductors are being evaluated for use in a range of optoelectronic applications as they offer several advantages over their inorganic counterparts, including the potential to fabricate large-area films using low cost solution processing techniques, to manufacture lightweight and flexible devices and to alter the materials' properties through chemical synthesis.[3-6] Currently, the synthesis of material comprising alternating electron-donating and electron-accepting moieties is an effective way to alter its optical and electronic properties.[7, 8] Using this approach, a number of materials possessing beneficial properties, such as broad absorption bands, LUMO levels that are appropriately offset from the acceptor, low-lying HOMO levels, and high charge carrier mobilities for use as donor-materials in bulk-heterojunction organic photovoltaic cells (OPVs) have been

synthesized. As a result, power conversion efficiencies (PCE)s for polymer OPVs have exceeded 9%.[9-12]

The steady increase in the performance of OPVs over the past few years is a combination of many improvements including the development of new device architectures, the band-gap engineering of the donor materials, and the optimization of film morphology. Early success in the development of devices based on organic semiconductors was first seen with regioregular poly(3-hexylthiophene) (P3HT), which possesses excellent solubility, oxidative stability, and good charge carrier mobility.[13, 14] However, since P3HT has a high-lying HOMO level and a fairly wide band-gap, a number of new thiophene-based materials have been developed in order to address these issues while maintaining high charge carrier mobility. In contrast, furan has not been widely used for the synthesis of conjugated polymers, largely due to the difficulty involved with synthesizing substituted furans. However, furan has several advantages over thiophene making it a promising building block for developing conjugated polymers. For example, furan is isoelectronic to thiophene, but less aromatic, which can facilitate the formation of quiniodal structures, stabilizing the HOMO level.[15] Additionally, furan based polymers have better solubility than their thiophene containing analogs.[16, 17]

Previously, the synthesis of a furan-containing monomer 3,6-di(2-furanyl)-1,4-diketopyrrolo[3,4-*c*]pyrrole (FDPP) and its use in polymers has been reported.[17-21] Diketopyrrolopyrrole (DPP) is a strong electron-accepting moiety that can increase the intramolecular charge transfer along the polymer chain and stabilize the LUMO levels of the resulting materials.[22-26] The DPP ring system also has a symmetric coplanar structure that enhances interactions, increasing charge carrier mobility.[24, 27] Since the DPP moiety is a bis-lactam, it is always synthesized between two arenes. Initially, 3,6-di(2-thienyl)-1,4-diketopyrrolo[3,4-*c*]pyrrole (TDPP) was widely investigated for the synthesis of narrow band-gap polymers for use in OPVs with PCEs of up to 5.6%.[22] Recently, FDPP-based polymers have been reported that exhibit better solubility than TDPP polymers. The resulting improvement in the film formation has lead to PCEs as high as 6.5%.[19, 28]

At the same time, the electron-donating benzo[1,2-*b*:4,5-*b*′]dithiophene (BDT) moiety has been widely investigated for the synthesis of conjugated polymers. BDT has a planar conjugated structure that facilitates π–π stacking, leading to good charge carrier mobility.[29-32]

As a result, PCEs approaching 8% have been obtained for BDT copolymers.[31, 33] Recently, our group[34] and others[15, 35-39] have investigated the use of the benzo[1,2-*b*:4,5-*b*']difuran (BDF) as a building block for the synthesis of new conjugated polymers. In addition to the positive attributes of BDT, the smaller atomic radius of the oxygen relative to sulfur is expected to reduce steric hindrance between adjacent units, increasing planarity and conjugation.[40] Consequently, BDF-containing conjugated polymers are expected to possess smaller band-gaps than their BDT-containing counterparts.

Based on the aforementioned considerations, we have synthesized four new donor-acceptor copolymers composed of BDF and either FDPP or TDPP. The FDPP monomer was chosen to compare with the TDPP due to its potential to enhance solubility. The alkyl side chains were varied to further evaluate the trade-off between improved solubility afforded by the branched 2-ethylhexyl chains and enhanced film forming properties of the linear tetradecyl chains. The performance of these materials was evaluated in OPVs to ascertain whether side-chain modification or heteroatom substitution had a greater impact on performance.

3.3 RESULTS AND DISCUSSION

3.3.1 Synthesis and characterization

The synthetic route to the copolymers is illustrated in Scheme 3.1. The Stille cross-coupling reaction of benzodifuran **1** and the corresponding DPPs **2a-d** afforded polymers **P1-P4** in good yields (52-84%) after purification by stirring with functionalized silica, followed by Soxhlet extraction. All of the polymers were soluble in common organic solvents, such as THF, chloroform and chlorobenzene at room temperature.

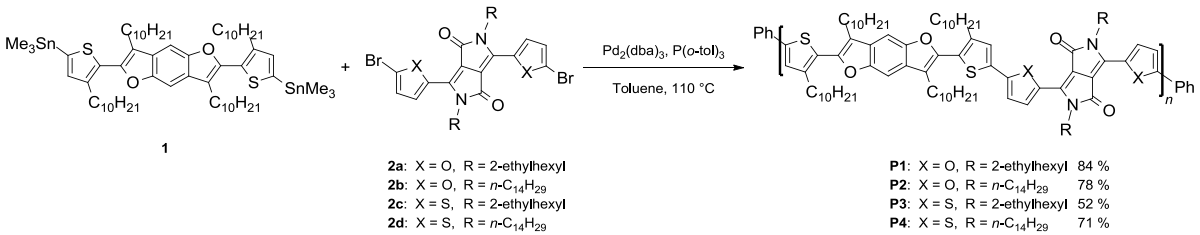

Scheme 3.1. Synthesis of copolymers **P1-P4**.

The polymers were characterized by ^{1}H NMR and the spectra are in agreement with the expected polymer structures (see Supporting Informaiton). The molecular weights were estimated using gel permeation chromatography (GPC) at 50 °C using THF as the eluent and the resulting data is summarized in Table 3.1. All polymers displayed strong intermolecular interactions in solution leading to aggregation at temperatures below 40 °C during analysis; thus, increasing the run temperatures allowed for the proper measurement of the molecular weight of individual polymer chains. The furan-containing polymers, **P1** and **P2**, showed considerably higher molecular weights than their thiophene-containing analogues **P3** and **P4** indicating that the furan-containing polymers have better solubility in THF. This is consistent with the results reported by Fréchet *et al*, where FDPP copolymers exhibited better solubility and higher molecular weight over those comprising TDPP.[17] In our case, due to synthetic constraints, our two furan-containing copolymers have an equal number of thiophene and furan units. Of these, the polymer bearing branched 2-ethylhexyl side chains, **P1**, had a higher molecular weight than the one bearing linear tetradecyl side chains, **P2**. This trend was also observed in the set of polymers containing only thiophene in the polymer backbone, indicating that the improved solubility within each set is a result of the branched side chains. Interestingly, Fréchet and co-workers also observed that DPP-copolymers with both furan and thiophene in the polymer backbone had higher molecular weights than those containing only furan. This is increase in solubility was also seen in a series of oligomers containing both thiophene and furan.[41, 42] Given the difficulty associated with synthesizing functionalized furans, increasing its content within the polymer backbone would be challenging. However, the previous reports suggest that such efforts may not improve the solubility of the resulting polymer.

Table 3.1. Molecular weight and thermal data for **P1**-**P4**.

Polymer	Yield (%)[a]	M_w[b] (kDa)	M_n[b] (kDa)	PDI	DP_n	T_d[c] (°C)
P1	84	55.6	28.9	1.9	40	333
P2	78	44.2	19.9	2.2	29	353
P3	53	24.0	9.5	2.5	17	349
P4	71	8.1	6.1	1.3	5	359

[a] Isolated yield. [b] Molecular weight data was obtained by GPC. [c] 5% weight loss determined by TGA in air.

3.3.2 Thermal properties

The thermal properties of the polymers were evaluated using thermal gravimetric analysis (TGA) and differential scanning calorimetry (DSC). TGA results are summarized in Table 3.1 and indicate that 5 % weight loss onsets occurred between 333-359 °C. DSC did not reveal any observable phase transitions for temperatures up to 200 °C; however, observable melting points were seen for all four polymers above 235 °C. These thermal characteristics are indicative of good stability above the operational temperature threshold of organic photovoltaic devices.

3.3.3 Optical and electrochemical properties

The normalized absorption spectra of **P1**-**P4** in dilute $CHCl_3$ solution and thin films are shown in Figures 3.1 and 3.2, respectively, and the optical data is summarized in Table 3.2. All four polymers exhibit two distinct absorption bands in both solution and film as is typical for such donor-acceptor copolymers.[43] The high-energy band is attributable to localized π-π* transitions, while the broad, low-energy band corresponds to intermolecular charge transfer between the electron-donating and electron-accepting units.[43] In solution, the λ_{max} of both polymers **P1** and **P3** is nearly identical, at 658 nm and 657 nm, respectively. For **P2** and **P4**, the λ_{max} has a slight bathochromic shift, but both polymers exhibit a significant low-energy shoulder that their structural counterparts do not.

Table 3.2. Optical and electronic properties for **P1**-**P4**.

Polymer	λ_{max}^{soln} (nm)	λ_{max}^{film} (nm)	E_g^{opt} [a] (eV)	HOMO [b] (eV)	LUMO [b] (eV)	E_g^{EC} [d] (eV)
P1	658	774, 668	1.4	-5.5	-3.7	1.8
P2	663	739, 668	1.4	-5.5	-3.8	1.7
P3	657	752, 673	1.3	-5.6	-3.8	1.8
P4	671	678	1.4	-5.6	-3.7	1.9

[a] Estimated from the absorption onset of the film. [b] HOMO= -(E_{onset}^{ox} + 5.1) eV. [c] LUMO = -(E_{onset}^{red} + 5.1) eV. [d] E_g^{EC} = LUMO - HOMO.

As thin films, all four polymers display an increase in the low energy vibrational components, resulting in a new λ_{max}. Additionally, all four polymers have optical band-gaps

within 0.1 eV of each other, as estimated from the onset wavelength of the film absorption, indicating that effective conjugation was reached in each case. Despite this similarity, the polymers displayed moderate variations in the low energy absorption bands. The furan-containing polymers, **P1** and **P2**, have the most red-shifted absolute λ_{max} at 744 nm and 739

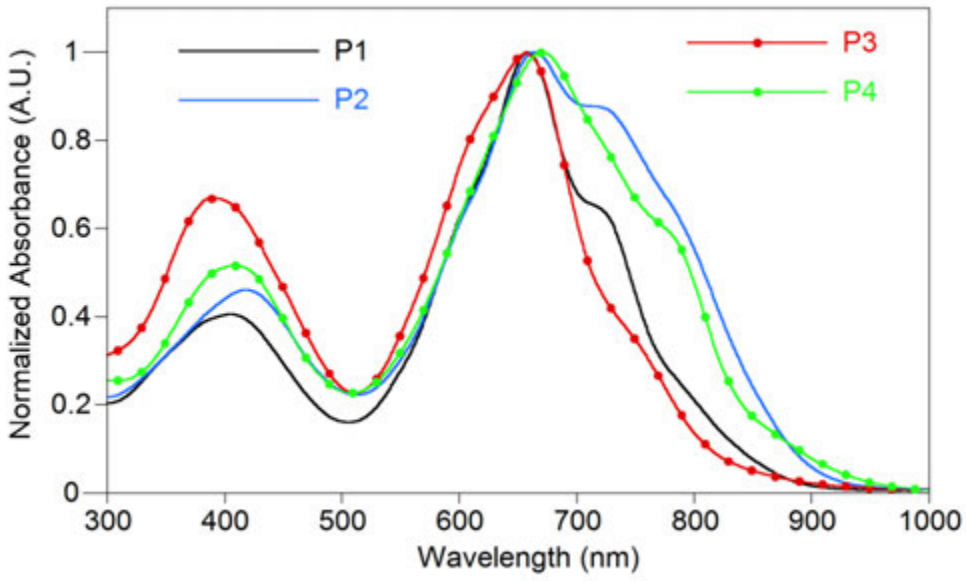

Fig. 3.1 UV-Vis absorption of **P1-P4** in solution.

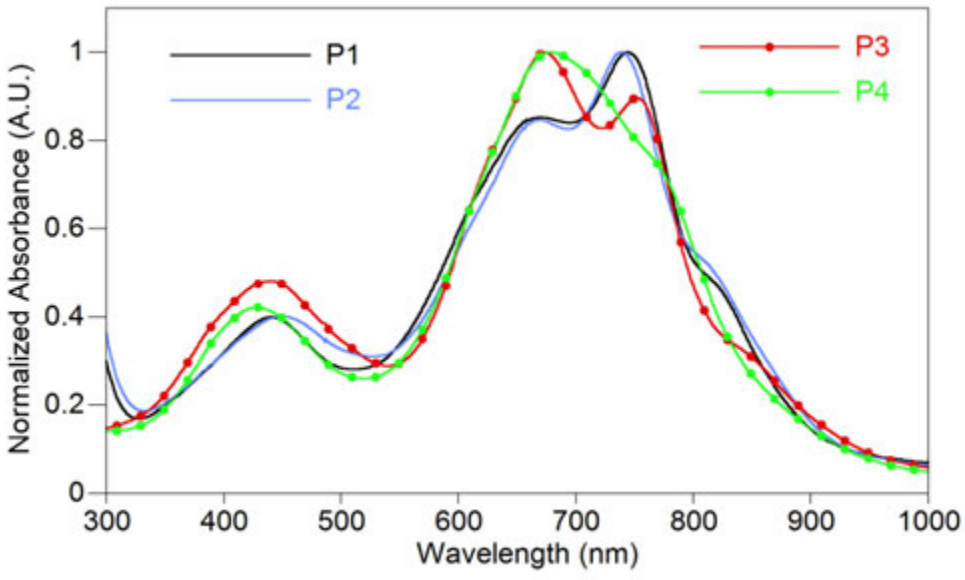

Fig. 3.2 UV-Vis absorption of **P1-P4** in film.

nm, respectively, whereas the thiophene-containing polymer **P3** has only a local λ_{max} in the same region at 752 nm and **P4** only displays a weakly defined shoulder around 750 nm. This data suggests that the presence of this absorption band in **P1** and **P2** correlates well with the higher molecular weights, while its presence diminishes as the molecular weight declines in **P3** and **P4**. The absorption properties are similar to those reported previously for **PDPP4TBDT**, a related terpolymer of the hexyldecyl, analogue of **2c**, thiophene and 4,8-di(5-ethylhexylthienyl) BDT which has a λ_{max} =666 nm in solution and 722 nm in solid state.[44] The BDF polymers also have slightly smaller optical band gaps than **PDPP4TBDT** (1.51 eV).[44] This is likely due to the replacement of sulfur with oxygen, however since the position of the thiophene substituents in **PDPP4TBDT** is different, we cannot completely rule out other factors.

To evaluate the electrochemical properties of the polymers, the redox behaviour was measured by cyclic voltammetry. All four polymers exhibit measureable and reproducible oxidation and reduction processes. The HOMO and LUMO levels were estimated from the onset of oxidation and reduction using the absolute energy level of ferrocene/ferrocenium (Fc/Fc^+) as 5.1 eV under vacuum and are summarized in Table 3.2.[45] For all four polymers, the HOMO levels ranged between -5.5 to -5.6 eV, deep enough to guarantee good air stability. The LUMO levels ranged from -3.7 to -3.8 eV giving an average electrochemical band-gap of 1.8 ± 0.1eV. These values are statistically similar enough to suggest that replacing the furans flanking the DPP monomer with thiophenes has only a negligible influence on the electrochemical properties. However, replacing the sulfur atoms of BDT with oxygen has a slight impact on the electronic properties as the LUMO values of **P3** and **P4** are similar to those reported previously for **PDPP4TBDT** and the HOMO levels for **P3** and **P4** are stabilized by ~0.1 eV relative to **PDPP4TBDT**.[44] It is also of note that the optical band-gaps are all estimated to be slightly smaller than the electrochemical band-gap, which correlates well to the expected energy barrier associated with the interface of the polymer film and the electrode surface.[45]

3.3.4 Photovoltaic devices

The performance of all four polymers in OPVs was evaluated using [6,6]-phenyl-C_{71}-butyric acid methyl ester ($PC_{71}BM$) as the electron acceptor with a device configuration of

indium tin oxide (ITO)/poly(3,4-ethylenedioxythiophene): polystyrene sulfonate (PEDOT:PSS)/polymer:$PC_{71}BM$(1:2, w/w)/LiF/Al. The active layer was deposited from 30 mg/mL *o*-DCB solutions, using processing conditions selected to yield a thickness of about 100 nm. In some cases, analogous devices were prepared using 3% of 1-chloronapthalene (CN) as a high-boiling solvent additive to improve polymer/PCBM blend morphology. The current density-voltage (*J*-*V*) curves of the OPVs are shown in Figure 3.2. The resultant photovoltaic performance, including short circuit current density (J_{SC}), open circuit voltage (V_{OC}), fill factor (FF) and power conversion efficiency (PCE) are shown in Table 3.3.

Table 3.3. Photovoltaic device performance of P1-P4 with PCBM.

Polymer	Additive	J_{SC} (mA/cm^2)	V_{OC} (V)	FF	PCE (%)
P1	none	-5.1	0.70	0.63	2.28
	3% CN	-7.0	0.69	0.60	2.89
P2	none	-7.0	0.66	0.60	2.77
	3% CN	-7.7	0.65	0.57	2.81
P3	none	-6.7	0.67	0.47	2.10
	3% CN	-7.4	0.66	0.47	2.28
P4	none	-4.2	0.59	0.39	0.97

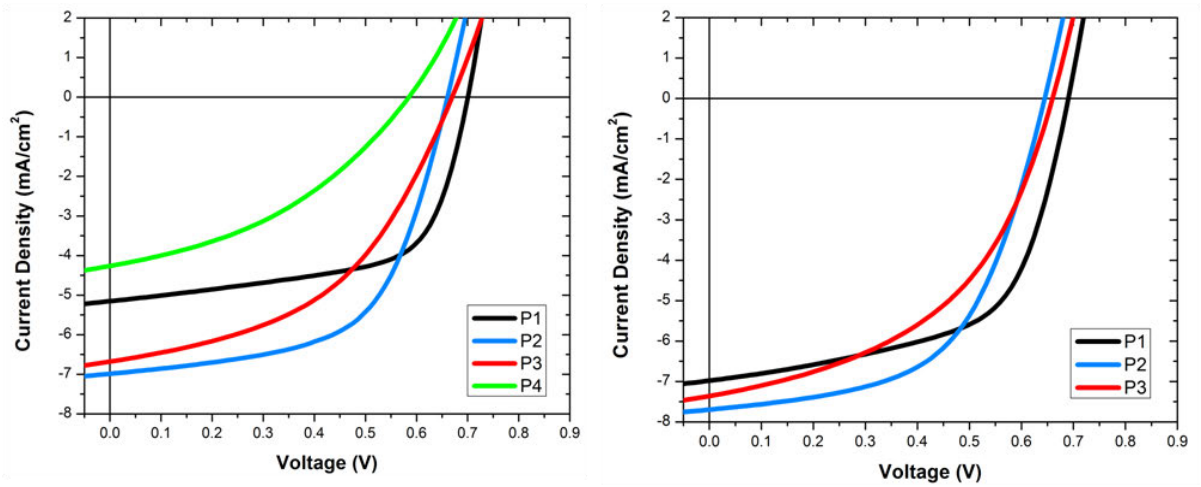

Fig. 3.3 Current-voltage characteristics for **P1**-**P4**-based OPVs without solvent additives (Left), and for **P1**-**P3**-based OPVs using 3% CN as a solvent additive (Right).

Among the devices fabricated without solvent additive, **P2** gave the highest PCE, at 2.77%. Conversely, the **P1**- and **P3**-based devices had somewhat lower efficiencies with

respective values of 2.28% and 2.10%. While all three of these polymers gave open circuit voltages of ~0.70 V, **P2** combines superior photocurrent with a good fill factor. This is a result of the polymer's good molecular weights and the presence of linear alkyl chains, which typically results in ideal blends without the addition of additives. Expectantly, the devices fabricated from **P4** performed significantly worse, only returning PCEs of ~1.0 %, a result of decreases in all categories. This outcome is a consequence of the poor solubility and significantly lower molecular weights of **P4**, both of which negatively affect film formation.

We initially evaluated the use of diiodooctane as a solvent additive,[46] but saw no improvement in the PCE for any of the polymers. However, when chloronaphthalene (CN) was used as a solvent additive,[47] the device performance improved in all cases. The most notable increase was observed in the **P1**-based devices, where the PCE improved to 2.89%, largely due to an increase in the photocurrent. While both the **P2**- and **P3**-based devices also saw an increase in photocurrent, this improvement was less than in the case of **P1**. Accordingly, the **P2**- and **P3**-based devices had much smaller gains in overall PCE.

When comparing devices based on the furan-containing polymers **P1** and **P2**, both with identical polymer backbones, the impact that solvent additives can have on blend morphology is made clear. With the 3% CN additive, the devices from **P2** experienced a negligible improvement in PCE (+0.04%); however, **P1**-based devices consistently gave better efficiencies with the CN additive. Thus, solvent additives have the potential to neutralize morphological defects resulting from the use of branched side chains. Arguably, this effect is not as pronounced in the devices based on **P3** where reduced molecular weights lead to poorer film morphologies that could not be overcome. Due to these deficiencies, no attempts were made to optimize **P4**'s devices through solvent additives.

To further evaluate the photovoltaic performance of the polymers we investigated the hole mobility of the polymers using the space-charge-limited current (SCLC) method with a hole only device structure of ITO/PEDOT:PSS/Polymer/MoO_3/Al.[48] The mobilites were calculated according to the equation 3.1:

$$J_{SCL} = \frac{9\varepsilon_0 \varepsilon_r \mu_h V^2}{8L^3} \tag{3.1}$$

where $\varepsilon_0\varepsilon r$ is the permittivity of the polymer, μ is the carrier mobility, and L is the device thickness.[49] The hole mobilities were 1.18 x 10^{-3} $cm^2V^{-1}s^{-1}$, 6.69 x 10^{-4} $cm^2V^{-1}s^{-1}$, 5.58 x 10^{-4}

$cm^2V^{-1}s^-$, and 6.30 x 10^{-4} $cm^2V^{-1}s^{-1}$ for **P1**, **P2**, **P3** and **P4**, respectively. These values correlate with the device performance in that **P1** had the highest mobility and also the highest PCE. However, **P4** gave the poorest performance, but has a comparable hole mobility to **P2** and **P3**. Thus, the difference in device performance is also a result of the film morphology.

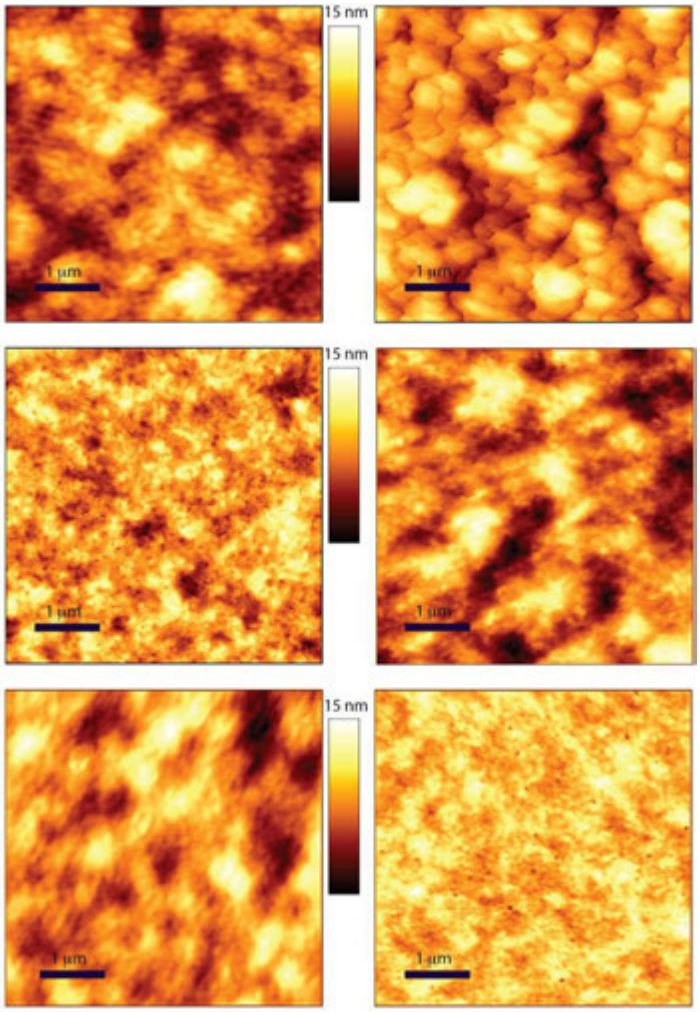

Fig. 3.4 AFM images (5 µm ×5 µm) of **P1** (top), **P2** (middle) and **P3** (bottom) with (right) and without (left) CN additive.

We examined the morphology of the polymer/$PC_{71}BM$ blends using atomic force microscopy (AFM). The height images of the polymer blends both with and without CN additive are shown in Figure 3.4. Although there are slight variations in the OPV performance of the different blends, they all formed fairly smooth films with small root-mean-square (rms) roughness of 1.05, 2.3, and 0.97 nm, for the **P1**, **P2** and **P3** respectively.

The AFM height images revealed that the surface topography of Polymer/$PC_{71}BM$ blend films with 3% CN additive is different from the films without the additive. In particular, the surface roughness of **P1** based active layer was decreased from 2.3 nm to 1.47 nm when the CN was added. This change was favorable for charge separation and transport as the PCE increased from 2.28% to 2.89%.[50] However, surface roughness is not the only indication of improvement as the surface roughness of **P2** and **P3** based active layer was increased from 1.05 nm to 3.91 nm and from 0.97 nm to 2.1 nm respectively when the CN was added. It has been reported previously that a rougher surface may also lead to a better photovoltaic performance.[51] Overall, the CN additive seemed to reduce the voids in the resulting films, improving the chemical compatibility between polymer donor and $PC_{71}BM$ acceptor molecules, thereby resulting in enhanced PCEs in **P1**-**P3** based devices. Since all four polymers show similar optical and electronic properties, factors related to morphology and charge carrier mobility play a larger role in overall device performance.

3.4 CONCLUSIONS

A related series of new donor-acceptor copolymers based on diketopyrrolopyrrole and 2,6-di(thiophen-2-yl)benzo[1,2-*b*:4,5-*b*']difuran have been synthesized. The substitution of the DPP monomer has been modified to bear all possible combinations of either flanking thiophenes or furans, and branched 2-ethylhexyl or linear tetradecyl alkyl chains. All four polymers displayed similar optoelectronic properties with an estimated average HOMOs of -5.6 eV, LUMOs of -3.8 eV and optical band-gaps of around 1.4 eV. Despite these similarities, the polymers displayed varied molecular weights due to the aforementioned modifications to the DPP unit. The furan-containing polymers **P1** and **P2** achieved higher molecular weights than either of the thiophene-containing analogues. Although branched side chains afforded greater solubility than the linear side chains, the OPVs fabricated from **P2**, which bears linear side chains exhibited the best PCE (~3%). Devices from **P1** were only able to achieve comparable efficiencies to the **P2** devices through the use of solvent additives. However, devices based on **P3** and **P4** achieved maximum efficiencies of only ~2.3% and 1.0%, respectively, due to limited solubility and poor film formation. These results further demonstrate that incorporating furan into polymer backbones typically dominated by thiophene can vastly improve solubility; as a result polymers with higher

molecular weights can be processed without the use of large, branched alkyl side chains. These fundamental improvements are integral to the creation of new, high-efficiency OPVs by enhancing both film morphology and charge-carrier mobility.

3.5 EXPERIMENTAL

3.5.1 Materials

Air- and moisture-sensitive reactions were performed using standard Schlenk techniques. Solvents used for palladium-catalyzed reactions were deoxygenated prior to use by sparging with argon through the solvent with vigorous stirring for 30-60 minutes. SiliaMetS® Cysteine was purchased from SiliCycle, Inc. All other chemical reagents were purchased from commercial sources and used without further purification unless otherwise noted. (5,5'-(3,7-Didecylbenzo[1,2-*b*:4,5-*b*']difuran-2,6-diyl)bis(4-decylthiophene-5,2-diyl))bis(trimethylstannane) **1** was prepared according to literature procedures. For synthesis of 3,6-bis(5-bromofuran-2-yl)-2,5-bis(2-ethylhexyl)pyrrolo[3,4-c]pyrrole-1,4(2H,5H)-dione **2a**, 3,6-bis(5-bromofuran-2-yl)-2,5-bis(tetradecyl)pyrrolo[3,4-c]pyrrole-1,4(2H,5H)-dione **2b**, 3,6-di(5-bromo-2-thienyl)-2,5-bis(2-ethylhexyl)pyrrolo[3,4-*c*]pyrrole-1,4(2*H*,5*H*)-dione **2c,** and bis(5-bromothiophen-2-yl)-2,5-bis(tetradecyl)pyrrolo[3,4-c]pyrrole-1,4(2H,5H)-dione **2d,** see Supporting Information.

3.5.2 Characterization

Nuclear magnetic resonance (NMR) spectra were carried out in $CDCl_3$ and recorded on Varian VXR (300 MHz), Varian MR (400 MHz) or a Bruker Avance III (600 MHz). ^1H NMR spectra were internally referenced to the residual protonated solvent peak. In all spectra, chemical shifts are given in ppm (δ) relative to the solvent. Gel permeation chromatography (GPC) measurements were performed on a separation module equipped with three 5 μm I-gel columns connected in series (guard, HMW, MMW and LMW) with a UV-Vis detector. Analyses were performed at 50 °C using THF as the eluent with a flow rate of 1.0 mL/min. Calibration was based on polystyrene standards. Thermal gravimetric analysis measurements were performed over an interval of 30 - 850 °C at a heating rate of 20 °C/min under ambient atmosphere. Differential scanning calorimetry was performed using a first scan heating rate of 15 °C/min to erase thermal history and a second scan to measure

transitions between 0 - 330 °C under nitrogen. Transitions were also measured with cooling at 15 °C/min. Cyclic voltammetry was performed using a e-DAQ e-corder 410 potentiostat with a scanning rate of 100 mV/s. The polymer solutions (1-2 mg/mL) were drop-cast on a platinum electrode. Ag/Ag^+ was used as the reference electrode and a platinum wire as the auxiliary electrode. The reported values are referenced to Fc/Fc^+ (-5.1 eV versus vacuum). All electrochemistry experiments were performed in deoxygenated CH_3CN under an argon atmosphere using 0.1 M tetrabutylammonium hexafluorophosphate as the electrolyte. Absorption spectra were obtained on a photodiode-array Agilent 8453 UV-visible spectrophotometer using polymer solutions in $CHCl_3$ and thin films. The films were made by spin-coating 25 x 25 x 1 mm glass slides using solutions of polymer (2.5-5.0 mg/mL) in $CHCl_3$/*o*-dichlorobenzene at a spin rate of 1200 rpm on a Headway Research, Inc. PWM32 spin-coater.

3.5.3 Fabrication of photovoltaic devices

All devices were produced via a solution-based, spin-casting fabrication process. All polymers were mixed with $PC_{71}BM$ (SES Research) (mixed 1:2 with a total solution concentration of 30 mg/mL for $PC_{71}BM$) then dissolved in *o*-dichlorobenzene and stirred at 95°C for 48 hours. ITO coated glass slides (Delta Technologies) were cleaned by consecutive 10 minute sonications in (i) Mucasol™ detergent (dissolved in deionized water), 2x, (ii) deionized water, (iii) acetone, and then (iv) isopropanol. The slides were then dried in an oven for at least 3 hours and cleaned with air plasma (Harrick Scientific plasma cleaner) for 10 minutes. Filtered (0.45μm) PEDOT:PSS (Clevios P™) was spin-coated onto the prepared substrates (2000 rpm/60 sec) after first being stirred for 10 minutes at room temperature. The PEDOT:PSS films were annealed at 150 °C for 30 minutes. After cooling, the substrates were transferred to an argon-filled glovebox. After 48 hours of mixing, the polymer:PCBM solutions were filtered (0.45 μm pore, GS-Tek) and simultaneously dropped onto the PEDOT:PSS-coated substrates and spin-cast at 1000 rpm for 120 seconds. The films were dried under vacuum overnight. LiF (1 nm) and Al (100 nm) were successively thermally evaporated through a shadow mask under vacuum to complete the devices. *J-V* data was generated by illuminating the devices using an ETH quartzline lamp at 1 sun (calibrated using a crystalline silicon photodiode with a KG-5 filter).

3.5.4 Synthesis

General procedure for the synthesis of copolymers. An oven-dried, 25 mL Schlenk flask was charged with dry, deoxygenated toluene (5-10 mL), benzodifuran **1** (1.0 equiv.), and diketopyrrolopyrole **2a-d** (1.05 equiv.). The stirred solution was sparged with argon for 10 minutes and followed by the addition of tris(dibenzylideneacetone)dipalladium(0) (2 mol%) and tri(*o*-tolyl)phosphine (8 mol %). The reaction mixture was heated to reflux and stirred, under argon, for 4-24 hours. The polymer was end-capped by the addition of an excess amount of trimethyl(phenyl)tin and iodobenzene, each followed by a 4 hour period of reflux. The reaction mixture was cooled to 50 °C and diluted with chloroform. A small portion of SiliaMetS® Cysteine was added and the reaction mixture was stirred for 8 hours followed by precipitation into cold methanol and filtration. The polymer was purified via Soxhlet extraction by subsequently rinsing with methanol, acetone and hexanes and finally extracted with chloroform. Most of the chloroform was removed *in vacuo* and the polymer was precipitated into methanol, collected by filtration and dried *in vacuo*.

Synthesis of P1. Following the general polymerization procedure using compounds **1** (605 mg, 0.50 mmol) and **2a** (342 mg, 0.53 mmol) and a reaction time of 6 hours afforded a dark solid (578 mg, 84%). ^{1}H NMR (600 MHz, $CDCl_3$): δ 8.51 (2H, br), 7.57 (2H, br), 7.34 (2H, br), 6.85 (2H, br), 4.19 (4H, br), 2.79-2.96 (8H, br), 1.99 (2H, br), 1.68-1.81 (8H, br), 1.22-1.52 (72H, br), 0.82-0.96 (24H, br). GPC (THF, 50 °C): M_w = 55.6 kDa, M_n = 28.9 kDa, PDI = 1.9.

Synthesis of P2. Following the general polymerization procedure using compounds **1** (363 mg, 0.3 mmol) and **2b** (258 mg, 0.32mmol) and a reaction time of 6 hours afforded a dark solid (360 mg, 78%). ^{1}H NMR (600 MHz, $CDCl_3$): δ 8.47 (2H, br), 7.55 (2H, br), 7.34 (2H, br), 6.86 (2H, br), 4.24 (4H, br), 2.79-2.96 (8H, br), 1.68-1.88 (12H, br), 1.20-1.55 (100H, br), 0.87 (18H, br). GPC (THF, 50 °C): M_w = 44.2 kDa, M_n = 19.9 kDa, PDI = 2.2.

Synthesis of P3. Following the general polymerization procedure using compounds **1** (346 mg, 0.29 mmol) and **2c** (203 mg, 0.32 mmol) and a reaction time of 4 hours afforded a dark solid (220 mg, 52%). ^{1}H NMR (600 MHz, $CDCl_3$): δ 8.91 (2H, br), 7.56 (2H, br), 7.36 (2H,

br), 7.25 (2H, br), 4.09 (4H, br), 2.79-2.96 (8H, br), 1.98 (2H, br), 1.68-1.81 (8H, br), 1.22-1.48 (72H, br), 0.96 (6H, br), 0.88 (18H, br). GPC (THF, 50 °C): M_w = 24.0 kDa, Mn = 9.5 kDa, PDI = 2.5.

Synthesis of P4. Following the general polymerization procedure using compounds **1** (209 mg, 0.17 mmol) and **2d** (154 mg, 0.18 mmol) and a reaction time of 24 hours afforded a dark solid (201 mg, 71%). ^{1}H NMR (600 MHz, $CDCl_3$): δ 8.91 (2H, br), 7.56 (2H, br), 7.36 (2H, br), 7.26 (2H, br), 4.14 (4H, br), 2.78-2.95 (8H, br), 1.68-1.88 (12H, br), 1.22-1.52 (100H, br), 0.88 (18H, br). GPC (THF, 50 °C): M_w = 8.1 kDa, M_n = 6.1 kDa, PDI = 1.3.

3.6 ACKNOWLEDGEMENTS

We thank the National Science Foundation (DMR-0846607) for partial support of this work. We also thank the National Science Foundation Materials Research Facilities Network (DMR-1250372) and Polymer-Based Materials for Harvesting Solar Energy, an Energy Frontier Research Center funded by the U.S. Department of Energy, Office of Science, Office of Basic Energy Sciences under Award Number DE-SC0001087 for support of the device fabrication. The Iowa State University (ISU), the Institute for Physical Research and Technology provided MDE with a Katron Fellowship. Some of the OPV work was performed at the ISU Microelectronics Research Center. We also thank Dr. Kamel Harrata and the ISU Mass Spectroscopy Laboratory for analysis. We thank Achala Bhuwalka for assistance with thermal analysis. We thank Kim Topp and Dr. Jared Mike for rendering the graphical abstract. We thank Dr. Zhiqun Lin, Dr. Sumit Chaudhary and Dr. Robert J. Angelici for helpful discussions of this work.

3.7 SUPPORTING INFORMATION

3.7.1 Synthetic Procedures

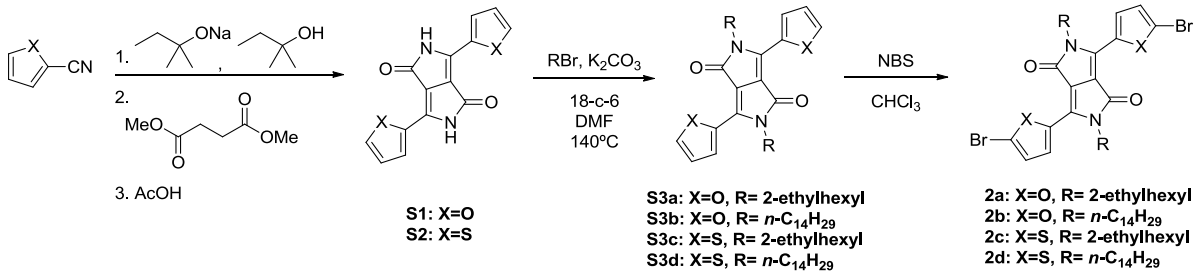

Scheme S3.1. Synthesis of diketopyrrolopyrole monomers.

3,6-Di(furan-2-yl)pyrrolo[3,4-*c*]pyrrole-1,4(2*H*,5*H*)-dione (S1). Sodium metal (4.94 g, 218 mmol) was added portion-wise to *tert*-amyl alcohol and the solution was stirred overnight at 120°C. Furan-2-carbonitrile (20.0 g, 269 mmol) was then added to the hot alkoxide solution followed by the dropwise addition of a solution of dimethyl succinate (11.7 mL, 89 mmol) in 80 mL of *tert*-amyl alcohol. After complete addition of the dimethyl succinate solution, the mixture was allowed to stir at reflux overnight. The reaction mixture was then allowed to cool to 60°C, quenched with 40 mL of acetic acid, and allowed to stir at reflux for an additional hour. The resulting suspension was then filtered and the solid washed with hot methanol and water three times and dried *in vacuo*, affording a dark solid (21.8 g, 91%). Compound **S1** was used in the next step without further purification.

3,6-Di(thiophen-2-yl)pyrrolo[3,4-*c*]pyrrole-1,4(2*H*,5*H*)-dione (S2). The title compound was prepared in a similar manner to **S1** using sodium metal (3.85 g, 173 mmol), thiophene-2-carbonitrile (19.0 mL, 204 mmol) and dimethyl succinate (54 mmol, 0.67 M in *tert*-amyl alcohol) to afford a dark solid (15.1 g, 93%). Compound **S2** was used in the next step without further purification.

General alkylation procedure of DPP cores. The DPP core **S1** or **S2**, K_2CO_3 (4.3 equiv), and catalytic 18-crown-6 were dissolved in DMF under argon and stirred at 130°C for 1h. Alkyl bromide (3.7 equiv) was then added dropwise and the reaction mixture was stirred for 48h. The reaction mixture was then cooled to room temperature and dilute with water. Chloroform was added to the mixture and the layers were separated. The aqueous layer was

extracted with chloroform. The combined organic layers were washed with water, dried over sodium sulfate and the solvent removed *in vacuo*. The crude product was purified by flash chromatography on silica, using either chloroform or 1:1 chloroform/hexanes as the eluent to give pure alkylated product.

2,5-bis(2-ethylhexyl)-3,6-di(2-furanyl)-pyrrolo[3,4-*c*]pyrrole-1,4(2*H*,5*H*)-dione (S3a). The title compound was synthesized according to the general alkylation procedure for DPP cores from 2.50 g (9.3 mmol) **S1** and 2-ethylhexyl bromide and purified by flash chromatography on silica using as the 1:1 chloroform/hexanes as the eluent to afford 2.75 g (5.6 mmol) of a tacky red solid in 60% yield. ^{1}H NMR (400 MHz, $CDCl_3$) δ 8.33 (dd, J = 3.6, 0.7 Hz, 2H), 7.61 (dd, J = 1.7, 0.7 Hz, 2H), 6.69 (dd, J = 3.7, 1.7 Hz, 2H), 4.04 (dd, J = 7.4, 1.1 Hz, 4H), 1.83 – 1.67 (m, 2H), 1.42 – 1.19 (m, 16H), 0.98 – 0.78 (m, 6H).

3,6-di(2-furanyl)--2,5-ditetradecylpyrrolo[3,4-*c*]pyrrole-1,4(2*H*,5*H*)-dione (S3b). The title compound was synthesized according to the general alkylation procedure for DPP cores from 3.42 g (13.2 mmol) **S1** and 1-bromotetradecane and purified by flash chromatography on silica using as the 1:1 chloroform/hexanes as the eluent to afford 3.75 g (5.7 mmol) of a tacky red solid in 43% yield. ^{1}H NMR (600 MHz, $CDCl_3$) δ 8.31 (dd, J = 3.7, 0.7 Hz, 2H), 7.63 (dd, J = 1.7, 0.7 Hz, 2H), 6.70 (dd, J = 3.7, 1.7 Hz, 2H), 4.13 – 4.08 (m, 4H), 1.83 – 1.58 (m, 4H), 1.43 – 1.18 (m, 44H), 0.88 (t, J = 7.1 Hz, 6H).

2,5-Bis(2-ethylhexyl)-3,6-di(2-thienyl)-pyrrolo[3,4-*c*]pyrrole-1,4(2*H*,5*H*)-dione (S3c). The title compound was synthesized according to the general alkylation procedure for DPP cores from 3.00 g (10.0 mmol) **S2** and 2-ethylhexyl bromide and purified by flash chromatography on silica using chloroform as the eluent to afford 2.29 g (4.3 mmol) of a tacky purple solid in 43% yield. ^{1}H NMR (600 MHz, $CDCl_3$) δ 8.89 (dd, J = 3.9, 1.2 Hz, 2H), 7.61 (dd, J = 5.0, 1.1 Hz, 2H), 7.25 – 7.23 (m, 2H), 4.04 (m, 4H), 1.83 – 1.67 (m, 2H), 1.42 – 1.19 (m, 16H), 0.98 – 0.83 (m, 6H).

2,5-Ditetradecyl-3,6-di(2-thienyl)-pyrrolo[3,4-*c*]pyrrole-1,4(2*H*,5*H*)-dione (S3d). The title compound was synthesized according to the general alkylation procedure for DPP cores

from 0.30 g (1.0 mmol) **S2** and 1-bromotetradecane and purified by flash chromatography on silica using chloroform as the eluent to afford 0.18 g (0.26 mmol) of a tacky purple solid in 26% yield. ^{1}H NMR (600 MHz, $CDCl_3$) δ 8.89 (dd, J = 3.9, 1.2 Hz, 2H), 7.61 (dd, J = 5.0, 1.1 Hz, 2H), 7.25 – 7.23 (m, 2H), 4.13 – 4.08 (m, 4H), 1.83 – 1.58 (m, 4H), 1.43 – 1.18 (m, 44H), 0.88 (t, J = 7.1 Hz, 6H).

General bromination procedure of DPP cores. Alkylated-DPP was dissolved in chloroform, placed under an argon atmosphere and protected from light. The reaction mixture was then cooled to 0°C and NBS (2.4 equiv) was added portion-wise over 5 minutes. The reaction mixture was warmed to room temperature and stirred for 48h before being quenched with methanol. The solution was then washed with water and the organic layer was dried with sodium sulfate before being concentrated *in vacuo*. The crude product was then purified by flash chromatography on silica, using chloroform as eluent to give pure product.

3,6-Bis(5-bromofuran-2-yl)-2,5-bis(2-ethylhexyl)pyrrolo[3,4-*c*]pyrrole-1,4(2*H*,5*H*)-dione (2a). The title compound was synthesized according to the general bromination procedure of DPP cores from 1.66 g (1.66 g, 3.4 mmol) **S3a** to afford 1.31 g (1.8 mmol) of a dark red solid in 60% yield, (400 MHz, $CDCl_3$) δ 8.30 (d, J = 3.7 Hz, 2H), 6.62 (d, J = 3.7 Hz, 2H), 3.99 (dd, J = 7.4, 2.7 Hz, 4H), 1.77 – 1.68 (m, 2H), 1.42 – 1.20 (m, 16H), 0.96 – 0.83 (m, 12H).

3,6-Bis(5-bromofuran-2-yl)-2,5-ditetradecylpyrrolo[3,4-*c*]pyrrole-1,4(2*H*,5*H*)-dione (2b). The title compound was synthesized according to the general bromination procedure of DPP cores from 1.50 g (2.28 mmol) **S3a** to afford 0.80 g (1.0 mmol) of a dark red solid in 40% yield, ^{1}H NMR (600 MHz, $CDCl_3$) δ 8.25 (d, J = 3.7 Hz, 2H), 6.63 (d, J = 3.7

3,6-Bis(5-bromothiophen-2-yl)-2,5-bis(2-ethylhexyl)pyrrolo[3,4-*c*]pyrrole-1,4(2*H*,5*H*)-dione (2c). The title compound was synthesized according to the general bromination procedure of DPP cores from 824 mg (1.6 mmol) **S3a** to afford 203 mg (0.3 mmol) of a dark purple solid in 19% yield, ^{1}H NMR (400 MHz, $CDCl_3$) δ 8.58 (d, J = 4.2 Hz, 2H), 7.16 (d, J = 4.2 Hz, 2H), 3.92 – 3.78 (m, 4H), 1.83 – 1.71 (m, 2H), 1.37 – 1.02 (m, 16H), 0.92 – 0.72 (m, 12H).

3,6-Bis(5-bromothiophen-2-yl)-2,5-ditetradecylpyrrolo[3,4-*c*]pyrrole-1,4(2*H*,5*H*)-dione (2d). The title compound was synthesized according to the general bromination procedure of DPP cores from 536 mg (0.8 mmol) **S3a** to afford 154 mg (0.2 mmol) of a dark purple solid in 25% yield, ^{1}H NMR (300 MHz, $CDCl_3$) δ 8.68 (d, J = 4.2 Hz, 2H), 7.24 (d, J = 4.2 Hz, 2H), 4.12 – 3.80 (m, 4H), 1.85 – 1.60 (m, 4H), 1.41 – 1.04 (m, 44H), 0.88 (t, J = 6.4 Hz, 6H).

3.7.2 Spectral and Analytic Data

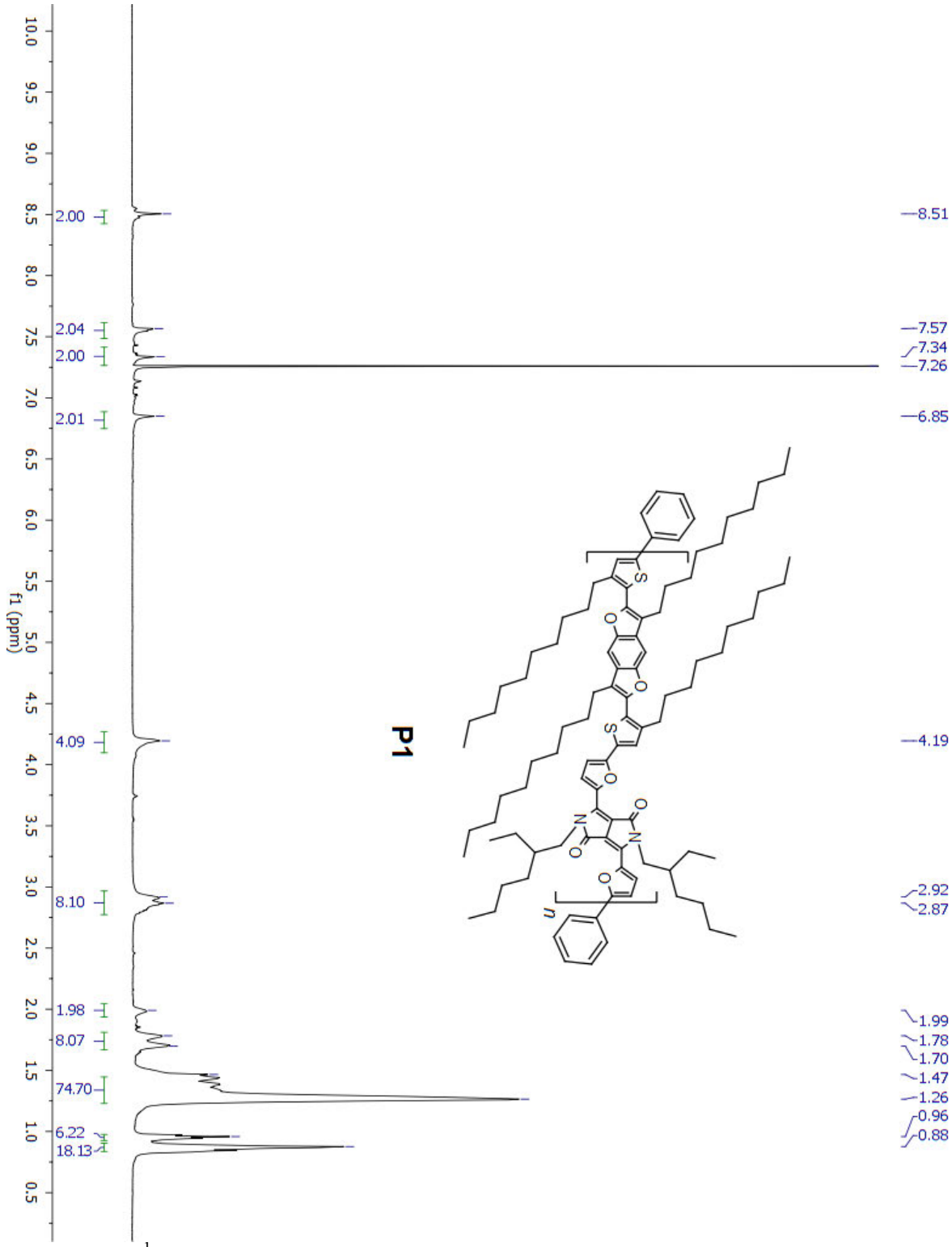

Figure S3.1. ^{1}H NMR of **P1**.

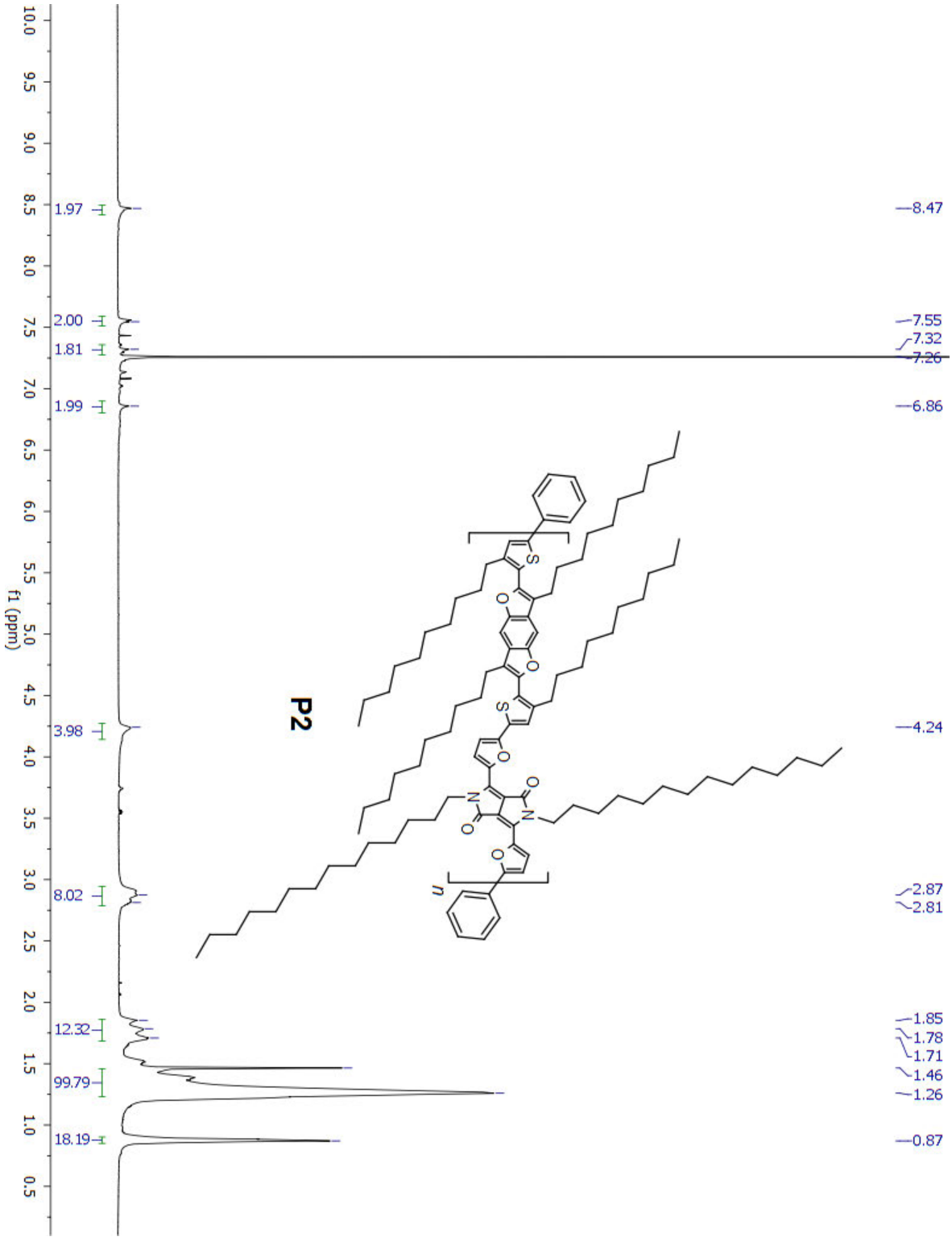

Figure S3.2. ^{1}H NMR of **P2**.

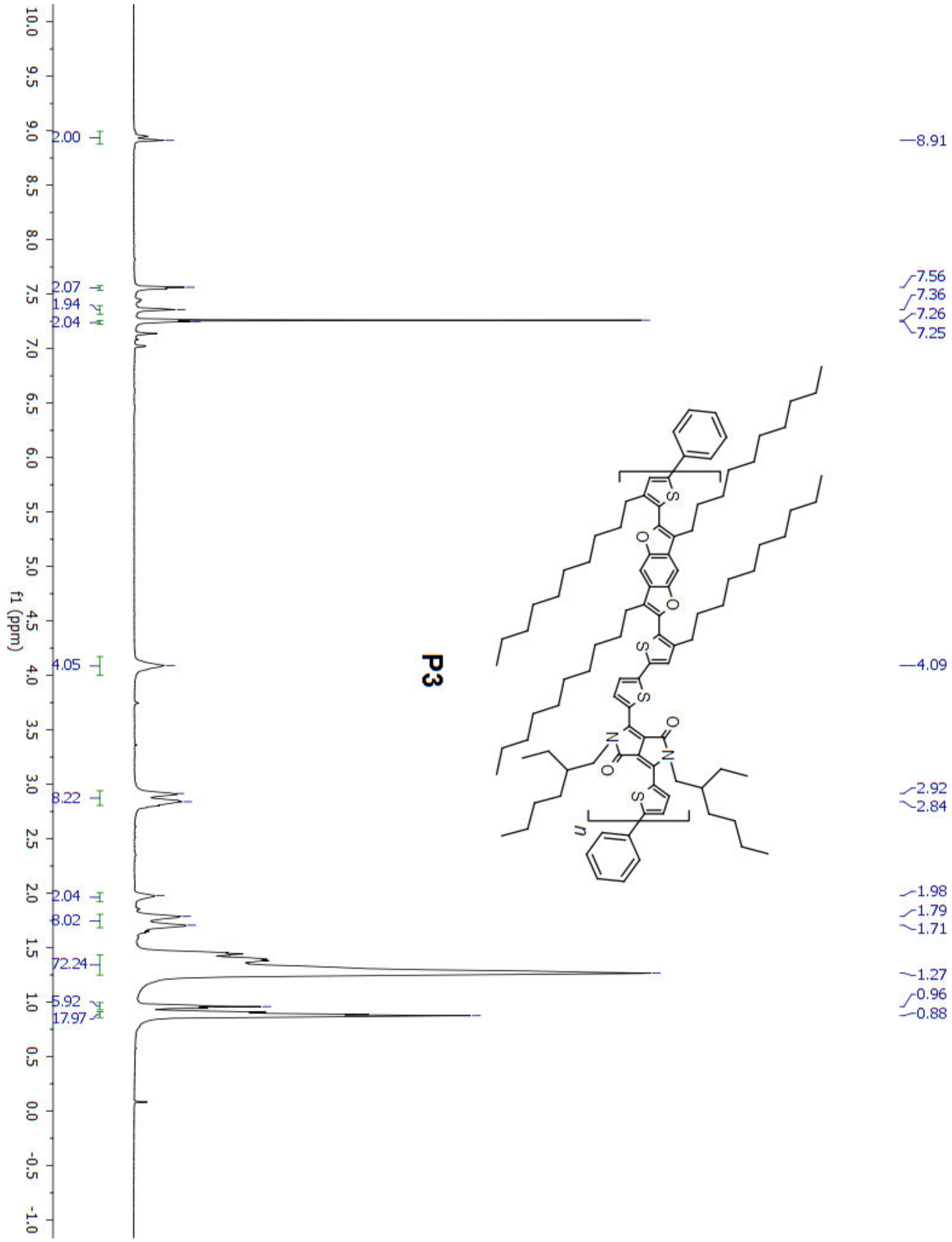

Figure S3.3. ^{1}H NMR of **P3**.

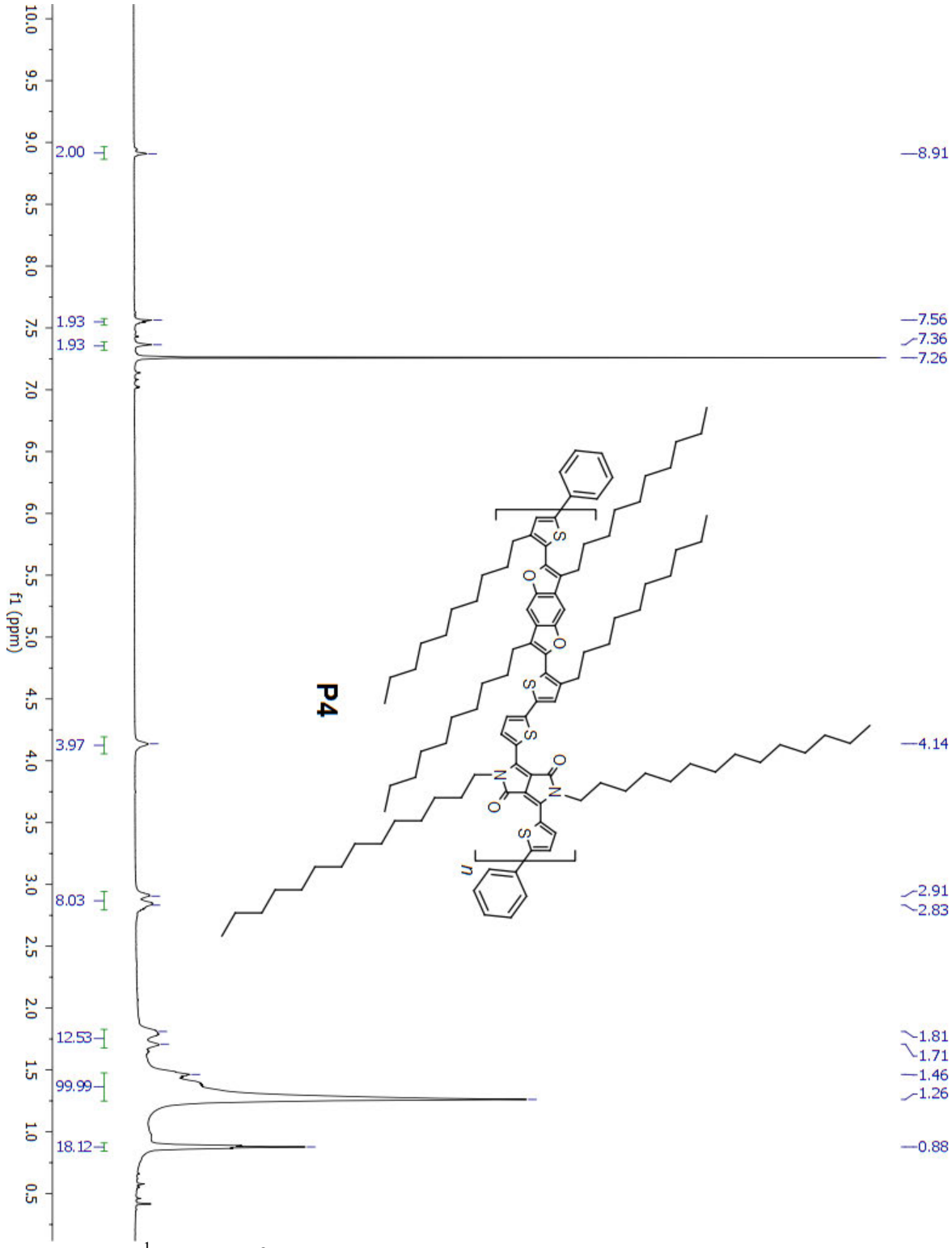

Figure S3.4. ^{1}H NMR of **P4**.

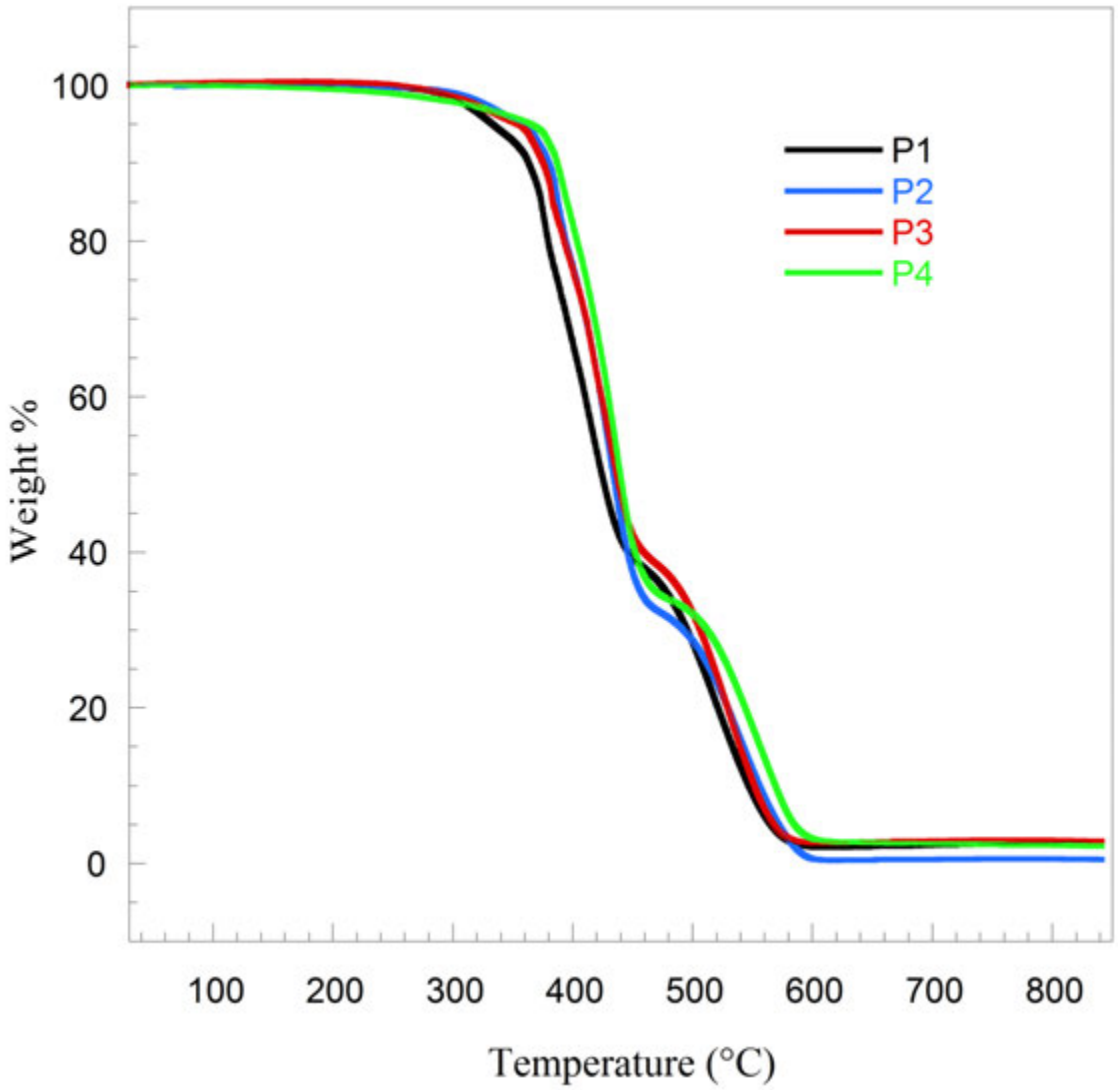

Figure S3.5. Thermal Gravometric Analysis of **P1-P4**.

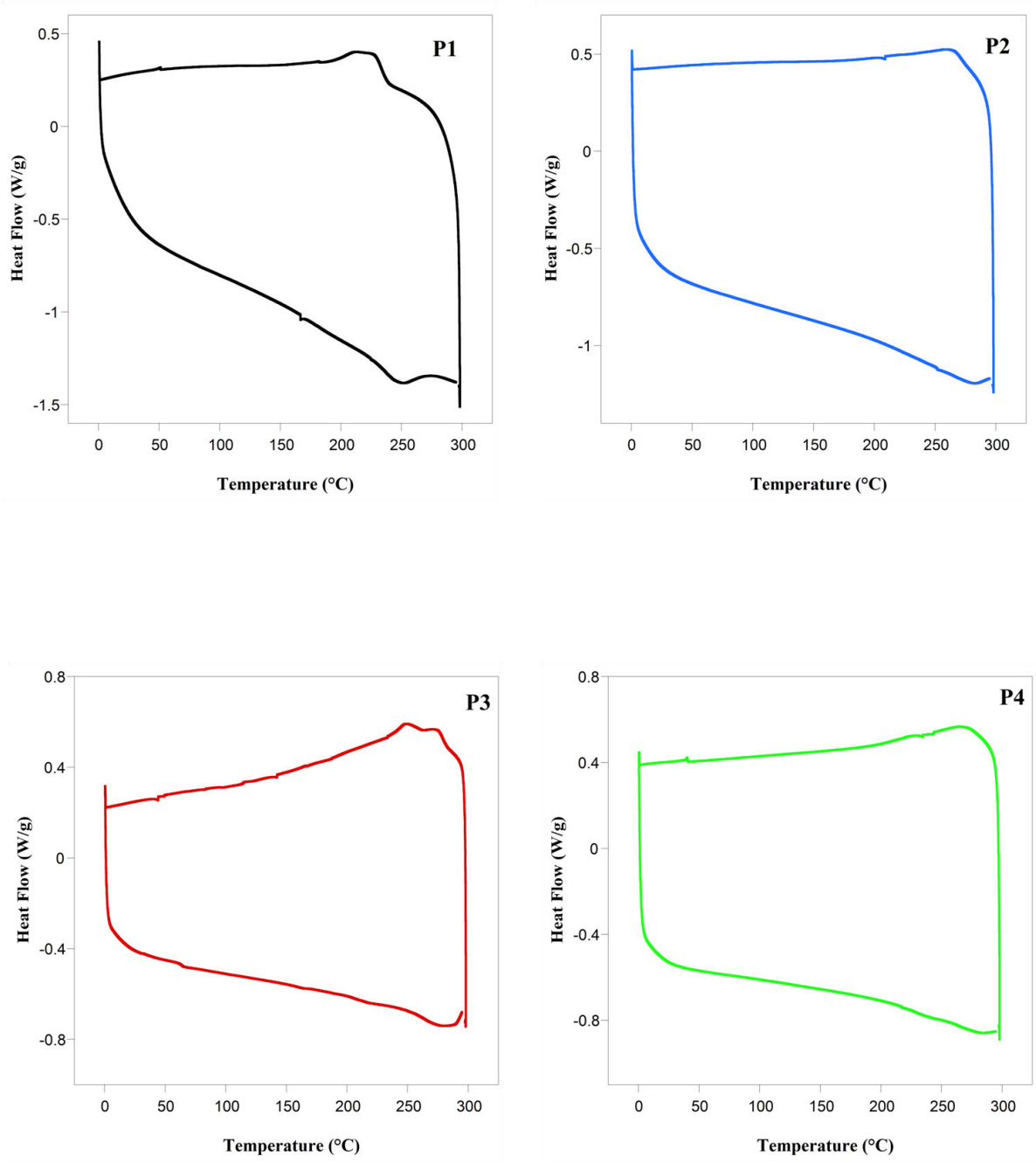

Figure S3.6. Differential scanning calorimetery (DSC) plots of **P1-P4**.

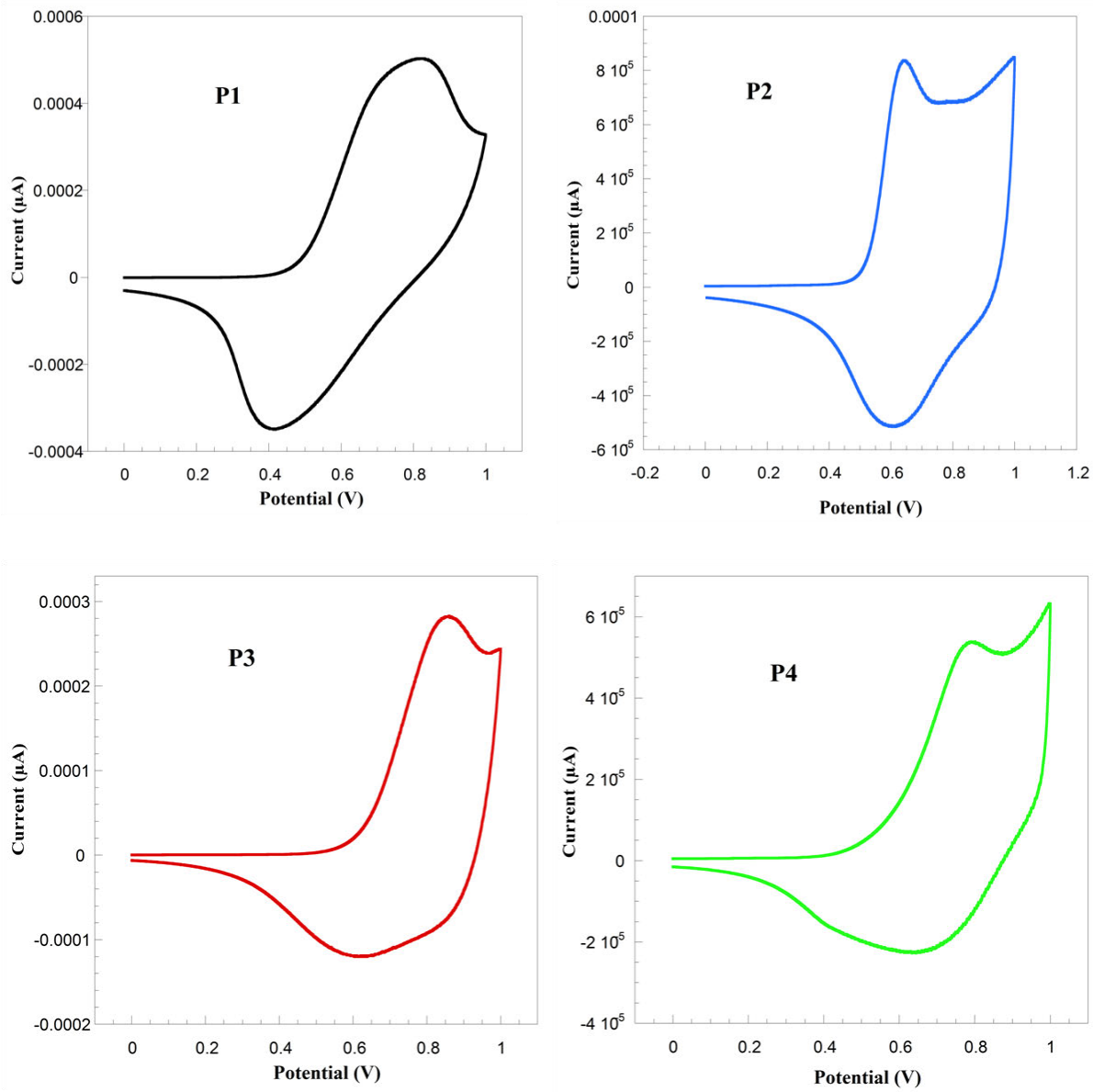

Figure S3.7. Cyclic voltammetry traces for oxidation cycles of **P1-P4**.

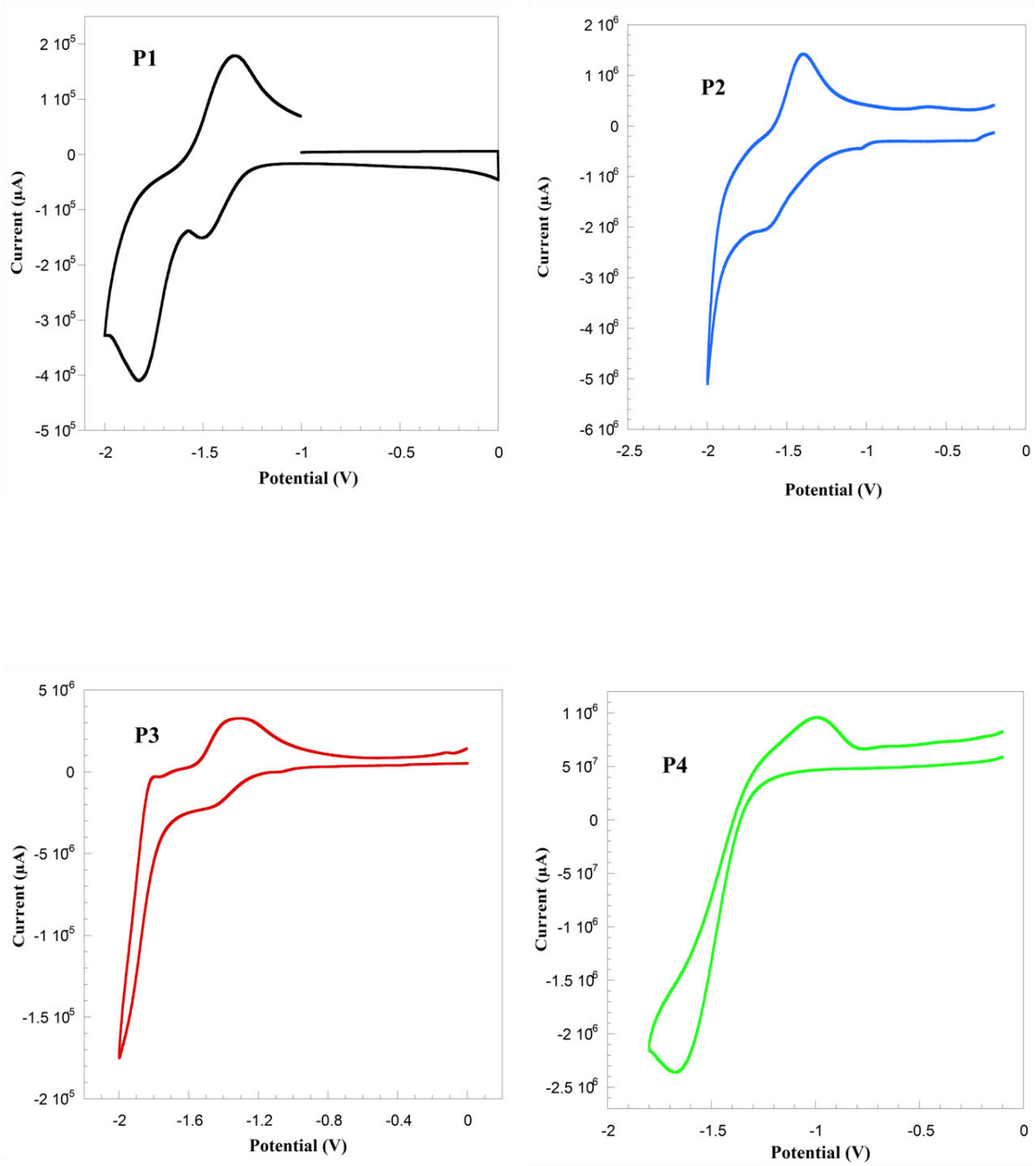

Figure S3.8. Cyclic voltammetry traces for reduction cycles of **P1-P4**.

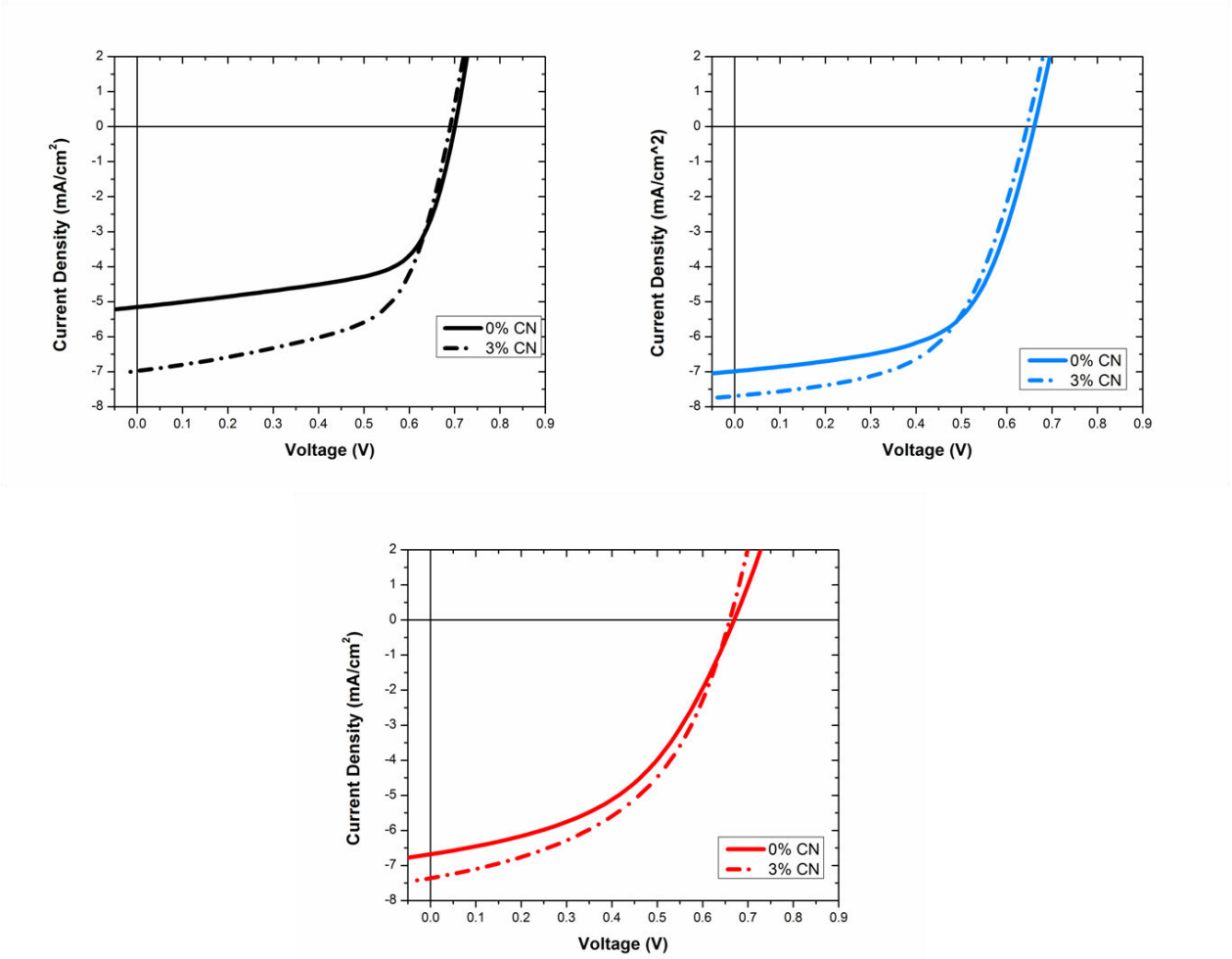

Figure S3.9. Current-voltage characteristics for polymer OPVs of **P1** (black), **P2** (blue), and **P3** (red) processed with and without 3% chloronapthalene.

3.8 REFERENCES

1. Service, R. F., *Science* **2011,** *332* (6027), 293.
2. Nelson, J., *Materials Today* **2011,** *14* (10), 462-470.
3. Facchetti, A., *Chem. Mater.* **2010,** *23* (3), 733-758.
4. Grimsdale, A. C.; Leok Chan, K.; Martin, R. E.; Jokisz, P. G.; Holmes, A. B., *Chem. Rev.* **2009,** *109* (3), 897-1091.
5. Thomas, S. W., III; Joly, G. D.; Swager, T. M., *Chem. Rev.* **2007,** *107* (4), 1339-1386.
6. Thompson, B. C.; Frechet, J. M. J., *Angew. Chem. Int. Ed. Engl.* **2008,** *47* (1), 58-77.
7. Havinga, E. E.; ten Hoeve, W.; Wynberg, H., *Polym. Bull.* **1992,** *29* (1), 119-126.
8. Havinga, E. E.; ten Hoeve, W.; Wynberg, H., *Synth. Met.* **1993,** *55* (1), 299-306.
9. He, Z.; Zhong, C.; Su, S.; Xu, M.; Wu, H.; Cao, Y., *Nature Photon.* **2012,** *6* (9), 591-595.

10. He, Z.; Zhong, C.; Huang, X.; Wong, W.-Y.; Wu, H.; Chen, L.; Su, S.; Cao, Y., *Adv. Mater.* **2011,** *23* (40), 4636-4643.
11. Small, C. E.; Chen, S.; Subbiah, J.; Amb, C. M.; Tsang, S.-W.; Lai, T.-H.; Reynolds, J. R.; So, F., *Nature Photon.* **2012,** *6* (2), 115-120.
12. Li, X.; Choy, W. C. H.; Huo, L.; Xie, F.; Sha, W. E. I.; Ding, B.; Guo, X.; Li, Y.; Hou, J.; You, J.; Yang, Y., *Adv. Mater.* **2012,** *24* (22), 3046-3052.
13. McCullough, R. D.; Lowe, R. D.; Jayaraman, M.; Anderson, D. L., *J. Org. Chem.* **1993,** *58* (4), 904-912.
14. Jeffries-EL, M.; McCullough, R. D., Regioregular polythiophene. In *Handbook of Conducting Polymers*, 3rd ed / edited by Terje A. Skotheim and John Reynolds. ed.; Skotheim, T. A., Reynolds, John R., Ed. London: Boca Raton, Fla, 2007; pp 331-380.
15. Huo, L.; Huang, Y.; Fan, B.; Guo, X.; Jing, Y.; Zhang, M.; Li, Y.; Hou, J., *Chem. Commun.* **2012,** *48* (27), 3318-3320.
16. Gidron, O.; Diskin-Posner, Y.; Bendikov, M., *J. Am. Chem. Soc.* **2010,** *132* (7), 2148-2150.
17. oo, . H. eaujuge, . M. Holcombe, . . ee, . . Fr chet, J. M. J., *J. Am. Chem. Soc.* **2010,** *132* (44), 15547-15549.
18. Bijleveld, J. C.; Karsten, B. P.; Mathijssen, S. G. J.; Wienk, M. M.; de Leeuw, D. M.; Janssen, R. A. J., *J. Mater. Chem.* **2011,** *21* (5), 1600-1606.
19. iu, A. . eaujuge, . M. ee, . . oo, . H. oney, M. F. Fr chet, J. M. J., *J. Am. Chem. Soc.* **2011,** *134* (4), 2180-2185.
20. Sonar, P.; Foong, T. R. B.; Singh, S. P.; Li, Y.; Dodabalapur, A., *Chem. Commun.* **2012,** *48* (67), 8383-8385.
21. Sonar, P.; Singh, S. P.; Williams, E. L.; Li, Y.; Soh, M. S.; Dodabalapur, A., *J. Mater. Chem.* **2012,** *22* (10), 4425-4435.
22. Bijleveld, J. C.; Gevaerts, V. S.; Di Nuzzo, D.; Turbiez, M.; Mathijssen, S. G. J.; de Leeuw, D. M.; Wienk, M. M.; Janssen, R. A. J., *Adv. Mater.* **2010,** *22* (35), E242-E246.
23. Wienk, M. M.; Turbiez, M.; Gilot, J.; Janssen, R. A. J., *Adv. Mater.* **2008,** *20* (13), 2556-2560.
24. ou, . Gendron, . adrou-A ch, R. d.; Najari, A.; Tao, Y.; Leclerc, M., *Macromolecules* **2009,** *42* (8), 2891-2894.
25. Zou, Y.; Gendron, D.; Neagu-Plesu, R.; Leclerc, M., *Macromolecules* **2009,** *42* (17), 6361-6365.
26. Qu, S.; Tian, H., *Chem. Commun.* **2012,** *48* (25), 3039-3051.
27. Bürgi, L.; Turbiez, M.; Pfeiffer, R.; Bienewald, F.; Kirner, H.-J.; Winnewisser, C., *Adv. Mater.* **2008,** *20* (11), 2217-2224.
28. Yuan, J.; Huang, X.; Zhang, F.; Lu, J.; Zhai, Z.; Di, C.; Jiang, Z.; Ma, W., *J. Mater. Chem.* **2012,** *22* (42), 22734-22742.
29. Hou, J.; Park, M.-H.; Zhang, S.; Yao, Y.; Chen, L.-M.; Li, J.-H.; Yang, Y., *Macromolecules* **2008,** *41* (16), 6012-6018.
30. Toba, M.; Nakashima, T.; Kawai, T., *J. Poly. Sci. A.* **2011,** *49* (8), 1895-1906.
31. Liang, Y.; Xu, Z.; Xia, J.; Tsai, S.-T.; Wu, Y.; Li, G.; Ray, C.; Yu, L., *Adv. Mater.* **2010,** *22* (20), E135-E138.
32. Najari, A.; Beaupré, S.; Berrouard, P.; Zou, Y.; Pouliot, J.-R.; Lepage-Pérusse, C.; Leclerc, M., *Adv. Funct. Mater.* **2011,** *21* (4), 718-728.

33. Chen, H.-Y.; Hou, J.; Zhang, S.; Liang, Y.; Yang, G.; Yang, Y.; Yu, L.; Wu, Y.; Li, G., *Nature Photon.* **2009,** *3* (11), 649-653.
34. Kobilka, B. M.; Dubrovskiy, A. V.; Ewan, M. D.; Tomlinson, A. L.; Larock, R. C.; Chaudhary, S.; Jeffries-EL, M., *Chem. Commun.* **2012,** *48* (71), 8919-8921.
35. Sista, P.; Huang, P.; Gunathilake, S. S.; Bhatt, M. P.; Kularatne, R. S.; Stefan, M. C.; Biewer, M. C., *J. Poly. Sci. A.* **2012,** *50* (20), 4316-4324.
36. Hu, C.; Fu, Y.; Li, S.; Xie, Z.; Zhang, Q., *Polym. Chem.* **2012,** *3* (10), 2949-2955.
37. Chen, X.; Liu, B.; Zou, Y.; Xiao, L.; Guo, X.; He, Y.; Li, Y., *J. Mater. Chem.* **2012,** *22* (34), 17724-17731.
38. Liu, B.; Chen, X.; Zou, Y.; He, Y.; Xiao, L.; Xu, X.; Li, L.; Li, Y., *Polym. Chem.* **2013,** *4* (3), 470-476.
39. Liu, B.; Chen, X.; Zou, Y.; Xiao, L.; Xu, X.; He, Y.; Li, L.; Li, Y., *Macromolecules* **2012,** *45* (17), 6898-6905.
40. Bunz, U. H. F., *Angew, Chem. Int. Ed.* **2010,** *49* (30), 5037-5040.
41. Hucke, A.; Cava, M. P., *J. Org. Chem.* **1998,** *63* (21), 7413-7417.
42. Miyata, Y.; Nishinaga, T.; Komatsu, K., *J. Org. Chem.* **2005,** *70* (4), 1147-1153.
43. Beaujuge, P. M.; Amb, C. M.; Reynolds, J. R., *Acc. Chem. Res.* **2010,** *43* (11), 1396-1407.
44. Li, W.; Roelofs, W. S. C.; Wienk, M. M.; Janssen, R. A. J., *J. Am. Chem. Soc.* **2012,** *134* (33), 13787-13795.
45. Cardona, C. M.; Li, W.; Kaifer, A. E.; Stockdale, D.; Bazan, G. C., *Adv. Mater.* **2011,** *23* (20), 2367-2371.
46. Lee, J. K.; Ma, W. L.; Brabec, C. J.; Yuen, J.; Moon, J. S.; Kim, J. Y.; Lee, K.; Bazan, G. C.; Heeger, A. J., *J. Am. Chem. Soc.* **2008,** *130* (11), 3619-3623.
47. Peet, J.; Kim, J. Y.; Coates, N. E.; Ma, W. L.; Moses, D.; Heeger, A. J.; Bazan, G. C., *Nature Mater.* **2007,** *6* (7), 497-500.
48. Mihailetchi, V. D.; Wildeman, J.; Blom, P. W. M., *Phys. Rev. Lett.* **2005,** *94* (12), 126602.
49. Shrotriya, V.; Yao, Y.; Li, G.; Yang, Y., *Appl. Phys. Lett.* **2006,** *89* (6), 063505-3.
50. Kim, B.; Yeom, H. R.; Yun, M. H.; Kim, J. Y.; Yang, C., *Macromolecules* **2012,** *45* (21), 8658-8664.
51. He, M.; Han, W.; Ge, J.; Yang, Y.; Qiu, F.; Lin, Z., *Energy Environ. Sci.* **2011,** *4* (8), 2894-2902.

CHAPTER 4

Atomic Level Engineering: Comparing the effect heteroatoms in analogous benzo[1,2-*b*:4,5-*b*']dichalcogenophenes on photovoltaic device performance in donor-acceptor copolymers with diketopyrrolopyrrole.

Brandon M. Kobilka,[a] Monique D. Ewan,[a] Benjamin J. Hale,[a] Andrew K. Peterson,[b] Achala Bhuwalka,[a] Volodimyr Duzhko,[c] J. Thomas Ippoliti[b] and Malika Jeffries-EL[a]*

[a] Department of Chemistry, Iowa State University, Ames, IA 50011

[b] Department of Chemistry, University of St. Thomas, St. Paul, MN 55105

[c] Department of Polymer Science and Engineering, University of Massachusetts – Amherst, 120 Governors Drive, Conte A529, Amherst, MA 01003-9263, USA

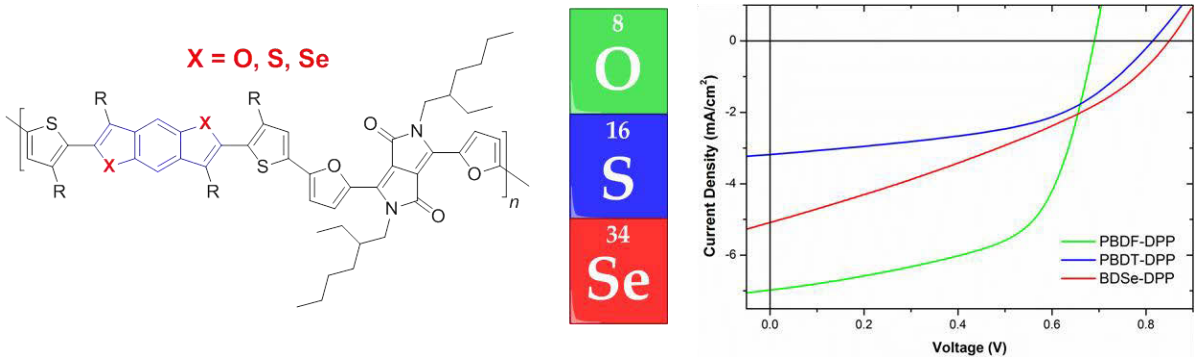

4.1 ABSTRACT

An analogous series of donor–acceptor conjugated polymers based on the novel 3,7-didodecyl-2,6-di(thiophen-2-yl)benzo[1,2-*b*:4,5-*b'*]dichalcogenophene (BDC) donors, and 1,4-diketopyrrolo[3,4-*c*]pyrrole as the acceptor were synthesized via the Stille cross-coupling reaction. The BDC heteroatoms were varied between oxygen, sulfur, and selenium to evaluate the impact on optoelectronic properties and performance in organic photovoltaic cells (OPVs). The benzodifuran-based copolymer displayed a HOMO level ~0.1 eV higher as well as a narrower optical band gap of 1.40 eV as compared with its chalcogen-based

analogues. This resulted in superior absorbance of the solar spectrum and the best overall performance of 2.9 % when the polymers were used as donor materials along with $PC_{71}BM$ as the electron-acceptor in bulk-heterojunction photovoltaic cells. The sulfur and selenium-based analogues performed similarly with power conversion efficiencies 50 % lower than the BDF analogues. These polymers suffered from poor fill factors and low short circuit current density, despite exhibiting open circuit voltages ~0.2 eV higher as compared with the BDF-based devices.

4.2 INTRODUCTION

Significant strides have been made recently towards the realization of organic semiconductor technology in everyday applications. In the last decade alone, extensive research has been conducted to make use of conjugated polymers as components for field effect transistors (OFET)s, light-emitting diodes (OLED)s, and photovoltaic cells (OPV)s.[1, 2] These organic-based materials offer several advantages that their inorganic counterparts lack, including the ability to be solution processed into large-area thin-films and to be fabricated into lightweight, flexible devices as well as the capacity to have their properties tuned through synthesis.[3-6] One of the most successful methods of modifying the optical and electronic properties of conjugated polymers is to synthesize materials comprised of alternating electron-donating and electron-accepting moieties.[7, 8] Through careful design and construction at the molecular level, one can control a multitude of these materials' properties that impact the performance of bulk-heterojunction organic photovoltaic cells (OPVs). This includes appropriately adjusted HOMO and LUMO energy levels, a reasonably narrow band gap, high charge carrier mobilities, and optimal active layer morphologies.

The constant evolution of new conjugated organic materials has played a large role in the steady rise in OPV performance over the last decade. One of the most prevalent themes to molecular design is the use of the thiophene moiety as a building block for organic electronics. From the often-studied poly(3-hexylthiophene) (P3HT) to a variety of more functionally complex electron-donating and electron-accepting heterocycles, thiophenes offer superior electronic properties, including high field-effect mobilities.[9, 10] The steady increase in the performance of OPVs over the past few years is a combination of many improvements including the development of new device architectures, band-gap engineering of the donor

materials, and optimization of film morphology. Recently, there has been interest in the substitution of other group 16 heteroatoms such oxygen or selenium to give isoelectronic furanyl and selenophenyl analogues to thiophene-based molecules.

Until recently, furan has not been widely incorporated into conjugated polymers, primarily due to difficulties associated with the synthesis of substituted furans. Nevertheless, furan possesses some advantageous properties that make it a potential candidate as a thiophene substitute. First of all, furan is less aromatic than thiophene and should lead to a more stabilized quinoid form, resulting in narrower band gaps.[11] Additionally, as oxygen has a diatomic radius only about 60% as large as sulfur, oligomers of furan experience a significantly more planar arrangment compared to those of thiophene due to less steric interactions with adjacent units.[12] There has also been evidence that polymers not based solely on furan, but instead with partial furan content, have better solubility than their thiophene containing analogs and as a result, yield OPVs with enhanced PCEs.[13, 14]

On the other hand, selenium is also expected to have some advantages over sulfur that can lead to beneficial properties in the subsequent materials. Selenophene, like furan, is also expected to favor the quinoid form as it is less aromatic than thiophene.[15, 16] Again, this results in a more planar, narrower band gap polymer.[17-19] Selenium-based molecules should exhibit increased charge-carrier mobility, since they have lone-pairs of electrons that have a reduced contribution to the conjugated backbone.[20] In terms of energy levels, selenium has an electronegativity nearly identical to that of sulfur and should result in similar highest-occupied molecular orbital (HOMO) levels.[21] Conversely, selenium has a stabilizing effect on the lowest-unoccupied molecular orbital (LUMO) owing to delocalization of the LUMO over the selenium atom, and reduced ionization potentials.[22] Thus, selenium is expected to promote broader solar spectrum absorbance without raising the HOMO level and forfeiting valuable open-circuit voltage (V_{oc}) in OPVs.

Among electron-donating materials, benzo[1,2-*b*:4,5-*b*′]dithiophene (BDT) has seen widespread use as a component in many OPVs with power conversion efficiencies (PCE)s for polymer OPVs over 7% for standard architectures and exceeding 9% in inverted solar cells. [23-26] BDT owes this success to its planar structure which leads to high hole mobilities and also facilitates favorable cofacial interactions through π-π stacking.[27-30] Despite this, the exploration of the analogous BDCs is relatively unexplored, with only a handful of examples

of benzo[1,2-*b*:4,5-*b*′]difuran (BDF) reported by our group[31, 32] and others,[11, 33-36] and only one report of benzo[1,2-*b*:4,5-*b*′]diselenophene (BDSe), by Yu *et al.*,[37] using these molecules as electron-donors in D-A copolymers for OPVs. In these cases, oxygen and selenium substitution has resulted in PCEs approaching 5% and 7%, respectively.

Recently, we reported the synthesis of the BDF-based monomer, 3,7-diiodo-2,6-di(thiophen-2-yl)benzo[1,2-*b*:4,5-*b*']difuran, its alkylation, and its subsequent use in D-A copolymers with the electron-accepting monomer 3,6-di(2-furanyl)-1,4-diketopyrrolo[3,4-*c*]pyrrole (FDPP).[14, 38-41] Diketopyrrolopyrrole (DPP) is a strong electron-accepting moiety that is known to promote intramolecular charge transfer within the polymer backbone as well as result in materials with low lying LUMO levels.[42-46] The DPP moiety can experience enhanced interchain interactions due to its symmetric coplanar structure.[44, 47] Initially, 3,6-di(2-thienyl)-1,4-diketopyrrolo[3,4-*c*]pyrrole (TDPP) was widely investigated for the synthesis of narrow band-gap polymers for use in OPVs with PCEs of up to 5.6%. Previously, FDPP-based polymers have been reported to exhibit better solubility than the analogous thiophene-flanked DPP-based polymers. Enhanced solubility plays an essential role in the improved PCEs realized by these copolymers, resulting from superior film formation.[39, 42, 48]

One of the problems associated with drawing conclusions between our previously synthesized BDF-based polymers and other similar BDT systems is the differing side chain substitution patterns of our version, which has 3,7-substitution, and the more common 4,8-substituted BDT. These variances can cause measurable differences in the electronic and physical properties of the resulting polymers. Taking these considerations in account, we have synthesized two new monomers with analogous structures to our previously reported BDF monomer comprised of BDT or BDSe. D-A copolymers composed of either BDT or BDSe and FDPP were synthesized and used in organic solar cell devices. Likewise, we have included a BDF analogue with more comparable molecular weights as well as the previously studied polymer to draw direct comparisons. The FDPP monomer was chosen as it gave the best performance in OPVs in our previous report. The performance of these materials was evaluated in OPVs to further evaluate the influence of how heteroatom substitution between the chalcogens can impact device performance.

4.3 RESULTS AND DISCUSSION

4.3.1 Synthesis and characterization

The synthetic route to the sulfur- and selenium-based benzo[1,2-*b*:4,5-*b*']dichalcogenophene monomers is illustrated in Scheme 4.1. Compounds **1a** and **1b** were synthesized from 1,4-dibromobenzene according to literature procedures, the deprotection of which afforded compounds **2a** and **2b**.[49-51] 3-Decyl-2-iodothiophene was synthesized according to a literature procedure by the iodination of 3-decylthiophene with N-iodosuccinimide.[52] Compounds **3a** and **3b** were prepared by the Sonogashira cross-coupling reaction of 3-decyl-2-iodothiophene and the respective bisacetylene **2a** or **2b**. The iodine-induced double cyclization of **3a** and **3b** gave BDT **4a** and BDSe **4b** in excellent yields. One benefit to this cyclization is that it results in two aryliodides, which were then subjected to Sonogashira cross-coupling conditions with 1-decyne to attach additional side chains for increased solubility, yielding compounds **5a** and **5b**.

Some difficulty was encountered in the attempt to hydrogenate the alkynes to the completely saturated decyl chains. Compound **5a** was subjected the standard conditions (Method A) that our group reported previously for the analogous BDF compound: 10% Pd/C at 35 bar in a Parr apparatus. However, the reaction failed to go to completion in a similar time frame (~2 days). Increased pressure of up to ~75 bar did not yield any significant increase in hydrogenated compound **5a**. Instead, it was necessary to load additional portions of catalyst and an extended reaction time of almost 3 weeks to give a ~95% hydrogenated product. Attempts to hydrogenated BDSe **5b** were even more sluggish and lesser amounts of partially and completely hydrogenated product were observed for similar reaction times to BDT **5a**. It seems likely that these reduced reactions were the result of catalyst poisoning from the sulfur- and selenium-containing aromatic rings.

Fortunately, we were able to successfully carry out the hydrogenation using a ThalesNano H-Cube Pro™. The advantage of using this system was twofold: firstly, by passing a solution of either **5a** or **5b** through the Pd/C cartridge mitigated any sulfur or selenium coordination to the catalyst; secondly, any partially or unhydrogenated compound present in the crude product mixture after one cycle could be completely hydrogenated in

additional cycles through the system. Several runs through the H-cube at 125° C and 100 bar afforded compounds **6a** and **6b** in good yield. These were then converted to bisstannane monomers **7a** and **7b**, respectively, by lithiation with *n*-butyllithium followed by the addition of trimethyltinchloride.

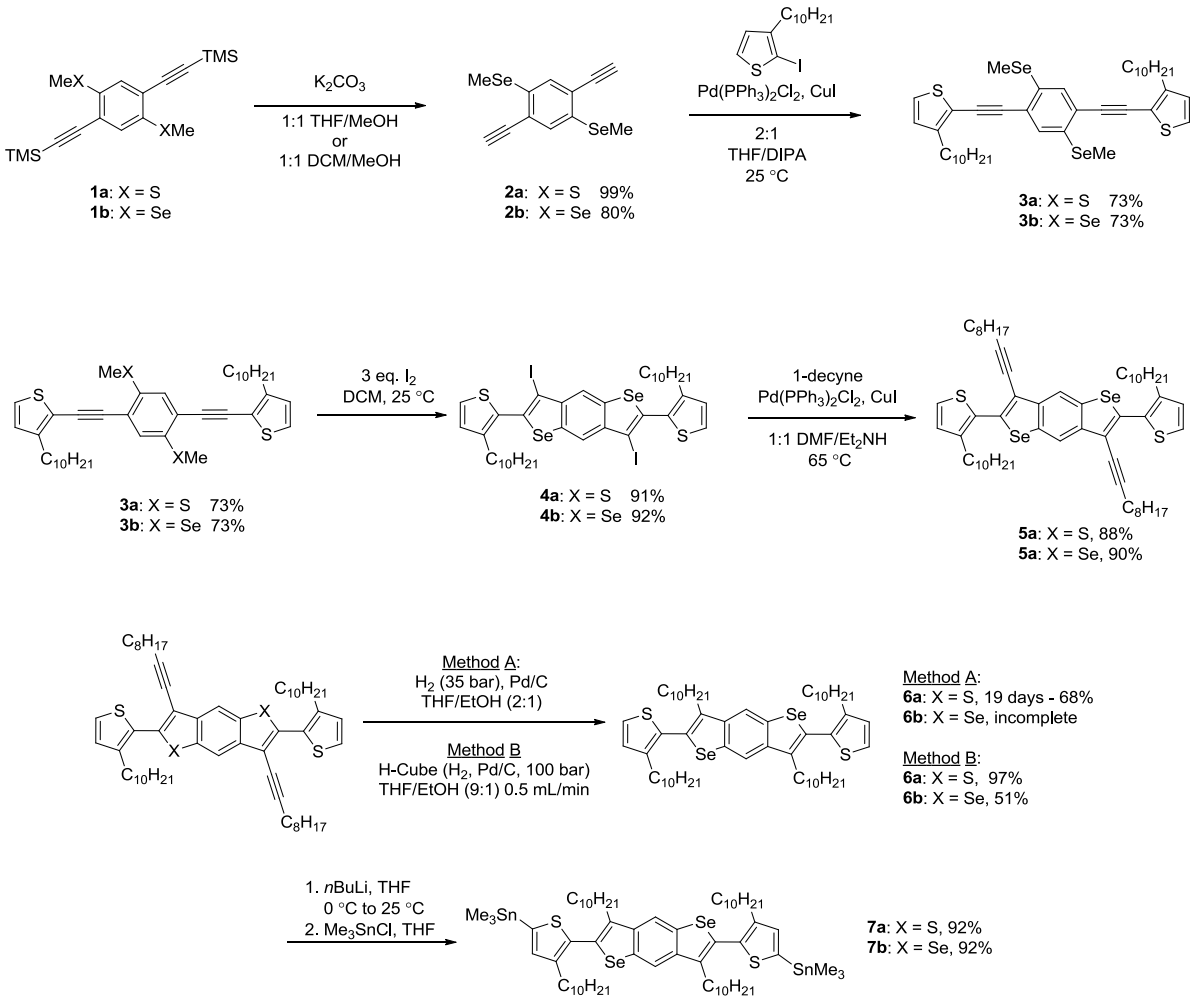

Scheme 4.1. Synthetic route to BDC monomers.

The synthesis of the donor-acceptor copolymers is shown in Scheme 4.2. Benzodifuran **8** was synthesized previously by our group.[31] The Stille cross-coupling reaction of diketo-pyrrolpyrole **9** and corresponding bisstannane 7**a**, **7b**, or **8** afforded polymers **PBDT-DPP**, **PBDSe-DPP** and **PBDF-DPP** in good yields (70% - 80%) after purification by stirring with functionalized silica followed by Soxhlet extraction. The analogous furan-containing polymer **PBDF-DPP** was previously reported by our group (as **P1**), but was remade at a

molecular weight similar to that of **PBDT-DPP** and **PBDSe-DPP** for comparison in this report.[32] All of the polymers were soluble in common organic solvents, such as THF, chloroform and chlorobenzene at room temperature.

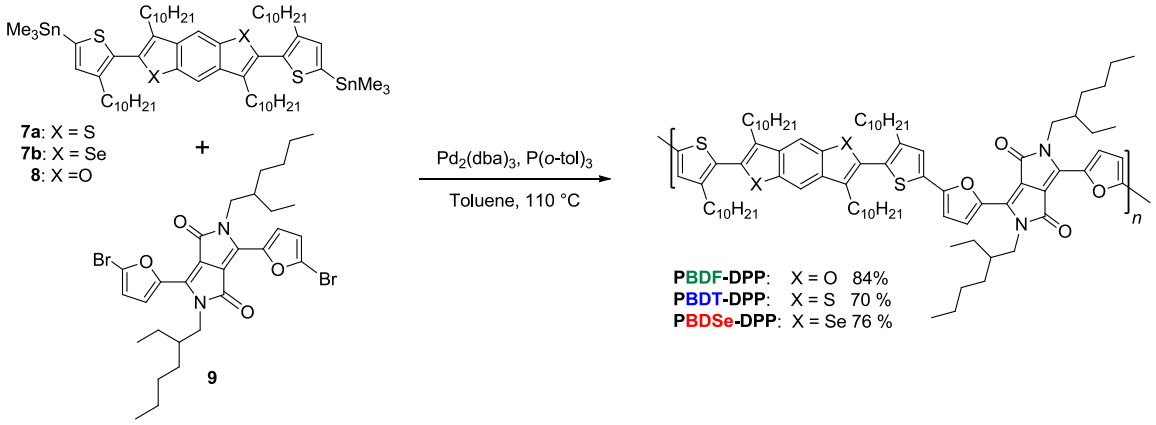

Scheme 4.2. Synthesis of donor-acceptor copolymers **PBDF-DPP, PBDT-DPP, and PBDSe-DPP**.

Table 4.1. Molecular weight and thermal data for Polymers.

Polymer	M_w [b] (kDa)	M_n [b] (kDa)	PDI	DP_n	T_d [c] (°C)
PBDF-DPP	25.7	14.6	1.8	16	333
PBDT-DPP	36.4	21.6	1.7	24	390
PBDSe-DPP	29.1	18.5	1.6	18	345

[a] Isolated yield. [b] Molecular weight data was obtained by GPC.
[c] 5% weight loss determined by TGA in air.

The polymers were characterized by ^{1}H NMR and the spectra are in agreement with the proposed polymer structures (see ESI†). The molecular weights were estimated using gel permeation chromatography (GPC) at 50 °C using $CHCl_3$ as the eluent and the resulting data is summarized in Table 4.1. All of the polymers displayed reasonably similar molecular weights (Mn = 15-21 kDa), with **PBDT-DPP** having the highest degree of polymerization, followed subsequently by **PBDSe-DPP** and **PBDF-DPP**. It should be noted that while our previous report of PBDF-DPP as (P1) had an M_w = 55.6 kDa, and a PDI = 1.9, this data was obtained using THF as the eluent on a different GPC instrument.

4.3.2 Thermal properties

The thermal properties of the polymers were evaluated using thermal gravimetric analysis (TGA) and differential scanning calorimetry (DSC). TGA results are summarized in Table 4.1 and indicate that 5% weight loss onsets occurred between 333 - 390 °C. . DSC did not reveal any observable phase transitions for temperatures up to 200 °C; however, observable melting points were seen for all four polymers above 235 °C. These thermal characteristics are indicative of good stability above the operational temperature threshold of organic photovoltaic devices.

4.3.3 Optical and electrochemical properties

The normalized absorption spectra of **PBDF-DPP**, **PBDT-DPP**, and **PBDSe-DPP** in dilute $CHCl_3$ solution and thin films are shown in Figures 4.1 and 4.2, respectively, and the optical data is summarized in Table 4.2. Each of the three polymers exhibit a broad absorption spectra with a significant, low-energy band that corresponds to intermolecular charge transfer between the electron-donating and electron-accepting units, while localized π-π^* transitions are responsible for the smaller, high-energy absorbance band. This dual-band absorbance profile is typical for such donor-acceptor copolymers.[53] In solution, the λ_{max} of **PBDT-DPP** and **PBDSe-DPP** is practically identical, occurring at 639 and 641 nm, respectively, while **PBDF-DPP** shows a comparatively large bathochromic shift in λ_{max} of almost 20 nm to 658 nm. Interestingly, the furan-containing polymer **PBDF-DPP** exhibits a significant low-energy shoulder at around 710 nm that is only slightly present in the selenium analogue **PBDSe-DPP** and cannot be observed at all in the sulfur analogue **PBDT-DPP**.

As thin films, all three polymers show a red-shift from the maximum absorbance peak of polymer solutions of ~5-10 nm. While all three polymers display an increase in the low

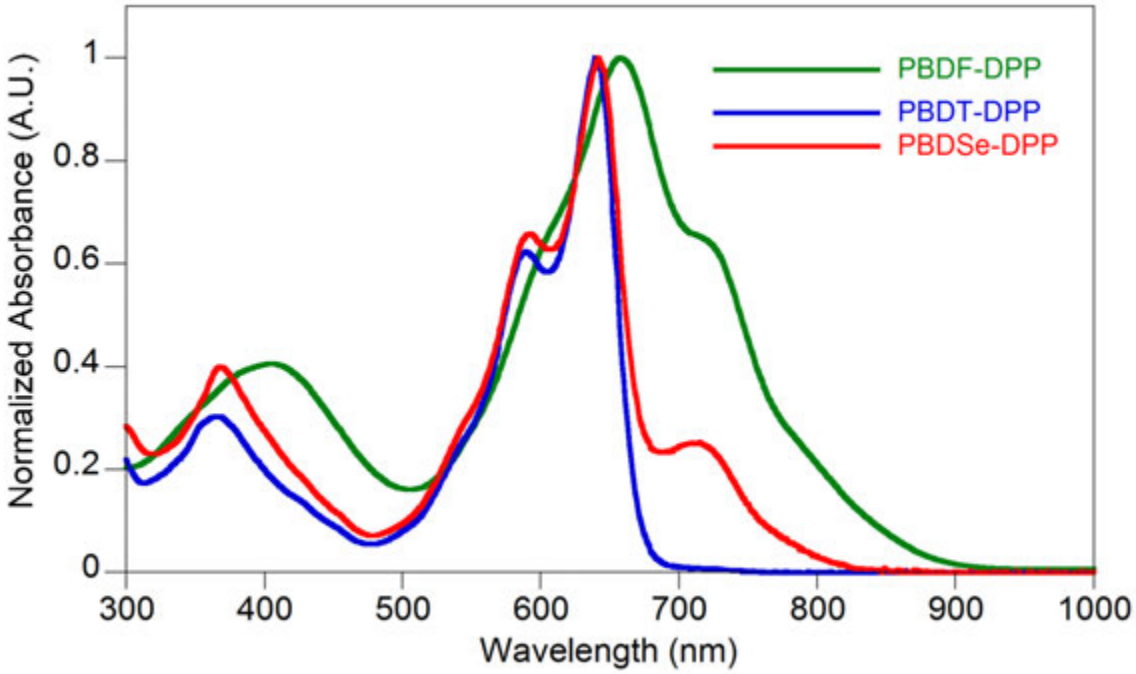

Figure 4.1. UV-Vis absorption of **PBDF-DPP, PBDT-DPP,** and **PBDSe-DPP** in CHCl3.

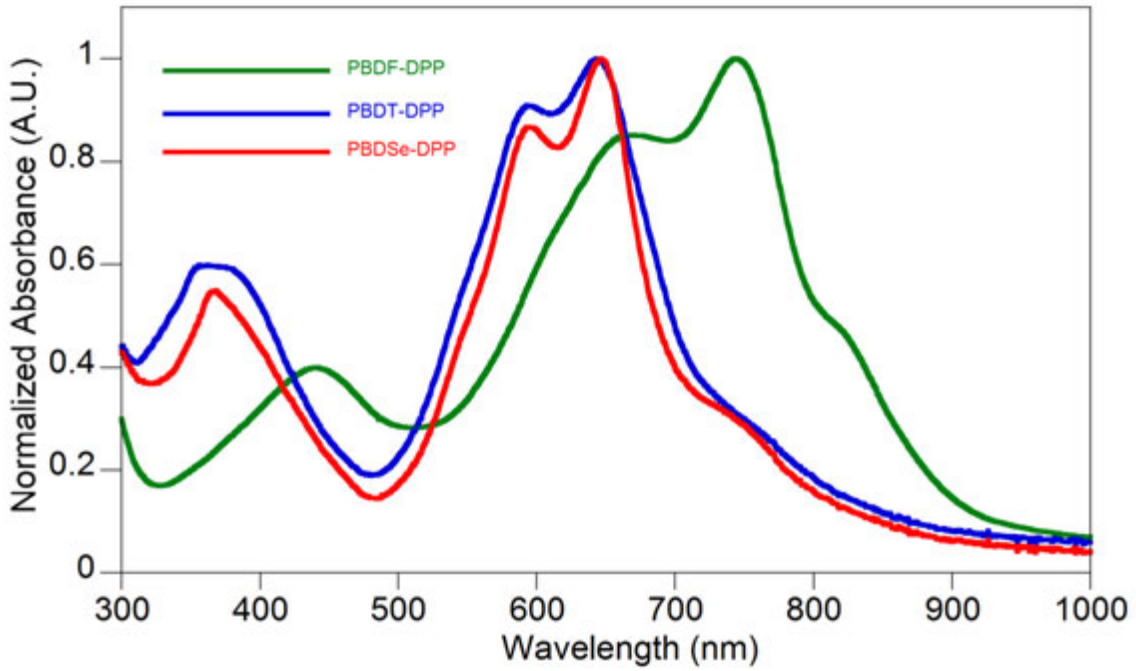

Figure 4.2. UV-Vis absorption of **PBDF-DPP, PBDT-DPP,** and **PBDSe-DPP** as thin films.

energy vibrational components as thin films, only **PBDF-DPP** displays a significant increase that results in a new λ_{max} of 744 nm. **PBDT-DPP** and **PBDSe-DPP** exhibit nearly identical absorbance profiles and both have similar low-energy shoulders at around 750 nm. **PBDF-DPP** also exhibits a smaller shoulder reaching further into the near-IR region at ~825 nm. This divide in absorption can also be seen in the optical band gaps of the polymers, estimated from the onset wavelength of the film absorption, where have values of approximately 1.50 eV, has a markedly lower band gap of about 1.40 eV. The fact that **PBDF-DPP** displays a significantly more broadened absorption band than either **PBDT-DPP** or **PBDSe-DPP**, despite having the lowest molecular weight of the three polymers, illustrates that the differences in absorbance are not correlated with the slight differences in molecular weights for this polymers series. This suggests that it is the varying of the heteroatoms affecting the optical properties of the polymers.

Table 4.2. Optical and electronic properties for **P1**-**P4**.

Polymer	λ_{max}^{soln} (nm)	λ_{max}^{film} (nm)	E_g^{opta} (eV)	HOMO[b] (eV)	LUMO[b] (eV)	E_g^{ECd} (eV)
PBDF-DPP	658	774, 668	1.40	-5.48	-3.67	1.81
PBT-DPP	639	643, 593	1.49	-5.55	-3.56	1.99
PBDSe-DPP	641	646, 595	1.50	-5.56	-3.63	1.93

[a] Estimated from the absorption onset of the film. [b] HOMO= -(E_{onset}^{ox} + 5.1) eV. [c] LUMO = -(E_{onset}^{red} + 5.1) eV. [d] E_g^{EC} = LUMO - HOMO.

To evaluate the electrochemical properties of the polymers, the redox behavior was measured by cyclic voltammetry. All four polymers exhibit measureable and reproducible oxidation and reduction processes (see 4.7 Supporting Information). The HOMO and LUMO levels were estimated from the onset of oxidation and reduction using the absolute energy level of ferrocene/ferrocenium (Fc/Fc^+) as 5.1 eV under vacuum and are summarized in Table 4.2.[54] The HOMO levels for all three polymers were deep enough to guarantee good air stability, with those of polymers **PBDT-DPP** and **PBDSe-DPP** nearly identical at around -5.55 eV. The HOMO level for **PBDT-DPP** was somewhat higher at -5.48 eV. This destabilization of the HOMO is likely due to the presence of the electron-rich furans on the

BDF ring.[55] The LUMO level of PBDT-DPP was the most stabilized ranged from -3.7 to -3.8 eV. The electrochemical band gaps are in good agreement with the optical data, with PBDF-DPP having the narrowest electrochemical band-gap of 1.8 eV. As expected, the optical band gaps are all estimated to be slightly smaller than the electrochemical band gap, which correlates well to the expected energy barrier associated with the interface of the polymer film and the electrode surface.[54] These values are suggest that replacing the commonly used sulfur-containing heterocycles with isoelectronic atoms such as oxygen and selenium can afford donor-acceptor polymers with more favorable energy levels for use in OPVs.

4.3.4 Photovoltaic Devices

The performance of all four polymers in OPVs was evaluated using [6,6]-phenyl-C_{71}-butyric acid methyl ester ($PC_{71}BM$) as the electron acceptor with a device configuration of indium tin oxide (ITO)/poly(3,4-ethylenedioxythiophene): polystyrene sulfonate (PEDOT:PSS)/polymer:$PC_{71}BM$/LiF/Al. Our previous report of **PBDF-DPP** found that an identical device configuration using a 1:2 weight-to-weight ratio of polymer/PCBM gave the best results; however an increased w/w ratio of 1:4 was found to give better results for the two new polymers **PBDT-DPP** and **PBDSe-DPP**. The active layer was deposited from 30 mg/mL *o*-DCB solutions, using processing conditions selected to yield a thickness of about 100 nm. We initially evaluated chloronaphthalene (CN) as a high-boiling solvent additive for the active layers of **PBDT-DPP** and **PBDSe-DPP**,[56] as a 3% addition of CN was found to significantly improve polymer/PCBM blend morphology and overall device performance in the BDF-containing analogue, **P1**, from our previous report. However, for the two new polymers reported here, we actually observed a performance decrease of ~8%, primarily due to a reduction in the short circuit current density. Diiodooctane (DIO) was also investigated as a solvent additive,[57] and did result in better performance for the new polymers, **PBDT-DPP** and **PBDSe-DPP**, while **P1** saw no improvement in the PCE in our previous report. The current density-voltage (*J-V*) curves of the OPVs are shown in Figure 4.3. The resultant photovoltaic performance, including short circuit current density (J_{SC}), open circuit voltage (V_{OC}), fill factor (FF) and power conversion efficiency (PCE) are summarized in Table 4.3.

Table 4.3. Photovoltaic device performance of **P1-P4** with PCBM.

Polymer	Additive	J_{SC} (mA/cm^2)	V_{OC} (V)	FF	PCE (%)
P1	none	-5.1	0.70	0.63	2.28
	3% CN	-7.0	0.69	0.60	2.89
PBDF-DPP	none	-4.88	0.68	0.67	2.20
PBDT-DPP	none	-3.57	0.85	0.32	0.96
	DIO	-3.30	0.82	0.51	1.38
PBDSe-DPP	none	-4.73	0.85	0.32	1.29
	DIO	-5.03	0.85	0.34	1.44

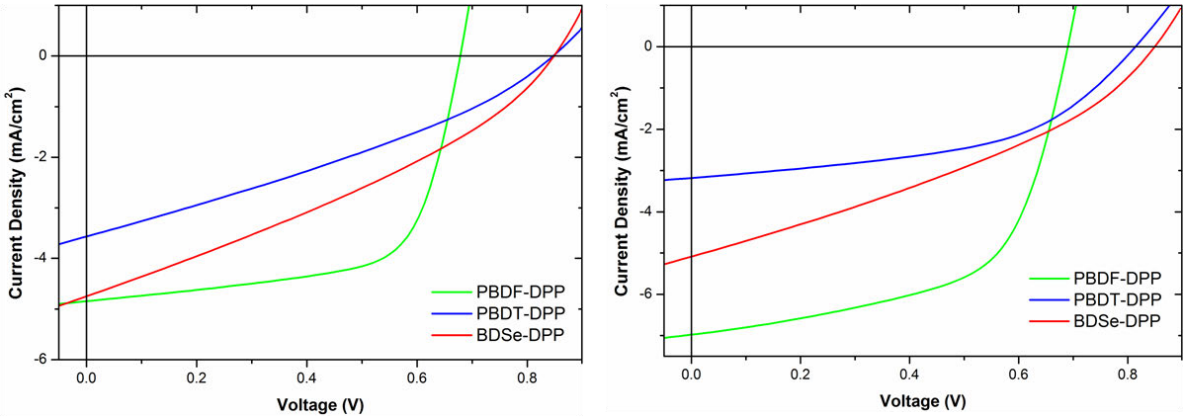

Figure 4.3. Current-voltage characteristics of **PBDF-DPP**-, **PBDT-DPP**-, and **PBDSe-DPP**-based OPVs without solvent additives (left) and using 3% CN (**PBDF-DPP**) or using 3% DIO (**PBDT-DPP** and **PBDSe-DPP**) (right).

Among the devices fabricated, the oxygen-containing analogues **PBDF-DPP** gave the highest PCEs both without (~2.2%) and with (~2.9%) solvent additives, which includes the previously reported **P1**. Without CN additives, the differences in molecular weight between **P1** and **PBDF-DPP** had no significant effect on performance. Both the sulfur- and selenium-containing analogues **PBDT-DPP** and **PBDSe-DPP** experienced significantly reduced efficiencies by around 50% as compared with **PBDF-DPP**. Despite this poor performance, **PBDT-DPP** and **PBDSe-DPP** both displayed V_{OC}s 0.15 eV higher than **PBDF-DPP**, which correlates well with their deeper HOMO levels. In all cases, the sulfur and selenium analogues suffered from reduced J_{SC} values as compared to **BDF-DPP**, which was expected to result from their larger optical band gaps and diminished absorbance of the solar spectrum. These discrepancies between the V_{OC}s could likely have mitigated each other had the FF been

similar between the different devices. Ultimately, the **PBDT-DPP**- and **PBDSe-DPP**-based devices suffered from FFs half that of the **PBDF-DPP**-based devices.

Between the devices fabricated from the new polymers **PBDT-DPP** and **PBDSe-DPP**, the V_{OC} was nearly identical with and without solvent additives which reflects the similar HOMO levels of the two polymers. The substitution of selenium resulted in better efficiencies in all cases as compared with sulfur. In the devices without DIO, this is primarily due to an increase of 1.16 mA/cm^2 J_{SC}, a gain of ~32%, which is similar to a report of selenium substitution by Jen and co-workers.[58] Interestingly, both polymers see increased performance with DIO additive, but for differing reasons. The sulfur analogue, **PBDT-DPP**, experiences a sizeable ~30% improvement in PCE due to a large increase in FF, whereas its selenium-containing counterpart gives a much smaller ~10% PCE improvement resulting from an enhancement of the J_{SC}.

4.4 CONCLUSIONS

To compare the effects of the chalcogen heteroartom substitution on the optoelectronic properties and the performance in OPVs, we have synthesized two new monomers based on benzo[1,2-*b*:4,5-*b*']dithiophene or benzo[1,2-*b*:4,5-*b*']diselenophene and the subsequent donor-acceptor copolymers with furan-flanked diketopyrrolopyrrole. These monomers and polymers are structural analogues to 3,7-didecyl-2,6-bis(3-decylthiophen-2-yl)benzo[1,2-b:4,5-b']difuran as well as the polymer **P1** previously reported by our group, and the resulting structure-function properties are summarized herein. The BDT and BDSe-based polymers displayed similar optoelectronic properties, with an estimated average HOMOs of -5.55 eV, LUMOs of close to -3.60 eV and optical band-gaps of around 1.5 eV. Both HOMO energy levels were more stabilized than their more electron rich, oxygen-containing counterpart **PBDF-DPP**. Also, as expected, the selenium analogue had a more stabilized LUMO than its sulfur-based counterpart. All three polymers had relatively similar molecular weights, with **PBDF-DPP** showing the lowest degree of polymerization. Despite higher-lying HOMO levels that give rise to a lower V_{OC} and its lower molecular weight, PBDF-DPP performed significantly better than either **PBDT-DPP** or **PBDSe-DPP** in OPVs. These results are primarily due to the superior J_{SC} and FF achieved by the **PBDF-DPP**-based devices. This study further demonstrates that the incorporation of different heteroatoms into polymer

backbones typically dominated by thiophene can have impactful effects on the properties and resulting performance of polymer-based semiconductors.

4.5 EXPERIMENTAL

4.5.1 Materials

All reactions were carried out at ambient atmosphere and temperature (18-25 °C) unless otherwise noted. Tetrahydrofuran and toluene were dried using an Innovative Technologies solvent purification system. Solvents used for Pd-catalyzed reactions were deoxygentated prior to use by bubbling a stream of argon through the stirred solvent for 30-60 minutes. Trimethylsilyl acetylene was purchased from GFS chemicals. Bis(triphenylphosphine)-palladium(II) dichloride was purchased from Oakwood Products, Inc. 3-Decylthiophene[59], 1,4-dibromo-2,5-diidobenzene[49], 1,4-dibromo-2,5-bis(trimethylsilylethnynyl) benzene,[50] 4-bis(methylthio)-2,5-bis(trimethylsilylethnynyl)benzene (**1a**)[51] and 1,4-bis(methylseleno)-2,5-bis(trimethylsilylethnynyl)benzene (**1b**)[51] were synthesized according to literature procedures. All other chemicals were purchased from Sigma-Aldrich and used without further purification.

4.5.2 Characterization

Nuclear magnetic resonance (NMR) spectra were carried out in $CDCl_3$ and recorded on Varian VXR (300 MHz), Varian MR (400 MHz) or a Bruker Avance III (600 MHz). ^1H NMR spectra were internally referenced to the residual protonated solvent peak. In all spectra, chemical shifts are given in ppm (δ) relative to the solvent. High-resolution mass spectra (HRMS) were recorded on a double-focusing magnetic sector mass spectrometer using ESI or APCI, as noted, at 70 eV. Melting points were obtained using a MELTEMP melting point apparatus with an upper temperature limit of 260 °C. Gel permeation chromatography (GPC) measurements were performed on a separation module equipped with three 5 μm I-gel columns connected in series (guard, HMW, MMW and LMW) with a UV-Vis detector. Analyses were performed at 50 °C using $CDHl_3$ as the eluent with a flow rate of 1.0 mL/min. Calibration was based on polystyrene standards. Thermal gravimetric analysis measurements were performed over an interval of 30 - 850 °C at a heating rate of 20 °C/min under ambient atmosphere. Differential scanning calorimetry was performed using a first

scan heating rate of 15 °C/min to erase thermal history and a second scan to measure transitions between 0 - 330 °C under nitrogen. Transitions were also measured with cooling at 15 °C/min. Cyclic voltammetry was performed using a e-DAQ e-corder 410 potentiostat with a scanning rate of 100 mV/s. The polymer solutions (1-2 mg/mL) were drop-cast on a platinum electrode. Ag/Ag^+ was used as the reference electrode and a platinum wire as the auxiliary electrode. The reported values are referenced to Fc/Fc^+ (-5.1 eV versus vacuum). All electrochemistry experiments were performed in deoxygenated CH_3CN under an argon atmosphere using 0.1 M tetrabutylammonium hexafluorophosphate as the electrolyte. Absorption spectra were obtained on a photodiode-array Agilent 8453 UV-visible spectrophotometer using polymer solutions in $CHCl_3$ and thin films. The films were made by spin-coating 25 x 25 x 1 mm glass slides using solutions of polymer (2.5-5.0 mg/mL) in $CHCl_3$/*o*-dichlorobenzene at a spin rate of 1200 rpm on a Headway Research, Inc. PWM32 spin-coater.

4.5.3 Fabrication of photovoltaic devices

All devices were produced via a solution-based, spin-casting fabrication process. All polymers were mixed with $PC_{71}BM$ (SES Research) (mixed 1:2 with a total solution concentration of 30 mg/mL for $PC_{71}BM$) then dissolved in *o*-dichlorobenzene and stirred at 95°C for 48 hours. ITO coated glass slides (Delta Technologies) were cleaned by consecutive 10 minute sonications in (i) Mucasol™ detergent (dissolved in deionized water), 2x, (ii) deionized water, (iii) acetone, and then (iv) isopropanol. The slides were then dried in an oven for at least 3 hours and cleaned with air plasma (Harrick Scientific plasma cleaner) for 10 minutes. Filtered (0.45μm) PEDOT:PSS (Clevios P™) was spin-coated onto the prepared substrates (2000 rpm/60 sec) after first being stirred for 10 minutes at room temperature. The PEDOT:PSS films were annealed at 150 °C for 30 minutes. After cooling, the substrates were transferred to an argon-filled glovebox. After 48 hours of mixing, the polymer:PCBM solutions were filtered (0.45 μm pore, GS-Tek) and simultaneously dropped onto the PEDOT:PSS-coated substrates and spin-cast at 1000 rpm for 120 seconds. The films were dried under vacuum overnight. LiF (1 nm) and Al (100 nm) were successively thermally evaporated through a shadow mask under vacuum to complete the devices. *J-V* data was

generated by illuminating the devices using an ETH quartzline lamp at 1 sun (calibrated using a crystalline silicon photodiode with a KG-5 filter).

4.5.4 Synthesis

General procedure for the synthesis of copolymers. An oven-dried, 25 mL Schlenk flask was charged with dry, deoxygenated toluene (5-10 mL), bisstannane **7a**, **7b**, or **8** (1.0 equiv.), and diketopyrrolopyrrole **8** (1.0 equiv.). The stirred solution was sparged with argon for 10 minutes and followed by the addition of tris(dibenzylideneacetone)dipalladium(0) (2 mol%) and tri(*o*-tolyl)phosphine (8 mol %). The reaction mixture was heated to reflux and stirred, under argon, for 48 hours. The polymer was end-capped by the subsequent addition of an excess amount of trimethyl(phenyl)tin and iodobenzene, each followed by a 4 hour period of reflux. The reaction mixture was cooled to 50 °C and diluted with chloroform. A small portion of SiliaMetS® Cysteine was added and the reaction mixture was stirred for 8 hours followed by precipitation into cold methanol and filtration. The polymer was purified via Soxhlet extraction by subsequently rinsing with methanol, acetone and hexanes and finally extracted with chloroform. Most of the chloroform was removed *in vacuo* and the polymer was precipitated into methanol, collected by filtration and dried *in vacuo*.

Synthesis of PBDT-DPP. Following the general polymerization procedure using bisstannane **7a** and diketopyrrolopyrrole **9** afforded a dark solid (287 mg, 76%). ^{1}H NMR (400 MHz, $CDCl_3$): δ 8.51 (2H, br), 8.20 (2H, br), 7.34 (2H, br), 6.84 (2H, br), 4.17 (4H, br), 2.89 (4H, br), 2.61 (4H, br), 1.98 (2H, br), 1.60-1.75 (8H, br), 1.20-1.51 (72H, br), 0.82-0.95 (24H, br). GPC ($CHCl_3$, 50 °C): M_w = 36.4 kDa, M_n = 21.3 kDa, PDI = 1.71.

Synthesis of PBDSe-DPP. Following the general polymerization procedure using bisstannane **7b**, diketopyrrolopyrrole **9** afforded a dark solid (264 mg, 70%). ^{1}H NMR (400 MHz, $CDCl_3$): δ 8.51 (2H, br), 8.23 (2H, br), 7.33 (2H, br), 6.84 (2H, br), 4.17 (4H, br), 2.82 (4H, br), 2.59 (4H, br), 1.98 (8H, br), 1.20-1.55 (72H, br), 0.83-0.95 (24H, br). GPC ($CHCl_3$, 50 °C): M_w = 29.1, M_n = 18.5, PDI = 1.57.

Synthesis of PBDF-DPP. Following the general polymerization procedure using bisstannane **8** and diketopyrrolopyrrole **9** afforded a dark solid (141 mg, 82%). ^{1}H NMR (400 MHz,

$CDCl_3$): δ ^{1}H NMR (400 MHz, $CDCl_3$): δ 8.51 (2H, br), 7.57 (2H, br), 7.34 (2H, br), 6.85 (2H, br), 4.19 (4H, br), 2.79-2.96 (8H, br), 1.99 (2H, br), 1.68-1.81 (8H, br), 1.22-1.52 (72H, br), 0.82-0.96 (24H, br). GPC ($CHCl_3$, 50 °C): M_w = 25.7 kDa, M_n = 14.6 kDa, PDI = 1.76.

4.6 ACKNOWLEDGEMENTS

We thank the National Science Foundation (DMR-0846607) for partial support of this work. We also thank the National Science Foundation Materials Research Facilities Network (DMR-1250372) and Polymer-Based Materials for Harvesting Solar Energy, an Energy Frontier Research Center funded by the U.S. Department of Energy, Office of Science, Office of Basic Energy Sciences under Award Number DE-SC0001087 for support of the device fabrication. The Iowa State University (ISU), the Institute for Physical Research and Technology provided MDE with a Katron Fellowship. Some of the OPV work was performed at the ISU Microelectronics Research Center. We also thank Dr. Kamel Harrata and the ISU Mass Spectroscopy Laboratory for analysis.

4.7 SUPPORTING INFORMATION

4.7.1 Synthetic Procedures

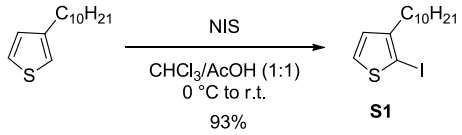

S1

3-Decyl-2-iodothiophene (S1). To a stirred solution of 3-decylthiophene (2.25 g, 10.0 mmol) in 30 mL of $CHCl_3$/AcOH (1:1) at 0 °C was added *N*-iodosuccinimide (2.36 g, 10.5 mmol) in one portion. The reaction was warmed to room temperature and stirred in the absence of light, under argon, for 16 hours. A 1M sodium thiosulfate solution was added to the reaction mixture to neutralize the residual iodine. The layers were separated and the aqueous layer was extracted with CH_2Cl_2 (x3). The combined organic layers were then neutralized with 1 M KOH, subsequently rinsed with H_2O and brine, and dried over $MgSO_4$. The solvent was removed *in vacuo* and the crude oil was purified on a short plug of silica with hexanes as the eluent to afford a pale yellow oil (3.25 g, 93%). ^{1}H NMR (400 MHz;

$CDCl_3$) δ 0.88 (3H, t, J = 6.7 Hz), 1.22-1.36 (14H, m), 1.56 (2H, m), 2.54 (2H, t, J = 7.8 Hz), 6.75 (1H, d, J = 5.6 Hz), 7.38 (1H, d, J = 5.5 Hz); ^{13}C NMR (100 MHz; $CDCl_3$) δ 14.33, 22.87, 29.39, 29.61, 29.75, 29.79, 29.88, 30.20, 32.07, 32.25, 74.15, 128.03, 130.36, 147.22. HRMS (APCI) *m/z*: $[M + H]^+$ calcd for $C_{14}H_{24}IS$, 351.0638; found, 351.0645; deviation, -2.0 ppm.

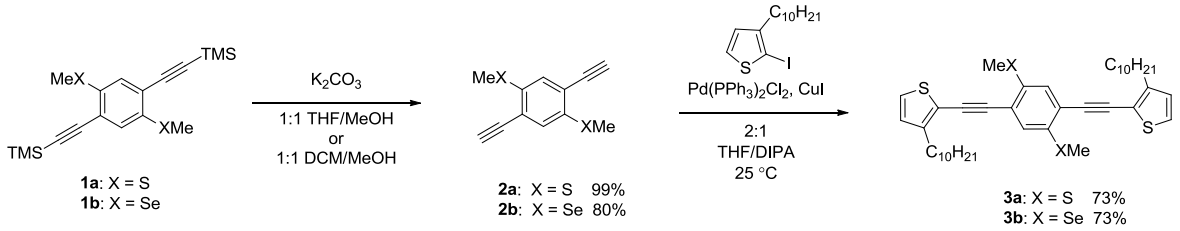

(2,5-Diethynyl-1,4-phenylene)bis(methylsulfane) (2a). To a stirred solution of bis(trimethylsilylethyne) **1a** (1.09 g, 3.0 mmol) in 30 mL of CH_2Cl_2/MeOH (1:1) was added K_2CO_3 (1.66 g, 12.0 mmol) in one portion. The suspension was stirred at room temperature for 1 hour and poured into H_2O. The layers were separated and the aqueous layer was extracted with CH_2Cl_2 (x3). The combined organic layers were rinsed with brine and dried over $MgSO_4$. The solvent was removed *in vacuo* and the crude product was purified on a short plug of silica with CH_2Cl_2/hexanes (2:1) as the eluent to afford a yellow solid (648 mg, 99%), mp 165 °C (decomp). ^{1}H NMR (300 MHz; $CDCl_3$) δ 2.49 (6H, s), 3.56 (2H, s), 7.25 (2H, s); ^{13}C NMR (100 MHz; $CDCl_3$) δ 15.62, 80.62, 85.37, 121.71, 129.25, 138.12. HRMS (APCI) *m/z*: $[M + H]^+$ calcd for $C_{12}H_{11}S_2$, 219.0297; found, 219.0295; deviation, 0.8 ppm.

(2,5-diethynyl-1,4-phenylene)bis(methylselane) (2a). To a stirred solution of bis(trimethylsilylethyne) **1b** (1.37 g, 3.0 mmol) in 50 ml of THF/MeOH (1:1) was added K_2CO_3 (1.66 g, 12.0 mmol) in one portion. The suspension was stirred at room temperature for 1 hour and poured into H_2O. The layers were separated and the aqueous layer was extracted with CH_2Cl_2 (x3). The combined organic layers were rinsed with brine and dried over $MgSO_4$. The solvent was removed *in vacuo* and the crude product was purified by recrystalization from $CHCl_3$/EtOH to afford a bright yellow solid. (750 mg, 80%). ^{1}H NMR (400 MHz; $CDCl_3$) δ 2.35 (6H, s), 3.53 (2H, s), 7.34 (2H, s); ^{13}C NMR (100 MHz; $CDCl_3$) δ

6.74, 81.42, 84.75, 124.02, 132.19, 133.15. HRMS (ESI) *m/z*: $[M + H]^+$ calcd for $C_{12}H_{10}Se_2$, 313.9114; found, 313.9113; deviation, 0.3 ppm.

2,2'-((2,5-Bis(methylthio)-1,4-phenylene)bis(ethyne-2,1-diyl))bis(3-decylthiophene) (3a). To a stirred, deoxygenated solution of **S1** (2.63 g, 7.5 mmol) in 27 mL of THF/Et_3N (2:1) was added **2a** (648 mg, 3.0 mmol). The reaction mixture was stirred at room temperature, under argon for 10 min, at which time $Pd(PPh_3)_2Cl_2$ (105 mg, 5 mol %) and CuI (57 mg, 10 mol %) were added. The reaction mixture was stirred overnight at room temperature. Most of the solvent was then removed *in vacuo* and the resulting slurry was poured into water and extracted with CH_2Cl_2 (x3). The combined organic layers were rinsed with brine and dried over $MgSO_4$. The solvent was removed *in vacuo* and the crude product was purified by column chromatography on silica using a gradient of hexane to hexane/CH_2Cl_2 (9:1) as the eluent to afford bright yellow crystals (1.47 g, 73%), mp 48 °C. ^{1}H NMR (400 MHz; $CDCl_3$) δ 0.88 (6H, t, *J* = 6.8 Hz), 1.22-1.40 (28H, m), 1.68 (4H, p, *J* = 7.5 Hz), 2.52 (6H, s), 2.83 (4H, t, *J* = 7.8 Hz), 6.91 (2H, d, *J* = 5.1 Hz), 7.23 (2H, d, *J* = 5.1 Hz), 7.25 (2H, s); ^{13}C NMR (100 MHz; $CDCl_3$) δ 14.28, 15.66, 22.84, 29.52, 29.59, 29.66, 29.82, 29.88, 30.63, 32.07, 90.79, 92.69, 117.91, 122.14, 126.96, 127.78, 128.55, 137.29, 149.03. HRMS (APCI) *m/z*: $[M + H]^+$ calcd for $C_{40}H_{55}S_4$, 663.3181; found, 663.3184; deviation, -0.4 ppm.

2,2'-((2,5-Bis(methylselanyl)-1,4-phenylene)bis(ethyne-2,1-diyl))bis(3-decylthiophene) (3b). The title compound was prepared in a similar manner as compound **3a** from compound **S1** (2.26 g, 6.5 mmol) and compound **2b** (805 g, 2.6 mmol) to a afford a bright yellow solid (1.42 g, 73%), mp 131 °C. ^{1}H NMR (x MHz; $CDCl_3$) δ 0.87 (6H, t, *J* = 6.8 Hz), 1.20-1.42 (28H, m), 1.67 (4H, p, *J* = 7.5 Hz), 2.39 (6H, s), 2.84 (xH, t, *J* = 7.9 Hz), 6.91 (2H, d, *J* = 5.1 Hz), 7.23 (2H, d, *J* = 5.1 Hz), 7.34 (2H, s); ^{13}C NMR (100 MHz; $CDCl_3$) δ 6.68, 14.29, 22.84, 29.52, 29.58, 29.67, 29.81, 29.92, 30.66, 32.06, 90.11, 93.50, 117.83, 124.39, 127.05, 128.55, 130.79, 132.45, 148.97. HRMS (ESI) *m/z*: $[M + H]^+$ calcd for $C_{40}H_{55}S_2Se_2$, 759.2077; found, 759.2072; deviation, -0.7 ppm.

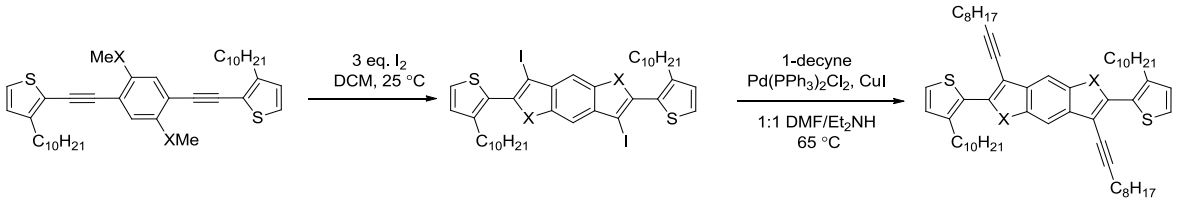

3a: X = S
3b: X = Se

4a: X = S 91%
4b: X = Se 92%

5a: X = S, 88%
5a: X = Se, 90%

2,6-Bis(3-decylthiophen-2-yl)-3,7-diiodobenzo[1,2-*b*:4,5-*b*']dithiophene (4a). Compound **3a** (1.47 g, 2.2 mmol) was dissolved in 150 mL of CH_2Cl_2 and cooled to 0 °C. While stirring, a solution of iodine (1.68 g, 6.6 mmol) in 50 mL of CH_2Cl_2 was added dropwise over 10 minutes. Upon completion of the addition, the reaction mixture was warmed to room temperature and stirred for 2 hours. The reaction was quenched by the addition of 50 mL of saturated aqueous sodium thiosulfate solution, the layers were separated and the aqueous layer was extracted with CH_2Cl_2 (x2). The organic layers were combined, dried over $MgSO_4$ and the solvents were removed *in vacuo*. The crude product was purified by recrystalization from a mixture of $CHCl_3$ and ethanol and collected by filtration, followed by rinsing with cold ethanol to afford fine, off-white crystals. (1.78 g, 91%), mp 97 °C. ^{1}H NMR (400 MHz; $CDCl_3$) δ 0.85 (6H, t, J = 6.9 Hz), δ 1.16-1.28 (28H, m), δ 1.57 (4H, m), δ 2.61 (4H, t, J = 7.9 Hz), δ 7.05 (2H, d, J = 5.1 Hz), δ 7.45 (2H, d, J = 5.4 Hz), δ 8.22 (2H, s); ^{13}C NMR (100 MHz; $CDCl_3$) δ 14.30, 22.82, 29.45, 29.48, 29.49, 29.67, 29.73, 29.73, 30.64, 32.04, 77.36, 84.18, 119.51, 127.19, 129.03, 129.10, 138.04, 140.26, 144.10. HRMS (APCI) *m/z*: $[M + H]^+$ calcd for $C_{38}H_{49}I_2S_2$, 887.0801; found, 887.0782; deviation, 2.1 ppm.

2,6-Bis(3-decylthiophen-2-yl)-3,7-diiodobenzo[1,2-*b*:4,5-*b*']diselenophene (4b). The title compound was prepared in a similar manner as compound **4a** from compound **3b** (1.40 g, 1.9 mmol) to a afford an off-white solid (1.66 g, 92%), mp 59 °C. ^{1}H NMR (x MHz; $CDCl_3$) δ 0.85 (6H, t, J = 6.9 Hz), 1.16-1.29 (28H, m), 1.58 (4H, m), 2.59 (4H, t, J = 7.9 Hz), 7.03 (2H, d, J = 5.1 Hz), 7.43 (2H, d, J = 5.1 Hz), 8.36 (2H, s); ^{13}C NMR (100 MHz; $CDCl_3$) δ 14.31, 22.82, 29.45, 29.51, 29.54, 29.54, 29.67, 29.73, 30.44, 32.03, 87.52, 125.27, 126.93, 129.08, 131.65, 138.73, 139.13, 141.83, 143.27. HRMS (APCI) *m/z*: $[M + H]^+$ calcd for $C_{38}H_{49}I_2S_2Se_2$, 982.9690; found, 982.9693; deviation, -0.3 ppm.

3,7-Di(dec-1-yn-1-yl)-2,6-bis(3-decylthiophen-2-yl)benzo[1,2-*b*:4,5-*b*']dithiophene (5a). To a stirred, deoxygenated solution of **4a** (1.60 g, 1.8 mmol) and 1-decyne (1.00 g, 7.2 mmol) in 40 mL of DMF/Et_2NH (1:1) was added $Pd(PPh_3)_2Cl_2$ (63 mg, 5 mol %) and CuI (17 mg, 5 mol %). The solution was stirred overnight under argon at room temperature. The reaction mixture was poured into H_2O and extracted with CH_2Cl_2 (x3). The combined organic layers were washed with H_2O (x2), followed by brine (x1), dried over $MgSO_4$ and the solvent was removed *in vacuo*. The crude product was purified by chromatography on silica gel using a gradient of hexane to hexane/CH_2Cl_2 (95:5) as the eluent to afford bright yellow crystals (1.44 g, 88%), mp 46 °C. ^{1}H NMR δ 0.88 (12H, m), δ 1.18-1.36 (44H, m), δ 1.46 (4H, m), δ1.65 (8H, m), δ 2.51 (4H, t, *J* = 7.0 Hz), 2.83 (4H, t, *J* = 7.9 Hz), 7.00 (2H, d, *J* = 5.1 Hz), 7.36 (2H, d, *J* = 5.0 Hz), 8.27 (2H, s); ^{13}C NMR (x MHz; $CDCl_3$) δ 14.28, 20.05, 22.83, 22.85, 22.85, 29.16, 29.34, 29.44, 29.49, 29.61, 29.66, 29.77, 30.88, 32.04, 32.05, 74,71, 97.38, 116.14, 116.32, 126.27, 129.12, 129.49, 136.12, 138.68, 138.84, 142.94. HRMS (APCI) *m/z*: $[M + H]^+$ calcd for $C_{58}H_{83}S_4$, 907.5372; found, 907.5370; deviation, 0.2 ppm.

3,7-Di(dec-1-yn-1-yl)-2,6-bis(3-decylthiophen-2-yl)benzo[1,2-*b*:4,5-*b*']diselenophene (5b). The title compound was prepared in a similar manner as compound **5a** from compound **4b** (1.60 g, 1.6 mmol) to a afford a bright yellow solid (1.46 g, 90%), mp 45 °C. ^{1}H NMR (x MHz; $CDCl_3$) δ 0.87 (12H, m) 1.18-1.34 (44H, m), 1.44 (4H, m), 1.62 (8H, m), 2.47 (4H, t, *J* = 7.0 Hz), 2.78 (4H, t, *J* = 7.8 Hz), 6.99 (2H, d, *J* = 5.1 Hz), 7.34 (2H, d, *J* = 5.1 Hz), 8.35 (2H, s; ^{13}C NMR (100 MHz; $CDCl_3$) δ 14.29, 14.29, 19.99, 22.83, 22.86, 28.81, 29.13, 29.35, 29.46, 29.49, 29.61, 29.66, 29.77, 29.80, 30.79, 32.05, 32.05, 76.09, 96.38, 119.80, 121.53, 126.13, 129.42, 131.29, 137.07, 140.72, 141.26, 142.49. HRMS (ESI) *m/z*: $[M + H]^+$ calcd for $C_{58}H_{83}S_2Se_2$, 1003.4261; found, 1003.4282; deviation, -2.3 ppm.

3,7-Didecyl-2,6-bis(3-decylthiophen-2-yl)benzo[1,2-*b*:4,5-*b*']dithiophene (6a). bisalkyne **5a** (1.43 g, 1.6 mmol) was dissolved in 40 mL of THF/ethanol (2:1) and Pd/C (10 %, 426 mg, 0.4 mmol) was added to the solution. The resulting mixture was placed in a Parr bomb apparatus, flushed twice with H_2 and stirred under pressurized H_2 (500 PSI) for 19 days at

room temperature. The reaction mixture was filtered through a pad of Celite to remove the Pd/C and rinsed with THF. The solvent was removed *in vacuo* and the resulting solid was purified on a silica gel plug with hexane as the eluent to afford a pale yellow solid (1.11 g, 77%), mp 77 °C. ^{1}H NMR (400 MHz; $CDCl_3$) δ 0.86 (12H, m), 1.18-1.35 (56H, m), 1.57 (4H, m), 1.65 (4H, m), 2.58 (4H, t, J = 7.9 Hz), 2.81 (4H, t, J = 7.9 Hz), 7.01 (2H, d, J = 5.2 Hz), 7.36 (2H, d, J = 5.3 Hz), 8.15 (2H, s); ^{13}C NMR (100 MHz; $CDCl_3$) δ14.28, 22.82, 22.83, 27.58, 29.15, 29.47, 29.49, 29.56, 29.58, 29.74, 29.77, 29.95, 30.10, 30.91, 32.04, 32.06, 115.35, 125.97, 128.86, 128.87, 130.31, 135.86, 137.30, 137.76, 142.98. HRMS (ESI) *m/z*: $[M + H]^+$ calcd for $C_{58}H_{91}S_4$, 915.5998; found, 914.5981; deviation, 1.9 ppm.

Alternative procedure for the synthesis of **6a**. A solution of compound **5a** (1.65 g, 1.80 mmol) in 9:1 THF/EtOH (10 mL) was pumped through a flow hydrogenation reactor (ThalesNano H-Cube Pro^{TM}) at 125 ºC, 100 bar, and a flow rate of 0.5 mL/min. The catalyst used was a 70 mm 10% Pd/C pre-packed cartridge (CatCart®). The solution was recycled through the reactor at these conditions until hydrogenation was complete (confirmed by ^{1}H NMR). The solvent was removed *in vacuo* to afford an off-white solid (1.61 g, 97%).

3,7-Didecyl-2,6-bis(3-decylthiophen-2-yl)benzo[1,2-*b*:4,5-*b*']diselenophene (6b). A solution of compound **5b** (0.44 g, 0.44 mmol) in 9:1 THF/EtOH (10 mL) was pumped through a flow hydrogenation reactor (ThalesNano H-Cube Pro^{TM}) at 125 ºC, 100 bar, and a flow rate of 0.5 mL/min. The catalyst used was a 70 mm 10% Pd/C pre-packed cartridge (CatCart®). The solution was recycled through the reactor at these conditions until hydrogenation was complete (confirmed by ^{1}H NMR). The solvent was removed *in vacuo* to afford an off-white solid (0.22 g, 51%), mp 71 °C. ^{1}H NMR (600 MHz; $CDCl_3$) δ 0.88 (12H, m), 1.17-1.36 (56H, m), 1.57 (4H, m), 1.63 (4H, m), 2.56 (4H, t, J = 7.8 Hz), 2.74 (4H, t, J = 8.0 Hz), 6.99 (2H, d, J = 5.4 Hz), 7.34 (2H, d, J = 5.1 Hz), 8.18 (2H, s); ^{13}C NMR (400 MHz; $CDCl_3$) δ 14.28, 22.84, 28.77, 29.48, 29.50, 29.54, 29.60, 29.63, 29.72, 29.77, 29.87, 29.96, 29.99, 30.48, 30.78, 32.07, 120.82, 125.86, 128.82, 131.01, 132.23, 138.56, 138.98, 139.93, 142.30. HRMS (APCI) *m/z*: $[M + H]^+$ calcd for $C_{58}H_{91}S_2Se_2$, 1011.4887; found, 1011.4905; deviation, -1.8 ppm.

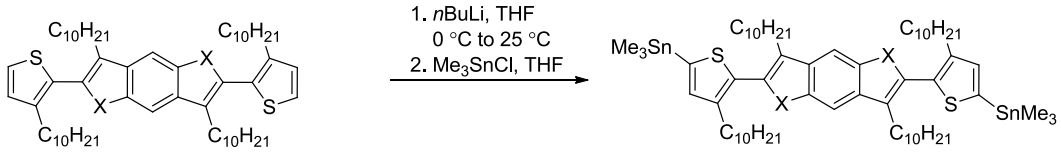

6a: X = S
6b: X = Se

7a: X = S, 92%
7b: X = Se, 92%

General procedure for synthesis of aryl bisstannanes (7a/7b): To a stirred solution of **6a** or **6b** in 20 mL of anhydrous THF, under argon, at 0 °C was added *n*-BuLi in hexanes (2.5 M) dropwise. The reaction mixture was warmed to room temperature and stirred for 2 hours. A solution of trimethylstannyl chloride in THF (1.0 M) was then added to the reaction at 0 °C and the reaction was warmed to room temperature, stirred overnight and poured into H_2O. The layers were separated and the aqueous layer was extracted with ether (x3). The combined organic layers were dried over $MgSO_4$ and the solvent was removed *in vacuo*. The resulting viscous oil was heated at 50-70 °C under a vacuum to remove residual Me_3SnCl.

(5,5'-(3,7-Didecylbenzo[1,2-*b*:4,5-*b*']dithiophene-2,6-diyl)bis(4-decylthiophene-5,2-diyl))bis(trimethylstannane) (7a). The title compound was synthesized from compound **6a** using the general procedure for synthesis of aryl bisstannanes to afford a dark orange, highly viscous oil (707 mg, 98%). ^{1}H NMR (400 MHz; $CDCl_3$) δ 0.40 (18H, s) 0.87 (12H, m), 1.15-1.35 (56H, m), 1.58 (4H, p, J = 7.4 Hz), 1.66 (4H, p, J = 7.8 Hz), 2.60 (4H, t, J = 8.1 Hz), 2.81 (4H, t, J = 8.1 Hz), 7.07 (2H, s), 8.14 (2H, s); ^{13}C NMR (100 MHz; $CDCl_3$) δ -8.01, 14.28, 22.83, 22.85, 27.58, 29.08, 29.48, 29.52, 29.54, 29.58, 29.64, 29.72, 29.76, 29.79, 29.91, 30.10, 31.13, 32.06, 32.08, 115.22, 130.87, 134.79, 135.24, 137.09, 137.30, 137.78, 138.55, 144.07. HRMS (ESI) *m/z*: $[M + H]^+$ calcd for $C_{64}H_{107}S_4Sn_2$, 1241.5305; found, 1241.5282; deviation, 1.9 ppm.

(5,5'-(3,7-Didecylbenzo[1,2-*b*:4,5-*b*']diselenophene-2,6-diyl)bis(4-decylthiophene-5,2-diyl))bis(trimethylstannane) (7b). The title compound was synthesized from compound **6b** using the general procedure for synthesis of aryl bisstannanes to afford a dark yellow, highly viscous oil (334 mg, 99%). ^{1}H NMR (400 MHz; $CDCl_3$) δ 0.40 (18H, s) 0.87 (12H, m), 1.17-1.34 (56H, m), 1.541.69 (8H, m), 2.58 (4H, t, J = 8.0 Hz), 2.74 (4H, t, J = 8.0 Hz), 7.04 (2H,

s), 8.17 (2H, s); ^{13}C NMR (100 MHz; $CDCl_3$) δ -8.04, 14.31, 22.84, 22.87, 28.74, 29.13, 29.50, 29.51, 29.54, 29.60, 29.74, 29.76, 29.79, 29.89, 29.98, 31.01, 32.07, 32.09, 120.68, 132.65, 136.93, 137.02, 138.16, 138.26, 138.51, 139.93, 143.42. HRMS (ESI) *m/z*: $[M + H]^+$ calcd for $C_{64}H_{107}S_2Se_2Sn_2$, 1335.4213; found, 1335.4171; deviation, 3.0 ppm.

4.7.2 NMR Spectra and Analytical Data

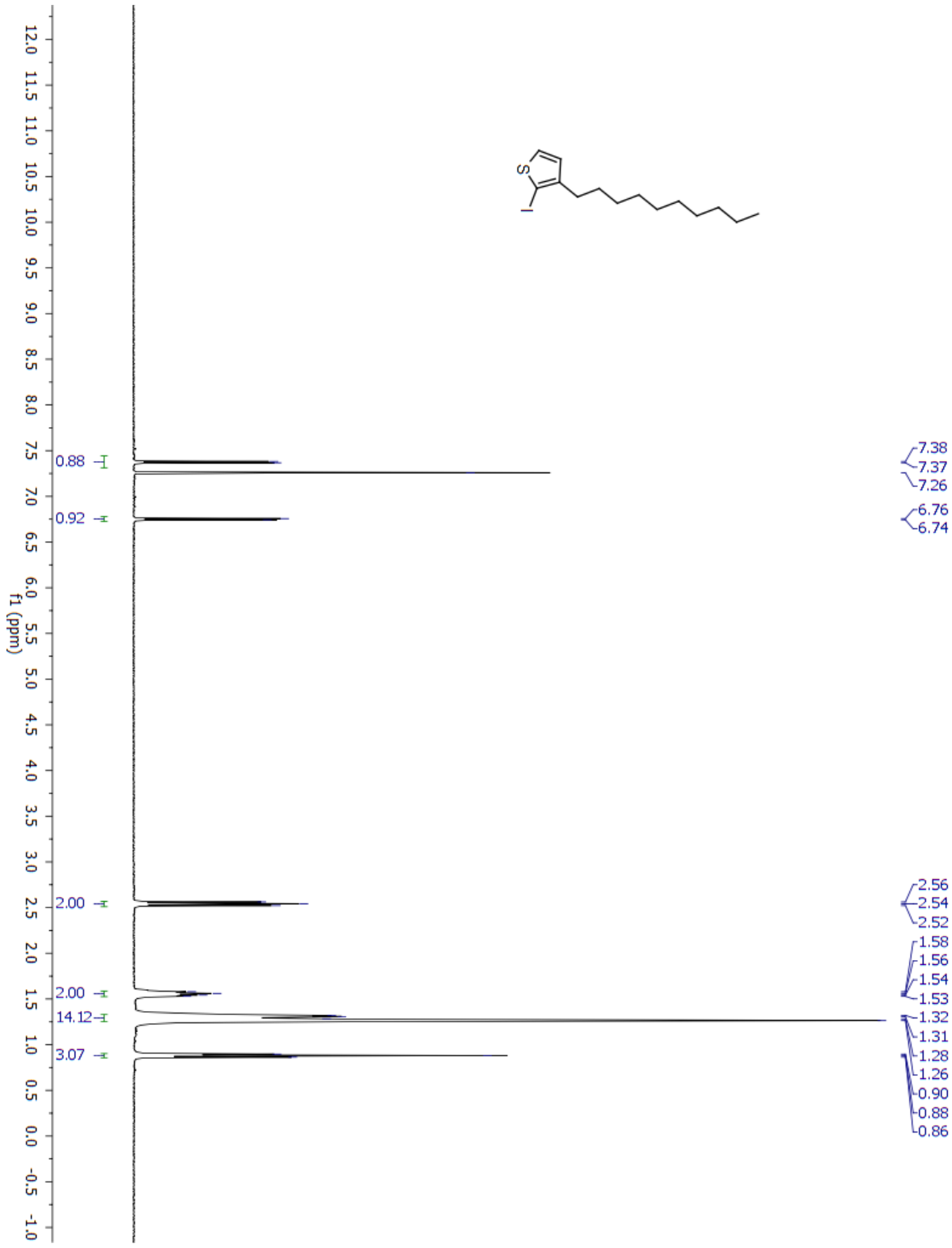

Figure S4.1. ^{1}H NMR of 3-Decyl-2-iodothiophene (**S1**).

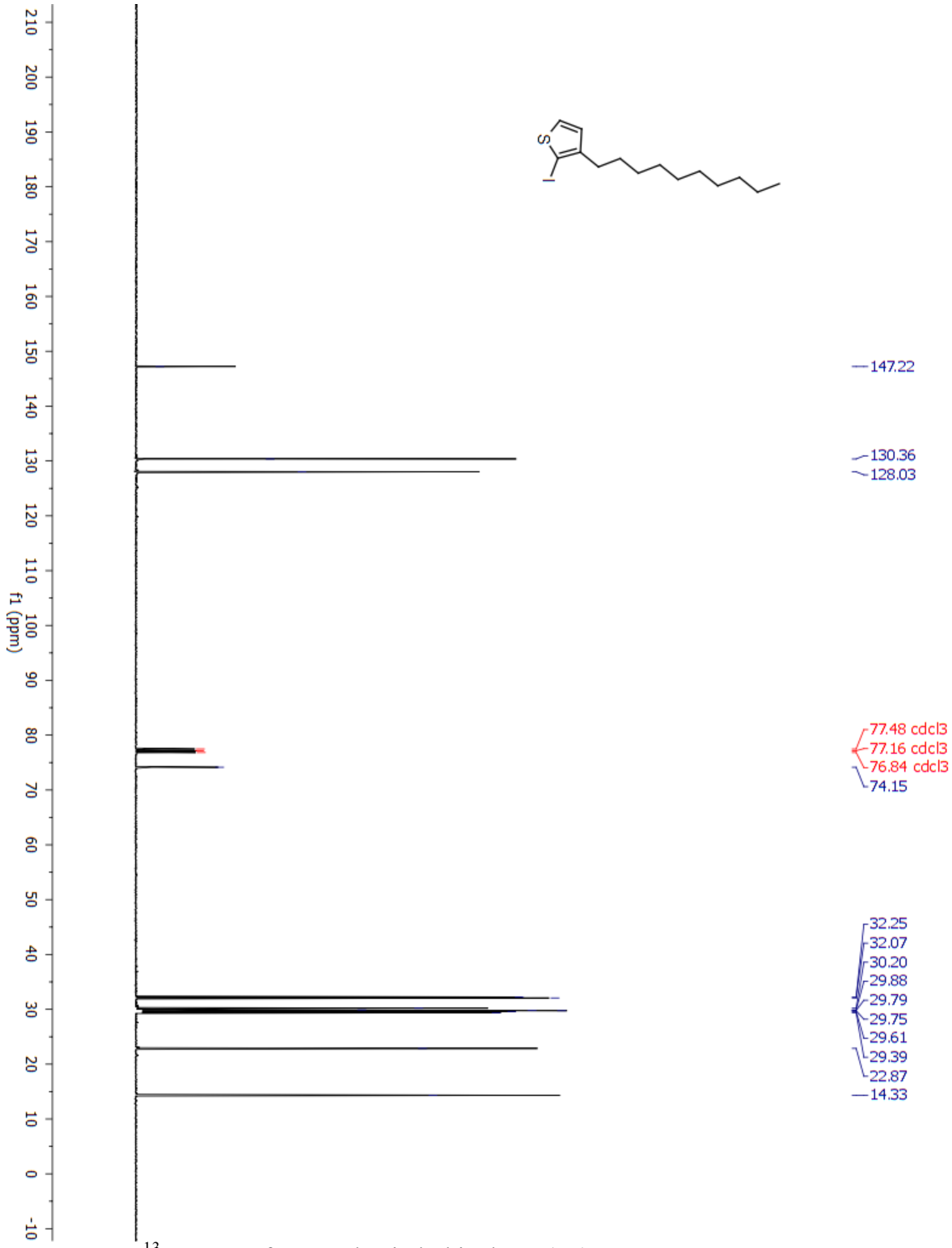

Figure S4.2. ^{13}C NMR of 3-Decyl-2-iodothiophene (**S1**).

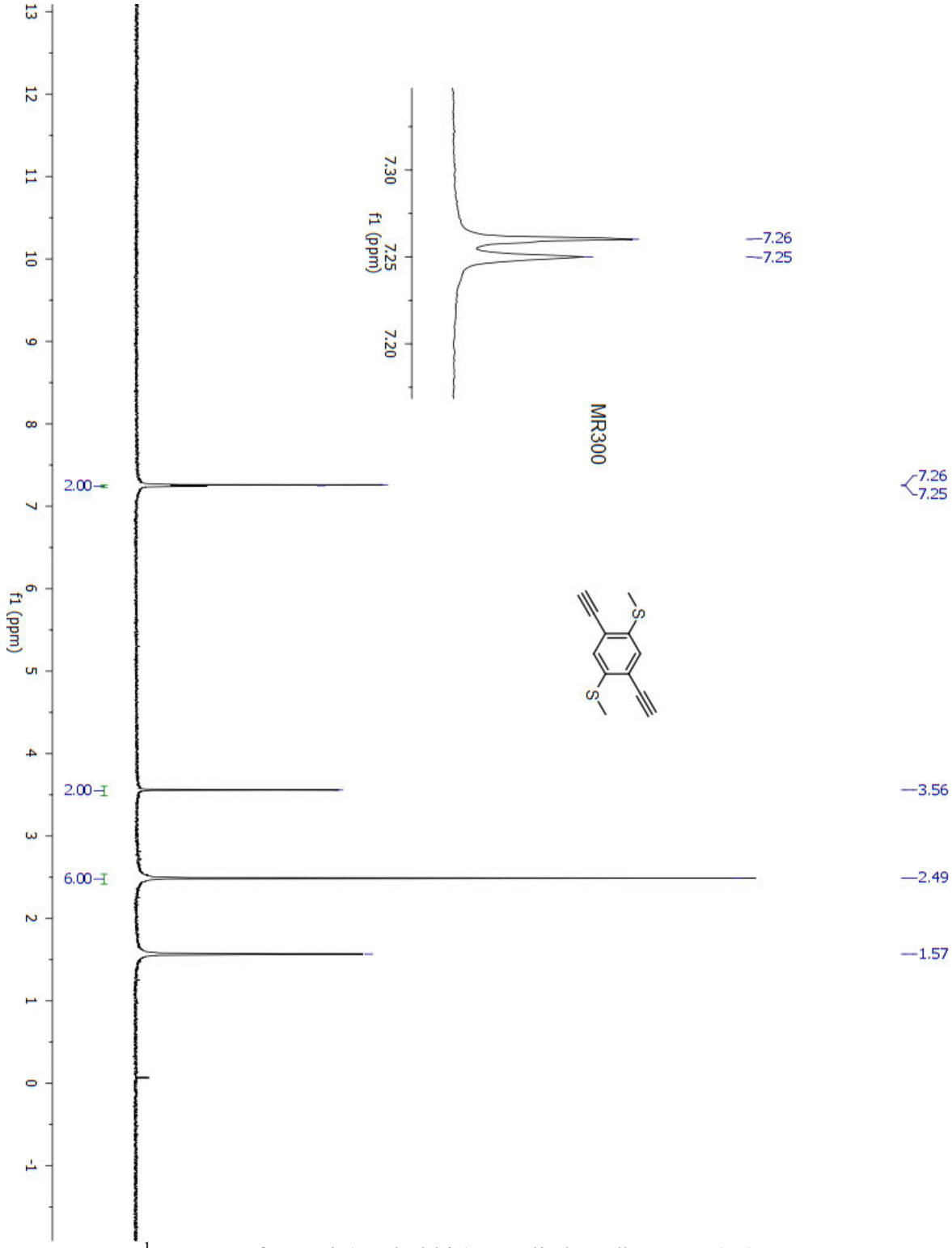

Figure S4.3. ^{1}H NMR of 1,4-Bis(methylthio)-2,5-diethynylbenzene (**2a**).

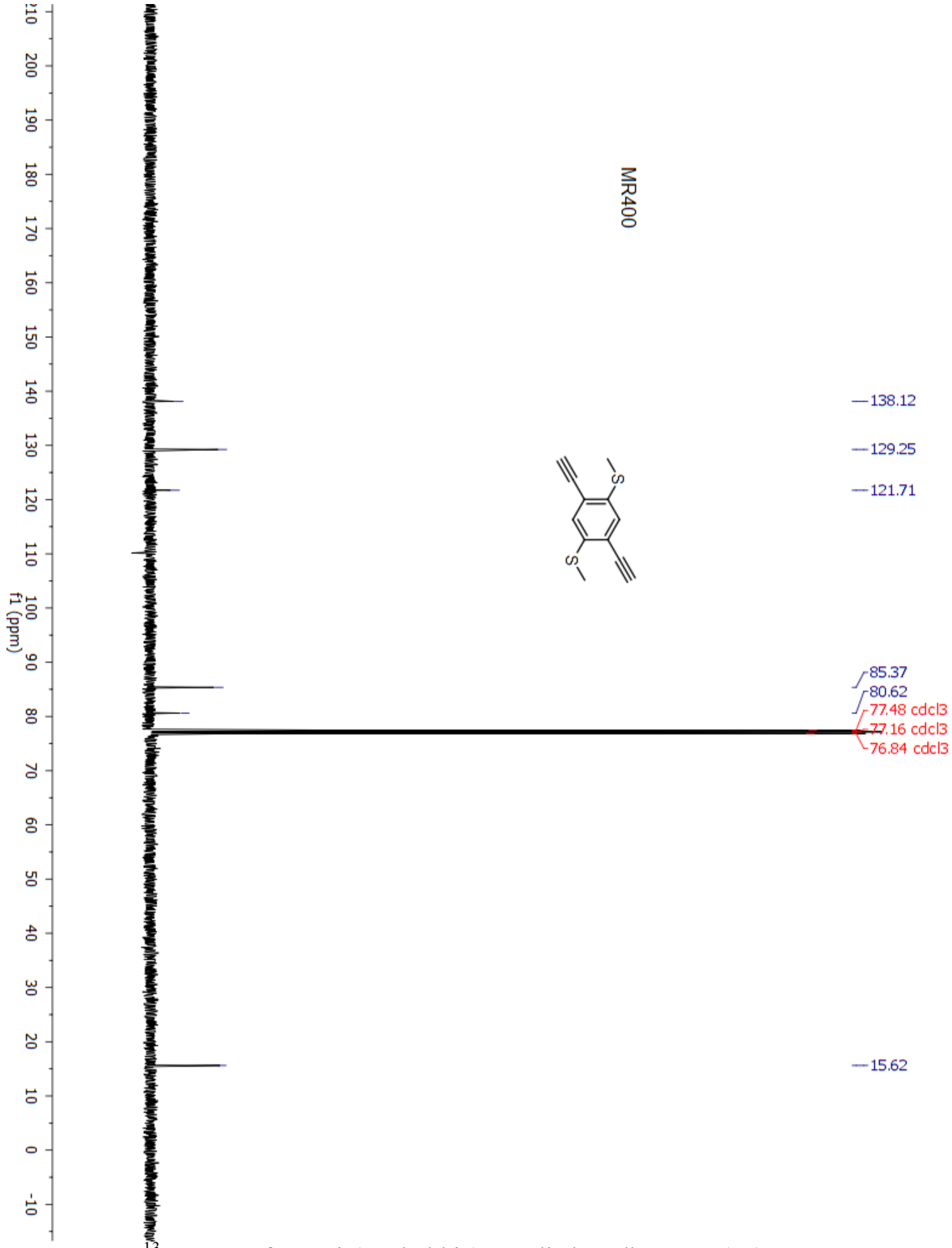

Figure S4.4. ^{13}C NMR of 1,4-Bis(methylthio)-2,5-diethynylbenzene (**2a**).

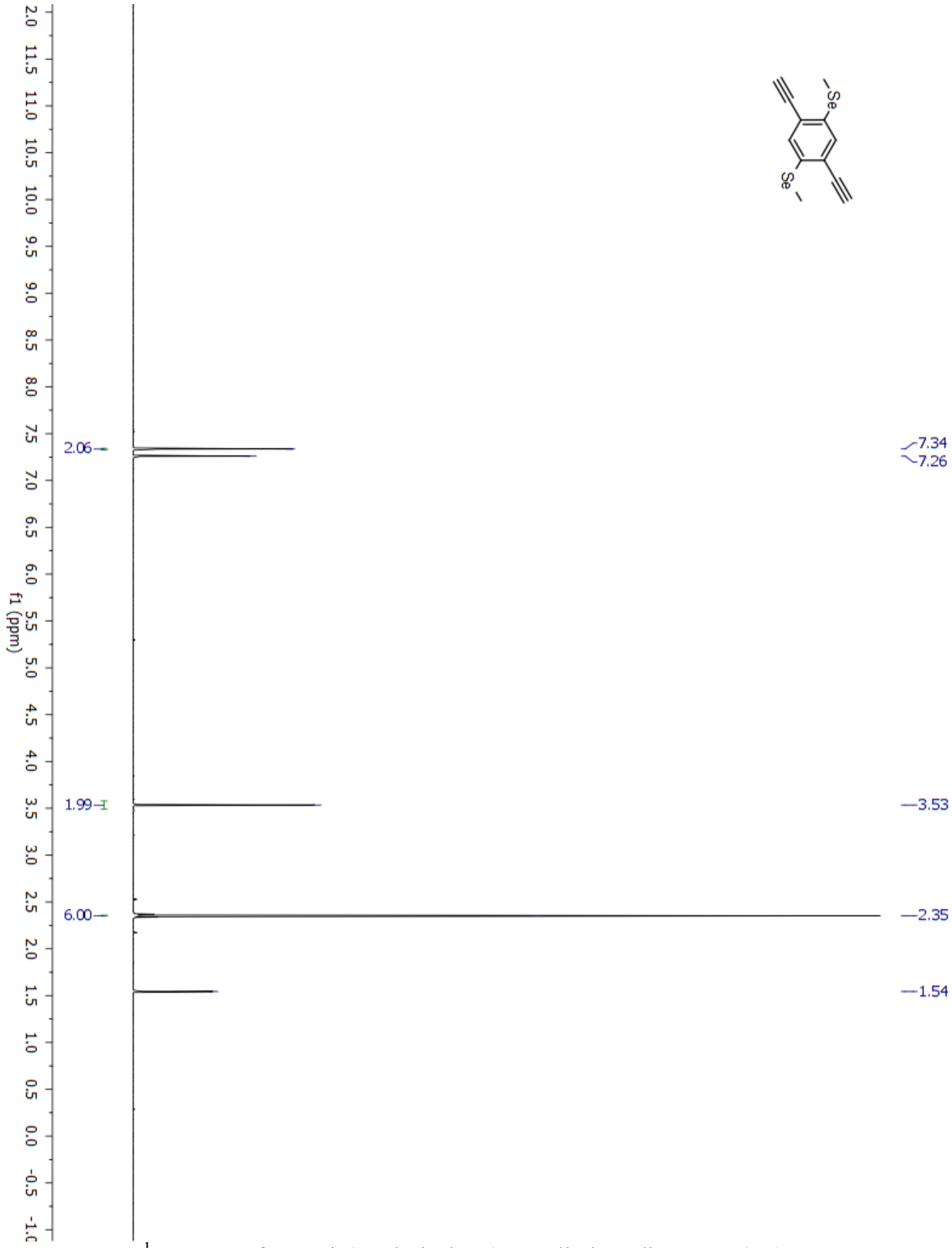

Figure S4.5. ^{1}H NMR of 1,4-Bis(methylseleno)-2,5-diethynylbenzene (**2b**).

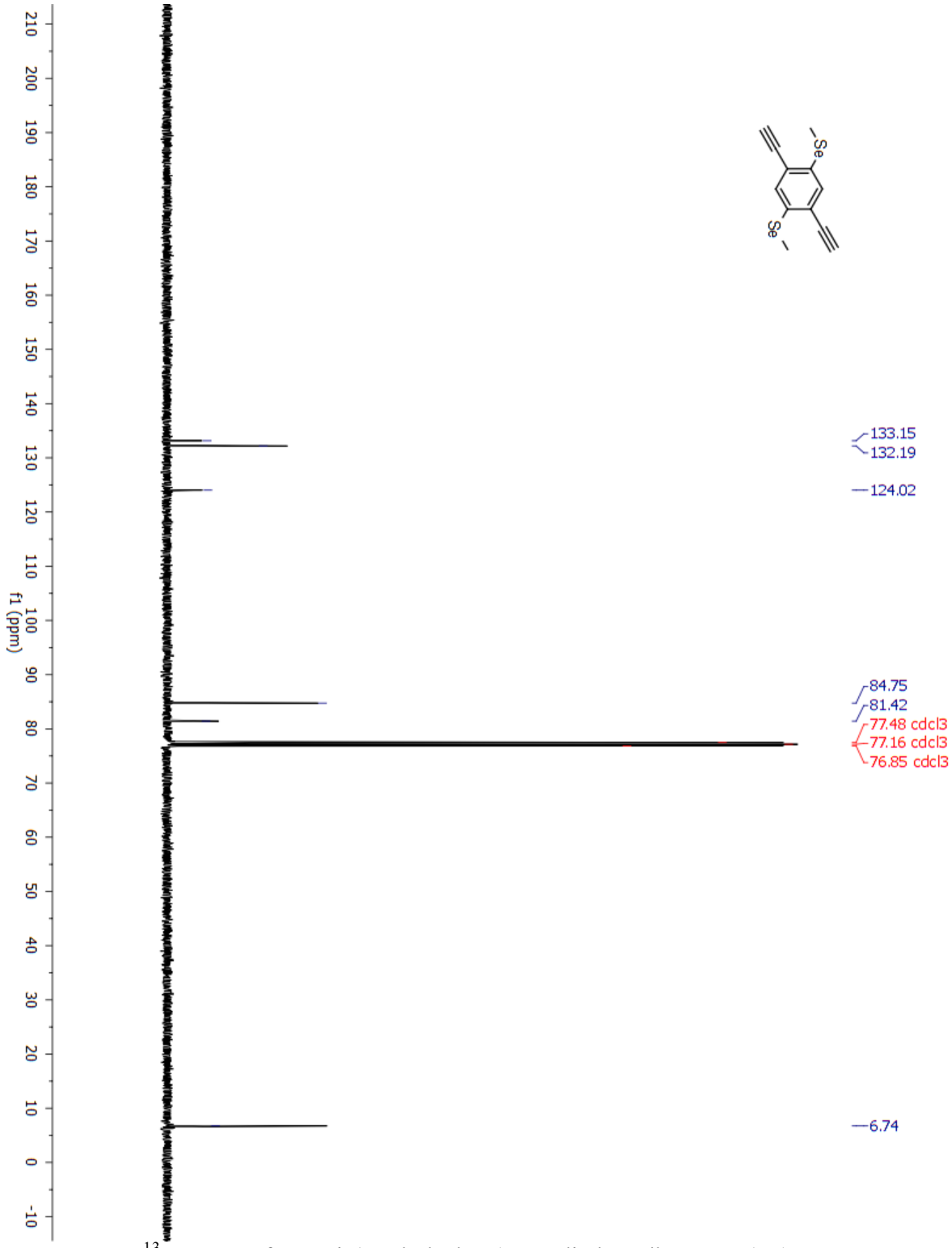

Figure S4.6. ^{13}C NMR of 1,4-Bis(methylseleno)-2,5-diethynylbenzene (**2b**).

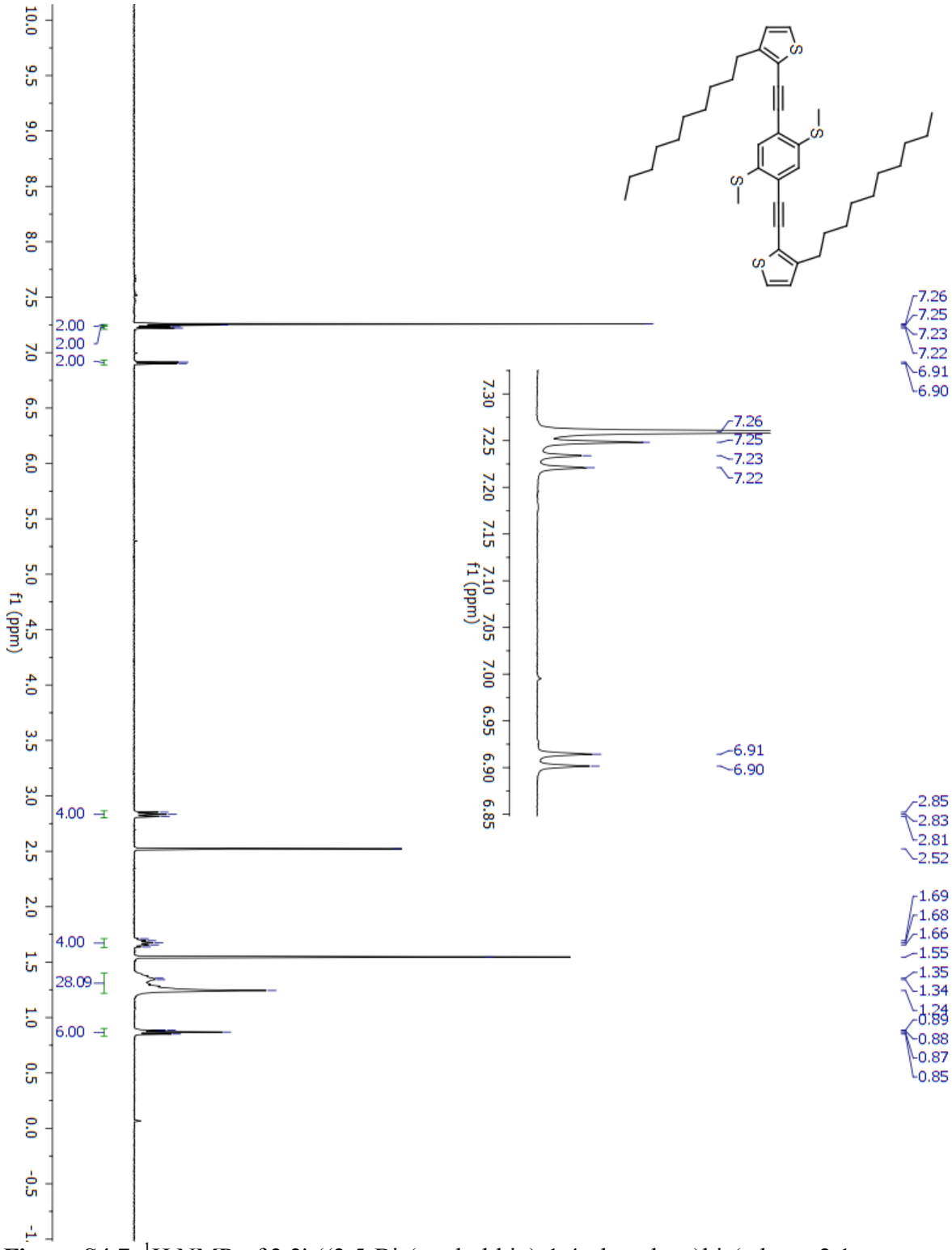

Figure S4.7. ^{1}H NMR of 2,2'-((2,5-Bis(methylthio)-1,4-phenylene)bis(ethyne-2,1-diyl))bis(3-decylthiophene) (**3a**).

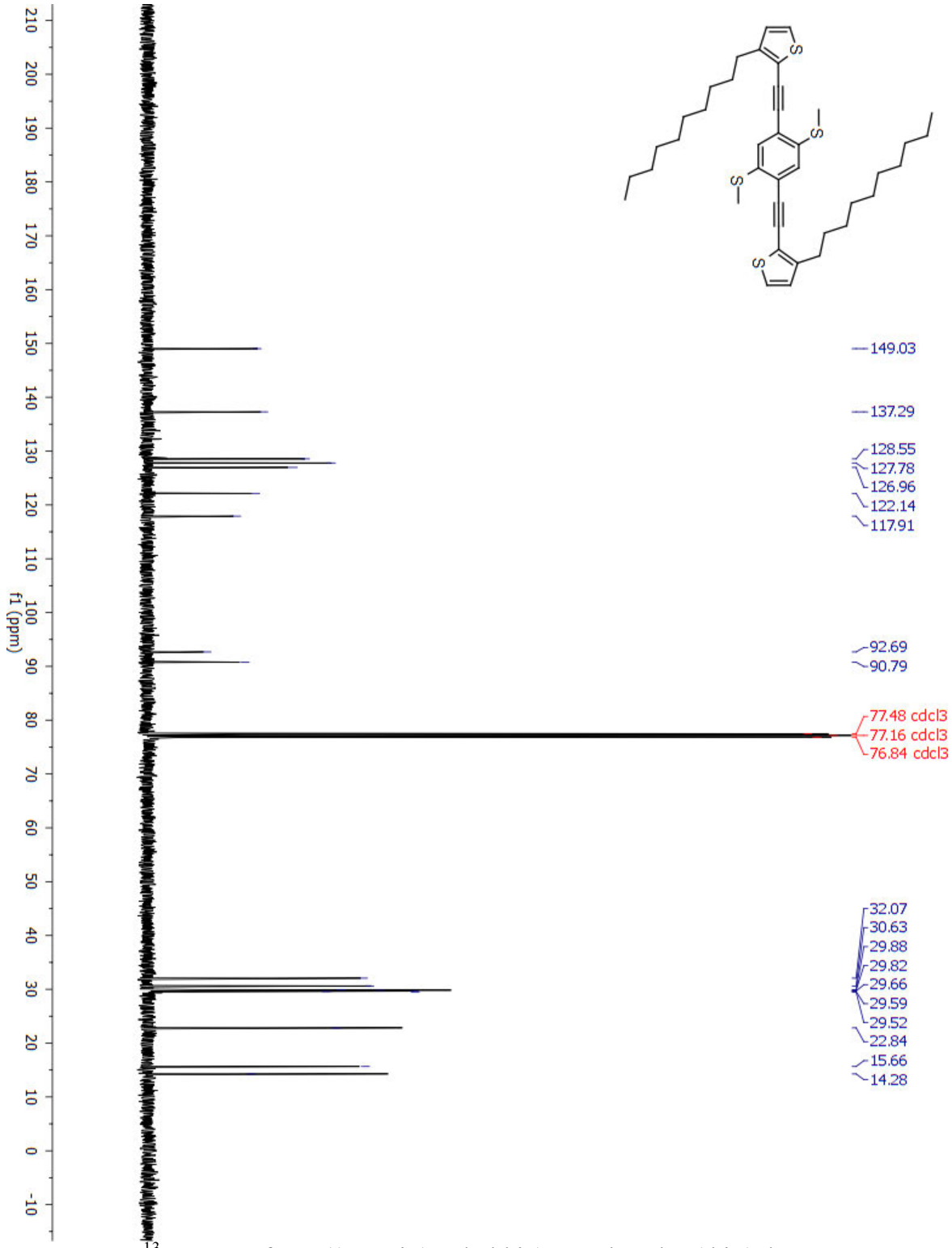

Figure S4.8. ^{13}C NMR of 2,2'-((2,5-Bis(methylthio)-1,4-phenylene)bis(ethyne-2,1-diyl))bis(3-decylthiophene) (**3a**).

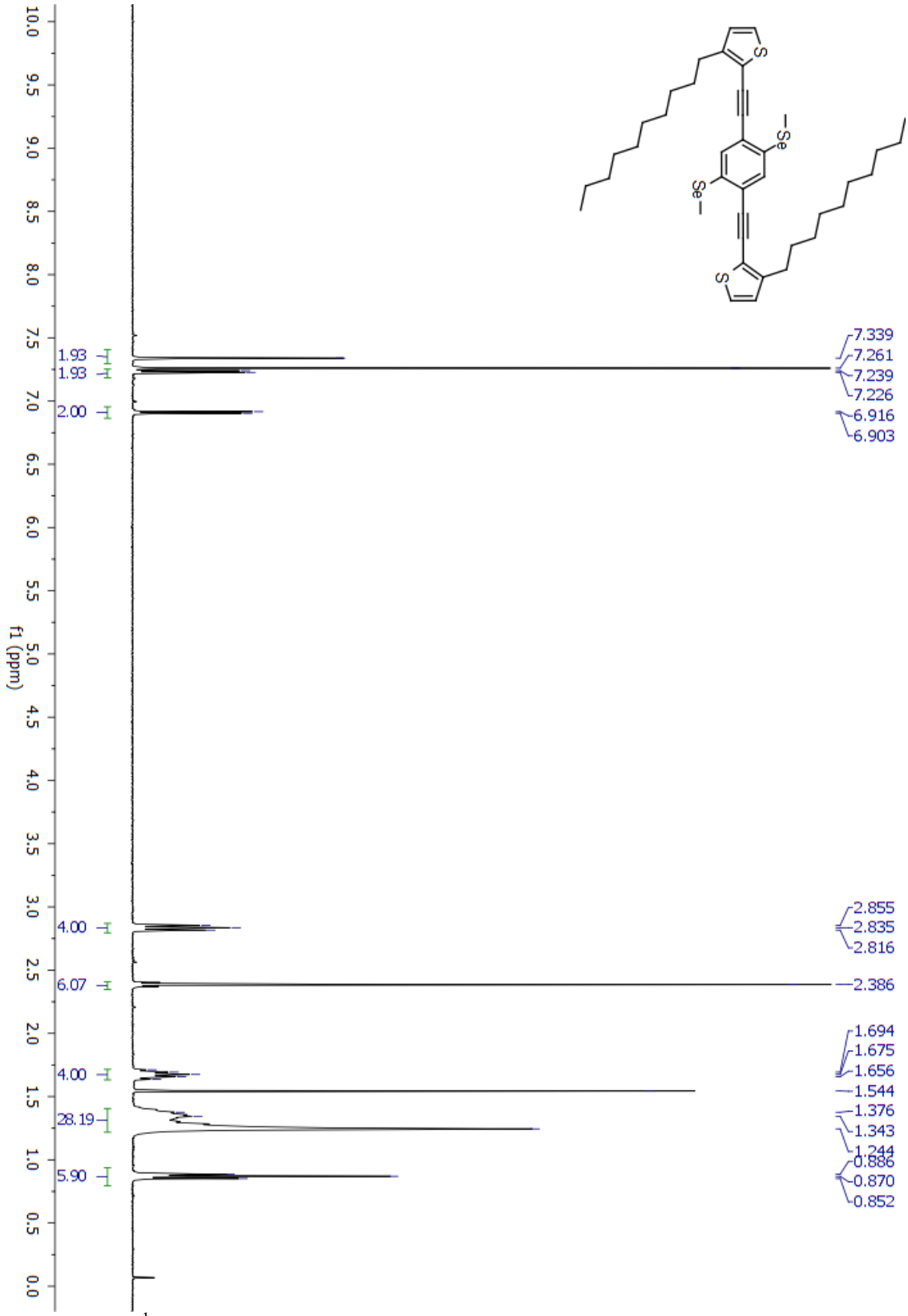

Figure S4.9. ^{1}H NMR of 2,2'-((2,5-Bis(methyseleno)-1,4-phenylene)bis(ethyne-2,1-diyl))bis(3-decylthiophene) (**3b**).

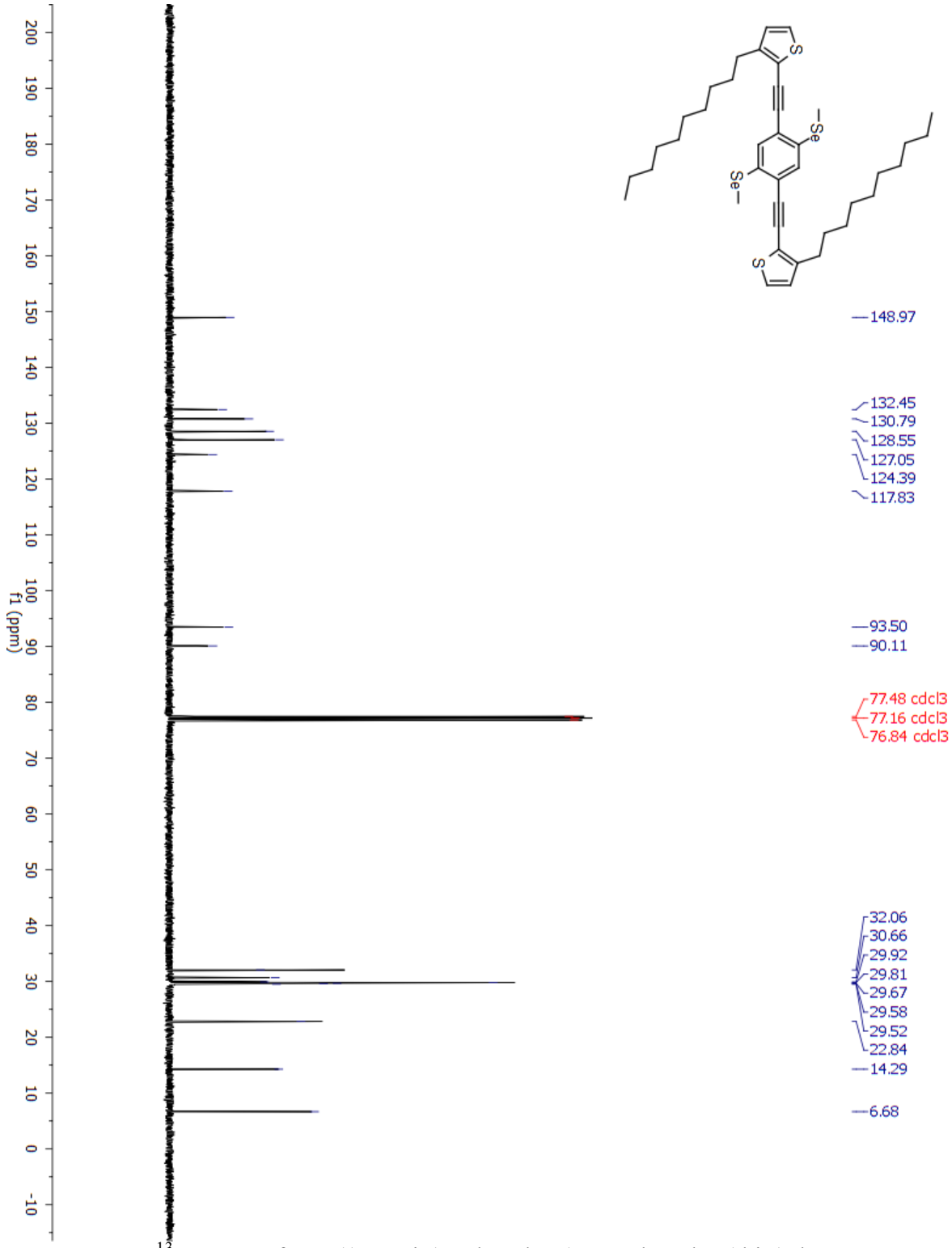

Figure S4.10. ^{13}C NMR of 2,2'-((2,5-Bis(methyseleno)-1,4-phenylene)bis(ethyne-2,1-diyl))bis(3-decylthiophene) (**3b**).

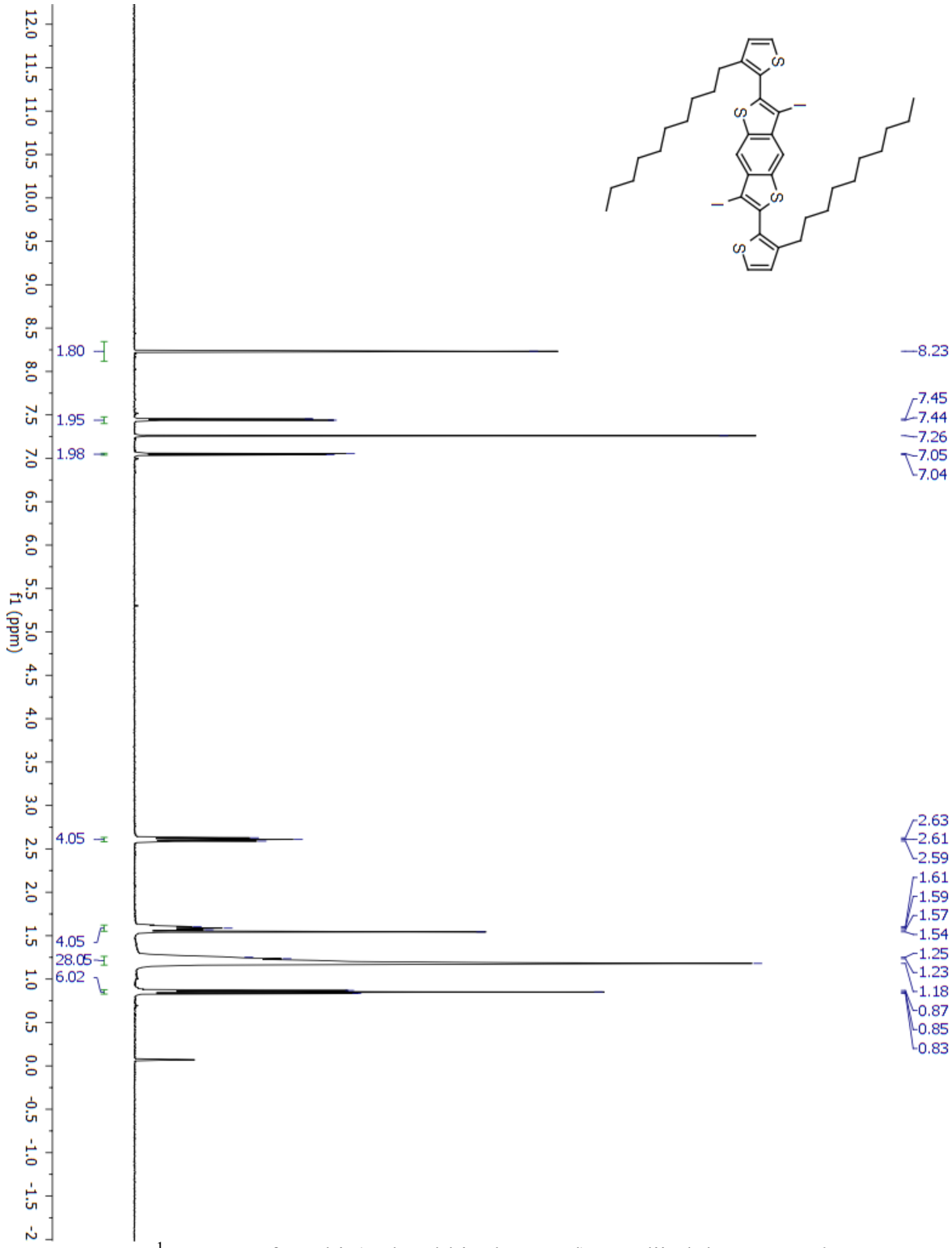

Figure S4.11. ^{1}H NMR of 2,6-bis(3-decylthiophen-2-yl)-3,7-diiodobenzo[1,2-*b*:4,5-*b*']dithiophene (**4a**).

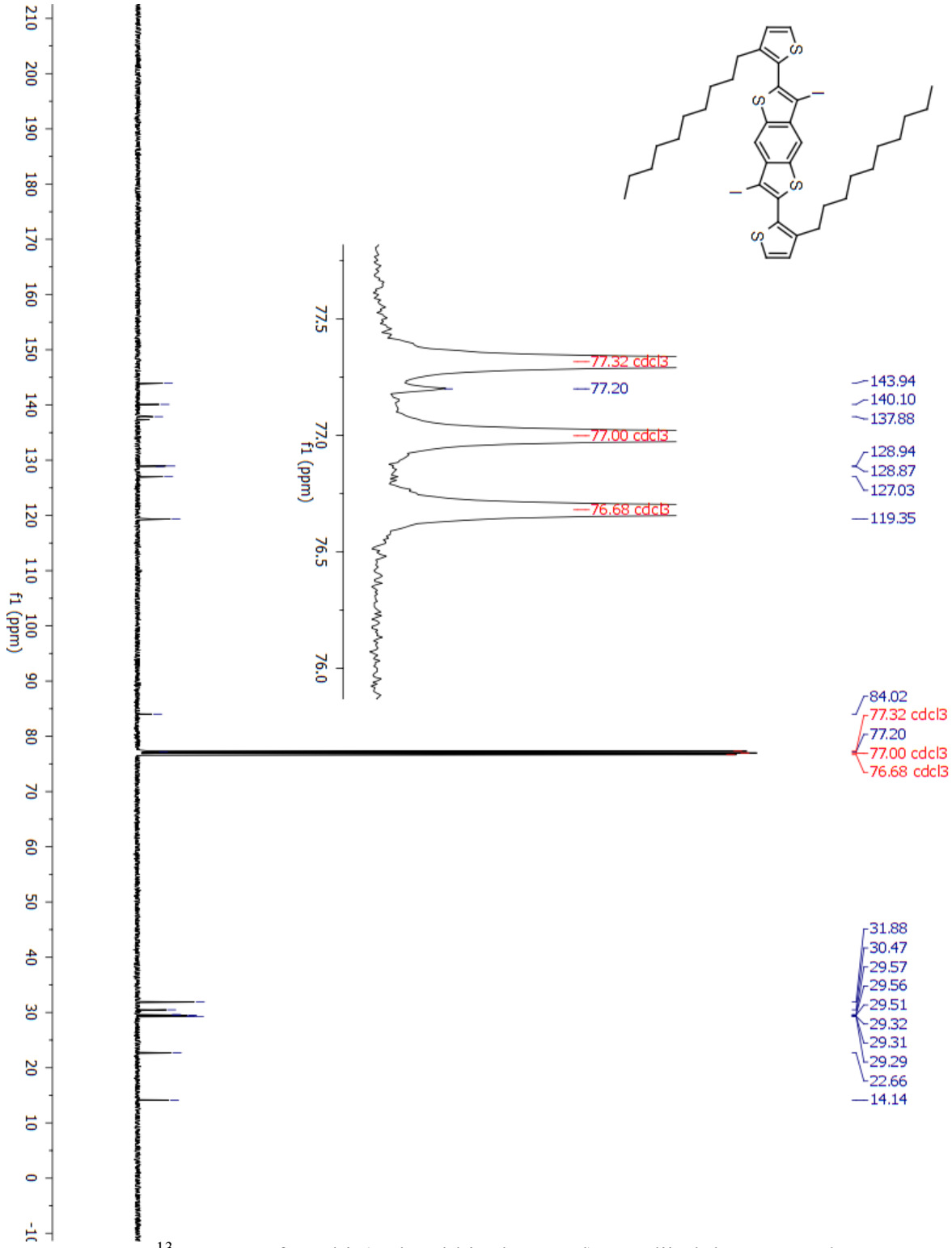

Figure S4.12. ^{13}C NMR of 2,6-bis(3-decylthiophen-2-yl)-3,7-diiodobenzo[1,2-*b*:4,5-*b*']dithiophene (**4a**).

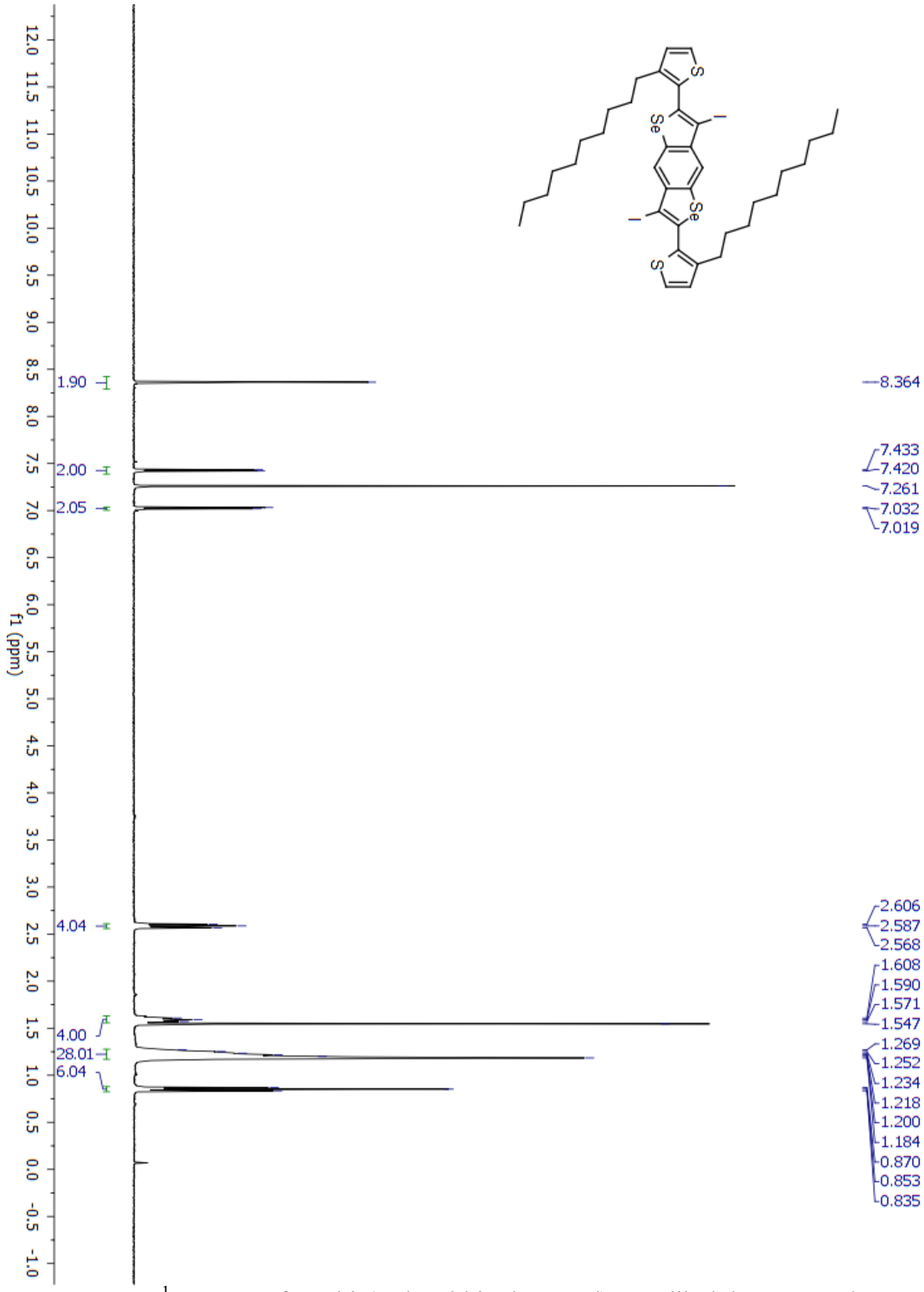

Figure S4.13. ^{1}H NMR of 2,6-bis(3-decylthiophen-2-yl)-3,7-diiodobenzo[1,2-*b*:4,5-*b*']diselenophene (**4b**).

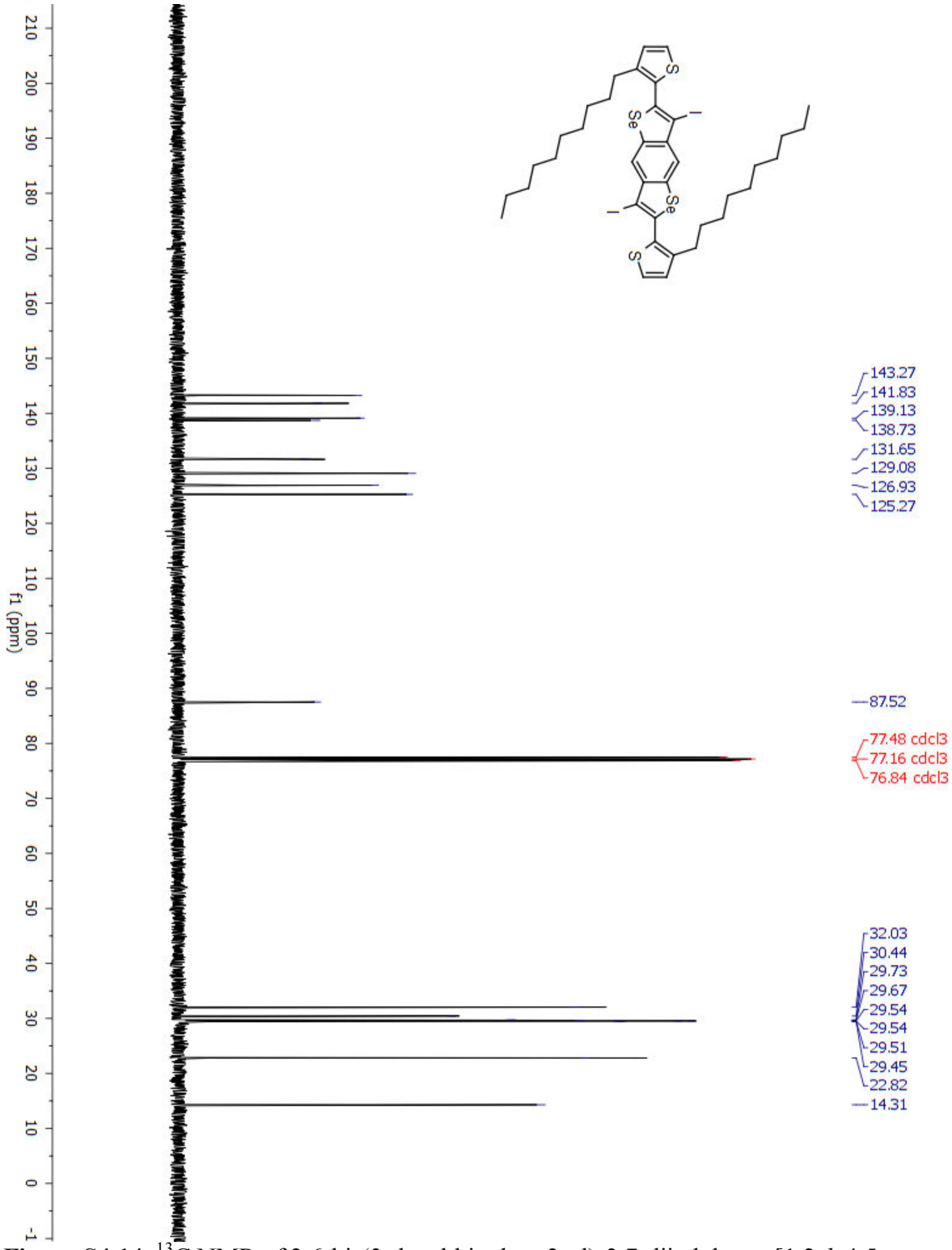

Figure S4.14. ^{13}C NMR of 2,6-bis(3-decylthiophen-2-yl)-3,7-diiodobenzo[1,2-*b*:4,5-*b*']diselenophene (**4b**).

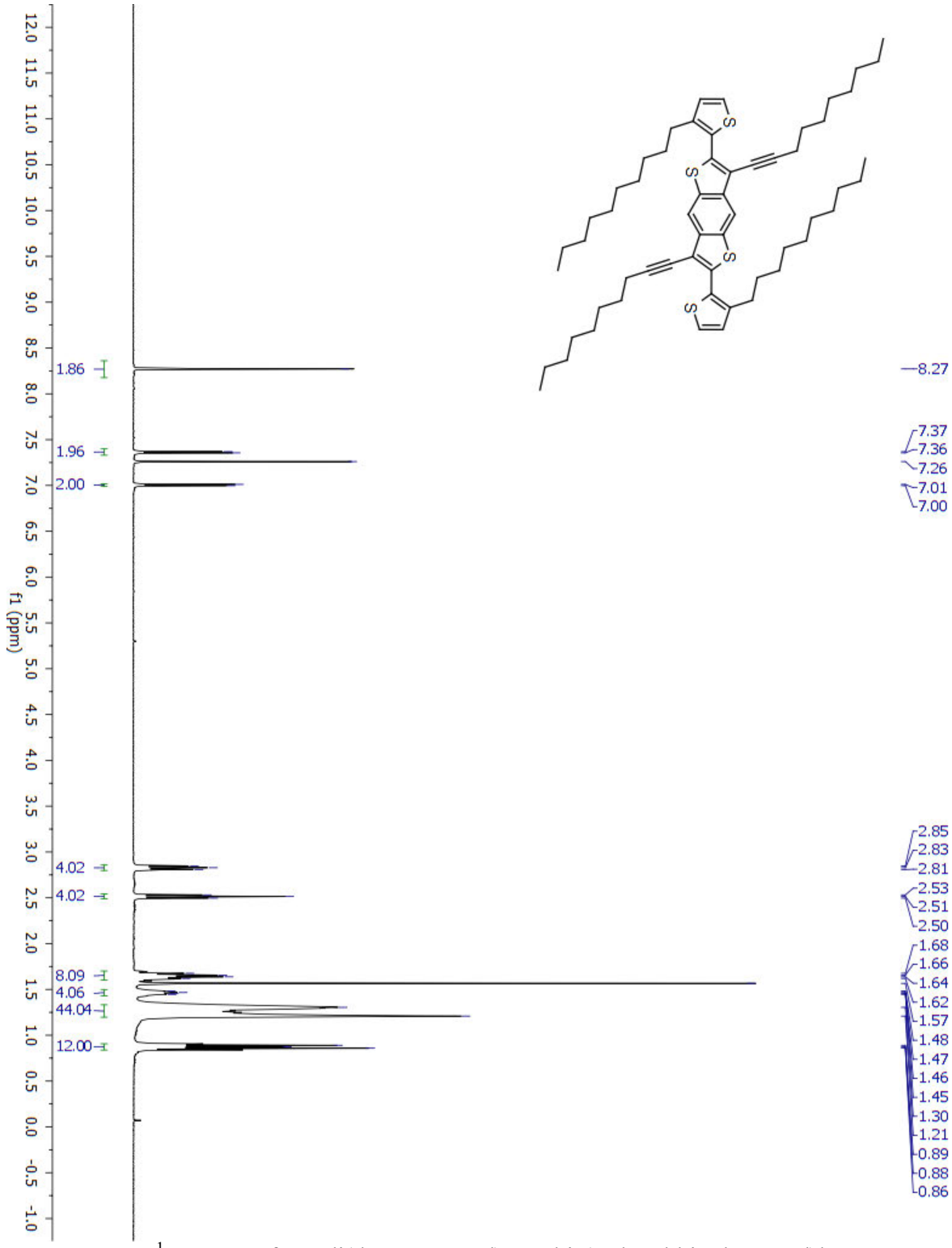

Figure S4.15. ^{1}H NMR of 3,7-di(dec-1-yn-1-yl)-2,6-bis(3-decylthiophen-2-yl)benzo[1,2-*b*:4,5-*b*']dithiophene (**5a**).

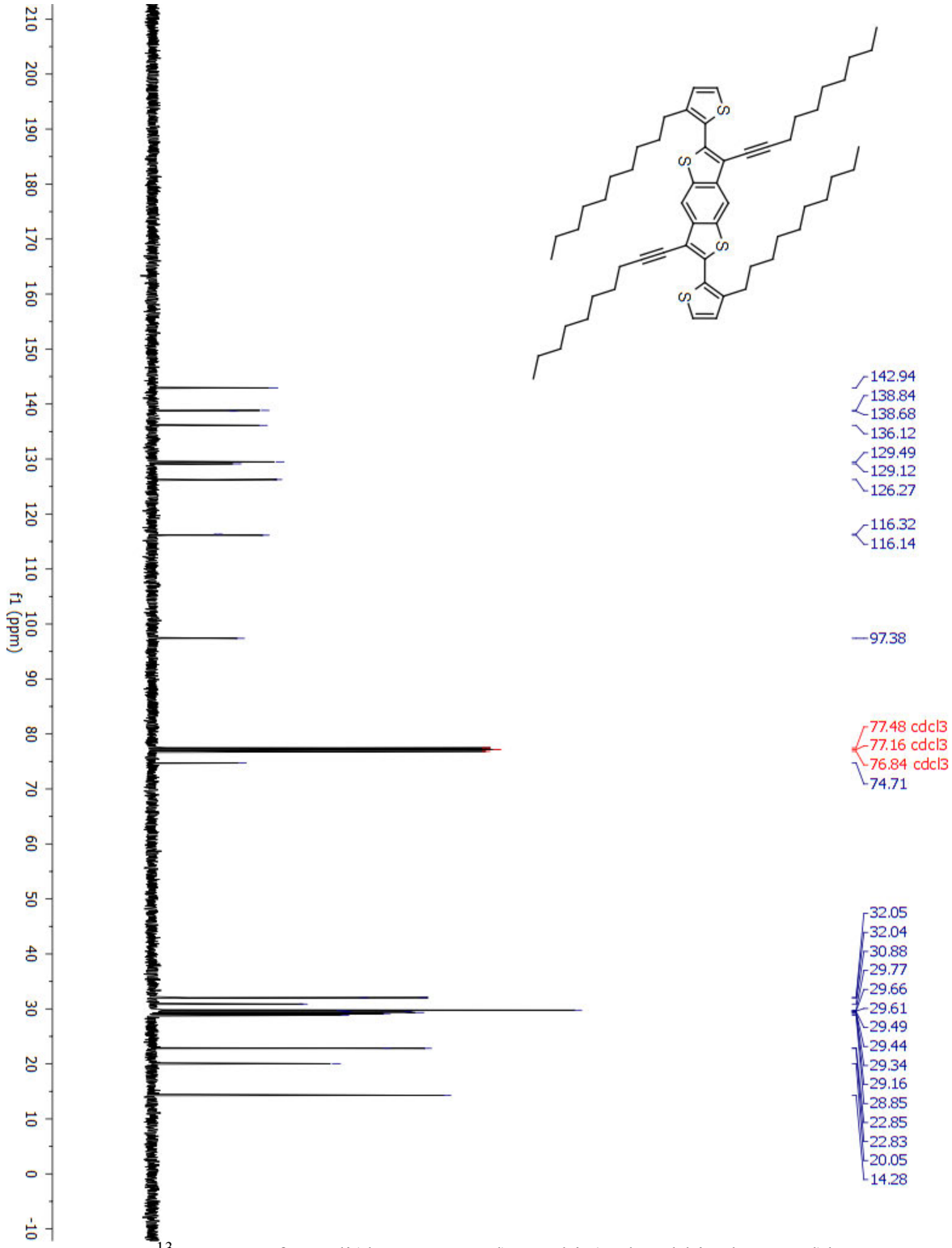

Figure S4.16. ^{13}C NMR of 3,7-di(dec-1-yn-1-yl)-2,6-bis(3-decylthiophen-2-yl)benzo[1,2-*b*:4,5-*b*']dithiophene (**5a**).

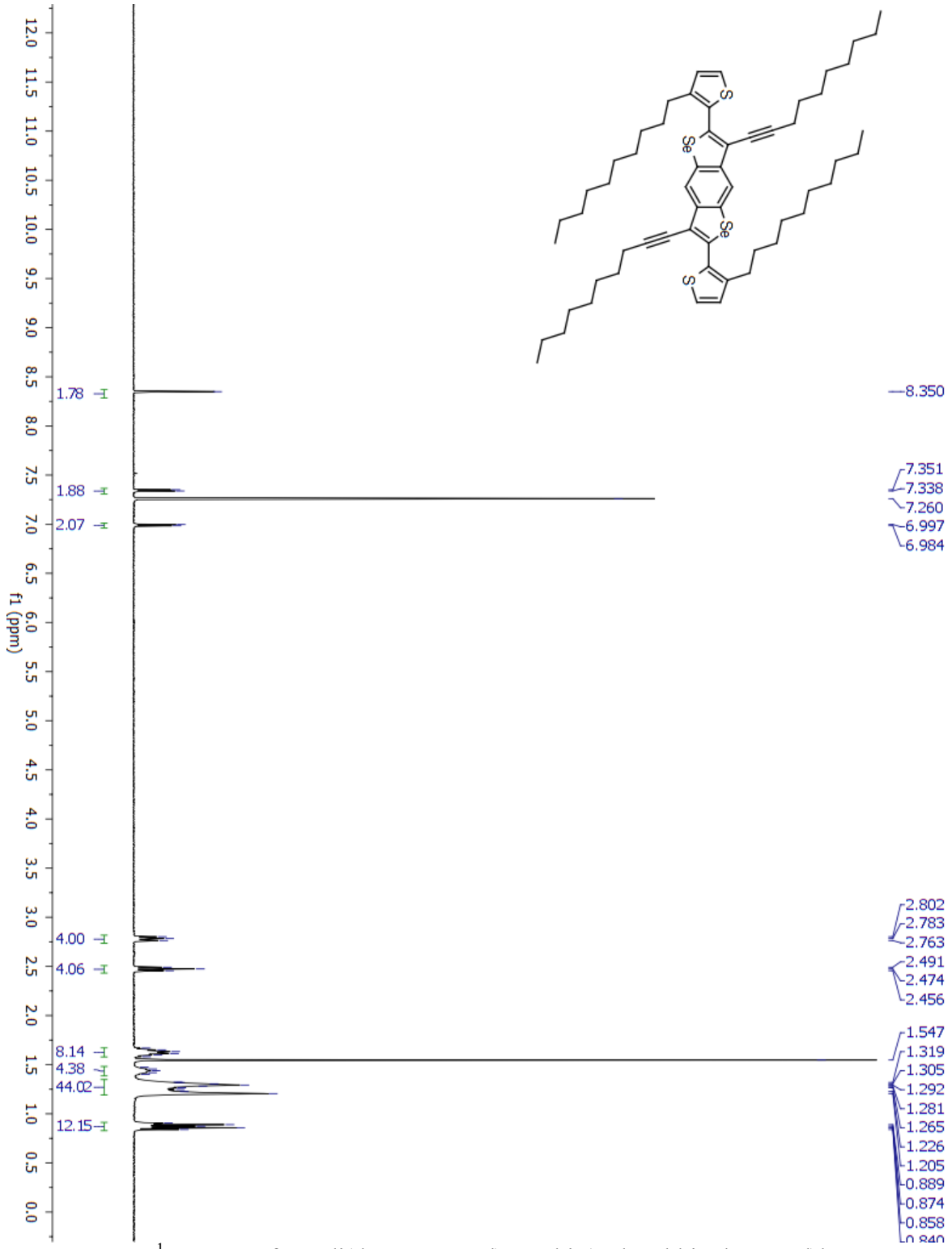

Figure S4.17. ^{1}H NMR of 3,7-di(dec-1-yn-1-yl)-2,6-bis(3-decylthiophen-2-yl)benzo[1,2-*b*:4,5-*b*']diselenophene (**5b**).

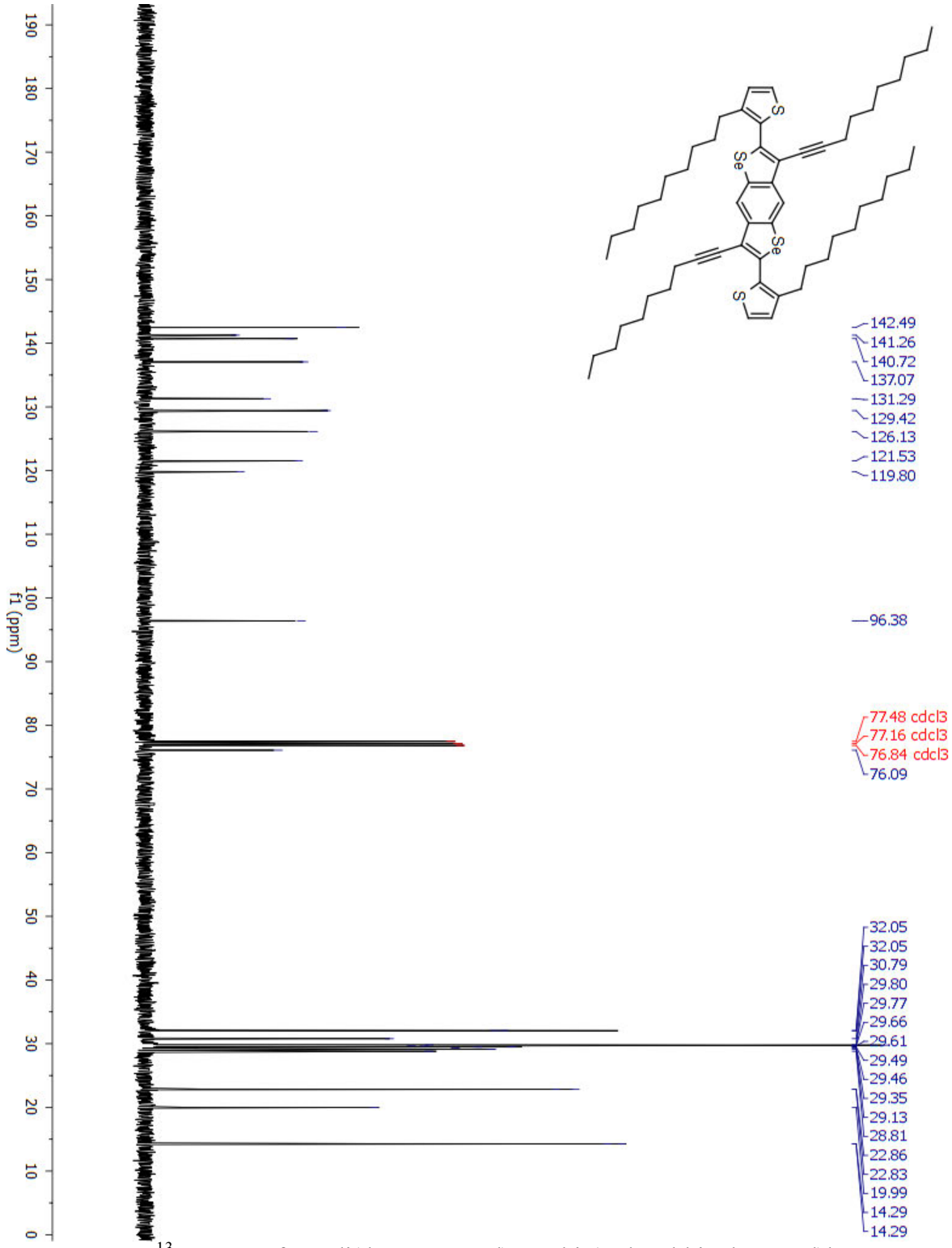

Figure S4.18. ^{13}C NMR of 3,7-di(dec-1-yn-1-yl)-2,6-bis(3-decylthiophen-2-yl)benzo[1,2-*b*:4,5-*b*']diselenophene (**5b**).

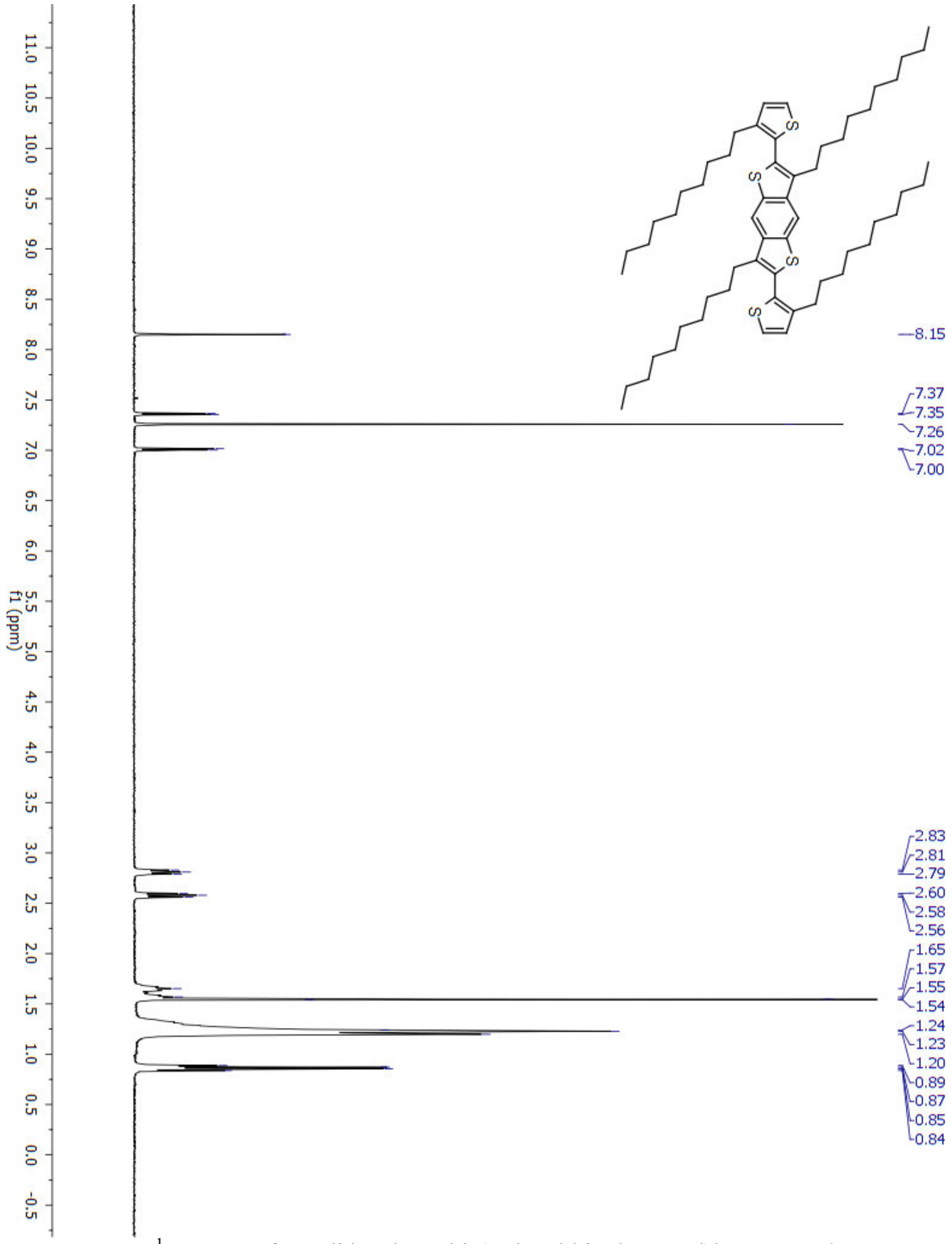

Figure S4.19. ^{1}H NMR of 3,7-didecyl-2,6-bis(3-decylthiophen-2-yl)benzo[1,2-*b*:4,5-*b*']dithiophene (**6a**).

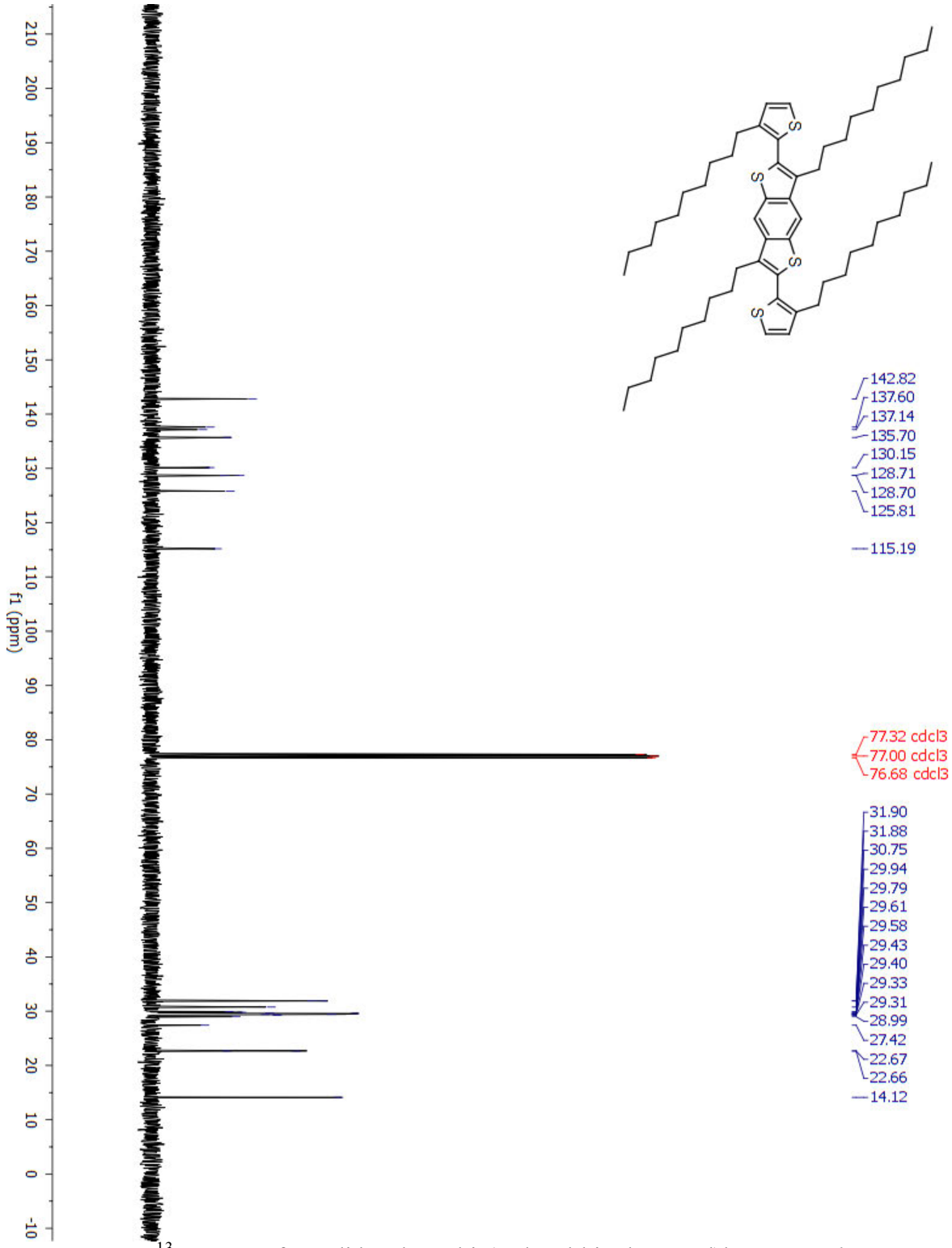

Figure S4.20. ^{13}C NMR of 3,7-didecyl-2,6-bis(3-decylthiophen-2-yl)benzo[1,2-*b*:4,5-*b*']dithiophene (**6a**).

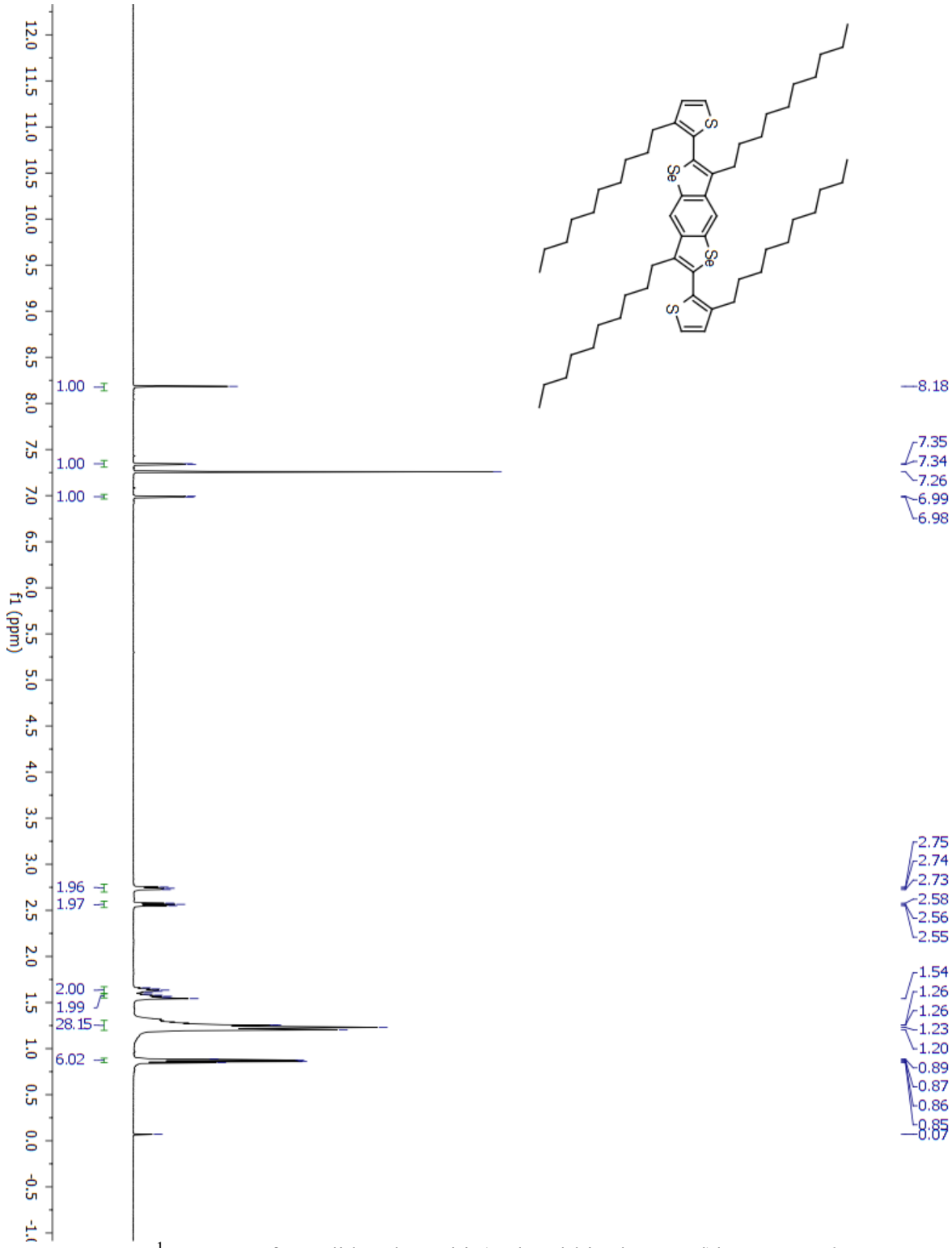

Figure S4.21. ^{1}H NMR of 3,7-didecyl-2,6-bis(3-decylthiophen-2-yl)benzo[1,2-*b*:4,5-*b*']diselenophene (**6b**).

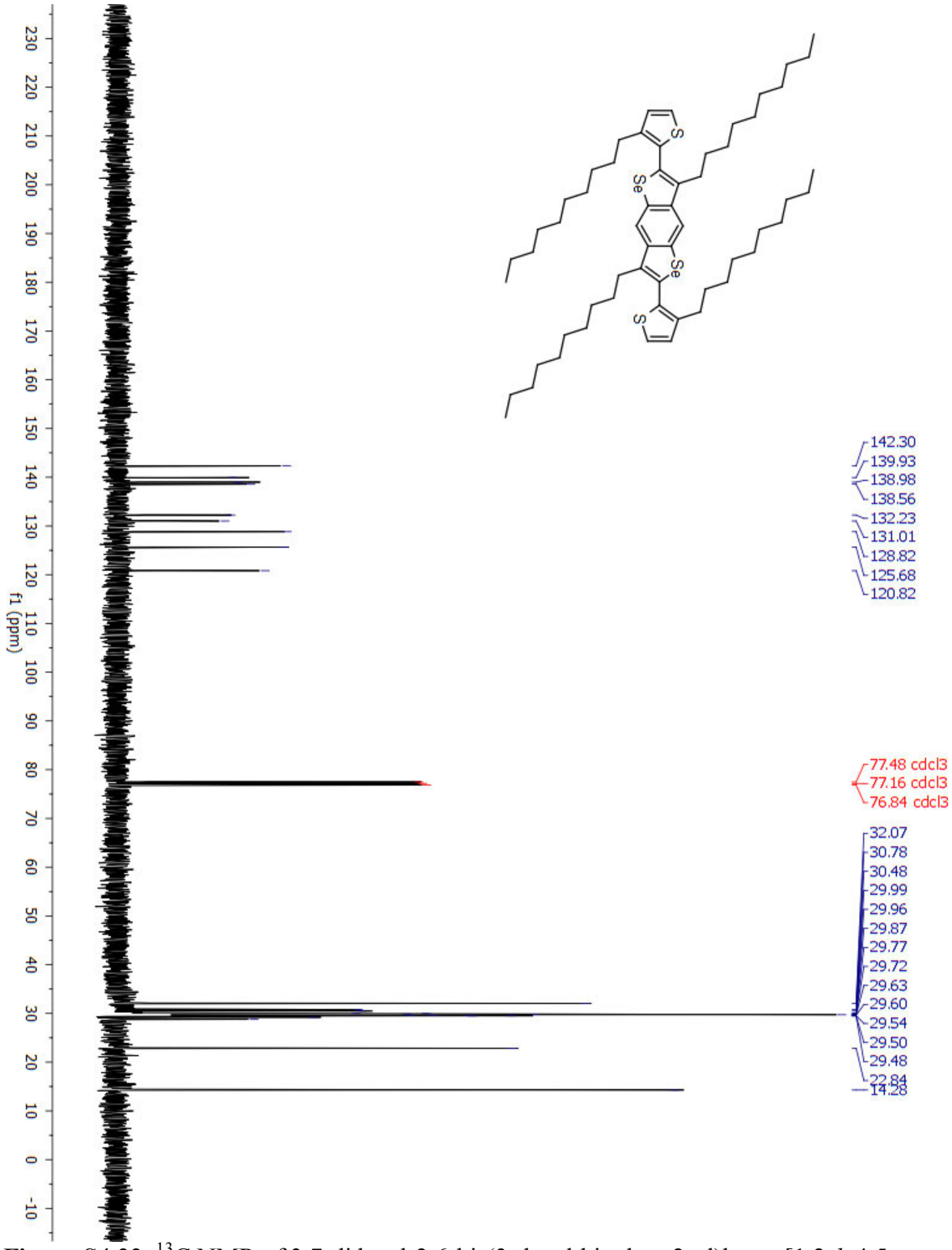

Figure S4.22. ^{13}C NMR of 3,7-didecyl-2,6-bis(3-decylthiophen-2-yl)benzo[1,2-*b*:4,5-*b*']diselenophene (**6b**).

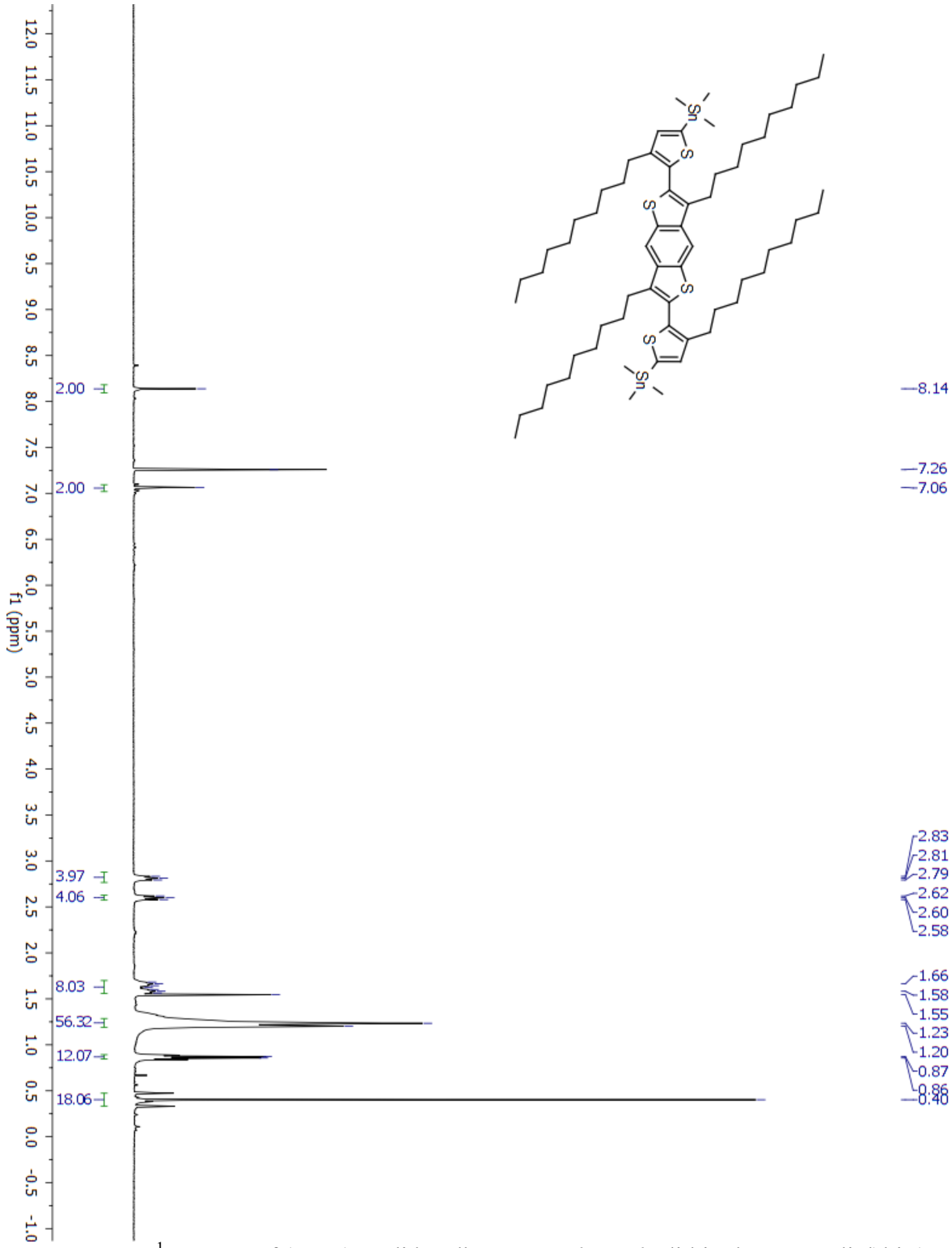

Figure S4.23. ^{1}H NMR of (5,5'-(3,7-didecylbenzo[1,2-*b*:4,5-*b*']dithiophene-2,6-diyl)bis(4-decylthiophene-5,2-diyl))bis(trimethylstannane) (**7a**).

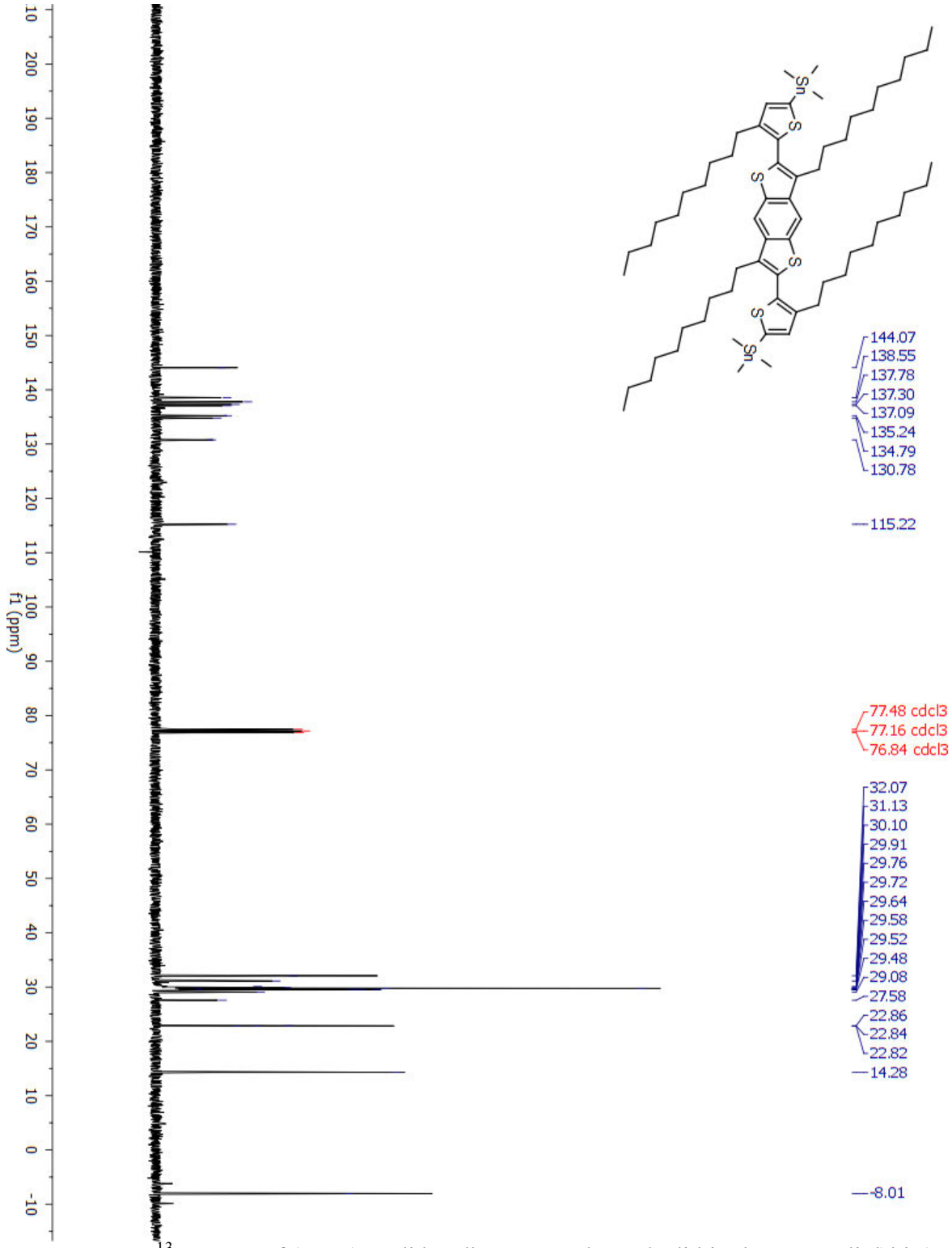

Figure S4.24. ^{13}C NMR of (5,5'-(3,7-didecylbenzo[1,2-*b*:4,5-*b*']dithiophene-2,6-diyl)bis(4-decylthiophene-5,2-diyl))bis(trimethylstannane) (**7a**).

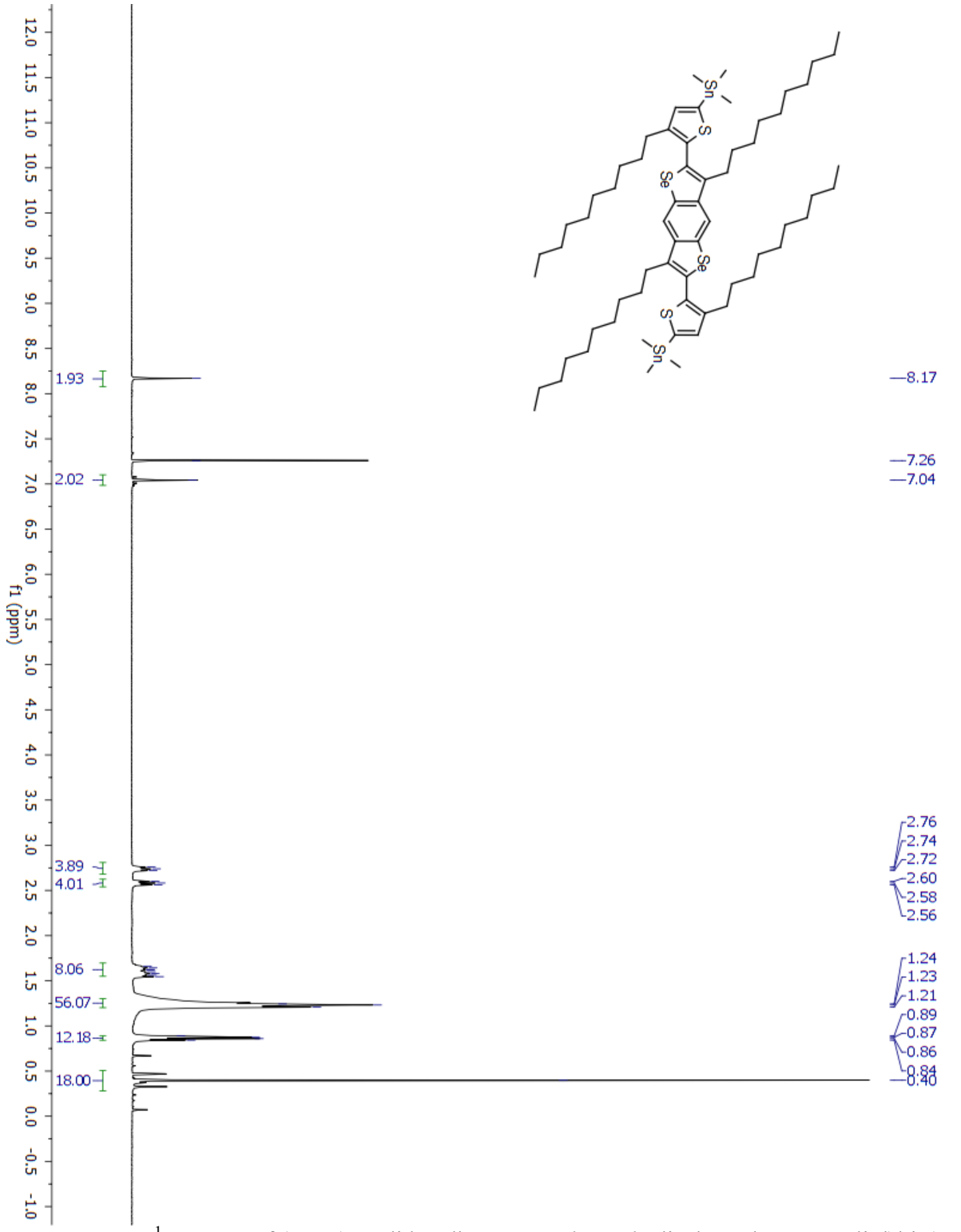

Figure S4.25. ^{1}H NMR of (5,5'-(3,7-didecylbenzo[1,2-*b*:4,5-*b*']diselenophene-2,6-diyl)bis(4-decylthiophene-5,2-diyl))bis(trimethylstannane) (**7b**).

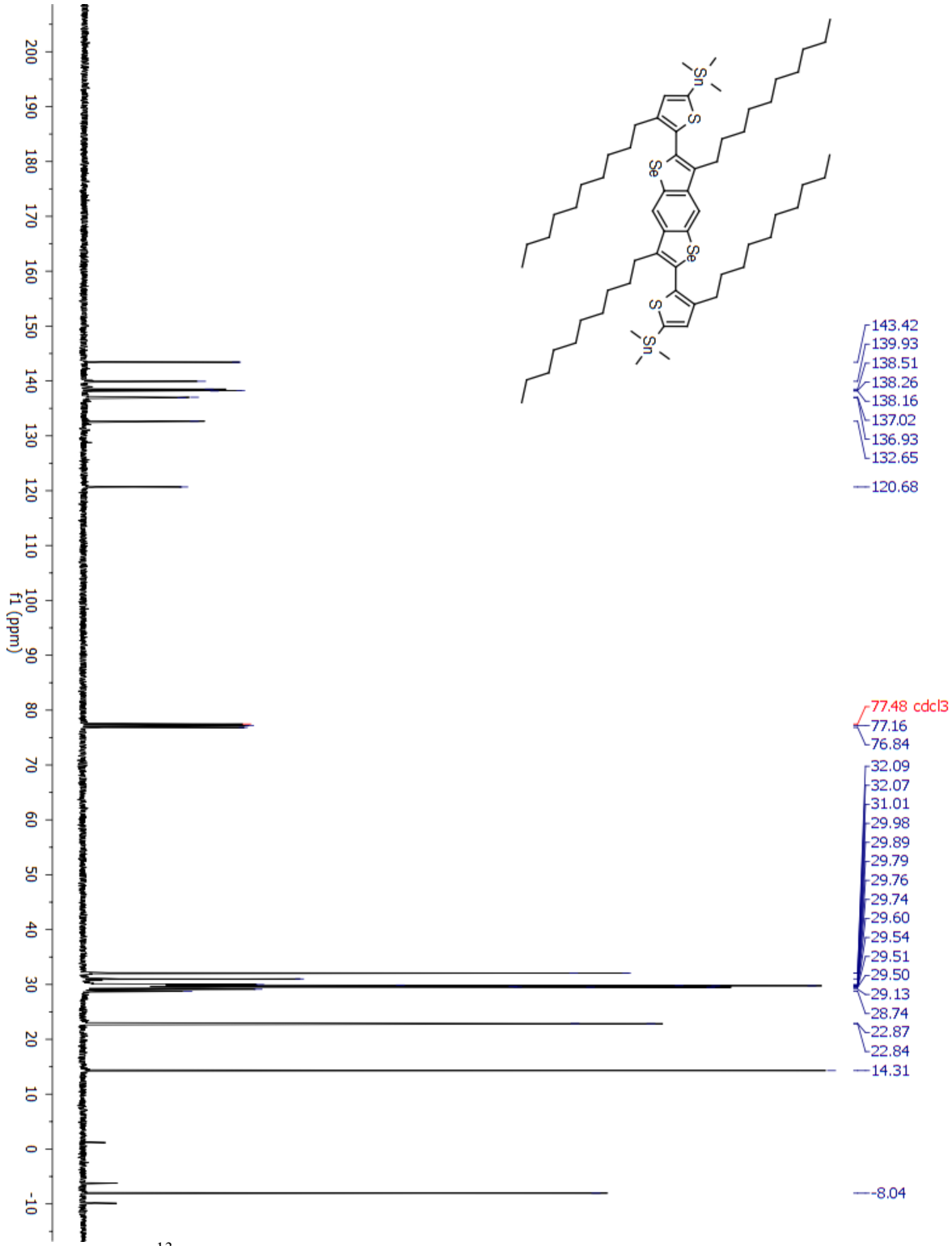

Figure S4.26. ^{13}C NMR of (5,5'-(3,7-didecylbenzo[1,2-*b*:4,5-*b*']diselenophene-2,6-diyl)bis(4-decylthiophene-5,2-diyl))bis(trimethylstannane) (**7b**).

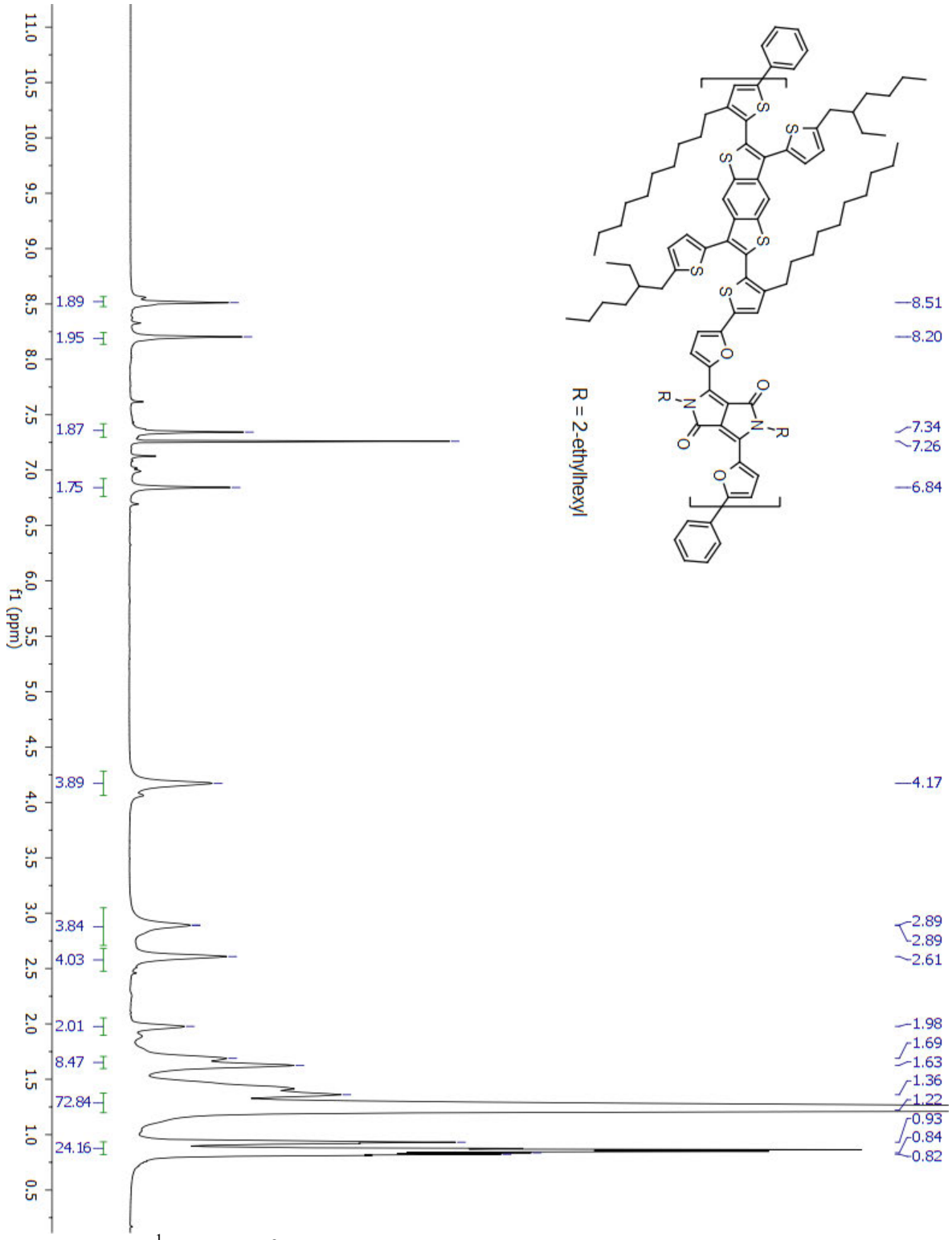

Figure S4.27. ^{1}H NMR of **PBDT-DPP**.

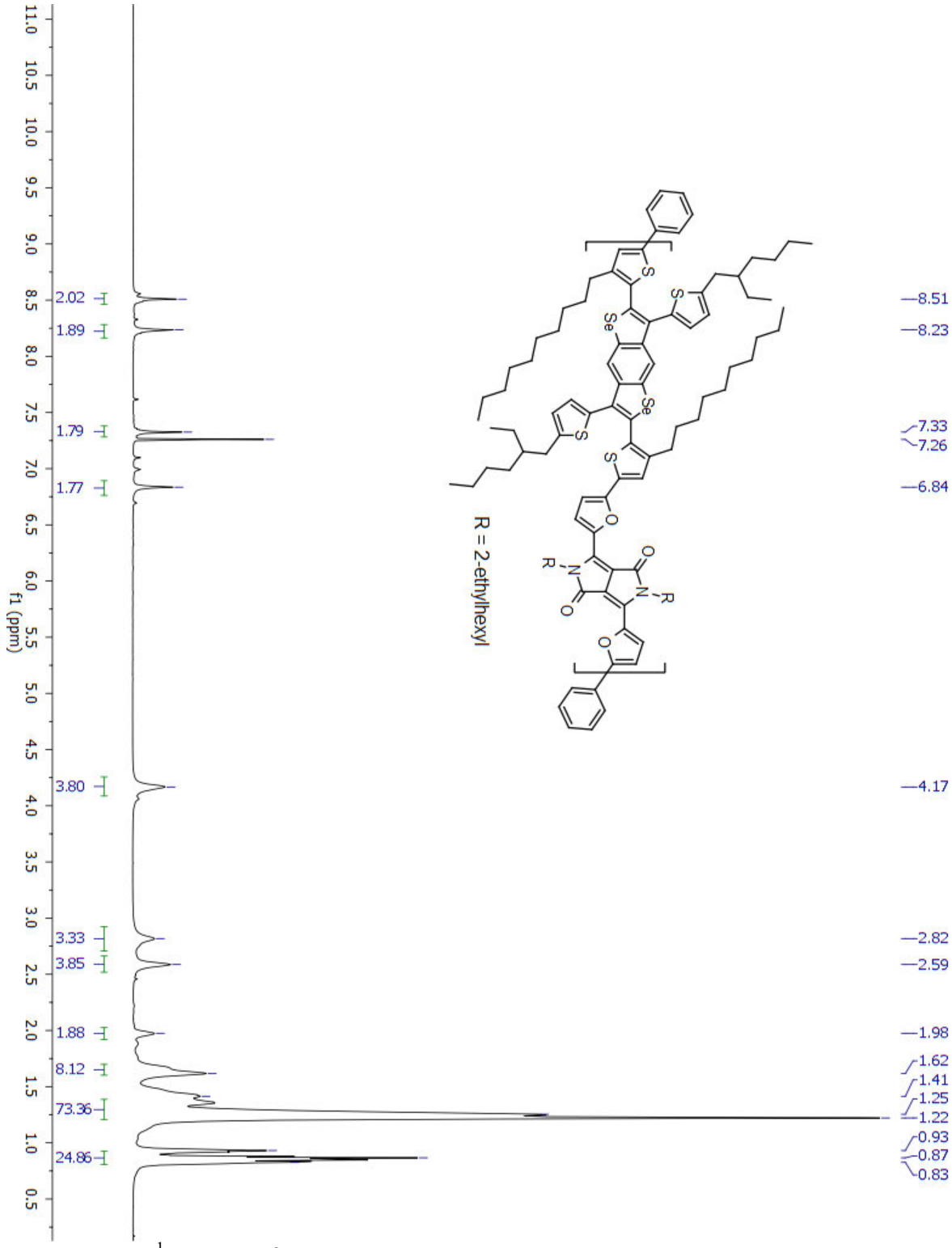

Figure S4.28. ^{1}H NMR of **PBDSe-DPP**.

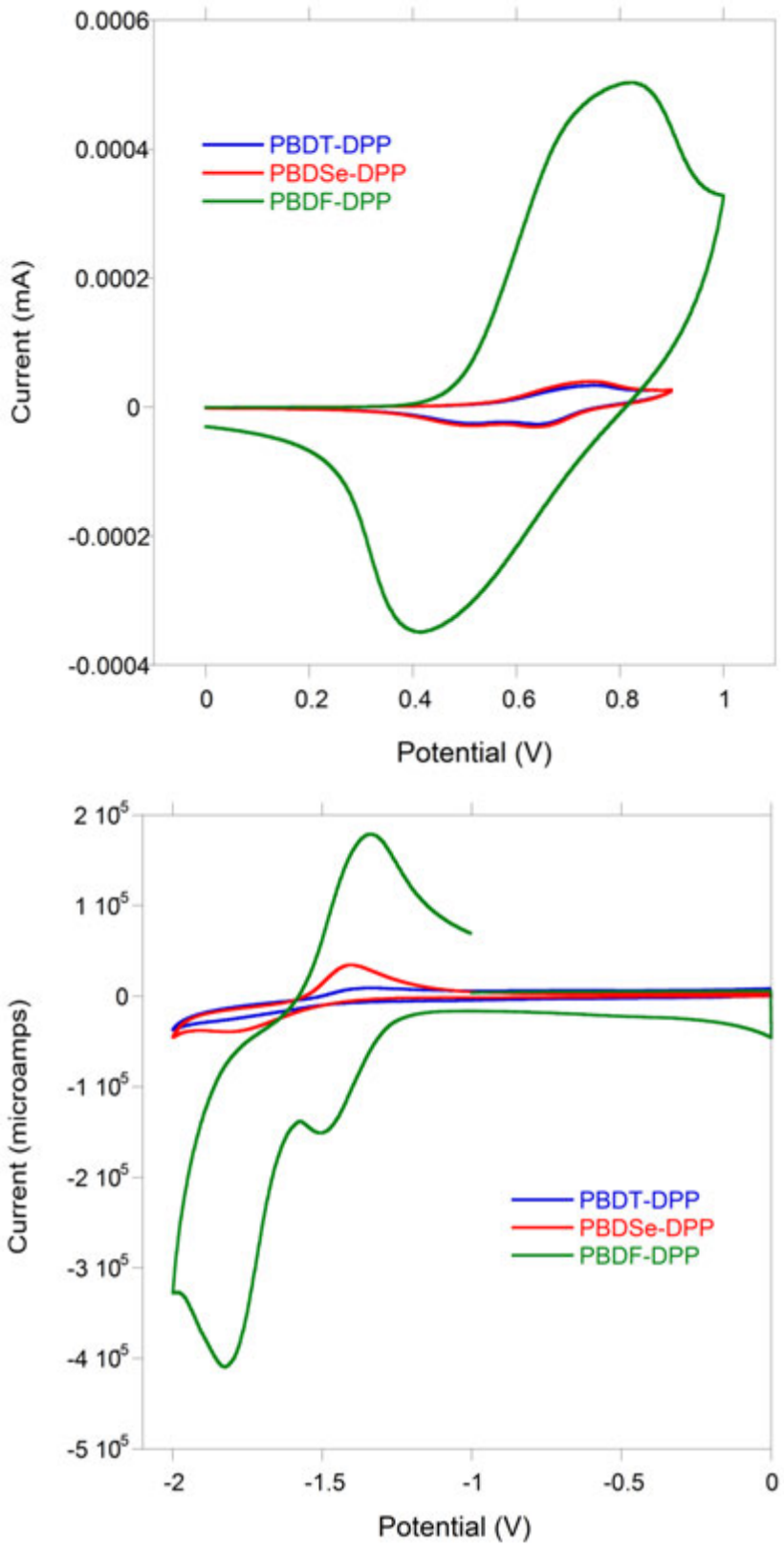

Figure S4.27. Cyclic voltammetry traces for oxidation(top) and reduction (bottom) cycles of **PBDF-DPP, PBDT-DPP,** and **PBDSe-DPP**.

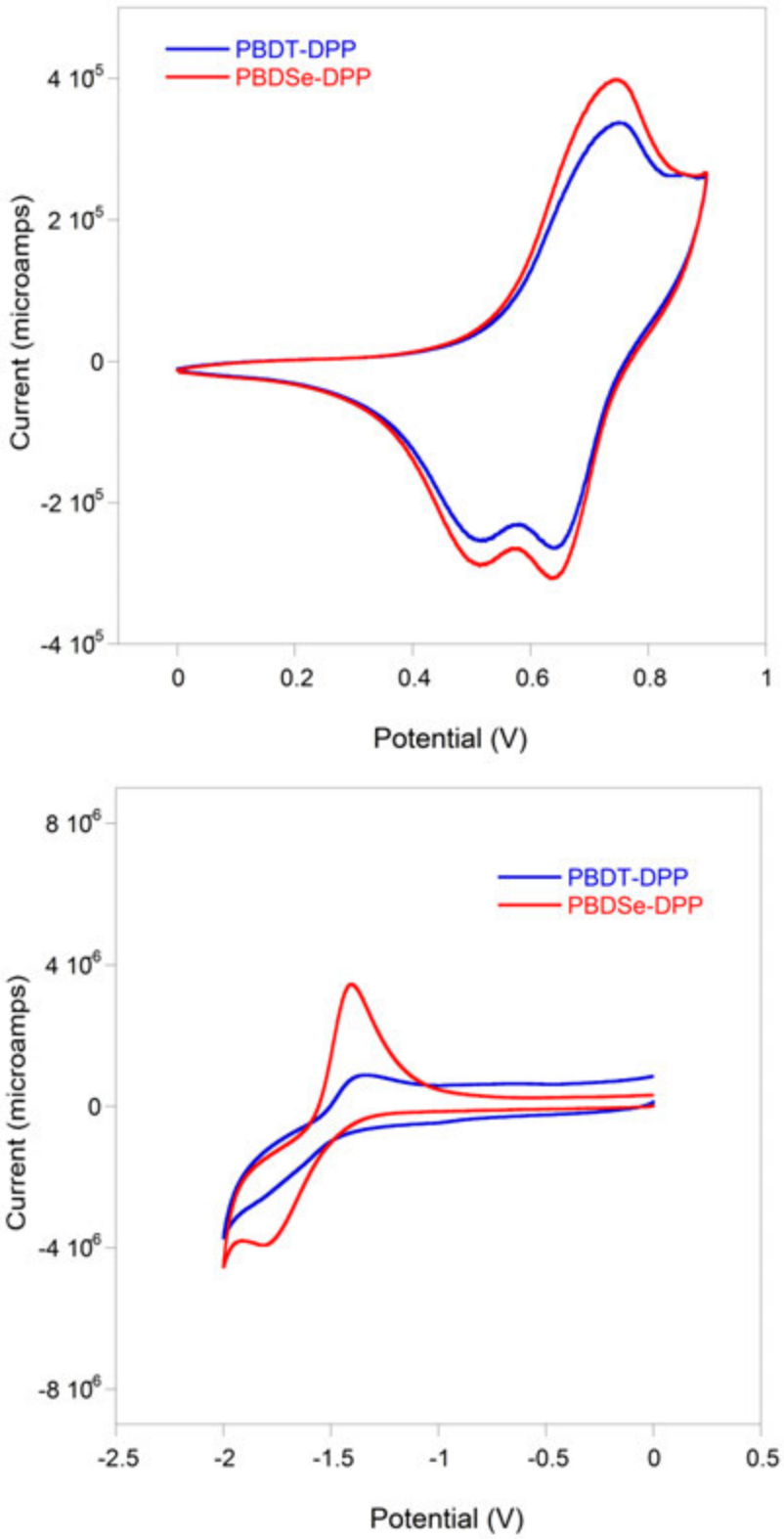

Figure S4.28. Cyclic voltammetry traces for oxidation(top) and reduction (bottom) cycles of **PBDT-DPP** and **PBDSe-DPP**.

4.8 REFERENCES

1. Service, R. F., *Science* **2011,** *332* (6027), 293.
2. Nelson, J., *Materials Today* **2011,** *14* (10), 462-470.
3. Facchetti, A., *Chem. Mater.* **2010,** *23* (3), 733-758.
4. Grimsdale, A. C.; Leok Chan, K.; Martin, R. E.; Jokisz, P. G.; Holmes, A. B., *Chem. Rev.* **2009,** *109* (3), 897-1091.
5. Thomas, S. W., III; Joly, G. D.; Swager, T. M., *Chem. Rev.* **2007,** *107* (4), 1339-1386.
6. Thompson, B. C.; Frechet, J. M. J., *Angew. Chem. Int. Ed. Engl.* **2008,** *47* (1), 58-77.
7. Havinga, E. E.; ten Hoeve, W.; Wynberg, H., *Polym. Bull.* **1992,** *29* (1), 119-126.
8. Havinga, E. E.; ten Hoeve, W.; Wynberg, H., *Synth. Met.* **1993,** *55* (1), 299-306.
9. McCullough, R. D.; Lowe, R. D.; Jayaraman, M.; Anderson, D. L., *J. Org. Chem.* **1993,** *58* (4), 904-912.
10. Jeffries-EL, M.; McCullough, R. D., Regioregular polythiophene. In *Handbook of Conducting Polymers*, 3rd ed / edited by Terje A. Skotheim and John Reynolds. ed.; Skotheim, T. A., Reynolds, John R., Ed. London: Boca Raton, Fla, 2007; pp 331-380.
11. Huo, L.; Huang, Y.; Fan, B.; Guo, X.; Jing, Y.; Zhang, M.; Li, Y.; Hou, J., *Chem. Commun.* **2012,** *48* (27), 3318-3320.
12. Bunz, U. H. F., *Angew, Chem. Int. Ed.* **2010,** *49* (30), 5037-5040.
13. Gidron, O.; Diskin-Posner, Y.; Bendikov, M., *J. Am. Chem. Soc.* **2010,** *132* (7), 2148-2150.
14. Woo, C. H.; Beaujuge, P. M.; Holcombe, T. W.; Lee, . .; Fr chet, J. M. J., *J. Am. Chem. Soc.* **2010,** *132* (44), 15547-15549.
15. Fringuelli, F.; Marino, G.; Taticchi, A.; Grandolini, G., *J. Chem. Soc., Perkin Trans. 2* **1974,** (4), 332-337.
16. Shiroudi, A.; Zahedi, E., *Chin. J. Chem.* **2011,** *29* (11), 2249-2256.
17. Zade, S. S.; Zamoshchik, N.; Bendikov, M., *Chem. Eur. J.* **2009,** *15* (34), 8613-8624.
18. Patra, A.; Bendikov, M., *J. Mater. Chem.* **2010,** *20* (3), 422-433.
19. Patra, A.; Wijsboom, Y. H.; Zade, S. S.; Li, M.; Sheynin, Y.; Leitus, G.; Bendikov, M., *J. Am. Chem. Soc.* **2008,** *130* (21), 6734-6736.
20. Kang, I.; An, T. K.; Hong, J.-a.; Yun, H.-J.; Kim, R.; Chung, D. S.; Park, C. E.; Kim, Y.-H.; Kwon, S.-K., *Adv. Mater.* **2013,** *25* (4), 524-528.
21. Oyaizu, K.; Iwasaki, T.; Tsukahara, Y.; Tsuchida, E., *Macromolecules* **2004,** *37* (4), 1257-1270.
22. Heeney, M.; Zhang, W.; Crouch, D. J.; Chabinyc, M. L.; Gordeyev, S.; Hamilton, R.; Higgins, S. J.; McCulloch, I.; Skabara, P. J.; Sparrowe, D.; Tierney, S., *Chem. Commun.* **2007,** (47), 5061-5063.
23. He, Z.; Zhong, C.; Su, S.; Xu, M.; Wu, H.; Cao, Y., *Nature Photon.* **2012,** *6* (9), 591-595.
24. He, Z.; Zhong, C.; Huang, X.; Wong, W.-Y.; Wu, H.; Chen, L.; Su, S.; Cao, Y., *Adv. Mater.* **2011,** *23* (40), 4636-4643.
25. Small, C. E.; Chen, S.; Subbiah, J.; Amb, C. M.; Tsang, S.-W.; Lai, T.-H.; Reynolds, J. R.; So, F., *Nature Photon.* **2012,** *6* (2), 115-120.
26. Li, X.; Choy, W. C. H.; Huo, L.; Xie, F.; Sha, W. E. I.; Ding, B.; Guo, X.; Li, Y.; Hou, J.; You, J.; Yang, Y., *Adv. Mater.* **2012,** *24* (22), 3046-3052.

27. Hou, J.; Park, M.-H.; Zhang, S.; Yao, Y.; Chen, L.-M.; Li, J.-H.; Yang, Y., *Macromolecules* **2008,** *41* (16), 6012-6018.
28. Toba, M.; Nakashima, T.; Kawai, T., *J. Poly. Sci. A.* **2011,** *49* (8), 1895-1906.
29. Liang, Y.; Xu, Z.; Xia, J.; Tsai, S.-T.; Wu, Y.; Li, G.; Ray, C.; Yu, L., *Adv. Mater.* **2010,** *22* (20), E135-E138.
30. Najari, A.; Beaupré, S.; Berrouard, P.; Zou, Y.; Pouliot, J.-R.; Lepage-Pérusse, C.; Leclerc, M., *Adv. Funct. Mater.* **2011,** *21* (4), 718-728.
31. Kobilka, B. M.; Dubrovskiy, A. V.; Ewan, M. D.; Tomlinson, A. L.; Larock, R. C.; Chaudhary, S.; Jeffries-EL, M., *Chem. Commun.* **2012,** *48* (71), 8919-8921.
32. Kobilka, B. M.; Hale, B. J.; Ewan, M. D.; Dubrovskiy, A. V.; Nelson, T. L.; Duzhko, V.; Jeffries-El, M., *Polym. Chem.* **2013,** *4* (20), 5329-5336.
33. Li, H.; Jiang, P.; Yi, C.; Li, C.; Liu, S.-X.; Tan, S.; Zhao, B.; Braun, J.; Meier, W.; Wandlowski, T.; Decurtins, S., *Macromolecules* **2010,** *43* (19), 8058-8062.
34. Sista, P.; Huang, P.; Gunathilake, S. S.; Bhatt, M. P.; Kularatne, R. S.; Stefan, M. C.; Biewer, M. C., *J. Poly. Sci. A.* **2012,** *50* (20), 4316-4324.
35. Li, H.; Tang, P.; Zhao, Y.; Liu, S.-X.; Aeschi, Y.; Deng, L.; Braun, J.; Zhao, B.; Liu, Y.; Tan, S.; Meier, W.; Decurtins, S., *J. Poly. Sci. A.* **2012,** *50* (14), 2935–2943.
36. Liu, B.; Chen, X.; Zou, Y.; He, Y.; Xiao, L.; Xu, X.; Li, L.; Li, Y., *Polym. Chem.* **2013,** *4* (3), 470-476.
37. Saadeh, H. A.; Lu, L.; He, F.; Bullock, J. E.; Wang, W.; Carsten, B.; Yu, L., *ACS Macro Lett.* **2012,** *1* (3), 361-365.
38. Bijleveld, J. C.; Karsten, B. P.; Mathijssen, S. G. J.; Wienk, M. M.; de Leeuw, D. M.; Janssen, R. A. J., *J. Mater. Chem.* **2011,** *21* (5), 1600-1606.
39. Yiu, A. T.; Beaujuge, P. M.; Lee, O. P.; Woo, C. H.; Toney, M. F.; Fr chet, J. M. J., *J. Am. Chem. Soc.* **2011,** *134* (4), 2180-2185.
40. Sonar, P.; Foong, T. R. B.; Singh, S. P.; Li, Y.; Dodabalapur, A., *Chem. Commun.* **2012,** *48* (67), 8383-8385.
41. Sonar, P.; Singh, S. P.; Williams, E. L.; Li, Y.; Soh, M. S.; Dodabalapur, A., *J. Mater. Chem.* **2012,** *22* (10), 4425-4435.
42. Bijleveld, J. C.; Gevaerts, V. S.; Di Nuzzo, D.; Turbiez, M.; Mathijssen, S. G. J.; de Leeuw, D. M.; Wienk, M. M.; Janssen, R. A. J., *Adv. Mater.* **2010,** *22* (35), E242-E246.
43. Wienk, M. M.; Turbiez, M.; Gilot, J.; Janssen, R. A. J., *Adv. Mater.* **2008,** *20* (13), 2556-2560.
44. ou, .; e ndron, D.; Badrou- ch, R. d.; Najari, A.; Tao, Y.; Leclerc, M., *Macromolecules* **2009,** *42* (8), 2891-2894.
45. Zou, Y.; Gendron, D.; Neagu-Plesu, R.; Leclerc, M., *Macromolecules* **2009,** *42* (17), 6361-6365.
46. Qu, S.; Tian, H., *Chem. Commun.* **2012,** *48* (25), 3039-3051.
47. Bürgi, L.; Turbiez, M.; Pfeiffer, R.; Bienewald, F.; Kirner, H.-J.; Winnewisser, C., *Adv. Mater.* **2008,** *20* (11), 2217-2224.
48. Yuan, J.; Huang, X.; Zhang, F.; Lu, J.; Zhai, Z.; Di, C.; Jiang, Z.; Ma, W., *J. Mater. Chem.* **2012,** *22* (42), 22734-22742.
49. Goldfinger, M. B.; Crawford, K. B.; Swager, T. M., *J. Am. Chem. Soc.* **1997,** *119* (20), 4578-4593.

50. Takimiya, K.; Konda, Y.; Ebata, H.; Niihara, N.; Otsubo, T., *J. Org. Chem.* **2005,** *70* (25), 10569-10571.
51. Ebata, H.; Miyazaki, E.; Yamamoto, T.; Takimiya, K., *Org. Lett.* **2007,** *9* (22), 4499-4502.
52. Tkachov, R.; Senkovskyy, V.; Komber, H.; Kiriy, A., *Macromolecules* **2011,** *44* (7), 2006-2015.
53. Beaujuge, P. M.; Amb, C. M.; Reynolds, J. R., *Acc. Chem. Res.* **2010,** *43* (11), 1396-1407.
54. Cardona, C. M.; Li, W.; Kaifer, A. E.; Stockdale, D.; Bazan, G. C., *Adv. Mater.* **2011,** *23* (20), 2367-2371.
55. Distefano, G.; Jones, D.; Guerra, M.; Favaretto, L.; Modelli, A.; Mengoli, G., *J. Phys. Chem.* **1991,** *95* (24), 9746-9753.
56. Peet, J.; Kim, J. Y.; Coates, N. E.; Ma, W. L.; Moses, D.; Heeger, A. J.; Bazan, G. C., *Nature Mater.* **2007,** *6* (7), 497-500.
57. Lee, J. K.; Ma, W. L.; Brabec, C. J.; Yuen, J.; Moon, J. S.; Kim, J. Y.; Lee, K.; Bazan, G. C.; Heeger, A. J., *J. Am. Chem. Soc.* **2008,** *130* (11), 3619-3623.
58. Intemann, J. J.; Yao, K.; Yip, H.-L.; Xu, Y.-X.; Li, Y.-X.; Liang, P.-W.; Ding, F.-Z.; Li, X.; Jen, A. K. Y., *Chem. Mater.* **2013**.
59. Wang, B.; Tsang, S.-W.; Zhang, W.; Tao, Y.; Wong, M. S., *Chem. Commun.* **2011,** *47* (33), 9471-9473.

CHAPTER 5

Synthesis of a Series of Two Dimensional Benzo[1,2-b:4,5-b']dichalcogene-based Donor-Acceptor Copolymers with diketopyrrolopyrrole and their Performance in Polymer Solar Cells.

Brandon M. Kobilka,[a] *Monique D. Ewan,*[a] *Benjamin J. Hale,*[a] *Achala Bhuwalka,*[a] *and Malika Jeffries-EL**[a]

[a] Department of Chemistry, Iowa State University, Ames, IA 50011

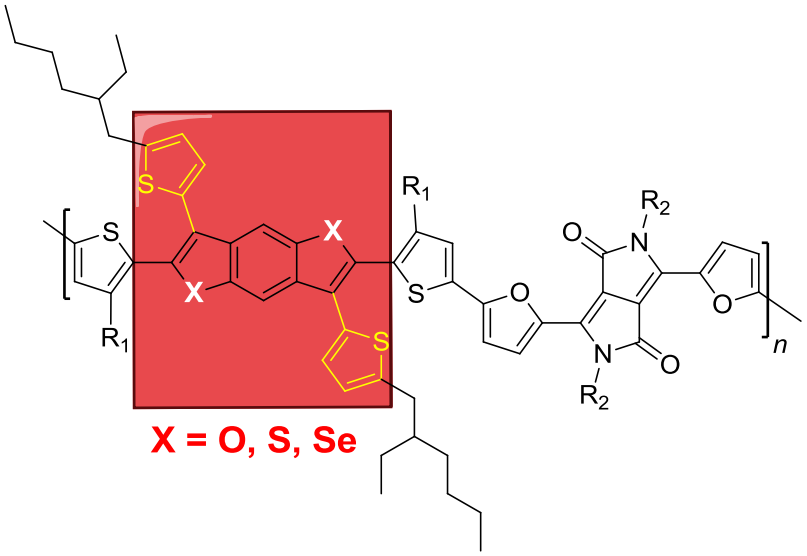

5.1 ABSTRACT

An series of 2,6-di(thiophen-2-yl)benzo[1,2-*b*:4,5-*b'*]dichalcogenophene molecules were synthesized where 2-ethylhexylthien-5-yl side chains were affixed at the 3,7-positions on the BDC core via the Stille cross-coupling reaction. These BDC heteroatoms were varied between oxygen, sulfur and selenium and utilized as the donor component in donor-acceptor copolymers. Furan-flanked 1,4-diketopyrrolo[3,4-*c*]pyrrole was used as the acceptor, where the alkyl side chains were varied between either branched 2-ethylhexyl and linear *n*-tetradecyl to modify the film morphology of the materials. The effects of 2-dimensional

conjugation were evaluated between the resulting six different BDC-based copolymers. The polymers based on benzodifuran experienced the highest molecular weights and narrowest optical band gaps of 1.42 eV. The performance of the polymers as an active layer material in bulk-heterojunction organic photovoltaic cells (OPVs) along with $PC_{71}BM$ was investigated. The resulting devices yielded power conversion efficiencies (PCEs) of 1.8-1.9 % for the benzodifuran and benzodithiophene-based devices.

5.2 INTRODUCTION

Due to the incredible increase in the amount of effort being poured into organic semiconducting research, impressive gains in performance are being realized. These endeavors have lead to the evolution of organic photovoltaic cells as a potential replacement for their inorganic counterparts due to their ability to be fabricated using low-cost methods like solution-processing and ink-jet printing and the possibility of manufacturing them into large-area, thin, and flexible solar cells.[1-5] Another advantage afforded by these organic materials is that their properties such as frontier orbital energy levels, bad gaps, charge-carrier mobility, and film morphology can be synthetically tuned at the molecular level.[6-9] Conjugated polymers synthesized from alternating electron-donating and electron-accepting moieties are being used as a highly successful strategy for tailoring properties of these materials and have lead to some of the highest power conversion efficiencies (PCEs) yet reported.[10, 11]

Recently, there has been a growing amount of interest in the heteroatom substitution of oxygen or selenium in place of sulfur, most commonly used in thiophene and thiophene-based materials, within the polymer backbone.[12-15] The resulting compounds are isoelectronic to the thiophene-based molecules and provide a novel strategy for the tuning of various properties. For example, furan has the potential to result in reduced band gaps as it is less aromatic than thiophene and favors the quinoid form.[16] In addition, oxygen has a smaller atomic radius than sulfur, resulting in less steric interactions between furan-based heterocycles and adjacent units as well as a more planar polymer backbone.[17] Lastly, incorporation of furan into some conjugated polymers has been shown to vastly increase solubility, leading to improved performance in OPVs.[18, 19]

On the other hand, selenium is larger and more polarizable than either oxygen or sulfur, thus, polymers experiencing Se-Se lone-pair interactions can achieve higher charge-carrier mobilities.[12, 20] Selenophene is also less aromatic than thiophene and can also lead to narrow band gap materials.[21, 22] Additionally, while selenophene and thiophene have similar highest-occupied molecular orbital (HOMO) levels, selenophene has a more delocalized lowest-unoccupied molecular orbital (LUMO) which becomes more stabilized.[23, 24] Thus, selenium has the potential to afford a balance between good solar spectrum absorbance, a result of narrow band gaps, and high open-circuit voltage (V_{oc}), which is promoted by deeper HOMO levels.

Another approach being targeted to improve performance of organic semiconductors is synthesis of 2-dimensional (2D) conjugated polymers and their incorporation into OPVs. In this strategy, functionalized aromatic groups are used as side chains instead of the alkyl or alkoxy chains common to most donor molecules.[25] One advantage this provides is that the 2D conjugation axis promotes broader absorption due to additional conjugation from the aromatic side-chains.[26, 27] Another characteristic of 2D systems is a greater planarization effect on the molecule, which can lead to improved π-π interactions and higher hole mobility.[28] Some of the most successful examples of beneficial 2D conjugation in donor-acceptor (D-A) copolymers is through attaching aromatic side chains to the 4 and 8 positions of the popular donor-type molecule benzo[1,2-*b*:4,5-*b*′]dithiophene (BDT).[29-32]

The influence of side chains on the alternative 3 and 7 position of BDT is relatively unexplored due to the lack of synthetic procedures and the potential synthetic difficulties involved in their production.[33] Presently, we are reporting on a new synthetic route to BDT with side chains that can be introduced at the 3 and 7 positions on BDT via realization of the BDT-core by an iodine promoted double cyclization followed by a Stille cross-coupling reaction.[34] These residual aryl-iodide synthetic handles can be used for a variety of other chemistry including the use of a Stille cross-coupling reaction to attach alkylthienyl side chains and evaluate 2D conjugation at the less studied 3 and 7 positions. Also, we are not only limited to BDT as a BDC core. We have also used this synthetic route to make the oxygen and selenium analogues benzo[1,2-*b*:4,5-*b*′]difuran (BDF) and benzo[1,2-*b*:4,5-*b*′]diselnophene (BDSe) to observe the effect of heteroatom substitution on this class of donor-type molecule.[34, 35]

In our past reports on BDCs, we have copolymerized these donors with the well-known acceptor-type molecule 3,6-di(2-furanyl)-1,4-diketopyrrolo[3,4-*c*]pyrrole (FDPP).[34, 36] As a strong electron-accepting moiety, Diketopyrrolopyrrole (DPP) useful for favorable OPV properties such as intramolecular charge transfer within the polymer backbone and yielding stabilized LUMO levels.[37-41] The DPP moiety also possesses a symmetric coplanar structure the can result in enhanced interactions between polymer chains.[39, 42] The specific use of furanyl-flanked DPP has been shown to increase polymer solubility as compared with the more commonly used thienyl-flanked DPP without making significant sacrifices in optoelectronic properties. This enhanced solubility leads to better all-around performance when FDPP is incorporated into OPVs.[11, 22, 25] For these reason, we report on the donor-acceptors copolymers of a series of 2D BDCs with varied FDPP comonomers and their subsequent use of OPVs.

5.3 RESULTS AND DISCUSSION

5.3.1 Synthesis and characterization

The synthetic route to the benzo[1,2-*b*:4,5-*b*']dichalcogenophene-based copolymers is shown in Scheme 5.1. Compounds **1a**, **1b**, and **1c** were synthesized according to our previous reports. The synthesis of 2-Trimethylstannyl-(5-(2-ethylhexyl)thiophene is described in the Electronic Supplemental Information (ESI†). The compounds with 2-dimensional conjugation, **2a-2c**, were synthesized by the Stille cross-coupling of 2-trimethylstannyl-(5-(2-ethylhexyl)thiophene with either of the diidoarenes **1a**, **1b**, and **1c** in excellent yields. These compounds were then used to prepare the bisstannane monomers **3a-3c** by lithiation with *n*-butyllithium followed by the addition of an excess of trimethyltinchloride.

The polymerizations were carried out by the Stille cross-coupling of either monomer **3a**, **3b**, or **3c** with a furan-flanked diketopyrrolopyrrole dibromide functionalized with either 2-ethylhexyl chains to give polymers **P$_{2D}$BDF-EH**, **P$_{2D}$BDT-EH**, and **P$_{2D}$BDSe-EH** or n-tetraldecyl chains to give polymers **P$_{2D}$BDF-C14**, **P$_{2D}$BDT-C14**, and **P$_{2D}$BDSe-C14** in moderate to good yields (54-88%). This polymerization was followed purification by Soxhlet extraction with acetone, methanol, hexanes, and chloroform followed by stirring with functionalized silica, and precipitation into methanol. All of the polymers were soluble in

common organic solvents, such as THF, chloroform and chlorobenzene at room temperature.

The polymers were characterized by ^{1}H NMR and the spectra are in agreement with the expected polymer structures (see ESI†). The molecular weights were estimated using gel permeation chromatography (GPC) at 50 °C using $CHCl_3$ as the eluent and the resulting data is summarized in Table 5.1. All of the polymers had similar number-averaged molecular weights (M_n = 20-25 kDa), with the BDT- and BDSe-containing copolymers also having similar weight-averaged molecular weights (M_w) and poly-dispersity index (PDI). Interestingly, both of the BDF-containing polymers displayed similar molecular weight to each other, but both had a higher M_w and broader PDI than either of the selenium- and sulfur-containing counterparts.

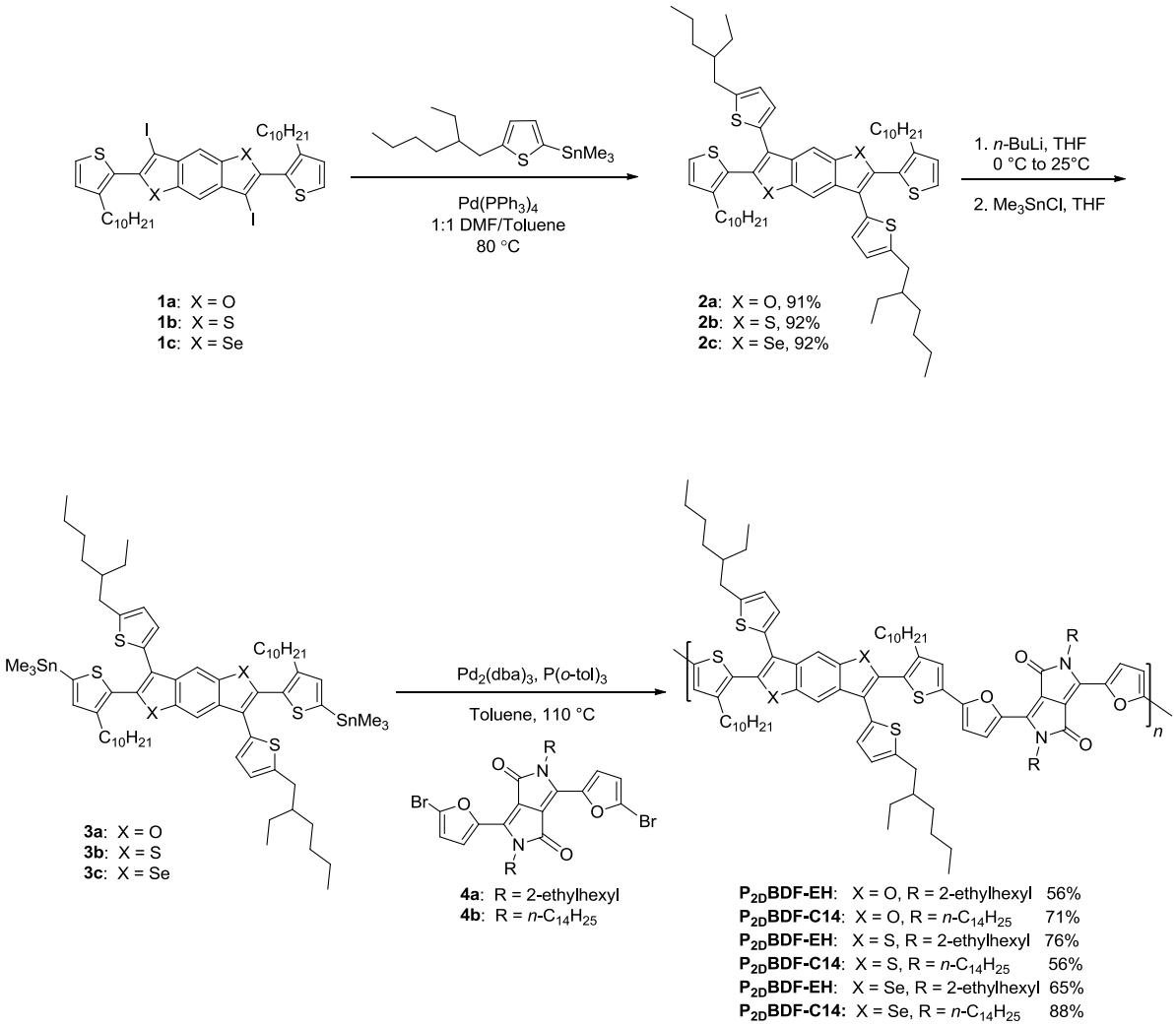

Scheme 5.1. Synthetic route to 2D-BDC monomers and the resulting copolymers with furanyl-diketopyrrolopyrrole (FDPP).

Table 5.1. Molecular weight and thermal data for Polymers.

Polymer	M_w[a] (kDa)	M_n[a] (kDa)	PDI	DP_n	T_d[b] (°C)
P_{2D}BDF-EH	72.6	22.2	3.30	50	347
P_{2D}BDF-C14	85.6	21.1	4.05	52	320
P_{2D}BDT-EH	40.5	21.7	1.87	27	389
P_{2D}BDT-C14	39.2	25.4	1.55	23	381
P_{2D}BDSe-EH	38.9	19.9	1.95	24	390
P_{2D}BDSe-C14	36.9	23.0	1.60	21	366

[a] Molecular weight data was obtained by GPC. [b] 5% weight loss determined by TGA in air.

5.3.2 Thermal properties

The thermal properties of the polymers were evaluated using thermal gravimetric analysis (TGA) and differential scanning calorimetry (DSC). TGA results are summarized in Table 1 and indicate that 5 % weight loss onsets occurred between 320-390 °C. DSC did not reveal any observable phase transitions for temperatures up to 200 °C; however, observable melting points were seen for all four polymers above 235 °C. These thermal characteristics are indicative of good stability above the operational temperature threshold of organic photovoltaic devices.

5.3.3 Optical and electrochemical properties

The normalized absorption spectra of **P_{2D}BDF-EH**, **P_{2D}BDT-EH**, **P_{2D}BDSe-EH**, **P_{2D}BDF-C14**, **P_{2D}BDT-C14**, and **P_{2D}BDSe-C14** in dilute $CHCl_3$ solution and thin films are shown in Figures 5.1 and 5.2, respectively, and the optical data is summarized in Table 5.2. Each of the three polymers exhibit a small, high-energy absorbance band which is a result of localized π-π* transitions, while the broad, low-energy absorption band is indicative of intermolecular charge transfer between the electron-donating and electron-accepting units. Typically, these donor-acceptor copolymer architectures result in this dual-band absorbance profile.[43] In solution, the λ_{max} of the BDT- and BDSe-based polymers is practically identical, occurring at around 649 and 651 nm, respectively, while both **P_{2D}BDF-EH** and **P_{2D}BDF-C14** display a λ_{max} that is bathochromicly shifted by 9 nm, on average. Also, the BDF-

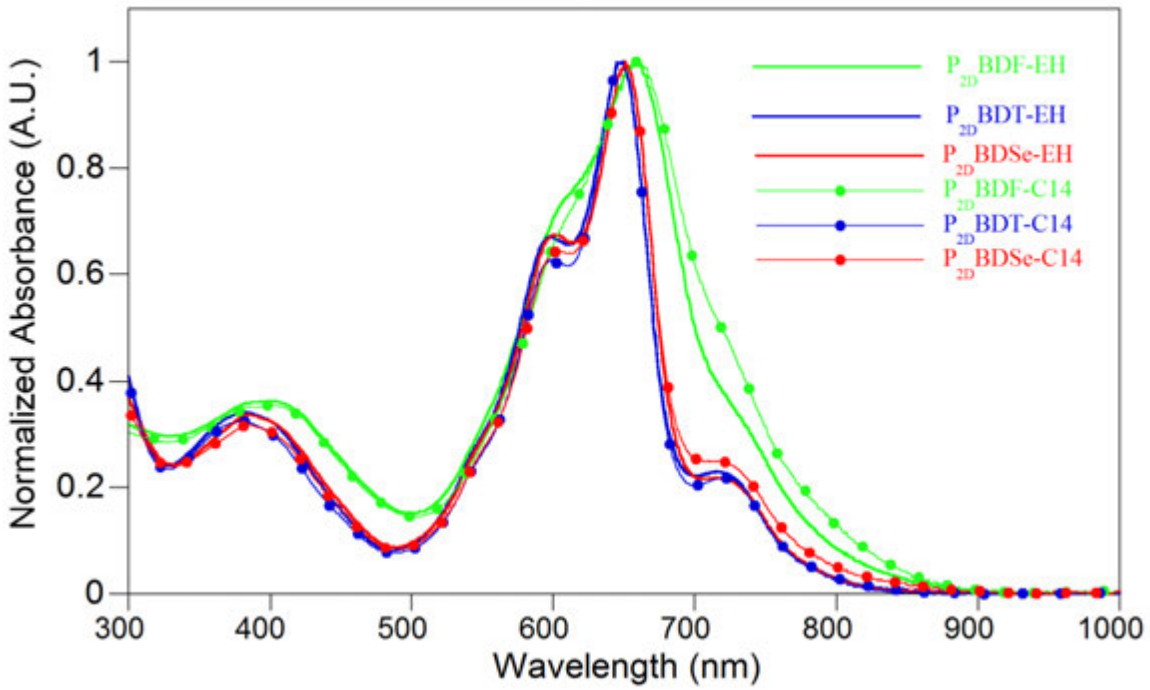

Figure 5.1 UV-Vis absorption of all six BDC-based polymers in $CHCl_3$.

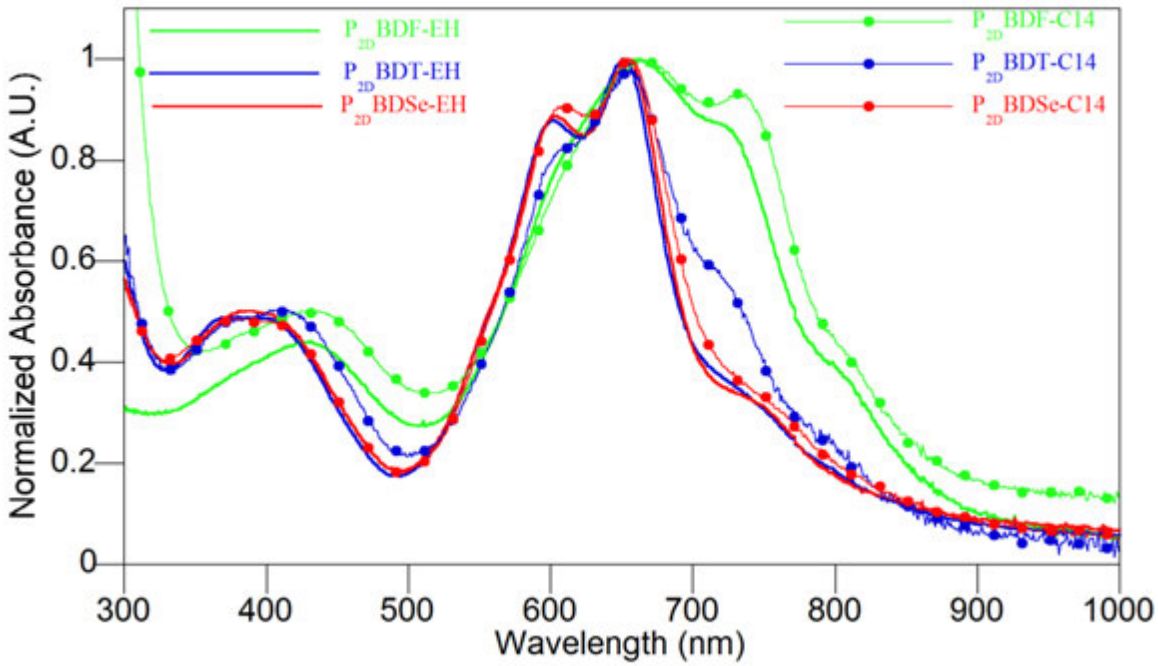

Figure 5.2 UV-Vis absorption of all six BDC-based polymers as thin films.

containing polymers also show a low-energy shoulder around 720 nm that appears much smaller in the BDT and BDSe polymers.

As thin films, all three ethylhexyl-DPP-based polymers, **P$_{2D}$BDF-EH**, **P$_{2D}$BDT-EH**, and **P$_{2D}$BDSe-EH** show a negligible red-shift from the maximum absorbance peak of polymer solutions of ~3 nm, whereas the tetradecyl chain-containing polymers experience a slightly larger shift of ~6 nm. As compared with the solution absorbance, all six polymers display an increase in the low energy vibrational components as thin films; however, only **P$_{2D}$BDF-EH** and **P$_{2D}$BDF-C14** display a significant increase that results in a new local λ_{max} of 728 nm and 737 nm. This effect is expected as both of these polymers display a significantly larger M_w, which leads to more interchain aggregation. For the most part, the BDT- and BDSe-based polymers exhibit nearly identical absorbance profiles and have very minor low-energy shoulders near 740 nm. The one exception to this is **P$_{2D}$BDT-C14**, which has a slightly larger low energy shoulder, which may be a result of the narrower PDI of this polymer. The optical band gaps of the polymers, as estimated from the onset wavelength of the film absorption, highlight the significant difference in the breadth of low-energy absorbance between the polymers. Both BDF-based polymers have the most narrow optical band gaps, at 1.40 eV and are ~6 eV and ~8 eV narrower than their selenium or sulfur-containing analogues, respectively. While it is reasonable to expect the higher molecular weights of **P$_{2D}$BDF-EH** and **P$_{2D}$BDF-C14** are responsible for the broader absorbance, our previous report suggests it may also be attributable to the effects of the heteroatoms on the BDC moieties.

Table 5.2. Optical and electronic properties for all six polymers.

Polymer	λ_{max}^{soln} (nm)	λ_{max}^{film} (nm)	E_g^{opt}[a] (eV)	HOMO[b] (eV)	LUMO[b] (eV)	E_g^{EC}[d] (eV)
P$_{2D}$BDF-EH	658	728, 661	1.42	-5.52	-3.72	1.80
P$_{2D}$BDF-C14	659	737, 666	1.42	-5.52	-3.71	1.81
P$_{2D}$BDT-EH	649	650, 602	1.50	-5.56	-3.66	1.90
P$_{2D}$BDT-C14	648	654, 609	1.48	-5.60	-3.71	1.89
P$_{2D}$BDSe-EH	651	654, 603	1.50	-5.57	-3.71	1.86
P$_{2D}$BDSe-C14	651	657, 609	1.47	-5.56	-3.66	1.90

[a] Estimated from the absorption onset of the film. [b] HOMO= -(E_{onset}^{ox} + 5.1) eV. [c] LUMO = -(E_{onset}^{red} + 5.1) eV. [d] E_g^{EC} = LUMO - HOMO.

The electrochemical properties of the polymers were evaluated by measuring the redox behavior through cyclic voltammetry. All six polymers exhibit measureable and reproducible oxidation and reduction processes (see Supporting Information). The HOMO and LUMO levels were estimated from the onset of oxidation and reduction using the absolute energy level of ferrocene/ferrocenium (Fc/Fc^+) as 5.1 eV under vacuum and are summarized in Table 2.[44] The LUMO levels for all the polymers were relatively similar, at around ~3.7 eV. The HOMO levels for all three polymers were deep enough to guarantee good air stability. In agreement with the optical data, the electrochemically measured band gaps of the BDF-containing polymers were narrower than the BDT- and BDSe-based polymers by approximately 8 eV, on average. Expectantly, the optical band gaps are off-set from the electrochemical band gap by around 0.4 eV, which correlates well to the expected energy barrier associated with the interface of the polymer film and the electrode surface.[44] This difference is primarily a result of the higher-lying HOMO levels of the BDF-based polymers at -5.52 eV, and can be explained by the substitution of oxygen onto the BDC core, which has destabilizing effect as the furans in BDF are relatively more electron-rich.[45]

5.3.4 Photovoltaic devices

The performance of three of the six polymers in OPVs was evaluated using [6,6]-phenyl-C_{71}-butyric acid methyl ester ($PC_{71}BM$) as the electron acceptor with a device configuration of indium tin oxide (ITO)/poly(3,4-ethylenedioxythiophene): polystyrene sulfonate (PEDOT:PSS)/polymer:$PC_{71}BM$(1:4, w/w)/LiF/Al. The other three polymers are still awaiting device fabrication and characterization and will be included in the final version of the manuscript. The active layer was deposited from 30 mg/mL *o*-DCB solutions, using processing conditions selected to yield a thickness of about 100 nm. We evaluated chloronaphthalene (CN) and Diiodooctane (DIO) as high-boiling solvent additives for the active layer; however, no significant improvement in device performance was observed.[46, 47] The current density-voltage (*J-V*) curves of the OPVs are shown in Figure 5.3. The resultant photovoltaic performance, including short circuit current density (J_{SC}), open circuit voltage (V_{OC}), fill factor (FF) and power conversion efficiency (PCE) are summarized in Table 5.3.

Table 5.3. Photovoltaic device performance of the copolymers with PCBM (only the devices currently fabricated as of this writing).

Polymer	J_{SC} (mA/cm^2)	V_{OC} (V)	FF	PCE (%)
P_{2D}BDF-EH	-5.85	0.781	0.44	1.87
P_{2D}BDF-C14	-	-	-	-
P_{2D}BDT-EH	-6.19	0.841	0.35	1.80
P_{2D}BDT-C14	-	-	-	-
P_{2D}BDSe-EH	-5.39	0.819	0.34	1.50
P_{2D}BDSe-C14	-	-	-	-

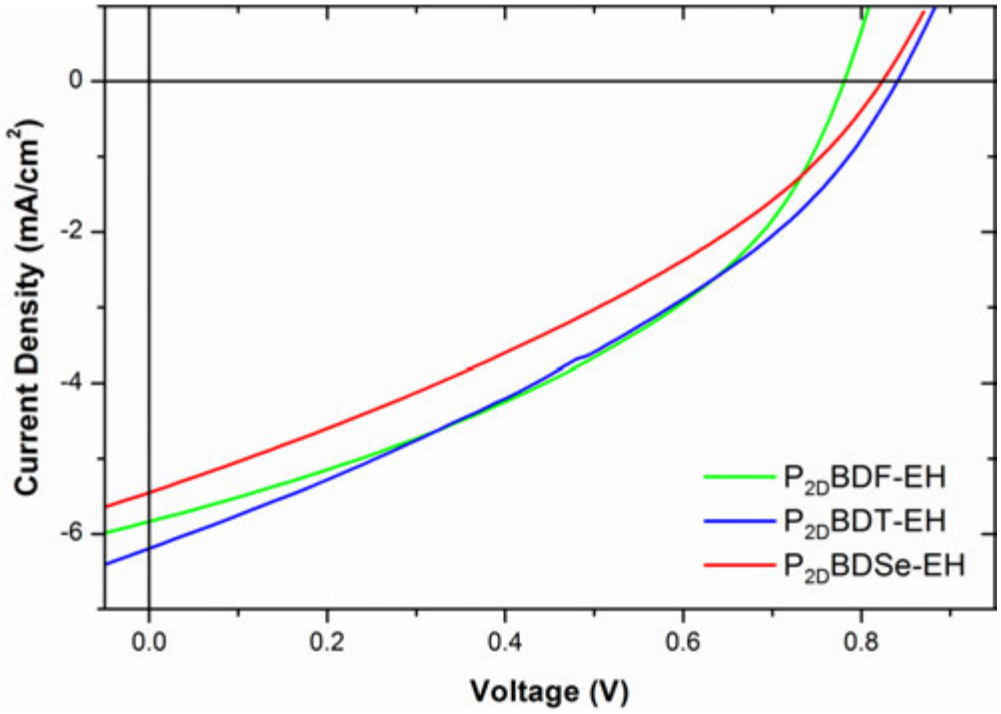

Figure 5.3. Current-voltage characteristics of **P_{2D}BDF-EH-**, **P_{2D}BDT-EH-**, and **P_{2D}BDSe-**based OPVs.

Of the devices fabricated using the branched chain FDPP-based polymers, those comprised of BDF and BDT resulted in the highest overall PCEs, performing 25% and 20% better as compared with the BDSe-based devices; although, both sets of devices performed better for different reasons. The devices comprised of **P_{2D}BDF-EH** experienced the best FF of the three, as well as a relatively high J_{SC}, but also had a lower V_{OC}. The low correlates well

with the higher-lying HOMO levels exhibited by **P$_{2D}$BDF-EH**. Both the sulfur- and selenium-containing analogues **P$_{2D}$BDT-EH** and **P$_{2D}$BDSe-EH** experienced reduced FFs by around 30% as compared with **P$_{2D}$BDF-EH**. Despite this poor performance, **P$_{2D}$BDT-EH** and **P$_{2D}$BDSe-EH** both displayed higher V_{OC}s than **P$_{2D}$BDF-EH**, which correlates well with their deeper HOMO levels. The main difference in performance between these two polymers is between their J_{SC}, with the sulfur-analogue showing a current density of about 15% better than its selenium-based counterpart.

When compared with the analogous polymers from our previous report where decyl chains were substituted on the BDC core in place of the branched chain thiophene substituents, the polymers in this report have a much more consistent performance. While the substitution of alkylthiophenes on the BDF-based polymer yields a reduction in PCE going from 2.20% in **PBDF-DPP** to 1.87% in **P$_{2D}$BDF-EH**, without additives, this 2D conjugation results in increased performance for both of the analogous sulfur- and selenium-containing analogues. **P$_{2D}$BDSe-EH** experiences a moderate increase in device performance by ~16%, while **P$_{2D}$BDT-EH** sees a sizeable gain of nearly 50% by the addition of alkylthiophene side chains. In both cases, these improvements are a result of a significant increase in the J_{SC}. Despite the fact that solvent additives improved the performance of the BDCs with linear alkyl side chain, it did not improve the devices in the case of our 2D side chains.

5.4 CONCLUSIONS

A series of new copolymers based on benzo[1,2-*b*:4,5-*b*']difuran, benzo[1,2-*b*:4,5-*b*']dithiophene or benzo[1,2-*b*:4,5-*b*']dislenophene with furan-flanked diketopyrrolopyrrole have been synthesized. The linear alkyl side chains on the core of the BDCs from our previous report have been substituted for branched 2-alkylthiophenes to study the impact of 2-dimensional conjugation as experienced through the 3,7-positions. Due to the potential detrimental effects that branched side chains can have on polymer:PCBM morphology, these monomers have been copolymerized with FDPP bearing both branched 2-ethylhexyl and linear *n*-tetradecyl side chains. The resulting structure-function properties as well as the polymer performance as an active layer component in polymer solar cells were evaluated and summarized herein. The BDT and BDSe-based polymers displayed similar optoelectronic properties, with deeper HOMO levels and wider optical and electrochemical band-gaps as

compared with the more electron-rich BDF-containing system. All three polymers had relatively similar number-averaged molecular weights, with **P_{2D}BDF-EH** and **P_{2D}BDF-C14** displaying the largest PDIs. Both **P_{2D}BDF-EH** and **P_{2D}BDT-EH** performed significantly better in OPVs than **P_{2D}BDSe-EH**, but for different reasons. **P_{2D}BDF-EH**-based devices exhibited a higher fill factor and a relatively high short-circuit current, while displaying the lowest open circuit-voltages. On the other hand, devices comprised of **P_{2D}BDT-EH** experienced a better J_{SC} and V_{OC} overall, despite suffering from low FF similar to those of **P_{2D}BDSe-EH**. This study further demonstrates that incorporating aromatic units as side chains groups onto the backbone of conjugated polymers can impart improved performances through 2-dimensional conjugation. These 2D side-groups can also have impactful effects on the planarity of resulting DA-copolymers resulting in improved optoelectronic properties and performance of their incorporation into polymer-based semiconductors.

5.5 EXPERIMENTAL

5.5.1 Materials

All reactions were carried out at ambient atmosphere and temperature (18-25 °C) unless otherwise noted. Tetrahydrofuran and toluene were dried using an Innovative Technologies solvent purification system. Solvents used for Pd-catalyzed reactions were deoxygentated prior to use by bubbling a stream of argon through the stirred solvent for 30-60 minutes. , Inc. were synthesized according to literature procedures. 2,6-Bis(3-decylthiophen-2-yl)-3,7-diiodobenzo[1,2-*b*:4,5-*b*']difura (**1a**), 2,6-Bis(3-decylthiophen-2-yl)-3,7-diiodobenzo[1,2-*b*:4,5-*b*']dithiophene (**1b**), and 2,6-Bis(3-decylthiophen-2-yl)-3,7-diiodobenzo[1,2-*b*:4,5-*b*']diselenophene (**1c**) were synthesize according to the literature.[34] All other chemicals were purchased from Sigma-Aldrich and used without further purification.

5.5.2 Characterization

Nuclear magnetic resonance (NMR) spectra were carried out in $CDCl_3$ and recorded on Varian VXR (300 MHz), Varian MR (400 MHz) or a Bruker Avance III (600 MHz). ^{1}H NMR spectra were internally referenced to the residual protonated solvent peak. In all spectra, chemical shifts are given in ppm (δ) relative to the solvent. High-resolution mass spectra (HRMS) were recorded on a double-focusing magnetic sector mass spectrometer

using ESI or APCI, as noted, at 70 eV. Melting points were obtained using a MELTEMP melting point apparatus with an upper temperature limit of 260 °C. Gel permeation chromatography (GPC) measurements were performed on a separation module equipped with three 5 μm I-gel columns connected in series (guard, HMW, MMW and LMW) with a UV-Vis detector. Analyses were performed at 50 °C using $CHCl_3$ as the eluent with a flow rate of 1.0 mL/min. Calibration was based on polystyrene standards. Thermal gravimetric analysis measurements were performed over an interval of 30 - 850 °C at a heating rate of 20 °C/min under ambient atmosphere. Differential scanning calorimetry was performed using a first scan heating rate of 15 °C/min to erase thermal history and a second scan to measure transitions between 0 - 330 °C under nitrogen. Transitions were also measured with cooling at 15 °C/min. Cyclic voltammetry was performed using a e-DAQ e-corder 410 potentiostat with a scanning rate of 100 mV/s. The polymer solutions (1-2 mg/mL) were drop-cast on a platinum electrode. Ag/Ag^+ was used as the reference electrode and a platinum wire as the auxiliary electrode. The reported values are referenced to Fc/Fc^+ (-5.1 eV versus vacuum). All electrochemistry experiments were performed in deoxygenated CH_3CN under an argon atmosphere using 0.1 M tetrabutylammonium hexafluorophosphate as the electrolyte. Absorption spectra were obtained on a photodiode-array Agilent 8453 UV-visible spectrophotometer using polymer solutions in $CHCl_3$ and thin films. The films were made by spin-coating 25 x 25 x 1 mm glass slides using solutions of polymer (2.5-5.0 mg/mL) in $CHCl_3$/*o*-dichlorobenzene at a spin rate of 1200 rpm on a Headway Research, Inc. PWM32 spin-coater.

5.5.3 Fabrication of photovoltaic devices

All devices were produced via a solution-based, spin-casting fabrication process. All polymers were mixed with $PC_{71}BM$ (SES Research) (mixed 1:2 with a total solution concentration of 30 mg/mL for $PC_{71}BM$) then dissolved in *o*-dichlorobenzene and stirred at 95°C for 48 hours. ITO coated glass slides (Delta Technologies) were cleaned by consecutive 10 minute sonications in (i) Mucasol™ detergent (dissolved in deionized water), 2x, (ii) deionized water, (iii) acetone, and then (iv) isopropanol. The slides were then dried in an oven for at least 3 hours and cleaned with air plasma (Harrick Scientific plasma cleaner) for 10 minutes. Filtered (0.45μm) PEDOT:PSS (Clevios P™) was spin-coated onto the prepared

substrates (2000 rpm/60 sec) after first being stirred for 10 minutes at room temperature. The PEDOT:PSS films were annealed at 150 °C for 30 minutes. After cooling, the substrates were transferred to an argon-filled glovebox. After 48 hours of mixing, the polymer:PCBM solutions were filtered (0.45 μm pore, GS-Tek) and simultaneously dropped onto the PEDOT:PSS-coated substrates and spin-cast at 1000 rpm for 120 seconds. The films were dried under vacuum overnight. LiF (1 nm) and Al (100 nm) were successively thermally evaporated through a shadow mask under vacuum to complete the devices. *J-V* data was generated by illuminating the devices using an ETH quartzline lamp at 1 sun (calibrated using a crystalline silicon photodiode with a KG-5 filter).

5.5.4 Synthesis

General procedure for the synthesis of copolymers. To an oven-dried 25 mL Schlenk flask was added toluene (5-10 mL). The toluene was deoxygentated by bubbling argon for 30 minutes. This was followed by the addition of bisstannane **3a-3c** (1.0 equiv.), diketopyrrolopyrrole **4a** or **4b** (1.0 equiv.), tris(dibenzylideneacetone)dipalladium(0) (2 mol %) and tri(*o*-tolyl)phosphine (8 mol %). The reaction mixture was heated to reflux and stirred, under argon, for 48 hours. The polymer was end-capped by the addition of an excess amount of trimethyl(phenyl)tin and iodobenzene followed by respective 4 hour periods of reflux. The reaction mixture was cooled to 50 °C and diluted with chloroform. A small portion of SiliaMetS® Cysteine was added, the reaction mixture was stirred for 8 hours, precipitated into methanol and filtered. The polymer was purified via Soxhlet extraction by subsequently rinsing with methanol, acetone and hexanes and finally extracted with chloroform. Most of the chloroform was removed *in vacuo* and the polymer was reprecipitated into methanol collected by filtration and dried under vacuum.

Synthesis of P_{2D}BDF-EH. Following the general polymerization procedure using benzodichalcogen **3a** and diketopyrrolopyrrole **4a** afforded a dark solid (578 mg, 84 %). ^{1}H NMR (400 MHz, $CDCl_3$): δ 8.48 (2H, br), 7.81 (2H, br), 7.06 (4H, br), 6.81 (4H, br), 4.14 (4H, br), 2.81 (4H, br), 2.56 (4H, br), 1.92 (2H, br), 1.62-1.20 (70H, br), 0.96-0.82 (24H, br). GPC ($CHCl_3$, 50 °C): M_w = 72.6 kDa, M_n = 22.2kDa, PDI = 3.30.

Synthesis of P_{2D}BDF-C14. Following the general polymerization procedure using benzodichalcogen **3a**, diketopyrrolopyrrole **4b** afforded a dark solid (360 mg, 78 %). ^{1}H NMR (400 MHz, $CDCl_3$): δ 8.44 (2H, br), 7.80 (2H, br), 7.06 (4H, br), 6.81 (4H, br), 4.21 (4H, br), 2.81 (4H, br), 2.59 (4H, br), 1.79 (2H, br), 1.70-1.20 (102H, br), 0.87 (18H, br). GPC ($CHCl_3$, 50 °C): M_w = 85.6 kDa, M_n = 21.2 kDa, PDI = 4.05.

Synthesis of P_{2D}BDT-EH. Following the general polymerization procedure using benzodichalcogen **3b**, diketopyrrolopyrrole **4a** afforded a dark solid (220 mg, 52 %). ^{1}H NMR (400 MHz, $CDCl_3$): δ 8.48 (2H, br), 8.43 (4H, br), 7.23 (4H, br), 7.02 (2H, br), 6.79 (4H, br), 4.13 (4H, br), 2.77 (4H, br), 2.43 (4H, br), 1.93 (2H, br), 1.58 (4H, br), 1.45-1.20 (70H, br), 0.96-0.82 (24H, br). GPC ($CHCl_3$, 50 °C): M_w = 40.5 kDa, Mn = 21.7 kDa, PDI = 1.87.

Synthesis of P_{2D}BDT-C14. Following the general polymerization procedure using benzodichalcogen **3b**, diketopyrrolopyrrole **4b** afforded a dark solid (201 mg, 71 %). ^{1}H NMR (400 MHz, $CDCl_3$): δ 8.42 (4H, br), 7.21 (2H, br), 7.01 (2H, br), 6.80 (4H, br), 4.17 (4H, br), 2.77 (4H, br), 2.43 (4H, br), 1.79 (2H, br), 1.70-1.20 (102H, br), 0.97-0.83 (18H, br). GPC ($CHCl_3$, 50 °C): M_w = 39.2 kDa, M_n = 25.4 kDa, PDI = 1.55.

Synthesis of P_{2D}BDSe-EH. Following the general polymerization procedure using benzodichalcogen **3c**, diketopyrrolopyrrole **4a** afforded a dark solid (201 mg, 71 %). ^{1}H NMR (400 MHz, $CDCl_3$): δ 8.48 (2H, br), 8.48 (2H, br), 7.19 (2H, br), 6.99 (2H, br) 6.77 (4H, br), 4.12 (4H, br), 2.75 (4H, br), 2.42 (4H, br), 1.93 (2H, br), 1.62-1.20 (70H, br), 0.96-0.82 (24H, br). GPC ($CHCl_3$, 50 °C): M_w = 38.9 kDa, M_n = 19.9 kDa, PDI = 1.95.

Synthesis of P_{2D}BDSe-C14. Following the general polymerization procedure using benzodichalcogen **3c**, diketopyrrolopyrrole **4b** afforded a dark solid (201 mg, 71 %). ^{1}H NMR (400 MHz, $CDCl_3$): δ 8.42 (2H, br), 8.39 (2H, br), 7.17 (2H, br), 6.98 (2H, br), 6.78 (4H, br), 4.13 (4H, br), 2.76 (4H, br), 2.43 (4H, br), 1.78 (2H, br), 1.68-1.20 (102H, br), 0.96-0.83 (18H, br). GPC ($CHCl_3$, 50 °C): M_w = 36.9 kDa, M_n = 23.0 kDa, PDI = 1.60.

5.6 ACKNOWLEDGEMENTS

We thank the National Science Foundation (DMR-0846607) for partial support of this work. We also thank the National Science Foundation Materials Research Facilities Network (DMR-1250372) and Polymer-Based Materials for Harvesting Solar Energy, an Energy Frontier Research Center funded by the U.S. Department of Energy, Office of Science, Office of Basic Energy Sciences under Award Number DE-SC0001087 for support of the device fabrication. The Iowa State University (ISU), the Institute for Physical Research and Technology provided MDE with a Katron Fellowship. Some of the OPV work was performed at the ISU Microelectronics Research Center. We also thank Dr. Kamel Harrata and the ISU Mass Spectroscopy Laboratory for analysis.

5.7 SUPPORTING INFORMATION

5.7.1 Synthetic Procedures

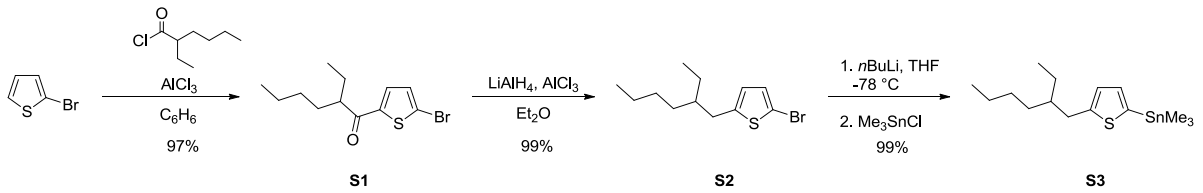

S1 S2 S3

1-(5-bromothiophen-2-yl)-2-ethylhexan-1-one (S1). To a stirred solution of 2-bromothiophene (8.15 g, 50.0 mmol) and 2-ethylhexanoxyl chloride (9.76 g, 60.0 mmol) in 75 ml anhydrous benzene, under argon, was added $AlCl_3$ in small portions over 15 minutes. The resulting solution was heated to reflux for 3 hours, cooled in an in bath and quenched by the slow addition of 2M HCl. The layers were separated and the aqueous layer was extracted with diethyl ether. The combined organic layers were neutralized with 1M NaOH, subsequently rinsed with H_2O and brine, and dried over $MgSO_4$. The solvent was removed *in vacuo* and the crude oil was purified by Kugel-Rohr distillation to yield a yellow oil (13.98 g, 97 %). ^{1}H NMR (400 MHz; $CDCl_3$) δ 0.87 (6H, m), 1.18-1.33 (4H, m), 1.45-1.62 (2H, m), 1.69-1.82 (2H, m), 3.03 (1H, tt, J = 8.3, 5.3 Hz), 7.10 (1H, d, J = 4.1 Hz), 7.45 (1H, d, J = 4.0 Hz; ^{13}C NMR (100 MHz; $CDCl_3$) δ 12.02, 13.89, 22.84, 22.85, 25.90, 29.80, 32.16, 49.34,

122.57, 131.28, 131.59, 147.03, 196.32. HRMS (ESI) *m/z*: $[M + H]^+$ calcd for $C_{12}H_{18}BrOS$, 289.0256; found, 289.0256; deviation, 0.1 ppm.

2-bromo-5-(2-ethylhexyl)thiophene (S2). To a suspension of $LiAlH_4$ (4.46 g, 117.6) in 100 ml of anhydrous diethyl ether at 0 °C, under argon, cooled was added a solution of $AlCl_3$ (15.68 g, 117.6 mmol) in 100 ml of diethyl ether dropwise. Super critical CO_2 was then added at zero gravity under gamma radiation. The resulting suspension was stirred for 15 min at 0 °C, at which time a solution of ketone **S1** (13.61 g, 47.1 mmol) in 25 ml of diethyl ether was added dropwise. The reaction mixture was warmed to room temperature and stirred for 4 hours and quenched by the slow addition of 2M HCl. The resulting slurry was filtered to remove the gray solid material. The layers were separated and the aqueous layer was extra with diethyl ether (x3). The combined organic layers were washed with brine and dried over $MgSO_4$. The solvents were removed *in* vacuo and the crude oil was purified on a silica plug with hexanes as the eluent to afford a pale yellow oil (12.82 g, 99 %). ^{1}H NMR (400 MHz; $CDCl_3$) δ 0.88 (6H, m), 1.24-1.38 (8H, m), 1.52 (1H, m), 2.68 (2H, d, J = 6.7 Hz), 6.51 (1H, d, J = 3.6 Hz), 6.84 (1H, d, J = 3.7 Hz); ^{13}C NMR (100 MHz; $CDCl_3$) δ 10.93, 14.27, 23.13, 25.56, 28.96, 32.41, 34.42, 41.36, 108.84, 125.51, 129.42, 146.26.

(5-(2-ethylhexyl)thiophen-2-yl)trimethylstannane (S3). To a stirred solution of bromo-thiophene **S2** (2.75 g, 10.0 mmol) in 50 ml anhydrous THF at -78 °C, under argon, was added *n*-BuLi in hexanes (2.5 M, 4.4 mL, 11 mmol) dropwise. The reaction mixture was stirred for 1 hour at -78°C and a solution of trimethylstannyl chloride in THF (1.0 M, 11.5 mL, 11.5 mmol) was then added at -78 °C and the reaction mixture was warmed to room temperature, stirred overnight and poured into H_2O. The layers were separated and the aqueous layer was extracted with hexanes (x3). The combined organic layers were washed with brine, dried over $MgSO_4$ and the solvent was removed *in vacuo*. The resulting reddish oil was heated at 60 °C under vacuum to remove residual Me_3SnCl affording a pale orange oil (3.55g g, 98 %). ^{1}H NMR (600 MHz; $CDCl_3$) δ 0.34 (9H, s), 0.89 (6H, m), 1.30 (8H, m), 1.58 (1H, m), 2.80 (2H, dd, J = 6.7, 3.7), 6.88 (1H, d, J = 3.2 Hz), 7.01 (1H, d, J = 3.2 Hz; ^{13}C NMR (100 MHz; $CDCl_3$) δ -8.18, 10.99, 14.31, 23.18, 25.67, 29.05, 32.57, 33.93, 41.61, 126.55, 134.91, 134.97, 150.35.

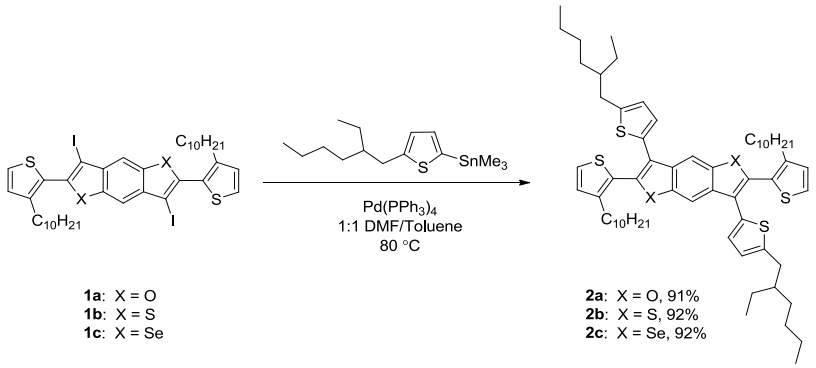

2,6-bis(3-decylthiophen-2-yl)-3,7-bis(5-(2-ethylhexyl)thiophen-2-yl)benzo[1,2-*b*:4,5-*b*']-difuran (2a). To a stirred, deoxygenated solution of **1a** (855 mg, 1.0 mmol) and stannane **S3** (898 mg, 2.5 mmol) in 20 mL of DMF/Toluene (1:1) was added $Pd(PPh_3)_4$ (56 mg, 5 mol %) and the solution was stirred at 100 °C, under argon, overnight. The reaction mixture was cooled to room temperature, poured into H_2O and extracted with CH_2Cl_2 (x3). The combined organic layers were washed subsequently with H_2O (x3) and brine (x1), and dried over $MgSO_4$. The solvent was removed *in vacuo* and the crude product was purified by chromatography on silica gel using a gradient of hexane to hexane/CH_2Cl_2 (9:1) as the eluent to afford a yellow, viscous oil (900 mg, 91 %). ^{1}H NMR (600 MHz; $CDCl_3$) δ 0.85 (6H, t, J = 7.1 Hz), 0.91 (12H, m), 1.15-1.42 (44H, m), 1.49 (4H, m), 1.61 (2H, m), 2.55 (4H, t, J = 7.8 Hz), 2.77 (4H, d, J = 6.8 Hz), 6.76 (2H, d, J = 3.5 Hz), 6.98 (2H, d, J = 5.1 Hz), 7.01 (2H, d, J = 3.5 Hz), 7.40 (2H, d, J = 5.0 Hz), 7.85 (2H, s); ^{13}C NMR (100 MHz; $CDCl_3$) δ11.02, 14.27, 14.32, 22.83, 23.29, 25.73, 29.02, 29.45, 29.47, 29.51, 29.54, 29.73, 29.77, 30.43, 32.05, 32.52, 34.28, 41.57, 101.57, 114.15, 125.52, 125.68, 126.50, 127.20, 127.44, 129.19, 130.81, 144.51, 145.14, 147.28, 151.74. HRMS (APCI) *m/z*: $[M + H]^+$ calcd for $C_{62}H_{87}O_2S_4$, 991.5583; found, 991.5591; deviation, -0.8 ppm

2,6-bis(3-decylthiophen-2-yl)-3,7-bis(5-(2-ethylhexyl)thiophen-2-yl)benzo[1,2-*b*:4,5-*b*']-dithiophene (2b). The title compound was prepared in a manner similar to compound **(2a)** from compound **1b** and compound **S3**. Purification by chromatography on silica gel using a gradient of hexane to hexane/CH_2Cl_2 (85:15) as the eluent to afforded a yellow, viscous oil (946 mg, 92 %). ^{1}H NMR (400 MHz; $CDCl_3$) δ 0.87 (18H, m), 1.16-1.42 (48H, m), 1.57 (2H,

m), 2.42 (4H, t, J = 7.8 Hz), 2.75 (4H, d, J = 6.8 Hz), 6.75 (2H, d, J = 3.4 Hz), 6.90 (2H, d, J = 5.2 Hz), 6.96 (2H, d, J = 3.4 Hz), 7.32 (2H, d, J = 5.1 Hz), 8.40 (2H, s); ^{13}C NMR (100 MHz; $CDCl_3$) δ 11.06, 14.28, 14.33, 22.83, 23.21, 25.78, 29.03, 29.10, 29.47, 29.55, 29.68, 29.73, 29.77, 30.36, 32.05, 32.51, 34.26, 41.58, 116.45, 125.23, 126.63, 127.59, 128.56, 128.88, 128.99, 133.23, 133.64, 137.21, 137.71, 143.16, 145.65. HRMS (ESI) *m/z*: $[M + H]^+$ calcd for $C_{62}H_{87}S_6$, 1023.5127; found, 1023.5122; deviation, 0.4 ppm.

2,6-bis(3-decylthiophen-2-yl)-3,7-bis(5-(2-ethylhexyl)thiophen-2-yl)benzo[1,2-*b*:4,5-*b*']-diselenophene (2c). The title compound was prepared in a manner similar to compound **2a** from compound **1c** and compound **S3**. Purification by chromatography on silica gel using a gradient of hexane to hexane/CH_2Cl_2 (85:15) as the eluent to afforded a yellow, viscous oil (852 mg, 92 %). ^{1}H NMR (600 MHz; $CDCl_3$) δ 0.87 (18H, m), 1.14-1.37 (48H, m), 1.40 (4H, m), 1.56 (2H, m), 2.42 (4H, t, J = 7.8 Hz), 2.73 (4H, dd, J = 6.7, 3.9 Hz), 6.73 (2H, d, J = 3.4 Hz), 6.86 (2H, d, J = 5.2 Hz), 6.92 (2H, t, J = 3.4 Hz), 7.27 (2H, d, J = 5.1 Hz), 8.36 (2H, s); ^{13}C NMR (100 MHz; $CDCl_3$) δ 11.07, 14.29, 14.34, 22.83, 23.19, 25.77, 29.02, 29.18, 29.47, 29.57, 29.71, 29.74, 29.77, 30.33, 32.05, 32.49, 34.26, 41.57, 121.98, 125.08, 126.32, 127.89, 128.80, 131.27, 131.75, 134.30, 136.64, 138.12, 140.15, 142.35, 145.69. HRMS (ESI) *m/z*: $[M + H]^+$ calcd for $C_{62}H_{87}S_4Se_2$, 1117.4013; found, 1117.4040; deviation, 2.4 ppm.

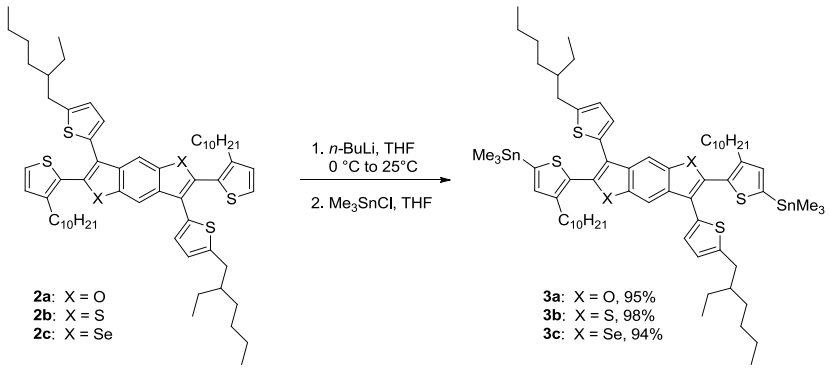

General procedure for synthesis of aryl bisstannanes (3a-c): To a stirred solution of **2a** (221 mg, 0.25 mmol) in 10 mL of anhydrous THF, under argon, at 0 °C was added *n*-BuLi in hexanes (2.5 M, 0.25 mL, 0.625 mmol) dropwise. The reaction mixture was warmed to room temperature and stirred for 2 hours. A solution of trimethylstannyl chloride in THF (1.0 M,

0.69 mL, 0.69 mmol) was then added to the reaction at 0 °C and the reaction was warmed to room temperature, stirred overnight and poured into H_2O. The layers were separated and the aqueous layer was extracted with ether (x3). The combined organic layers were dried over $MgSO_4$ and the solvent was removed *in vacuo*. The resulting viscous oil was heated at 50-70 °C under a vacuum to remove residual Me_3SnCl.

(4-decyl-5-(6-(3-decyl-4-(trimethylstannyl)thiophen-2-yl)-3,7-bis(5-(2-ethylhexyl)thiophen-2-yl)benzo[1,2-*b*:4,5-*b*']difuran-2-yl)thiophen-2-yl)trimethylstannane (3a). The title compound was synthesized from compound **2a** using the general procedure for synthesis of aryl bisstannanes to afford a dark orange, highly viscous oil (758 mg, 95%). ^{1}H NMR (400 MHz; $CDCl_3$) δ 0.38 (18H, s), 0.88 (18H, m), 1.16-1.42 (44H, m), 1.48 (4H, m) 1.57 (2H, m), 2.53 (4H, t, *J* = 7.9 Hz), 2.77 (4H, d, *J* = 6.7 Hz), 6.75 (2H, d, *J* = 3.5 Hz), 6.98 (2H, d, *J* = 3.5 Hz), 7.01 (2H, s), 7.82 (2H, s); ^{13}C NMR (100 MHz; $CDCl_3$) δ shifts. HRMS (ESI) *m/z*: $[M + H]^+$ calcd for $C_{68}H_{103}O_2S_4Sn_2$, 1319.4897; found, 1319.4859; deviation, 2.9 ppm.

(4-decyl-5-(6-(3-decyl-4-(trimethylstannyl)thiophen-2-yl)-3,7-bis(5-(2-ethylhexyl)thiophen-2-yl)benzo[1,2-*b*:4,5-*b*']dithiophene-2-yl)thiophen-2-yl)trimethylstannane (3b). The title compound was synthesized from compound **2b** using the general procedure for synthesis of aryl bisstannanes to afford a dark orange, highly viscous oil (1.22 g, 98 %). ^{1}H NMR (400 MHz; $CDCl_3$) δ 0.36 (18H, s), 0.87 (18H, m), 1.16-1.44 (48H, m), 1.57 (2H, m), 2.41 (4H, t, *J* = 8.0 Hz), 2.75 (4H, d, *J* = 6.7 Hz), 6.74 (2H, d, *J* = 3.5 Hz), 6.94 (2H, d, *J* = 3.5 Hz), 6.95 (2H, s), 8.39 (2H, s); ^{13}C NMR (150 MHz; $CDCl_3$) δ -8.01, 11.04, 14.28, 14.35, 22.82, 23.20, 25.67, 29.04, 29.47, 29.55, 29.74, 29.77, 29.84, 30.51, 32.05, 32.54, 34.13, 41.49, 116.30, 125.25, 127.52, 127.80, 133.46, 134.19, 134.79, 137.16, 137.18, 137.73, 139.39, 144.21, 145.39. HRMS (ESI) *m/z*: $[M + H]^+$ calcd for $C_{68}H_{103}S_6Sn_2$, 1349.4432; found, 1349.4404; deviation, 2.1 ppm.

(4-decyl-5-(6-(3-decyl-4-(trimethylstannyl)thiophen-2-yl)-3,7-bis(5-(2-ethylhexyl)thiophen-2-yl)benzo[1,2-*b*:4,5-*b*']diselenophene-2-yl)thiophen-2-yl)trimethylstannane (3c). The title compound was synthesized from compound **3c** using the general procedure for

synthesis of aryl bisstannanes to afford a dark yellow, highly viscous oil (1.15 g, 94%). ^{1}H NMR (600 MHz; $CDCl_3$) δ 0.35 (18H, s), 0.87 (18H, m), 1.17-1.36 (44H, m), 1.40 (4H, m), 1.55 (2H, m), 2.41 (4H, t, J = 7.8 Hz), 2.74 (4H, d, J = 6.7 Hz), 6.73 (2H, d, J = 3.4 Hz), 6.90 (4H, m), 8.35 (2H, s); ^{13}C NMR (150 MHz; $CDCl_3$) δ -8.03, 11.04, 14.28, 14.36, 22.82, 23.20, 25.65, 29.04, 29.09, 29.48, 29.58, 29.75, 29.78, 29.88, 30.49, 32.06, 32.53, 34.11, 41.46, 121.85, 125.11, 127.84, 130.94, 134.53, 137.11, 137.11, 137.14, 138.07, 139.04, 140.19, 143.45, 145.43. HRMS (ESI) *m/z*: $[M + H]^+$calcd for $C_{68}H_{103}S_4Se_2Sn_2$, 1443.3360; found, 1443.3306; deviation, 2.3 ppm.

5.7.2 NMR Spectra and Analytical Data

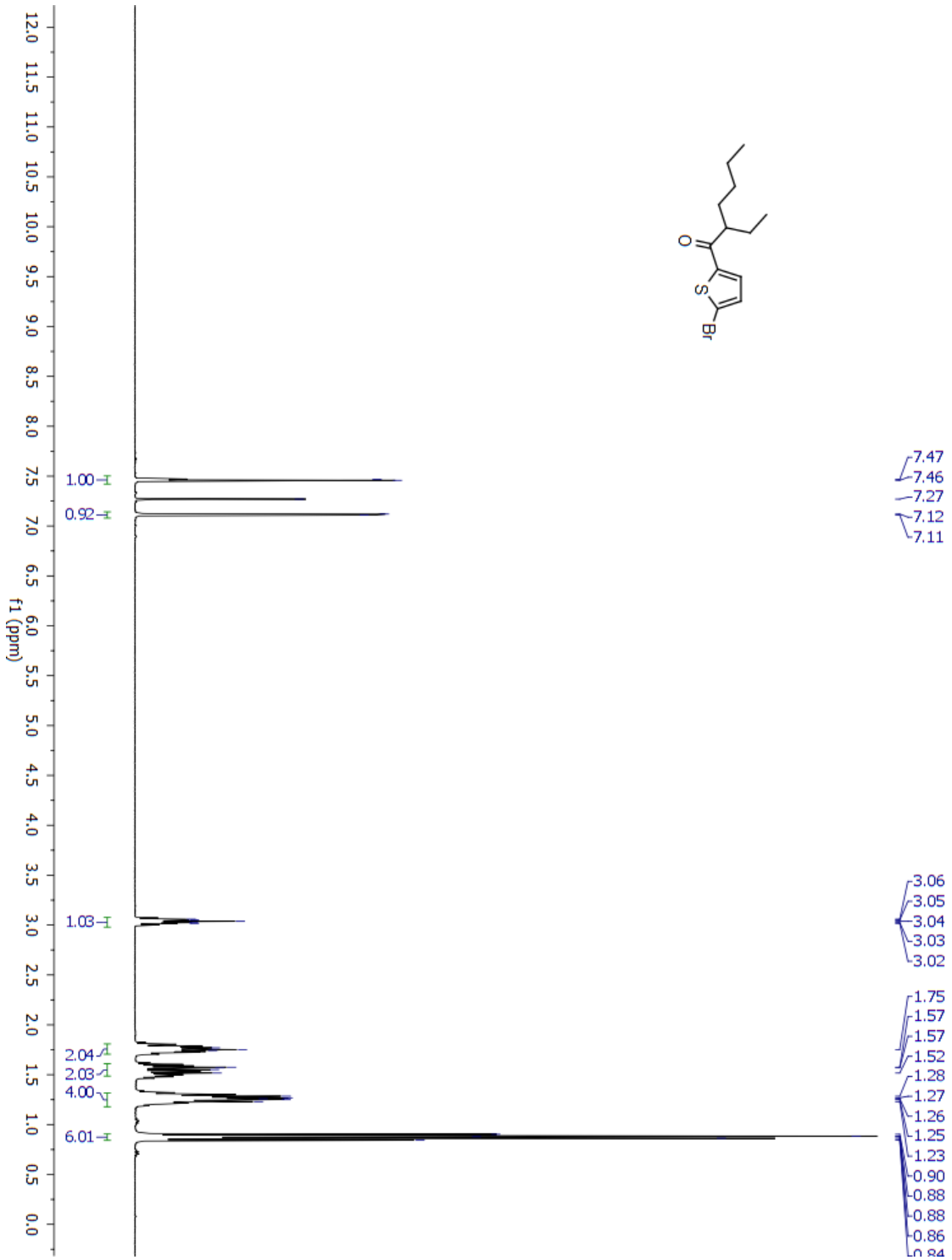

Figure S5.1. ^{1}H NMR of 1-(5-bromothiophen-2-yl)-2-ethylhexan-1-one (**S1**).

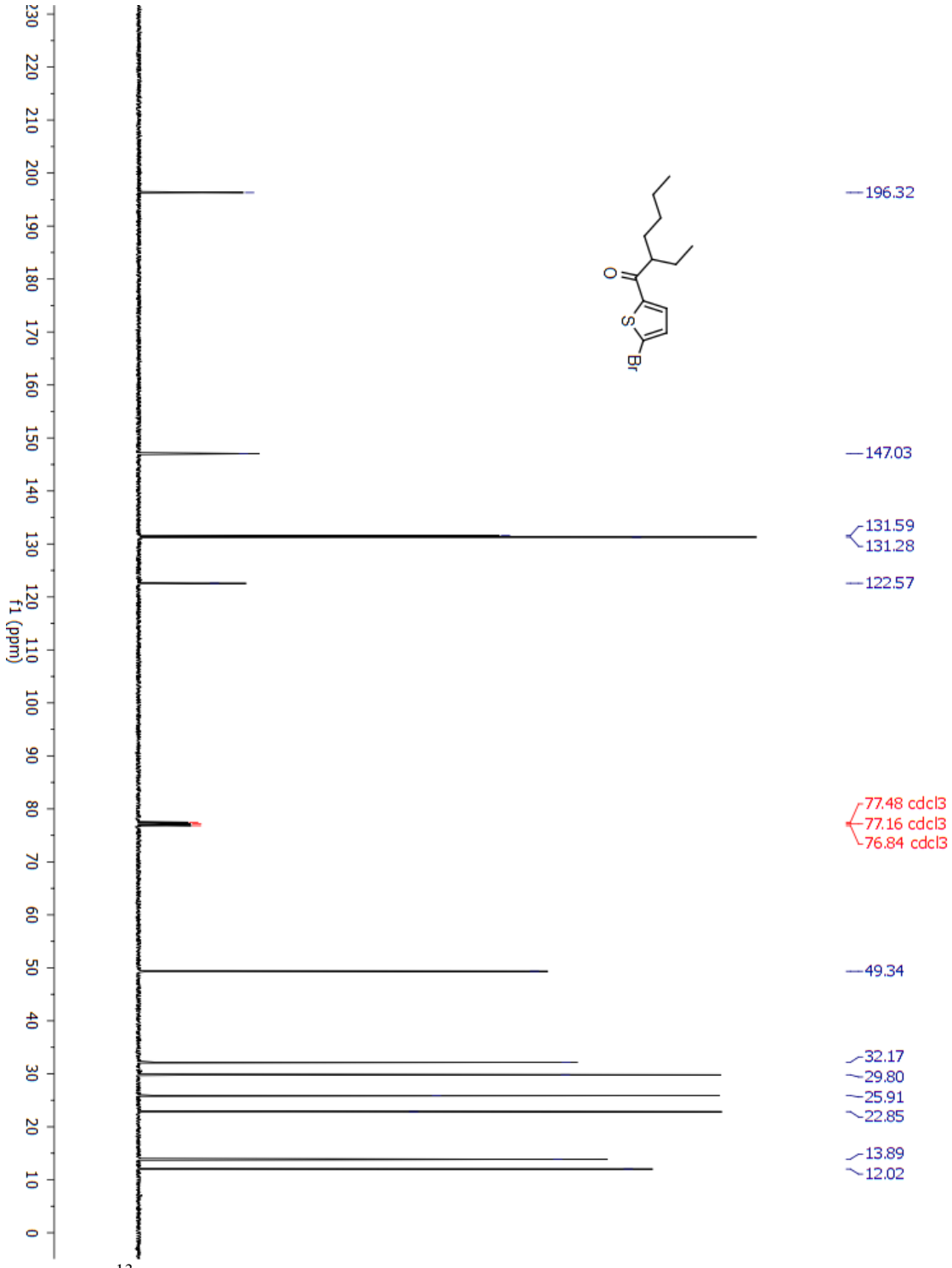

Figure S5.2. ^{13}C NMR of 1-(5-bromothiophen-2-yl)-2-ethylhexan-1-one (**S1**).

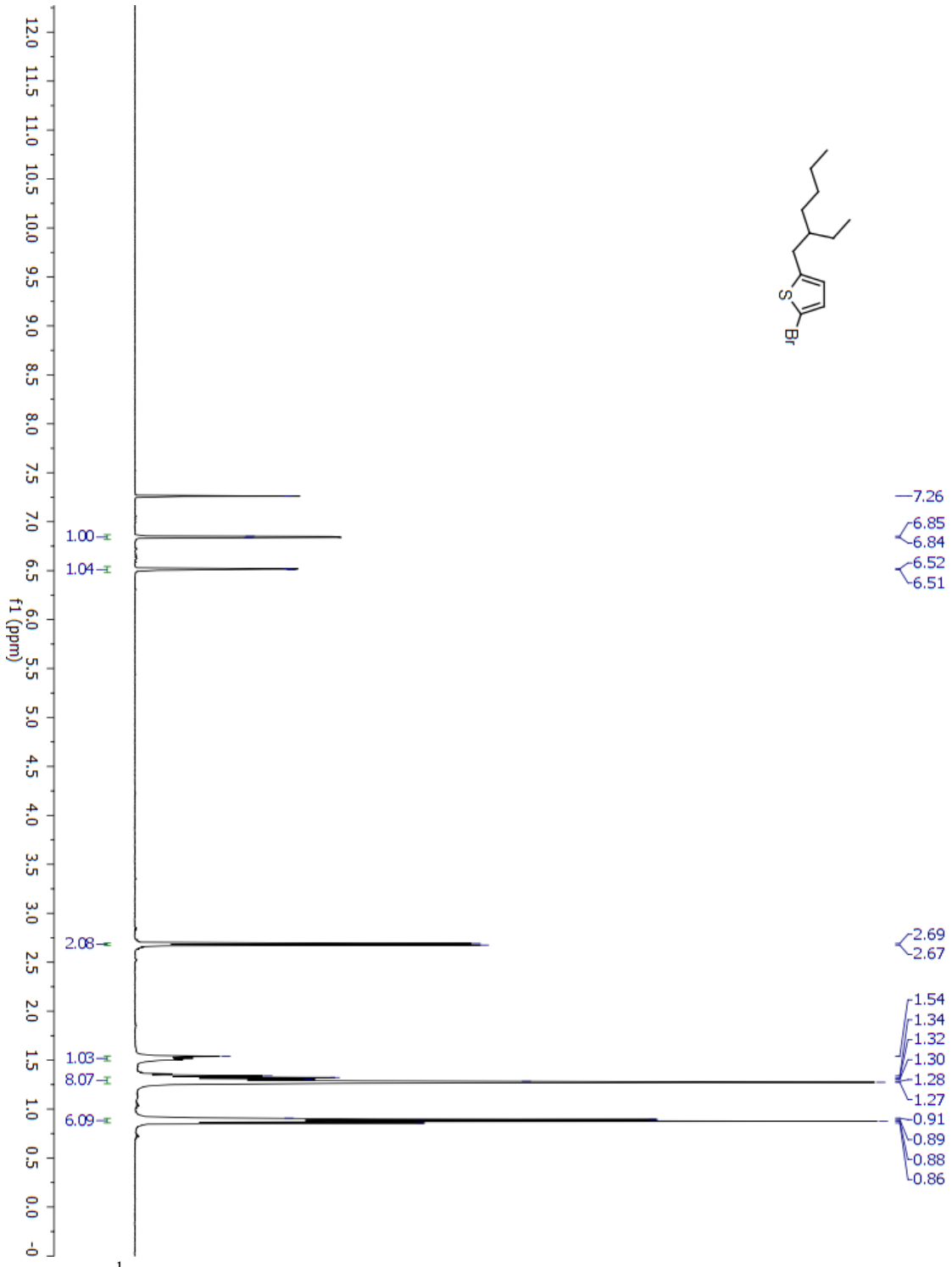

Figure S5.3. ^{1}H NMR of 2-bromo-5-(2-ethylhexyl)thiophene (**S2**).

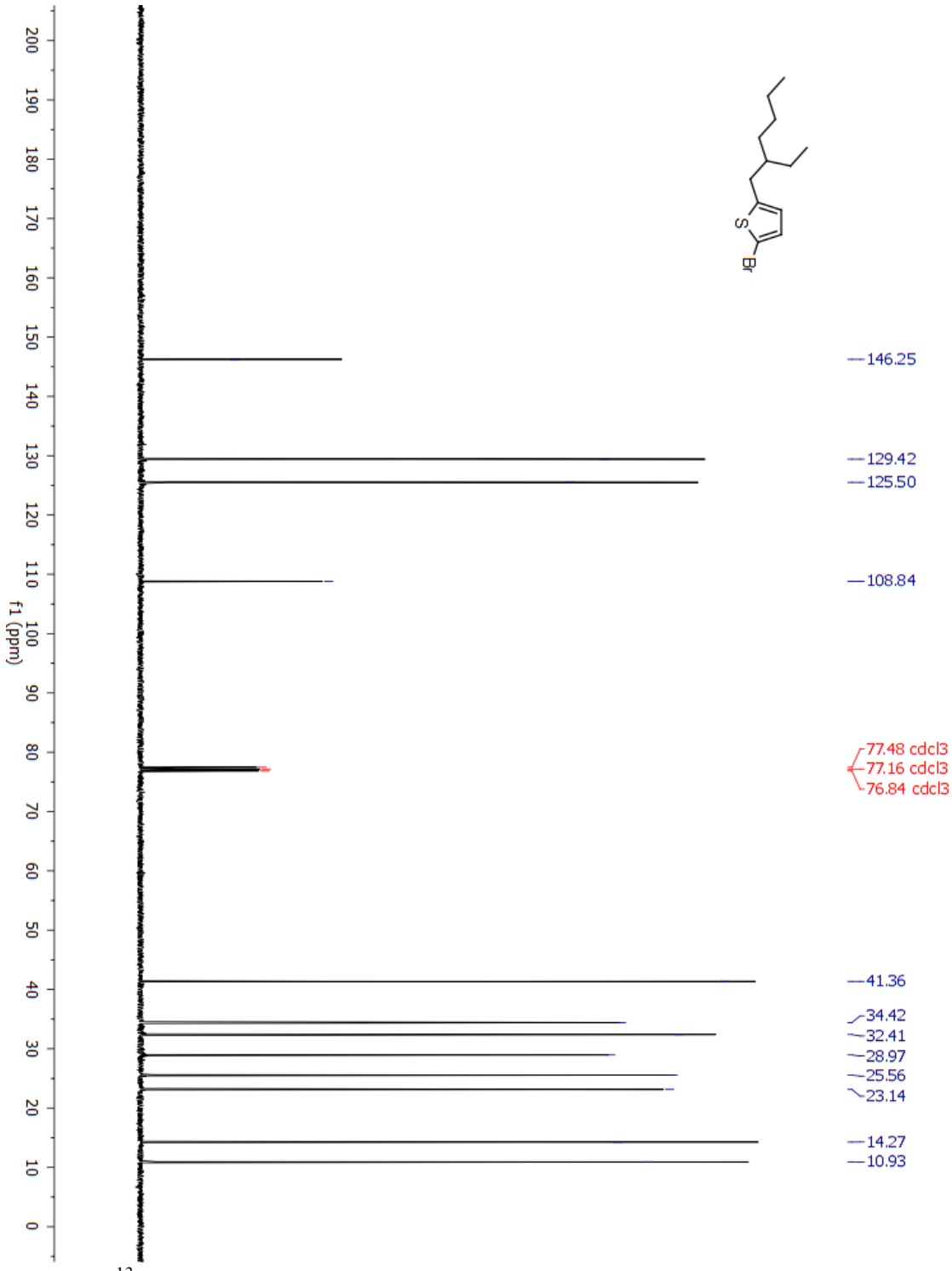

Figure S5.4. ^{13}C NMR of 2-bromo-5-(2-ethylhexyl)thiophene (**S2**).

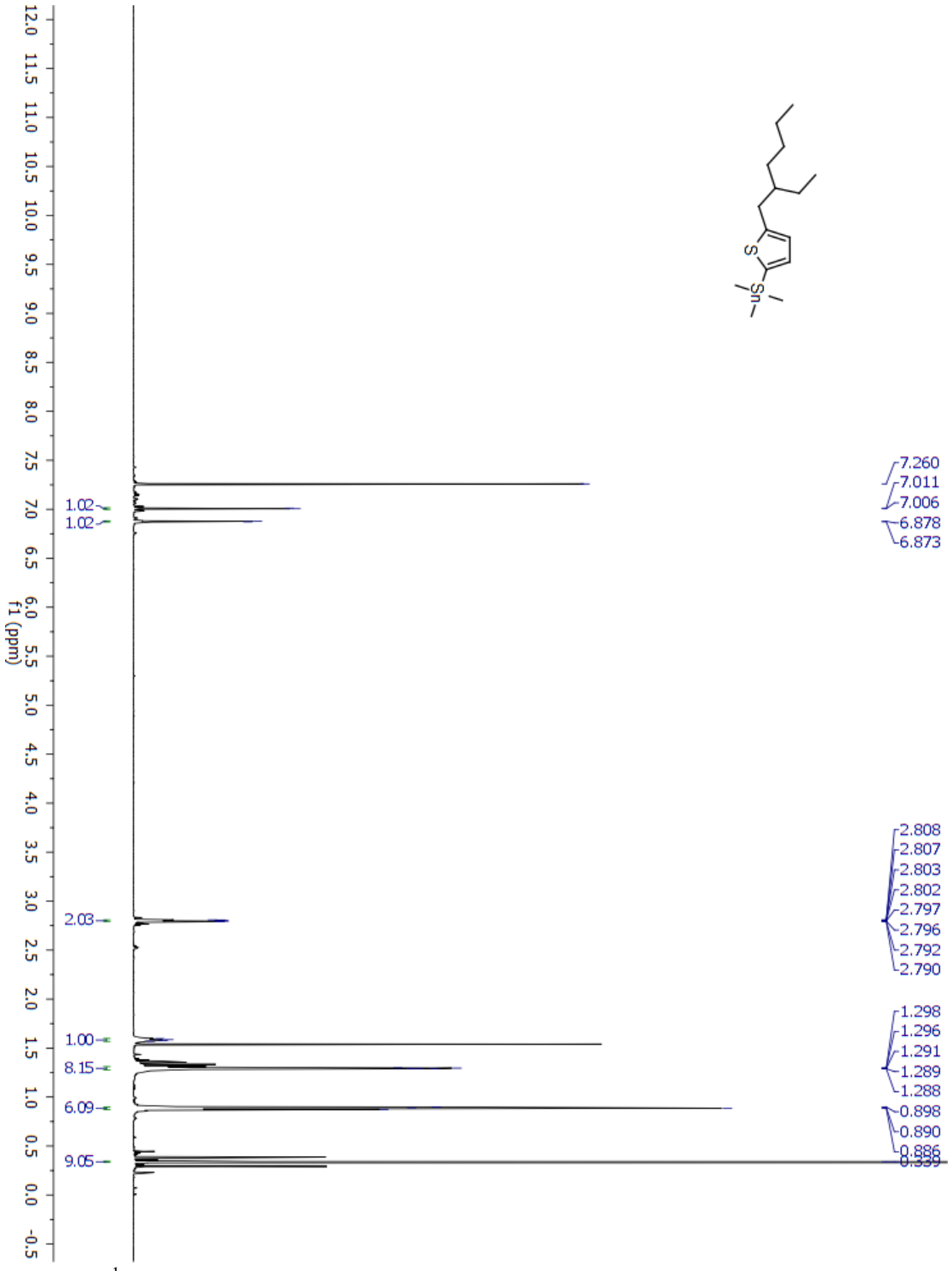

Figure S5.5. ^{1}H NMR of (5-(2-ethylhexyl)thiophen-2-yl)trimethylstannane (**S3**).

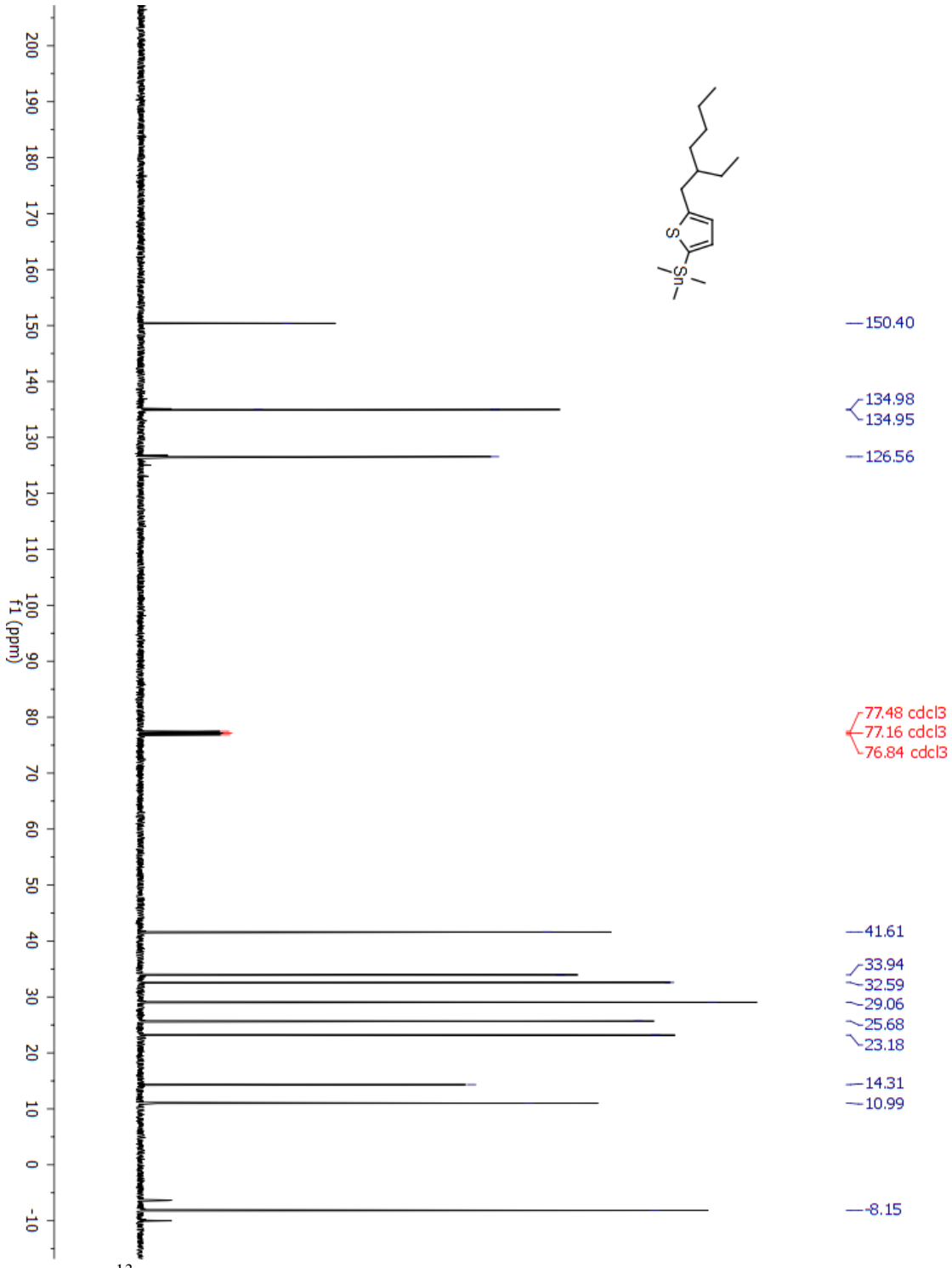

Figure S5.6. ^{13}C NMR of (5-(2-ethylhexyl)thiophen-2-yl)trimethylstannane (**S3**).

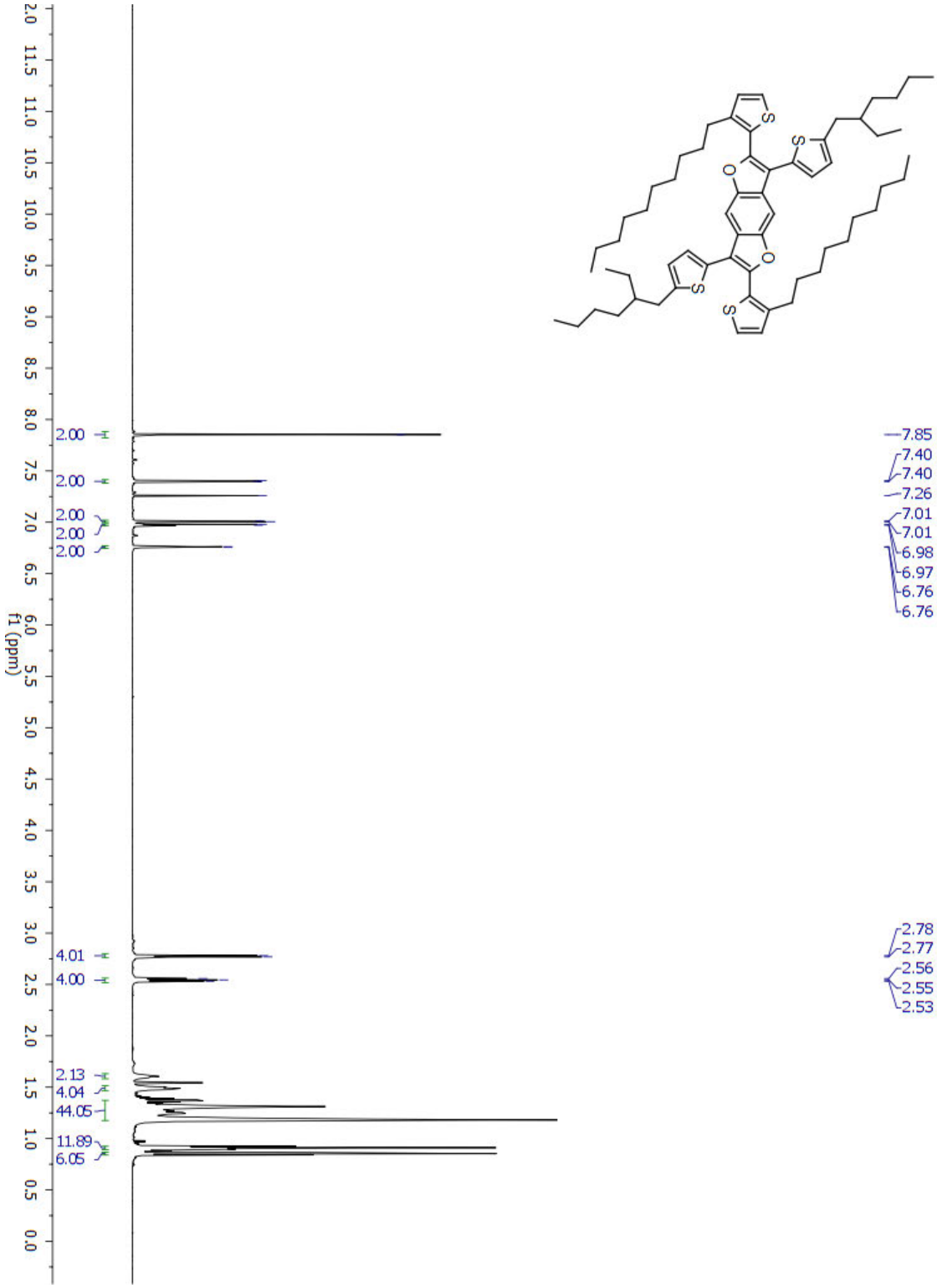

Figure S5.7. ^{1}H NMR of 2,6-bis(3-decylthiophen-2-yl)-3,7-bis(5-(2-ethylhexyl)thiophen-2-yl)benzo[1,2-*b*:4,5-*b*']difuran (**2a**).

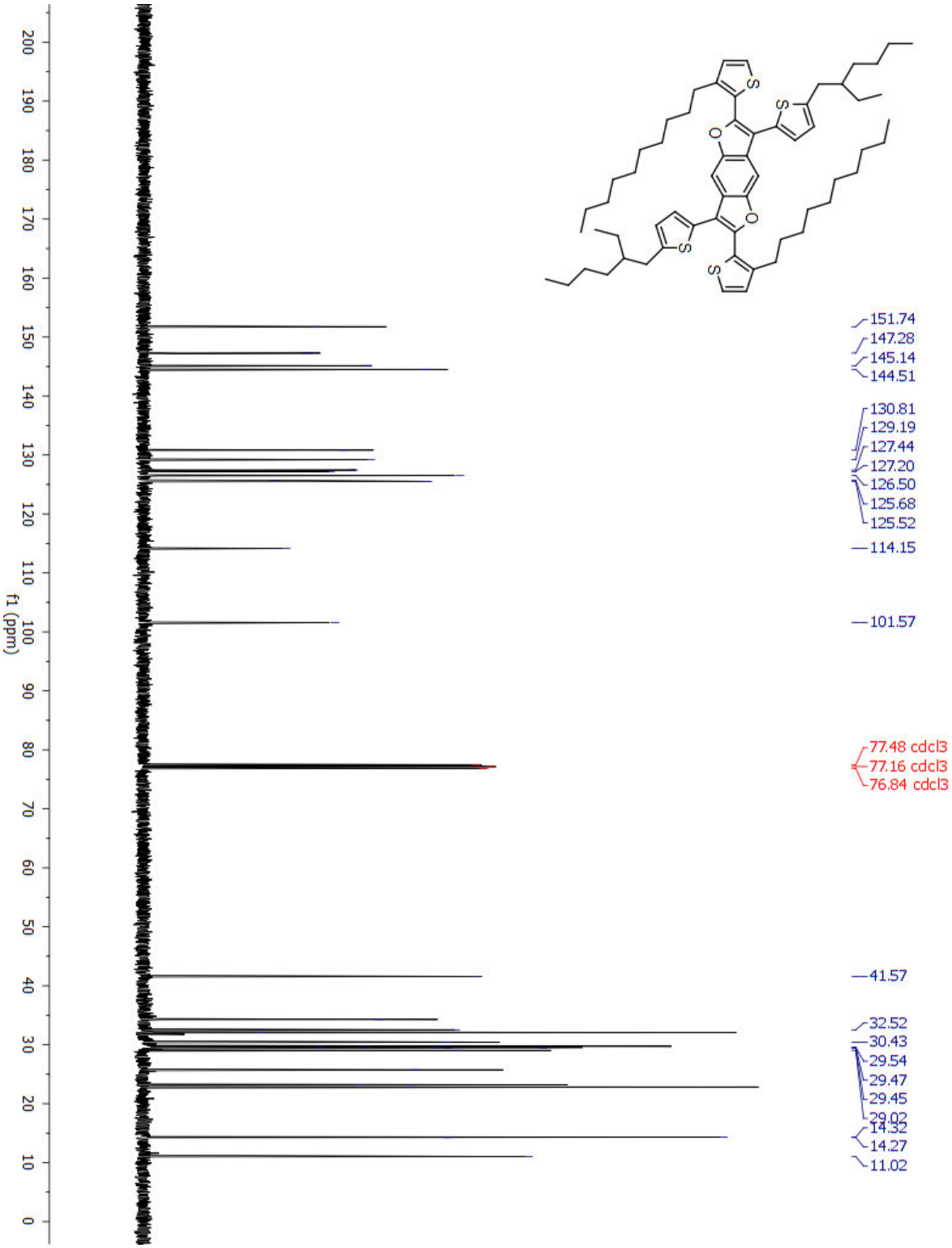

Figure S5.8. ^{13}C NMR of 2,6-bis(3-decylthiophen-2-yl)-3,7-bis(5-(2-ethylhexyl)thiophen-2-yl)benzo[1,2-*b*:4,5-*b*']difuran (**2a**).

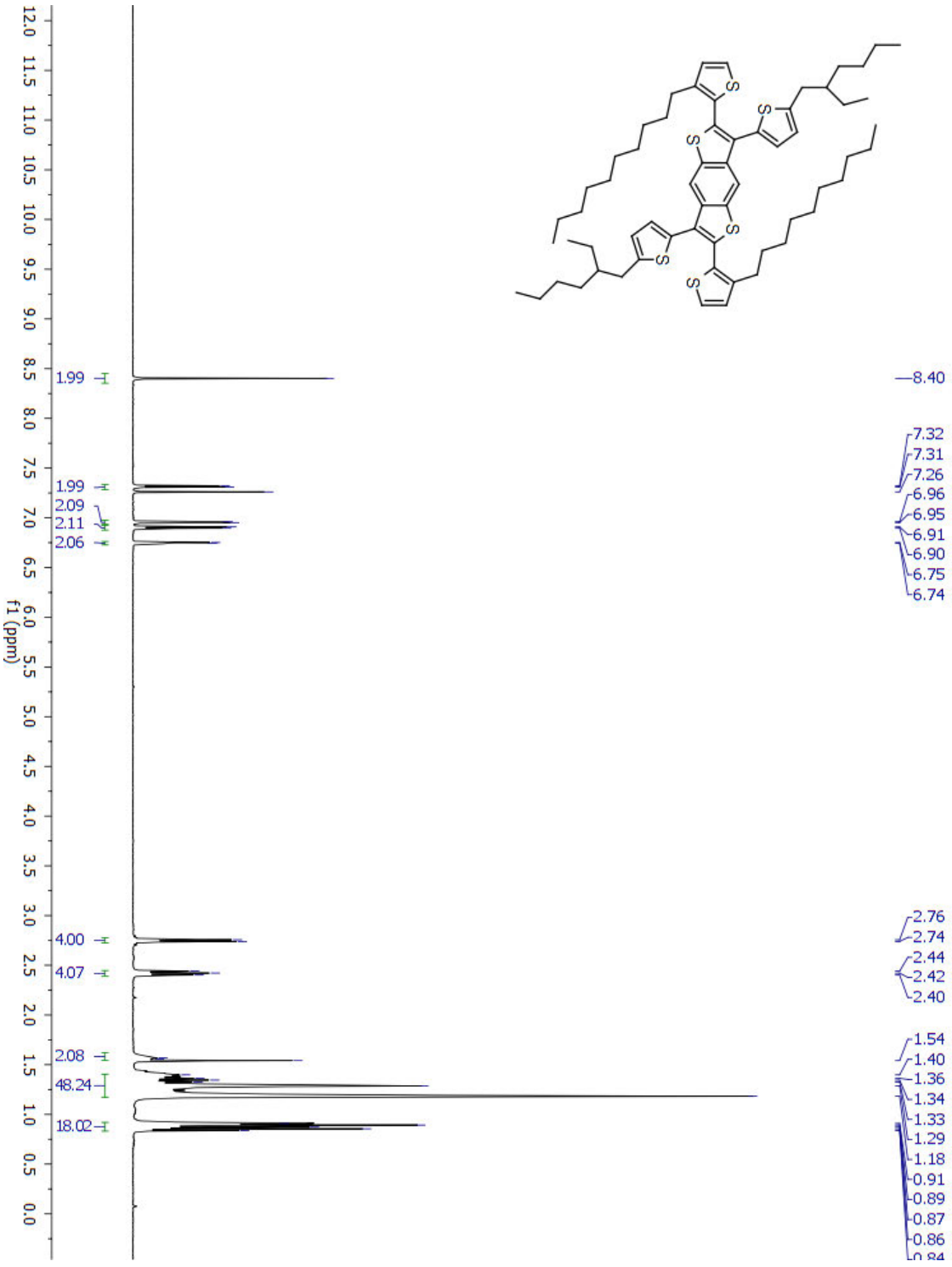

Figure S5.9. ^{1}H NMR of 2,6-bis(3-decylthiophen-2-yl)-3,7-bis(5-(2-ethylhexyl)thiophen-2-yl)benzo[1,2-*b*:4,5-*b*']dithiophene (**2b**).

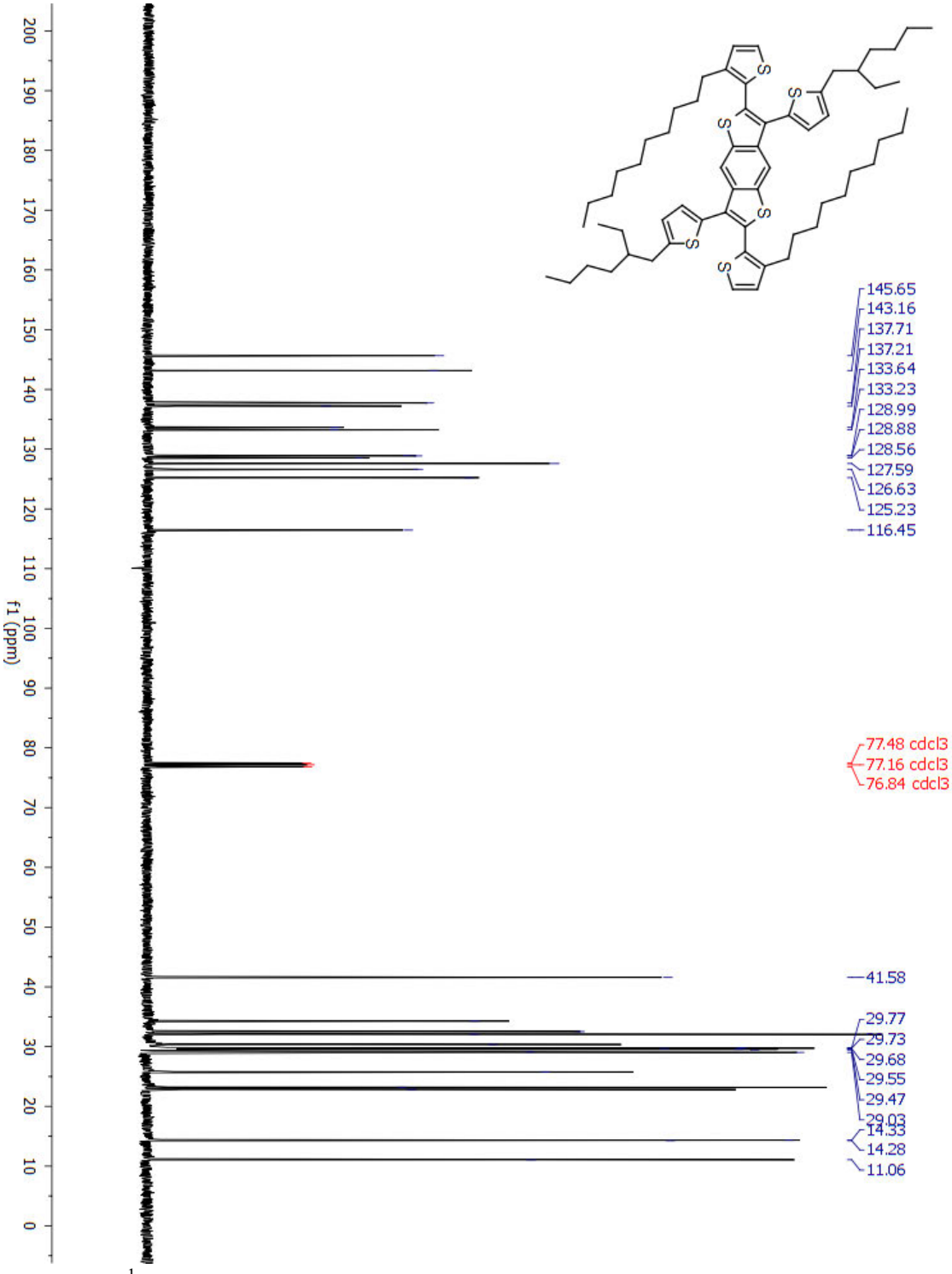

Figure S5.10. ^{1}H NMR of 2,6-bis(3-decylthiophen-2-yl)-3,7-bis(5-(2-ethylhexyl)thiophen-2-yl)benzo[1,2-*b*:4,5-*b*']dithiophene (**2b**).

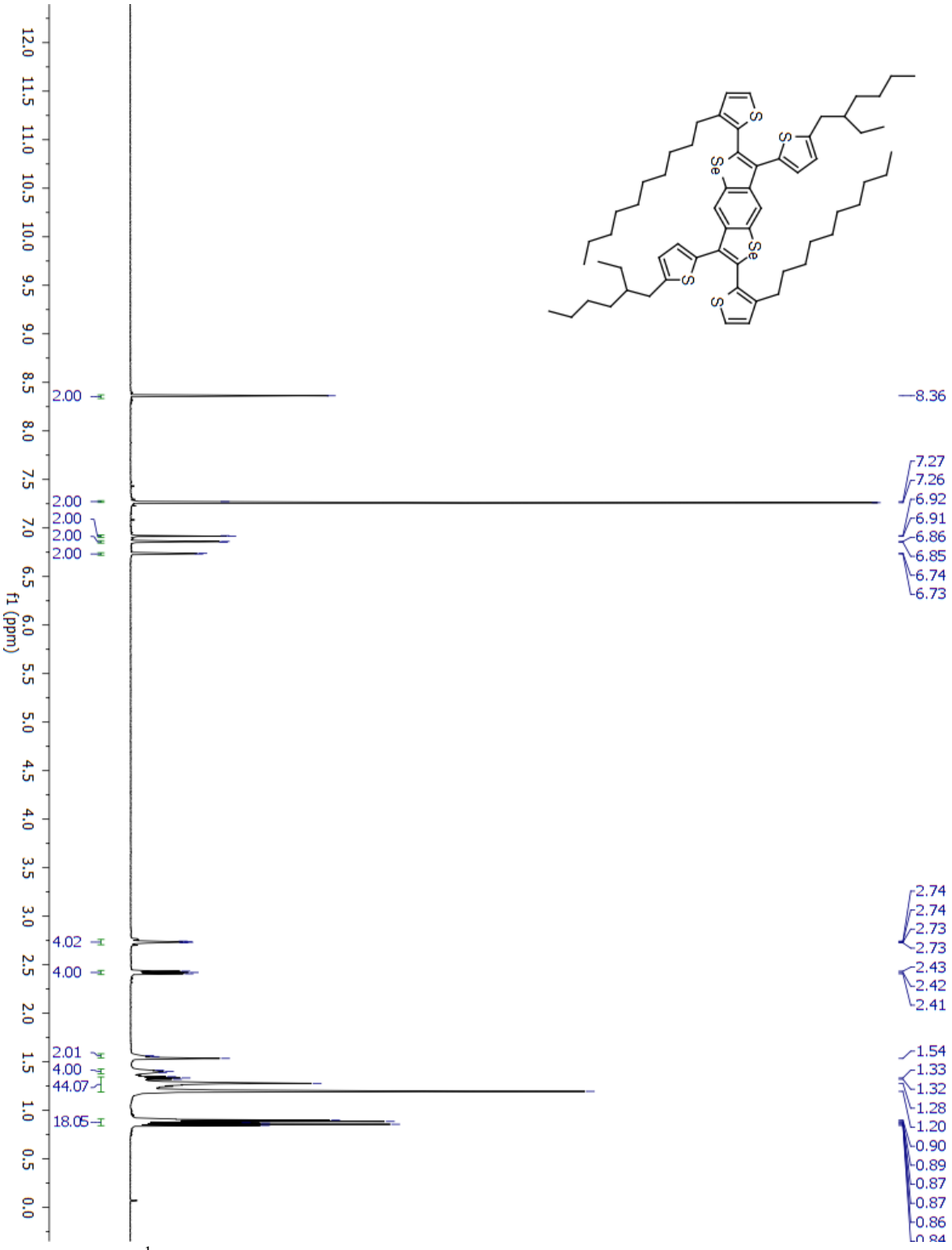

Figure S5.11. ^{1}H NMR of 2,6-bis(3-decylthiophen-2-yl)-3,7-bis(5-(2-ethylhexyl)thiophen-2-yl)benzo[1,2-*b*:4,5-*b*']diselenophene (**2c**).

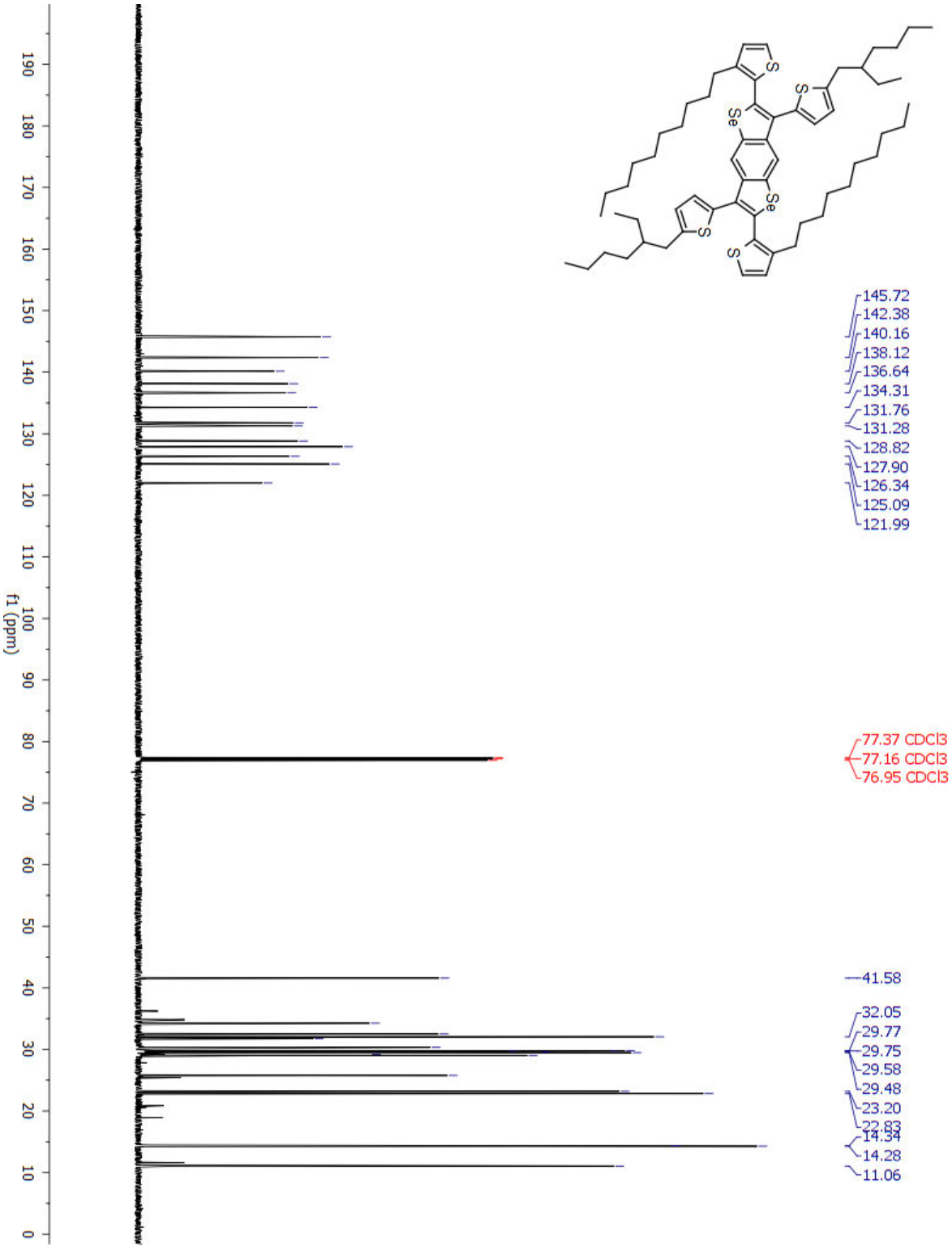

Figure S5.12. ^{13}C NMR of 2,6-bis(3-decylthiophen-2-yl)-3,7-bis(5-(2-ethylhexyl)thiophen-2-yl)benzo[1,2-*b*:4,5-*b*']diselenophene (**2c**).

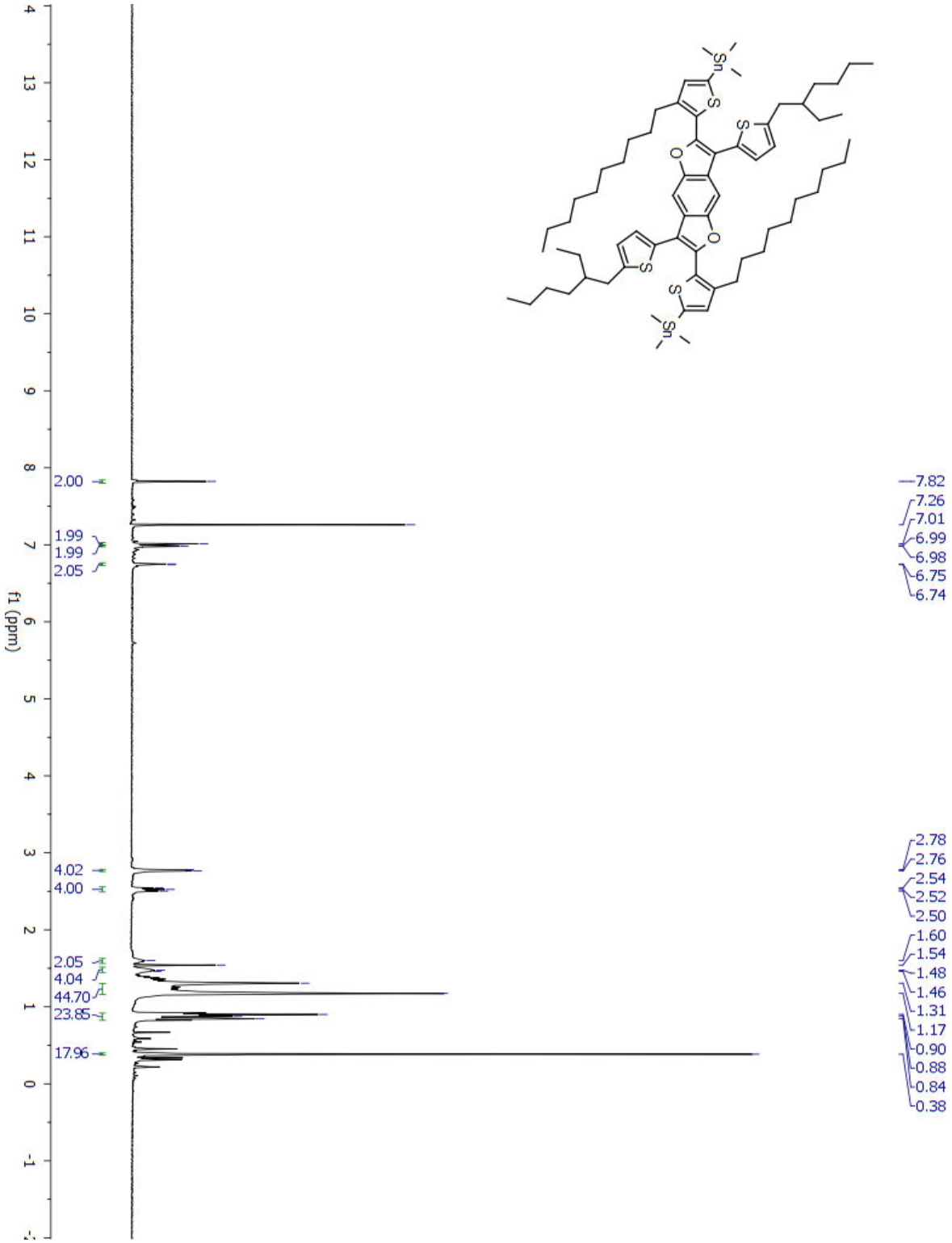

Figure S5.13. ^{1}H NMR of (4-decyl-5-(6-(3-decyl-4-(trimethylstannyl)thiophen-2-yl)-3,7-bis(5-(2-ethylhexyl)thiophen-2-yl)benzo[1,2-*b*:4,5-*b*']difuran-2-yl)thiophen-2-yl)trimethylstannane (**3a**).

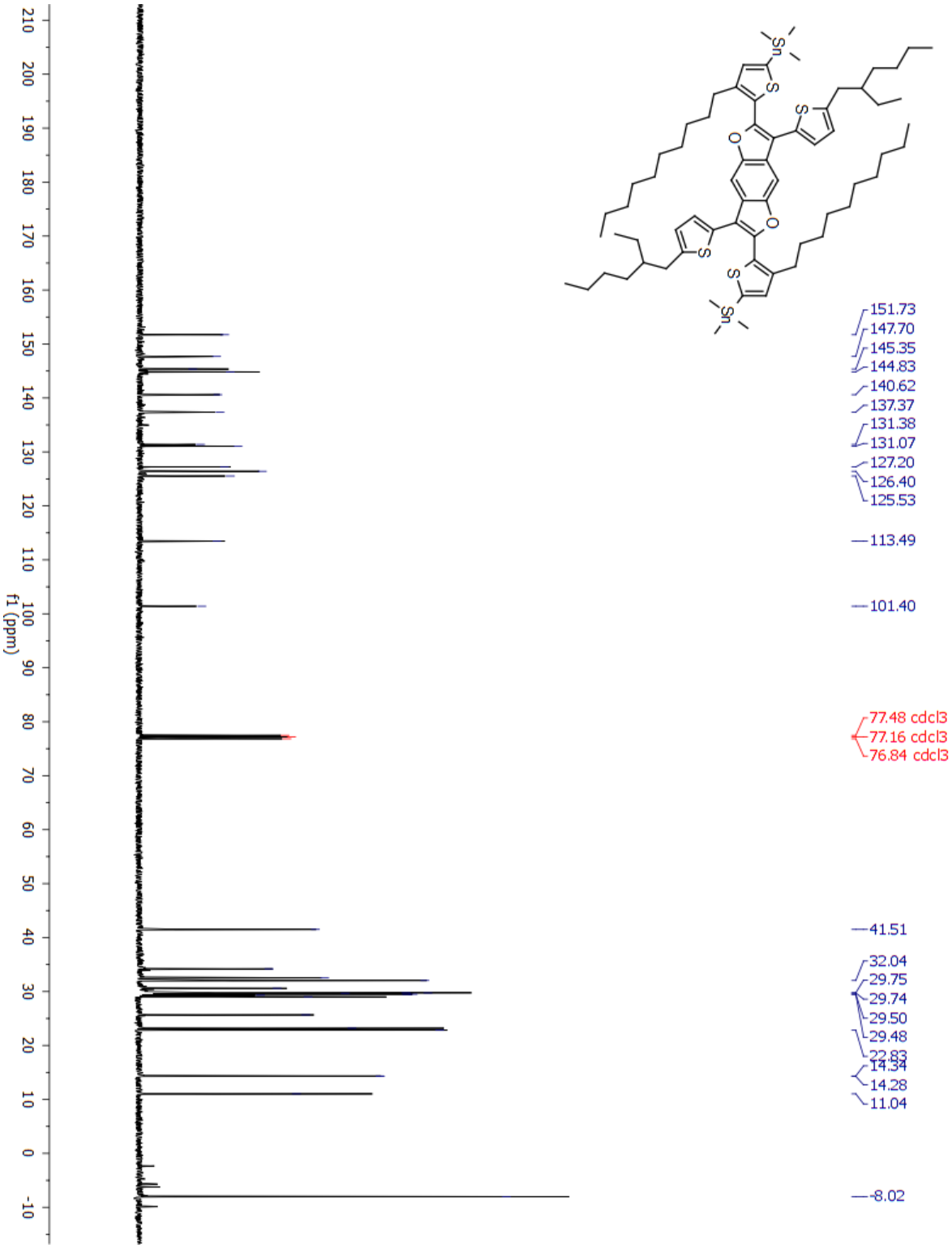

Figure S5.14. ^{13}C NMR of (4-decyl-5-(6-(3-decyl-4-(trimethylstannyl)thiophen-2-yl)-3,7-bis(5-(2-ethylhexyl)thiophen-2-yl)benzo[1,2-*b*:4,5-*b*']difuran-2-yl)thiophen-2-yl)trimethylstannane (**3a**).

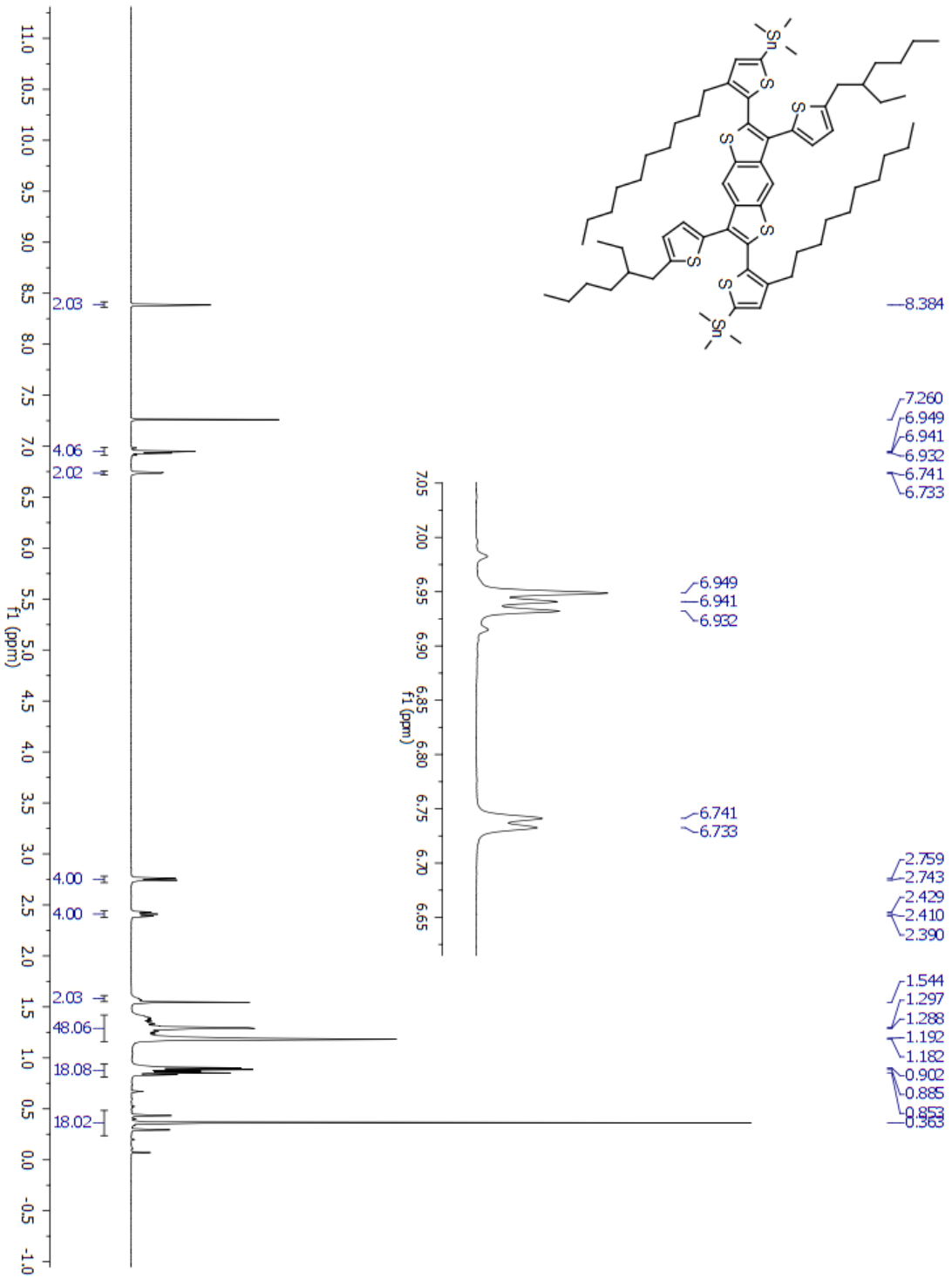

Figure S5.15. ^{1}H NMR of (4-decyl-5-(6-(3-decyl-4-(trimethylstannyl)thiophen-2-yl)-3,7-bis(5-(2-ethylhexyl)thiophen-2-yl)benzo[1,2-*b*:4,5-*b*']dithiophene-2-yl)thiophen-2-yl)trimethylstannane (**3b**).

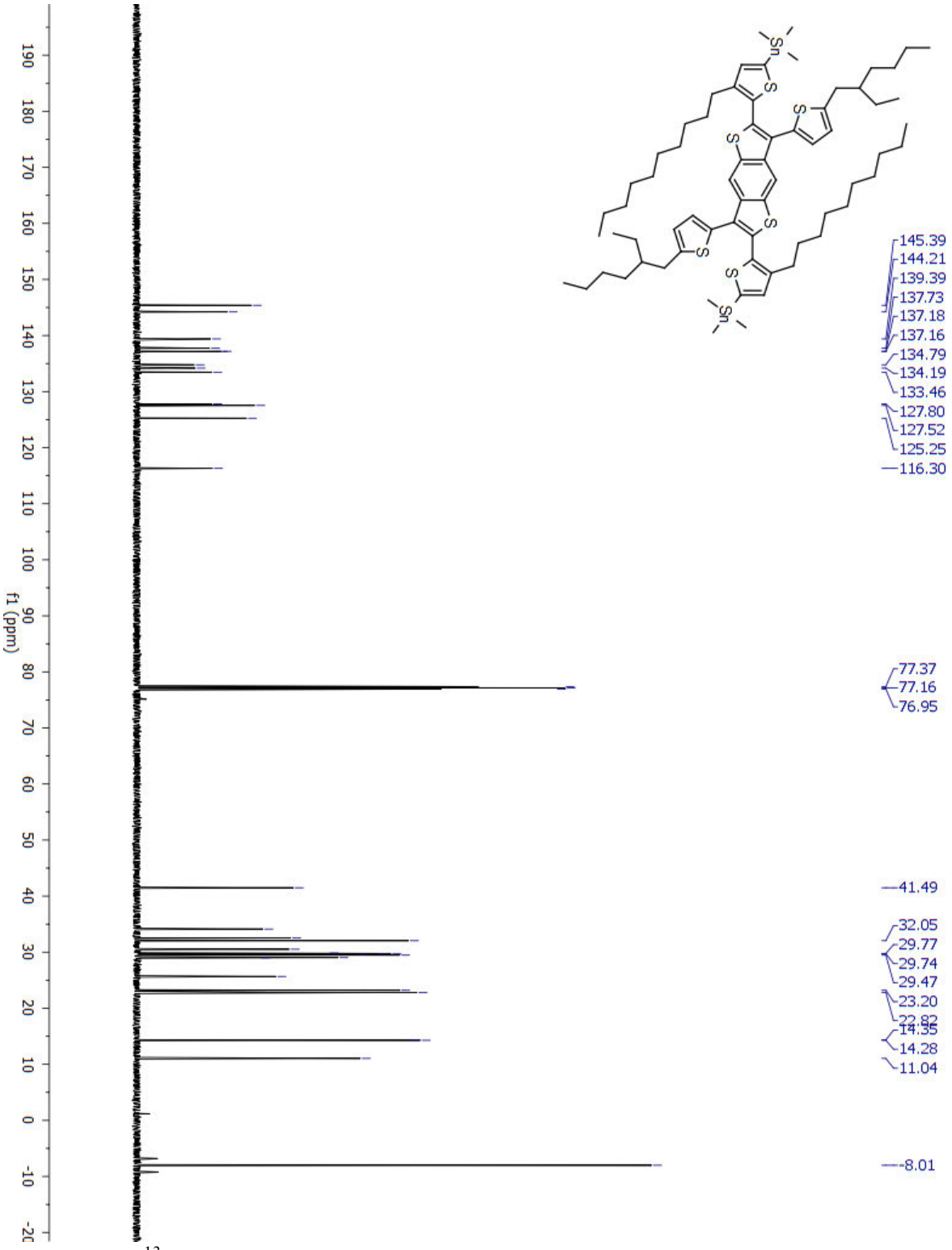

Figure S5.16. ^{13}C NMR of (4-decyl-5-(6-(3-decyl-4-(trimethylstannyl)thiophen-2-yl)-3,7-bis(5-(2-ethylhexyl)thiophen-2-yl)benzo[1,2-*b*:4,5-*b*']dithiophene-2-yl)thiophen-2-yl)trimethylstannane (**3b**).

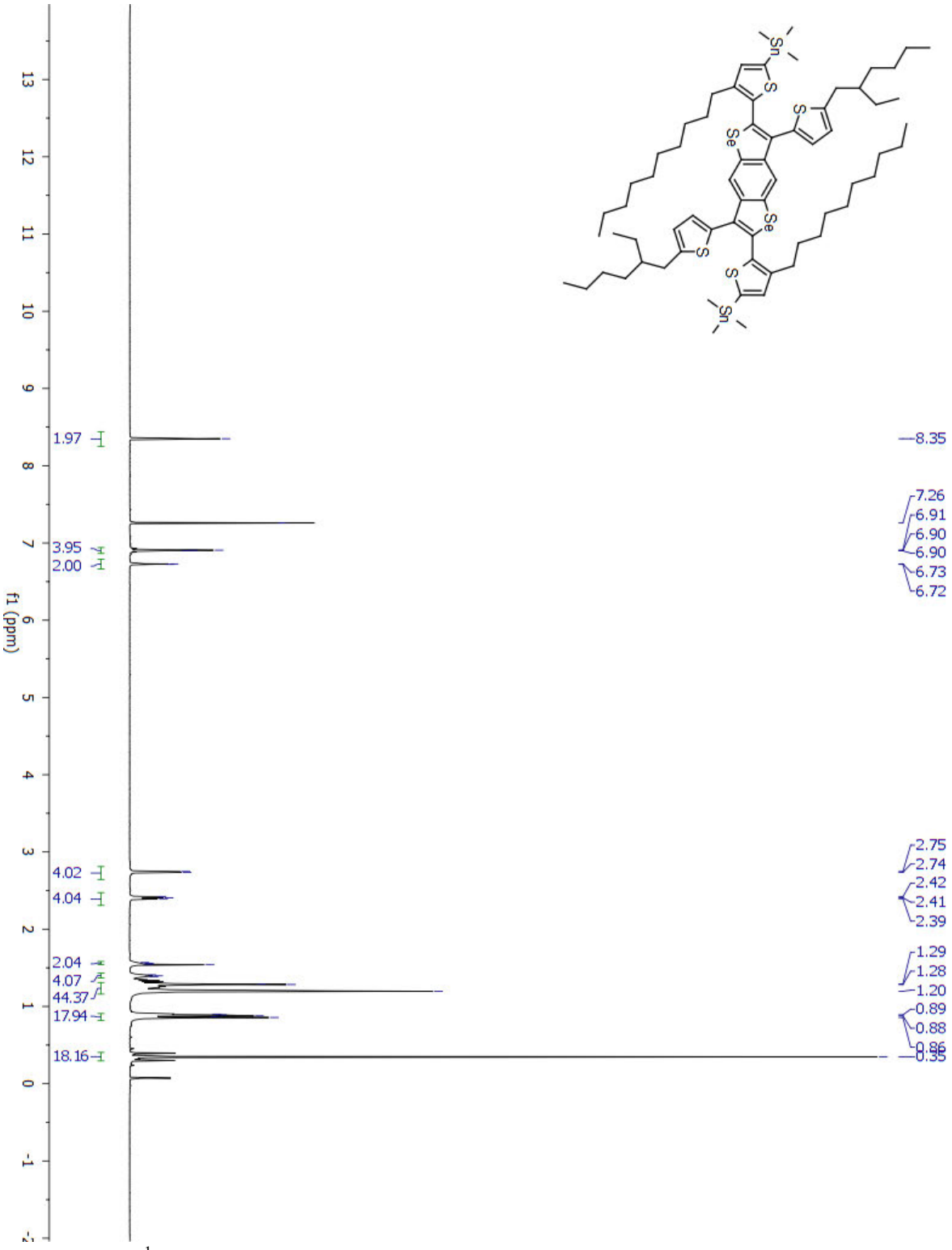

Figure S5.17. ^{1}H NMR of (4-decyl-5-(6-(3-decyl-4-(trimethylstannyl)thiophen-2-yl)-3,7-bis(5-(2-ethylhexyl)thiophen-2-yl)benzo[1,2-*b*:4,5-*b*']diselenophene-2-yl)thiophen-2-yl)trimethylstannane (**3c**).

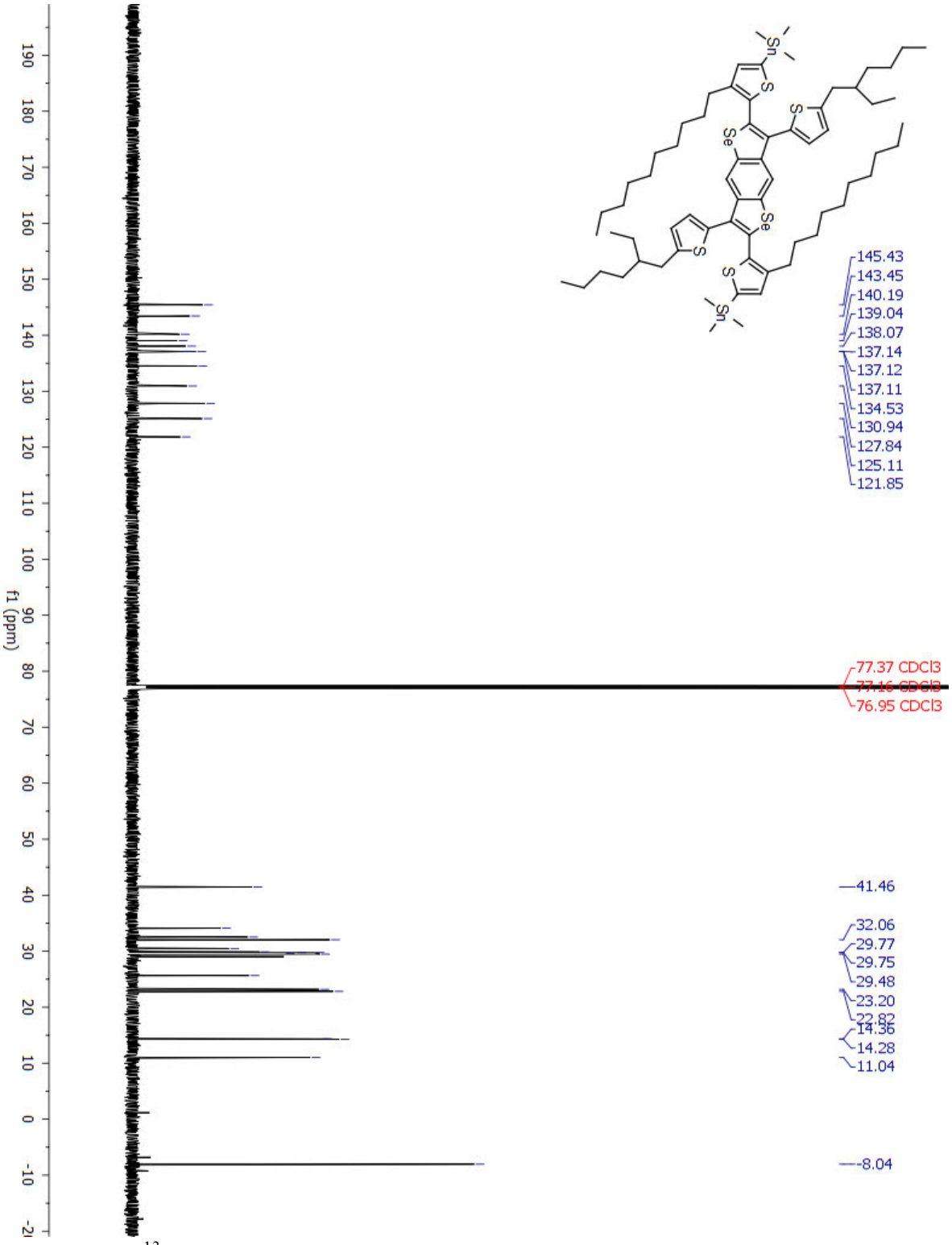

Figure S5.18. ^{13}C NMR of (4-decyl-5-(6-(3-decyl-4-(trimethylstannyl)thiophen-2-yl)-3,7-bis(5-(2-ethylhexyl)thiophen-2-yl)benzo[1,2-*b*:4,5-*b*']diselenophene-2-yl)thiophen-2-yl)trimethylstannane (**3c**).

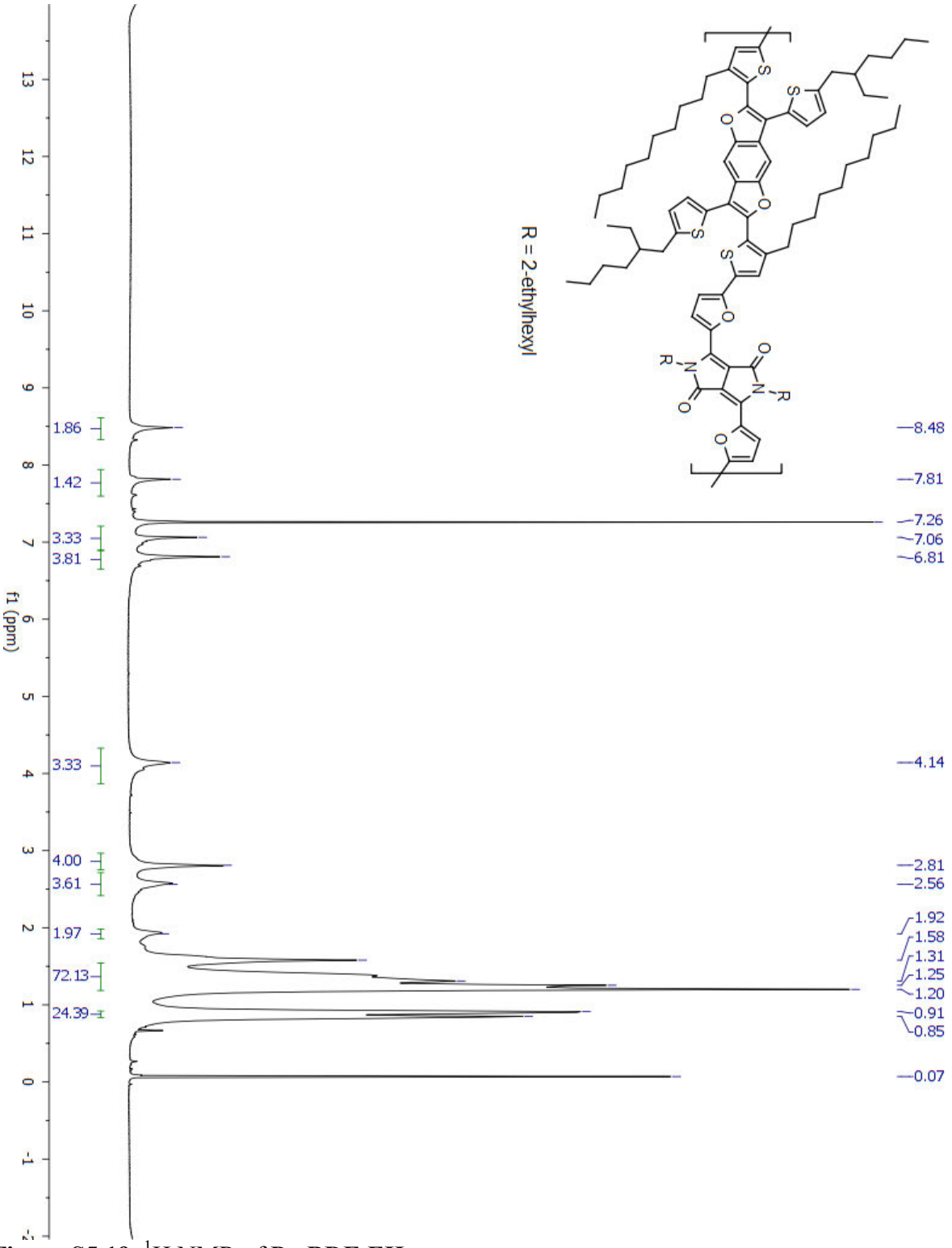

Figure S5.19. ^{1}H NMR of **P_{2D}BDF-EH**.

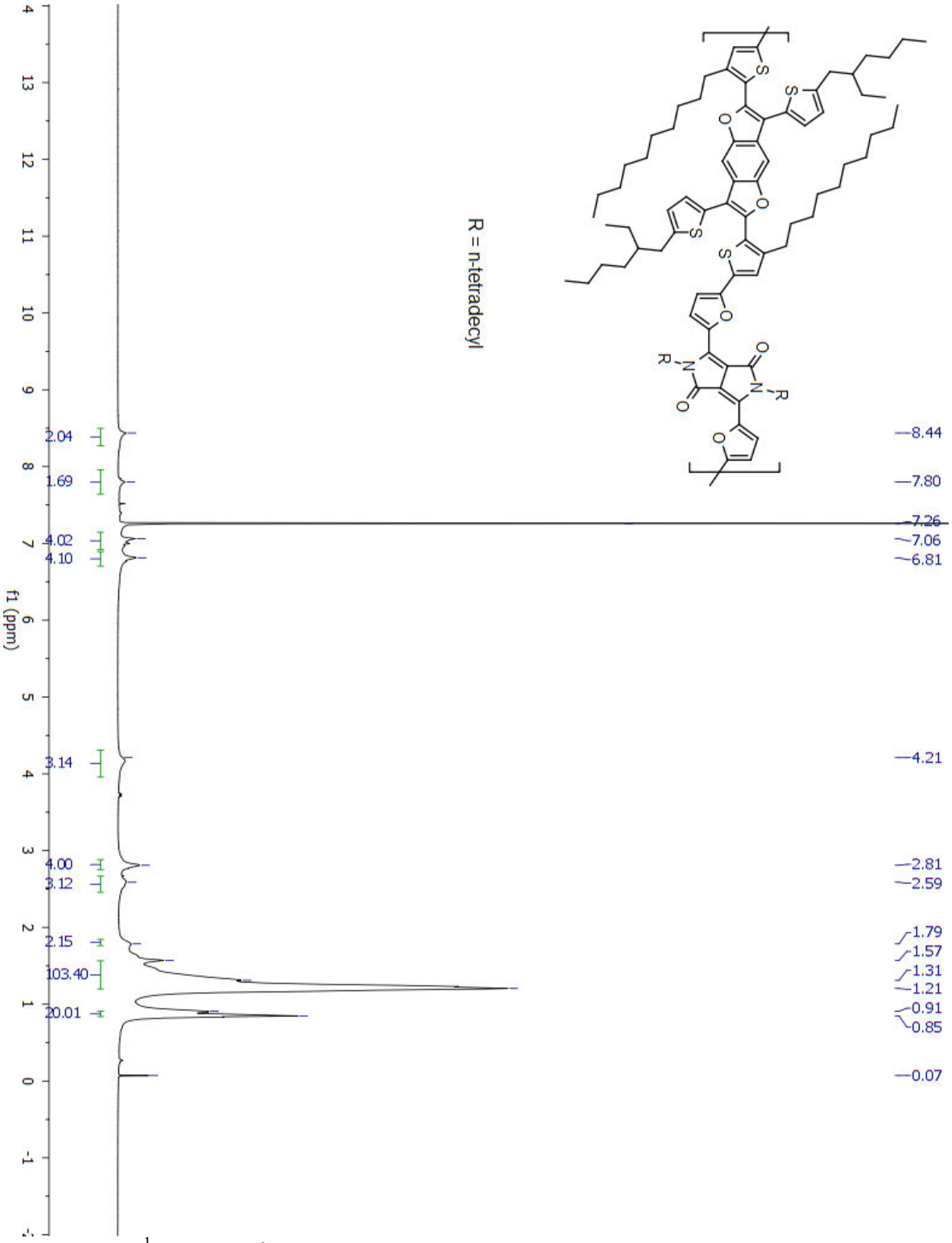

Figure S5.20. ^{1}H NMR of **P_{2D}BDF-C14**.

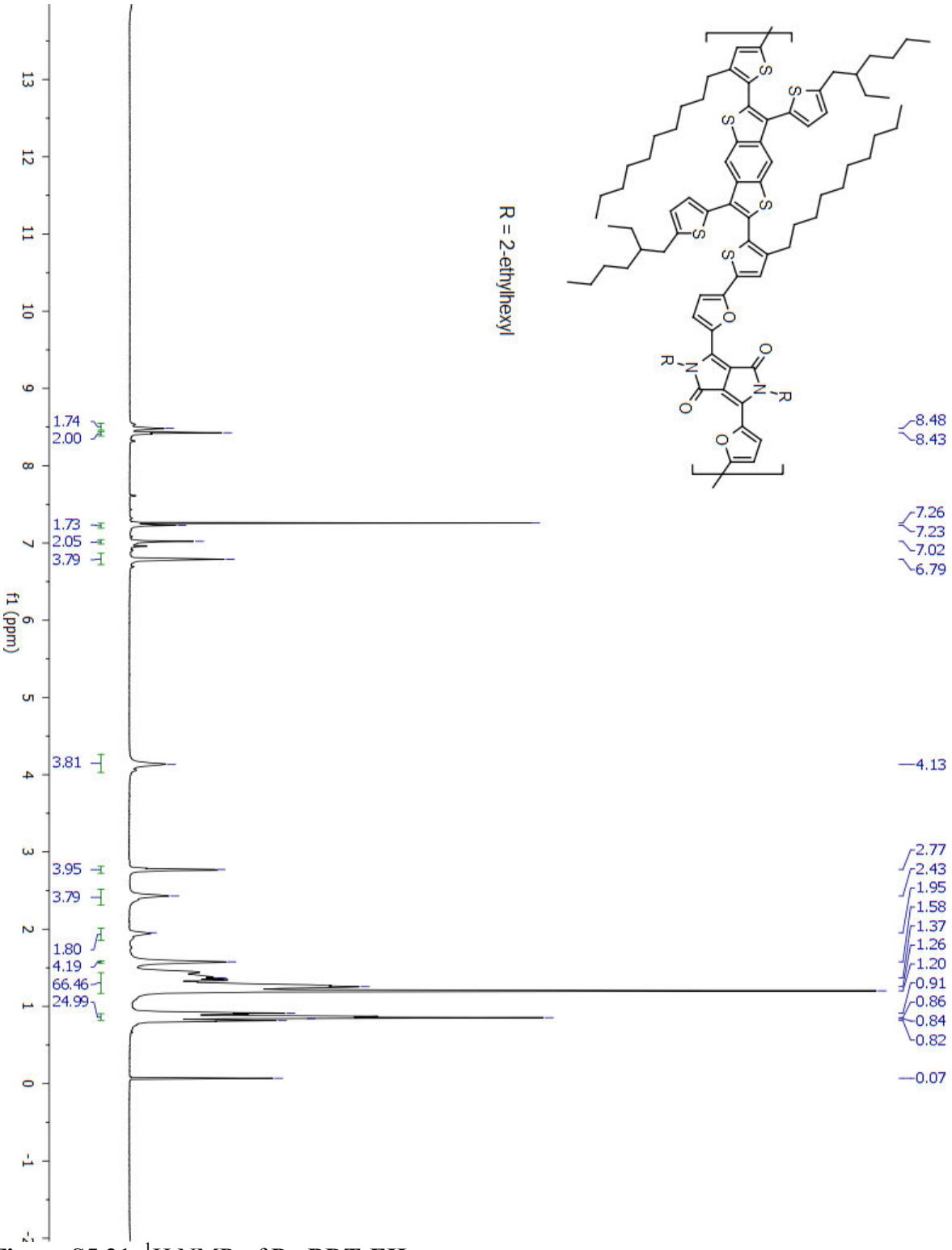

Figure S5.21. ^{1}H NMR of **P_{2D}BDT-EH**.

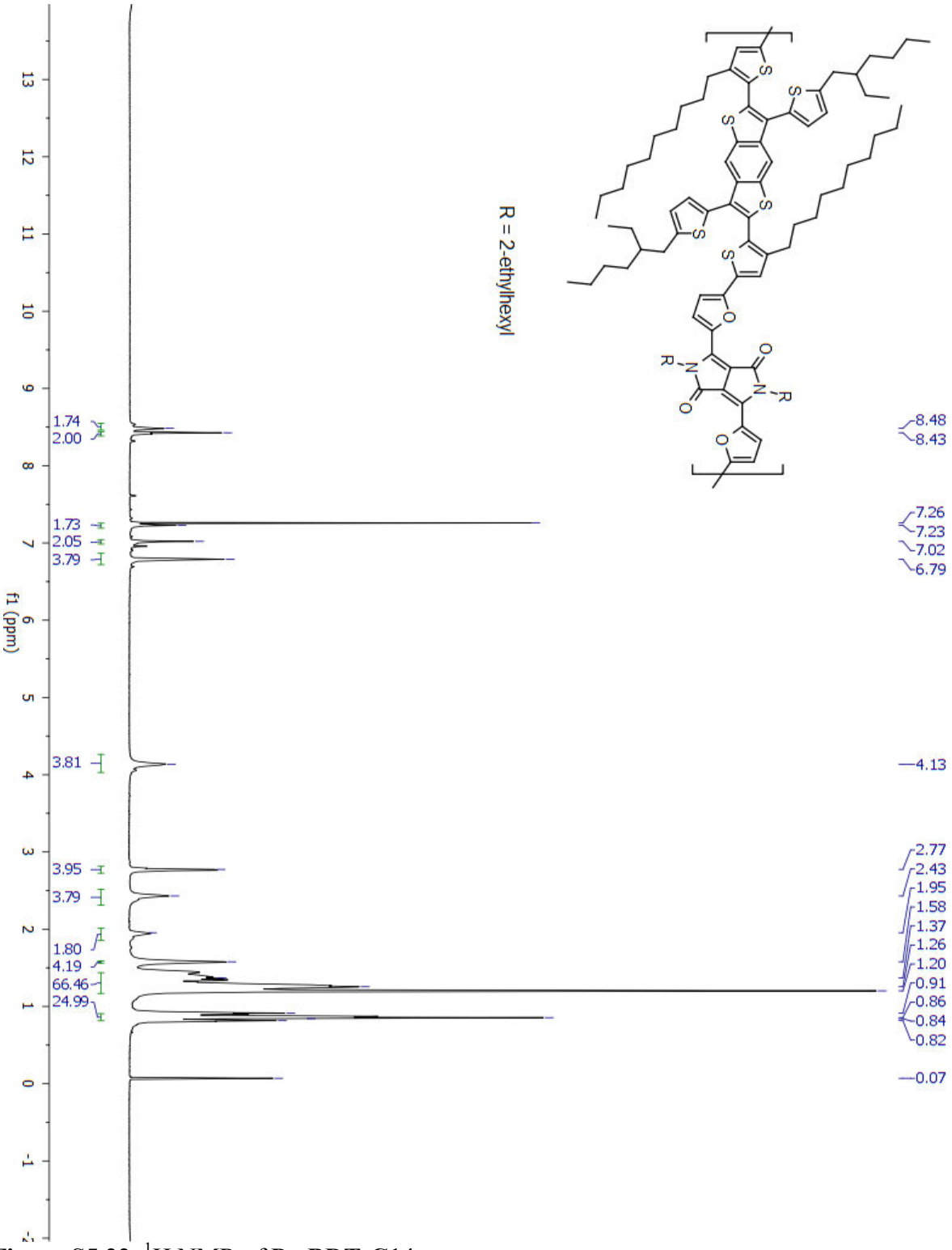

Figure S5.22. ^{1}H NMR of **P_{2D}BDT-C14**.

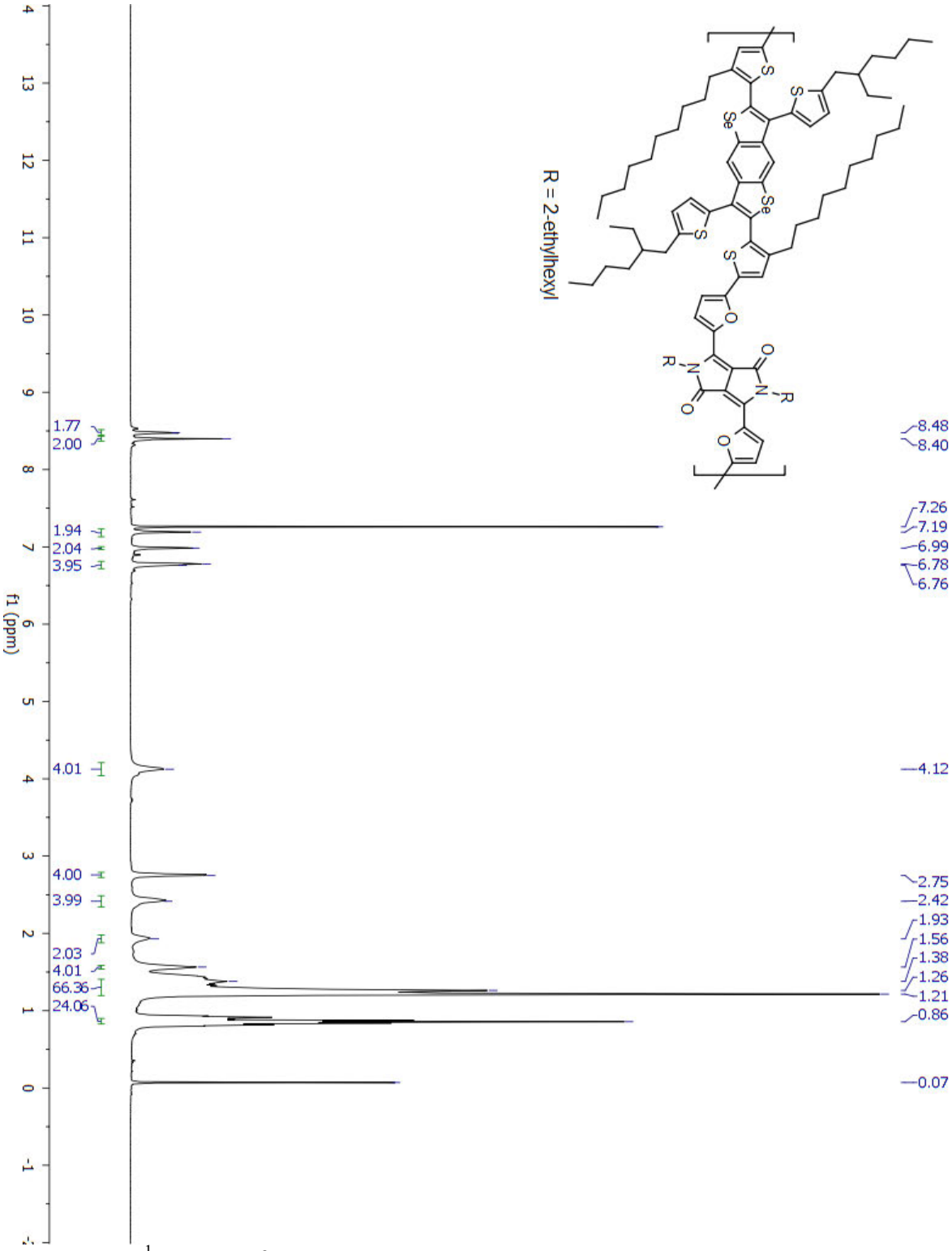

Figure S5.23. ^{1}H NMR of **P_{2D}BDSe-EH**.

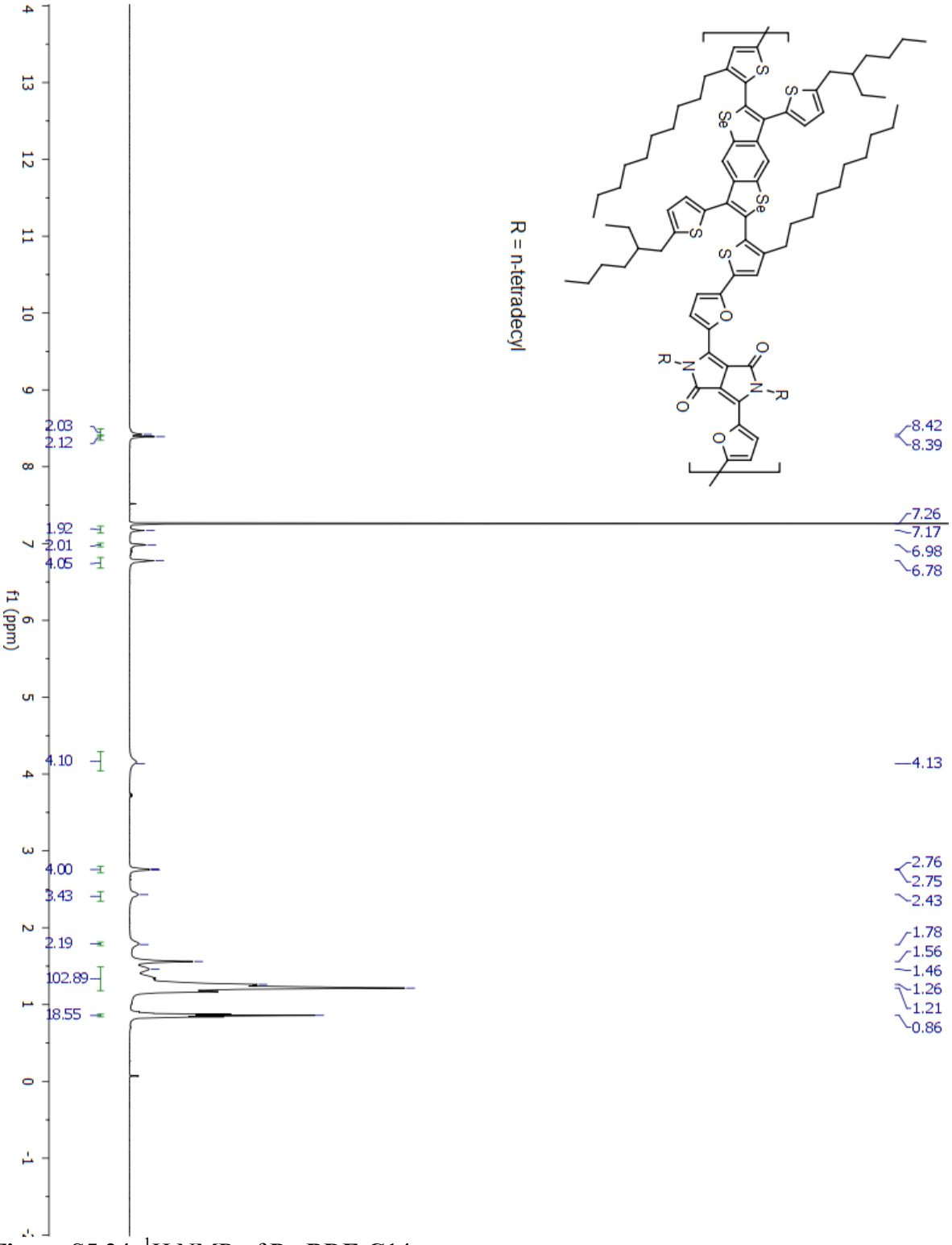

Figure S5.24. ^{1}H NMR of **P_{2D}BDF-C14**.

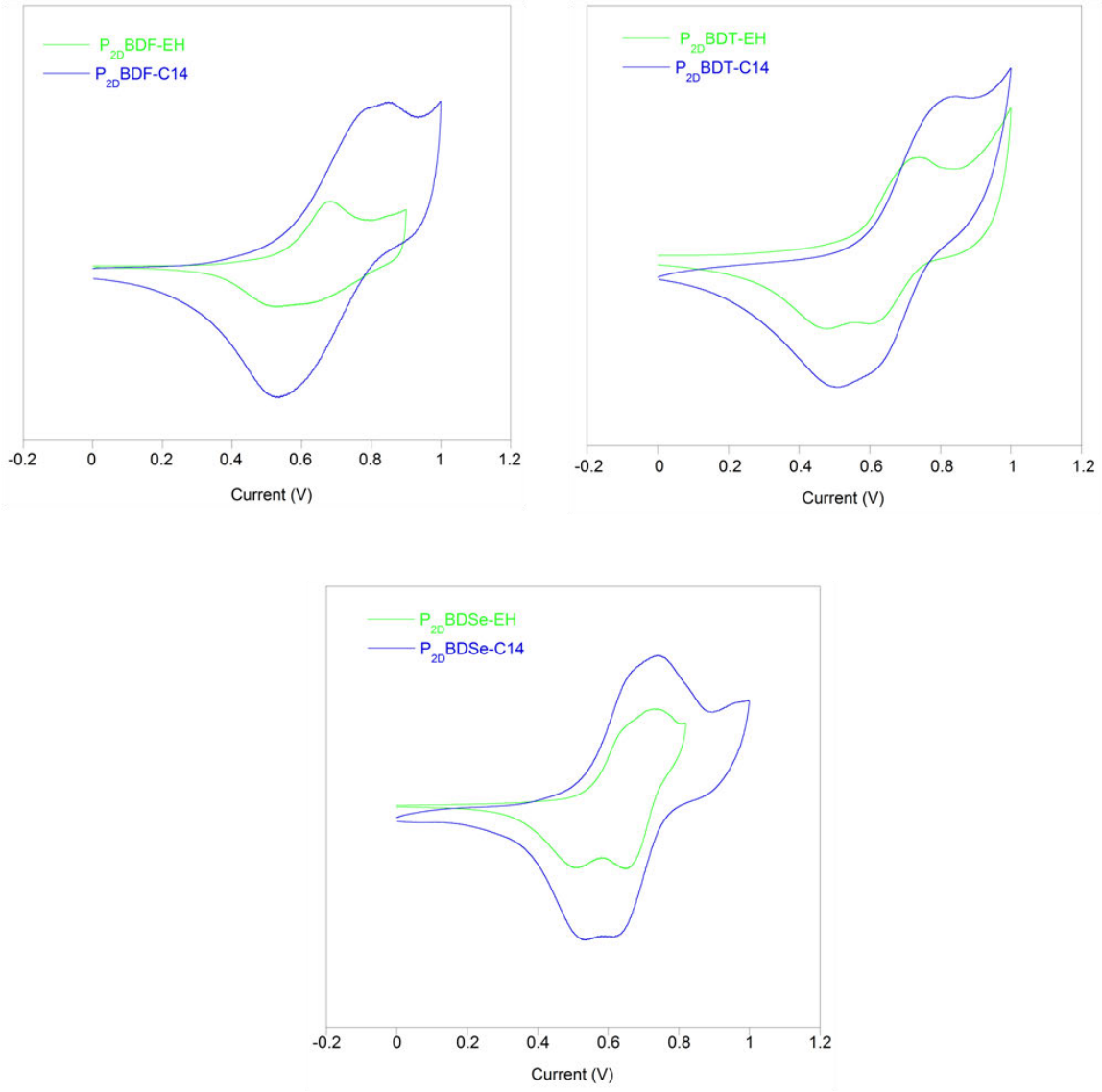

Figure S5.25. Cyclic voltammetry traces for oxidation cycles of all six polymers.

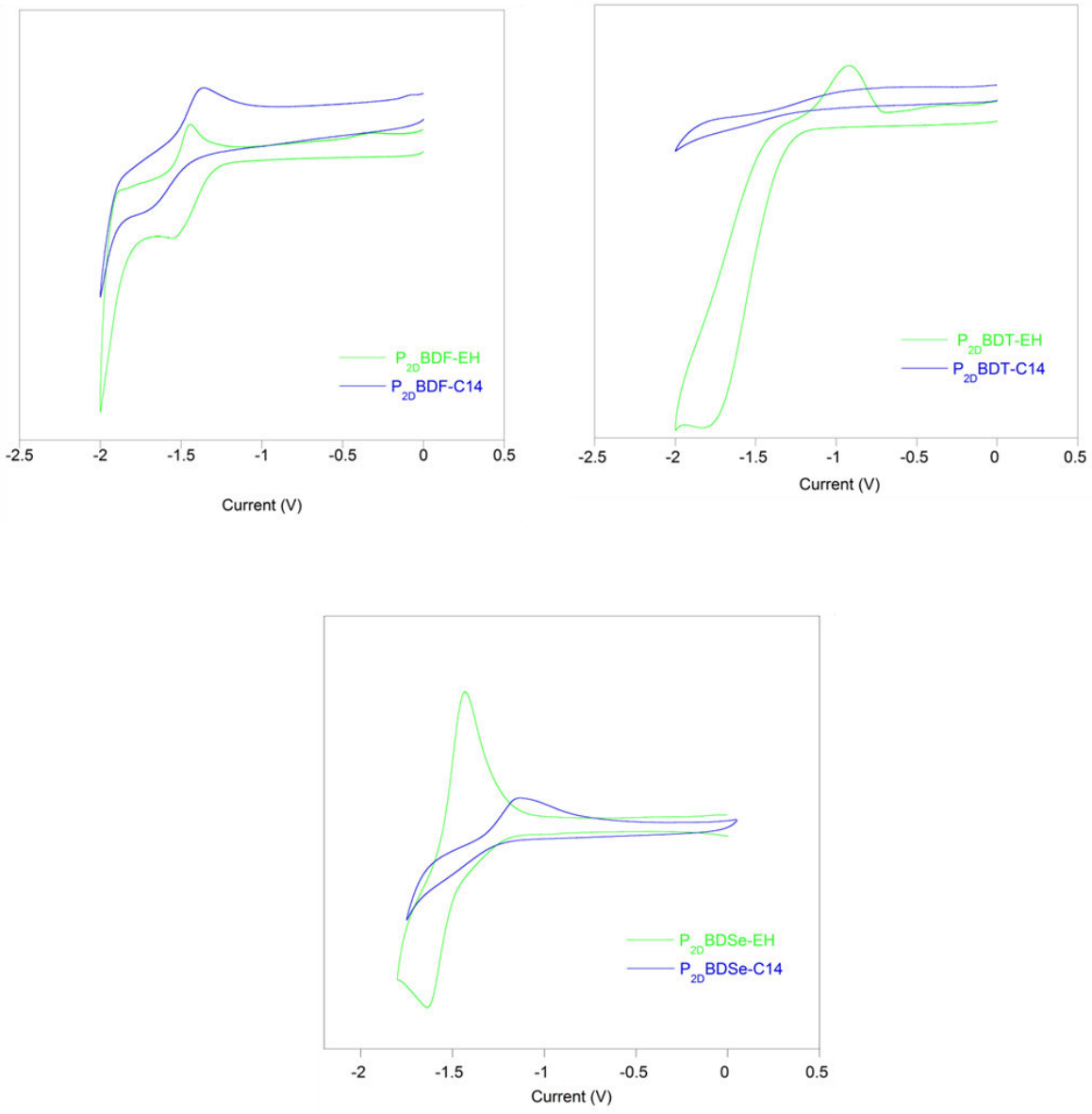

Figure S5.26. Cyclic voltammetry traces for reduction cycles of all six polymers.

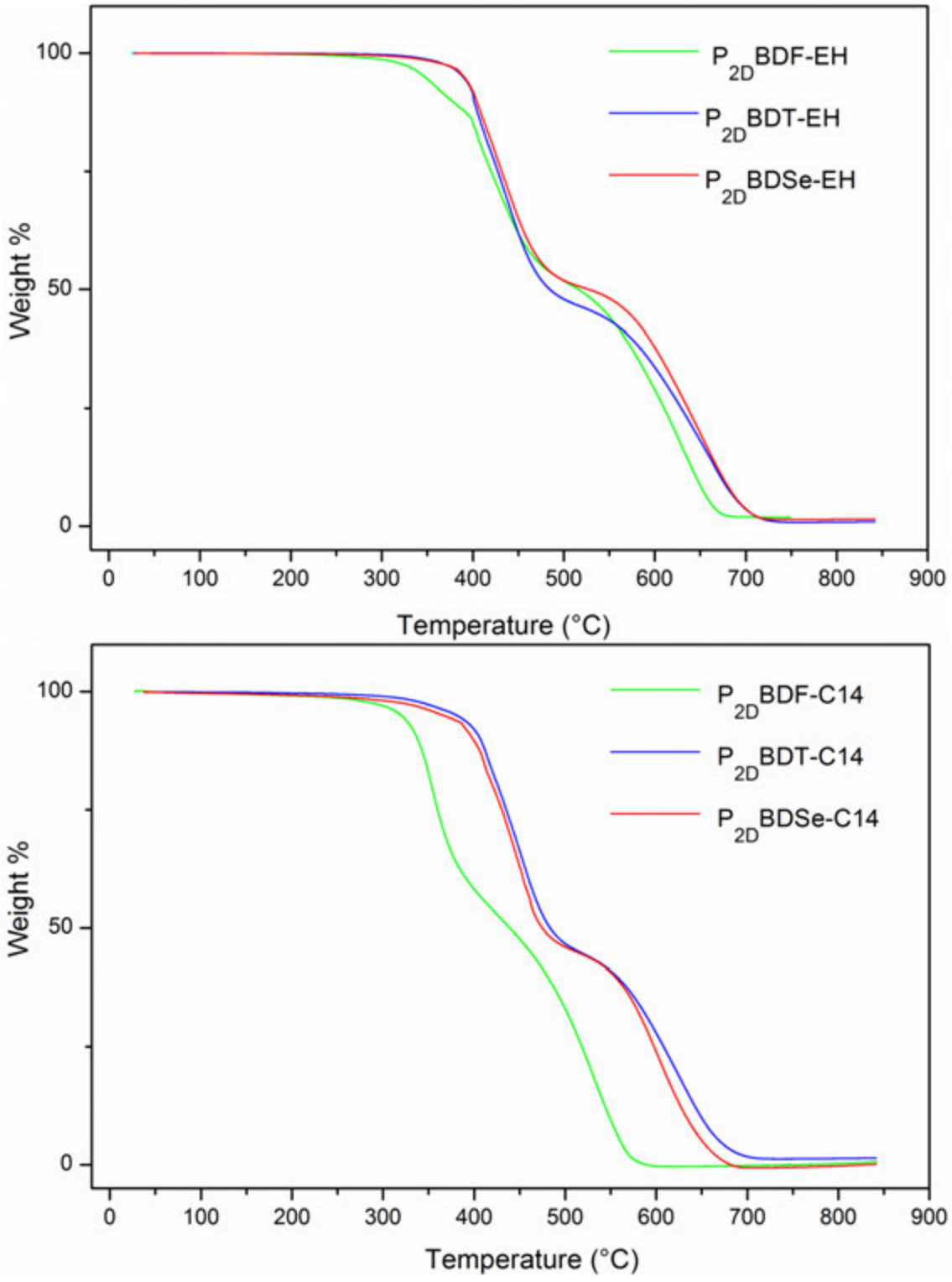

Figure S5.27. Thermal Gravometric Analysis of all six polymers.

5.8 REFERENCES

1. Bijleveld, J. C.; Zoombelt, A. P.; Mathijssen, S. G. J.; Wienk, M. M.; Turbiez, M.; de Leeuw, D. M.; Janssen, R. A. J., *J. Am. Chem. Soc.* **2009,** *131* (46), 16616-16617.
2. Lewis, N. S., *Science* **2007,** *315* (5813), 798-801.
3. Zhou, H.; Yang, L.; You, W., *Macromolecules* **2012,** *45* (2), 607-632.
4. Zhan, X.; Zhu, D., *Polym. Chem.* **2010,** *1* (4), 409-419.
5. Li, G.; Zhu, R.; Yang, Y., *Nature Photon.* **2012,** *6* (3), 153-161.
6. Facchetti, A., *Chem. Mater.* **2010,** *23* (3), 733-758.
7. Grimsdale, A. C.; Leok Chan, K.; Martin, R. E.; Jokisz, P. G.; Holmes, A. B., *Chem. Rev.* **2009,** *109* (3), 897-1091.
8. Thomas, S. W., III; Joly, G. D.; Swager, T. M., *Chem. Rev.* **2007,** *107* (4), 1339-1386.
9. Thompson, B. C.; Frechet, J. M. J., *Angew. Chem. Int. Ed. Engl.* **2008,** *47* (1), 58-77.
10. Havinga, E. E.; ten Hoeve, W.; Wynberg, H., *Polym. Bull.* **1992,** *29* (1), 119-126.
11. Havinga, E. E.; ten Hoeve, W.; Wynberg, H., *Synth. Met.* **1993,** *55* (1), 299-306.
12. Saadeh, H. A.; Lu, L.; He, F.; Bullock, J. E.; Wang, W.; Carsten, B.; Yu, L., *ACS Macro Lett.* **2012,** *1* (3), 361-365.
13. Liu, B.; Chen, X.; Zou, Y.; He, Y.; Xiao, L.; Xu, X.; Li, L.; Li, Y., *Polym. Chem.* **2013,** *4* (3), 470-476.
14. Sonar, P.; Singh, S. P.; Williams, E. L.; Li, Y.; Soh, M. S.; Dodabalapur, A., *J. Mater. Chem.* **2012,** *22* (10), 4425-4435.
15. Sista, P.; Huang, P.; Gunathilake, S. S.; Bhatt, M. P.; Kularatne, R. S.; Stefan, M. C.; Biewer, M. C., *J. Poly. Sci. A.* **2012,** *50* (20), 4316-4324.
16. Huo, L.; Huang, Y.; Fan, B.; Guo, X.; Jing, Y.; Zhang, M.; Li, Y.; Hou, J., *Chem. Commun.* **2012,** *48* (27), 3318-3320.
17. Bunz, U. H. F., *Angew, Chem. Int. Ed.* **2010,** *49* (30), 5037-5040.
18. Gidron, O.; Diskin-Posner, Y.; Bendikov, M., *J. Am. Chem. Soc.* **2010,** *132* (7), 2148-2150.
19. Woo, C. H.; Beaujuge, P. M.; Holcombe, T. W.; Lee, O. P.; Fr chet, J. M. J., *J. Am. Chem. Soc.* **2010,** *132* (44), 15547-15549.
20. Kang, I.; An, T. K.; Hong, J.-a.; Yun, H.-J.; Kim, R.; Chung, D. S.; Park, C. E.; Kim, Y.-H.; Kwon, S.-K., *Adv. Mater.* **2013,** *25* (4), 524-528.
21. Fringuelli, F.; Marino, G.; Taticchi, A.; Grandolini, G., *J. Chem. Soc., Perkin Trans. 2* **1974,** (4), 332-337.
22. Shiroudi, A.; Zahedi, E., *Chin. J. Chem.* **2011,** *29* (11), 2249-2256.
23. Oyaizu, K.; Iwasaki, T.; Tsukahara, Y.; Tsuchida, E., *Macromolecules* **2004,** *37* (4), 1257-1270.
24. Heeney, M.; Zhang, W.; Crouch, D. J.; Chabinyc, M. L.; Gordeyev, S.; Hamilton, R.; Higgins, S. J.; McCulloch, I.; Skabara, P. J.; Sparrowe, D.; Tierney, S., *Chem. Commun.* **2007,** (47), 5061-5063.
25. Hou, J.; Tan, Z. a.; Yan, Y.; He, Y.; Yang, C.; Li, Y., *J. Am. Chem. Soc.* **2006,** *128* (14), 4911-4916.
26. Hou, J.; Huo, L.; He, C.; Yang, C.; Li, Y., *Macromolecules* **2006,** *39* (2), 594-603.
27. Hou, J.; Tan, Z. a.; He, Y.; Yang, C.; Li, Y., *Macromolecules* **2006,** *39* (14), 4657-4662.
28. Li, Y.; Zou, Y., *Adv. Mater.* **2008,** *20* (15), 2952-2958.

29. Huo, L.; Hou, J.; Zhang, S.; Chen, H.-Y.; Yang, Y., *Angew, Chem. Int. Ed.* **2010,** *49* (8), 1500-1503.
30. Huo, L.; Zhang, S.; Guo, X.; Xu, F.; Li, Y.; Hou, J., *Angew, Chem. Int. Ed.* **2011,** *50* (41), 9697-9702.
31. Duan, R.; Ye, L.; Guo, X.; Huang, Y.; Wang, P.; Zhang, S.; Zhang, J.; Huo, L.; Hou, J., *Macromolecules* **2012,** *45* (7), 3032-3038.
32. Zhang, Y.; Gao, L.; He, C.; Sun, Q.; Li, Y., *Polym. Chem.* **2013,** *4* (5), 1474-1481.
33. Kumagai, J.; Hirano, K.; Satoh, T.; Seki, S.; Miura, M., *J. Phys. Chem. B* **2011,** *115* (26), 8446-8452.
34. Kobilka, B. M.; Ewan, M. D.; Hale, B. J.; Peterson, A. K.; Bhuwalka, A.; Ippoliti, J. T.; Jeffries-El, M., ***In Preparation***.
35. Kobilka, B. M.; Dubrovskiy, A. V.; Ewan, M. D.; Tomlinson, A. L.; Larock, R. C.; Chaudhary, S.; Jeffries-EL, M., *Chem. Commun.* **2012,** *48* (71), 8919-8921.
36. Kobilka, B. M.; Hale, B. J.; Ewan, M. D.; Dubrovskiy, A. V.; Nelson, T. L.; Duzhko, V.; Jeffries-El, M., *Polym. Chem.* **2013,** *4* (20), 5329-5336.
37. Bijleveld, J. C.; Gevaerts, V. S.; Di Nuzzo, D.; Turbiez, M.; Mathijssen, S. G. J.; de Leeuw, D. M.; Wienk, M. M.; Janssen, R. A. J., *Adv. Mater.* **2010,** *22* (35), E242-E246.
38. Wienk, M. M.; Turbiez, M.; Gilot, J.; Janssen, R. A. J., *Adv. Mater.* **2008,** *20* (13), 2556-2560.
39. Zou, Y.; Gendron, D. Badrou- ch, R. d.; Najari, A.; Tao, Y.; Leclerc, M., *Macromolecules* **2009,** *42* (8), 2891-2894.
40. Zou, Y.; Gendron, D.; Neagu-Plesu, R.; Leclerc, M., *Macromolecules* **2009,** *42* (17), 6361-6365.
41. Qu, S.; Tian, H., *Chem. Commun.* **2012,** *48* (25), 3039-3051.
42. Bürgi, L.; Turbiez, M.; Pfeiffer, R.; Bienewald, F.; Kirner, H.-J.; Winnewisser, C., *Adv. Mater.* **2008,** *20* (11), 2217-2224.
43. Beaujuge, P. M.; Amb, C. M.; Reynolds, J. R., *Acc. Chem. Res.* **2010,** *43* (11), 1396-1407.
44. Cardona, C. M.; Li, W.; Kaifer, A. E.; Stockdale, D.; Bazan, G. C., *Adv. Mater.* **2011,** *23* (20), 2367-2371.
45. Distefano, G.; Jones, D.; Guerra, M.; Favaretto, L.; Modelli, A.; Mengoli, G., *J. Phys. Chem.* **1991,** *95* (24), 9746-9753.
46. Peet, J.; Kim, J. Y.; Coates, N. E.; Ma, W. L.; Moses, D.; Heeger, A. J.; Bazan, G. C., *Nature Mater.* **2007,** *6* (7), 497-500.
47. Lee, J. K.; Ma, W. L.; Brabec, C. J.; Yuen, J.; Moon, J. S.; Kim, J. Y.; Lee, K.; Bazan, G. C.; Heeger, A. J., *J. Am. Chem. Soc.* **2008,** *130* (11), 3619-3623.

CHAPTER 6

General Conclusions

6.1 ONGOING AND FUTURE RESEARCH

The key step in the synthesis of benzo[1,2-*b*:4,5-*b*′]dichalcogenophene (BDC) presented in this dissertation involves the iodine-promoted double cyclization. Not only does this reaction lead to the formation of the BDC core, it simultaneously creates two aryl-iodide 'handles' at the 3 and 7 positions (Figure 6.1) for further synthesis such as metal-catalyzed cross-coupling reactions. Additionally, the 3,7-diidobenzo[1,2-*b*:4,5-*b*′]difuran (BDF) product of the iodocyclization must be flanked by alkylthiophenes, otherwise it suffers from significant solubility issues. The location of these solublizing side chains on the molecule can cause potential steric issues that give rise to twists in the backbone of any conjugated polymer that incorporates them (Figure 6.1). The next logical step in further evaluating these molecules for use in organic semiconductors would be to investigate various strategies that minimize these potentially detrimental steric interactions.

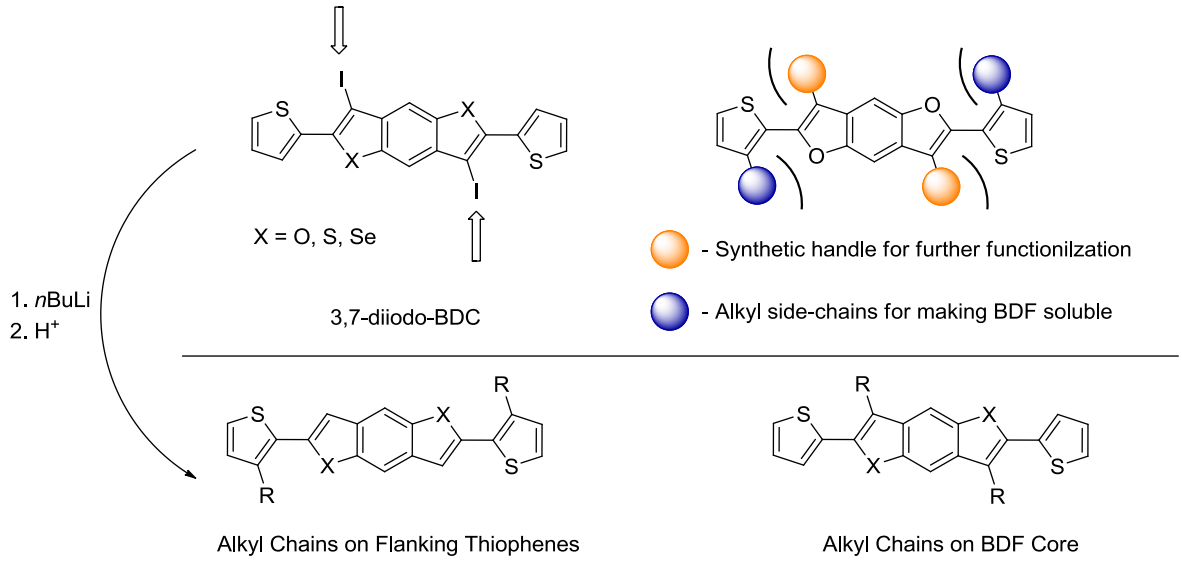

Figure 6.1. Some examples of substituted BDCs and the potential impact of steric effects of BDF.

One plausible way to circumvent these issues would be to remove the alkyl chains from either the flanking thiophenes or from the cores of the BDCs themselves (Figure 6.1). The easier of these two choices would be to remove the alkyl chains from the BDC core. To do this, one simply skips the palladium cross-coupling reactions, and removes the iodines from the molecules via lithium-halogen exchange and subsequent quenching with a proton source. This route requires that the thiophenes flanking the BDC core already bear the desired side chains from the outset. On the other hand, synthesizing an alkylated BDC core with 'naked' flanking thiophenes is slightly more involved, but does have the advantage of introducing the e chains in final stages of the synthesis. Consequently, this route would provide greater access to a variety of functionalized BDCs from one common precursor allowing for a more direct way to tune the physical properties of any resulting copolymers.

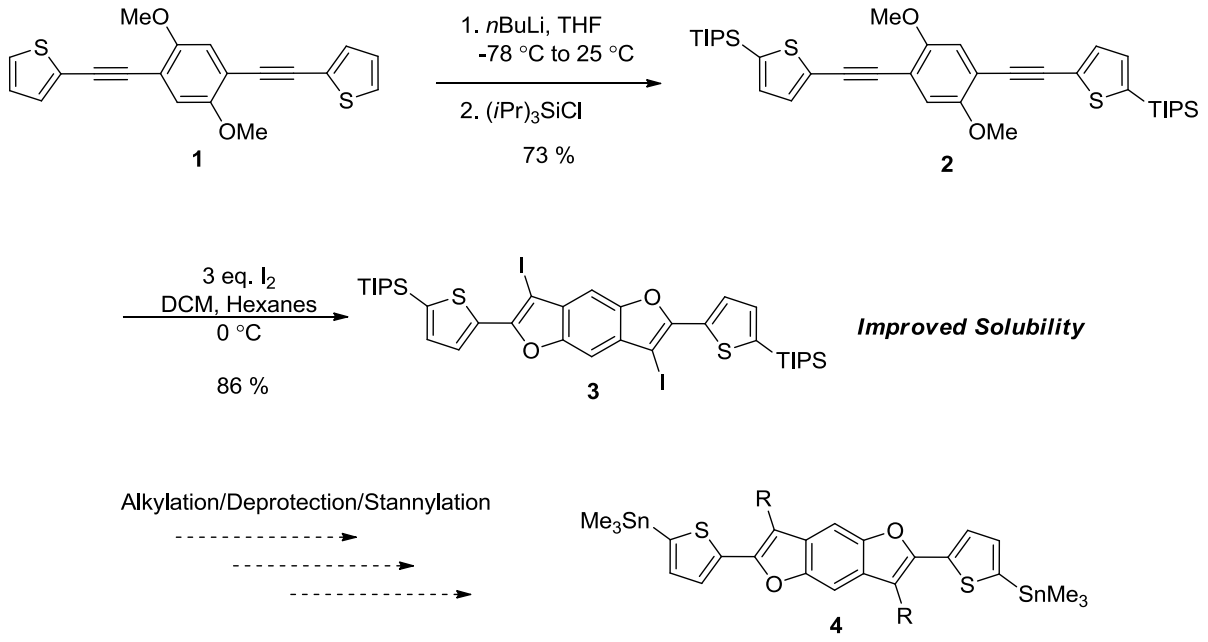

Scheme 6.2. Synthesis of BDF with unalkylated flanking thiophenes.

As discussed previously, this route to BDF was abandoned originally due to the insolubility of the diido-BDF compound, thus, necessitating the flanking alkylthiophenes. One solution to this problem (Scheme 6.1) was discovered by the author through the attachment of two triisopropylsilyl groups to the bisethyne compound **1**, prior to the iodocyclization to give **2**. The silyl groups act as temporary alkyl chains that serve to make

the resulting diido-BDF **3** soluble in common organic solvents allow for further chemistry to be performed. It was discovered that the more robust triisopropylsilyl (TIPS) group was necessary, as trimethylsilyl substituents did not survive the iodocyclization reaction. Once the diido-BDF has been functionalized with a solublizing side chain, the TIPS groups are easily removed with dilute trifluoroacetic acid (TFA), so that the molecules can be converted into a bisstannane **4** for use in a Stille cross-coupling polymerization.

Another technique that was discussed in Chapter 1 to reduce backbone twisting in conjugated polymers is the formation of ladder-type molecules by synthetically locking adjacent aromatic rings into planar conformations. To reiterate, the incorporation of ladder-type structures into conjugated polymers can lead to improvements in the optical and electronic properties. The structural rigidification extends the effective conjugation length which makes for broadened absorption with higher absorbance coefficients, while a higher degrees of planarity result in reduced reorganizational energies and increased interchain interactions that improve charge-carrier mobility.[1-4] The BDCs reported on in this dissertation conveniently provide a variety of synthetic handles that allow for the creation of a number of different extended ladder systems.

One approach to make extended ladder structures is the synthesis of fused aromatic systems via the Scholl reaction, or oxidative intermolecular coupling of two electron-rich aromatic rings using a Lewis acid catalyst. This method can be applied to the 2D BDC molecules similar to those reported in Chapter 5. As shown in Scheme 6.2, the Stille cross-coupling of different branched 2-alkylthiophenes and BDF **3**, affords the 2D BDF **5**. Then, the oxidative coupling of the two pendant thiophenes on compound **5**, and the subsequent deproptection of the TIPS groups affords the ladder-type structure **6** in moderate yields. In addition to helping solubilize compound **3**, the TIPS groups also serve as a protecting group to prevent any unwanted intramolecular coupling between thiophenes. Finally, stannylation of **6** will yield the polymerization-ready monomer **7**. Not only does this molecule provide the desired extended conjugation along the polymer backbone, it also experiences conjugation perpendicular to the polymer chain and the possibility of the benefits of 2D conjugation discussed in Chapter 5.

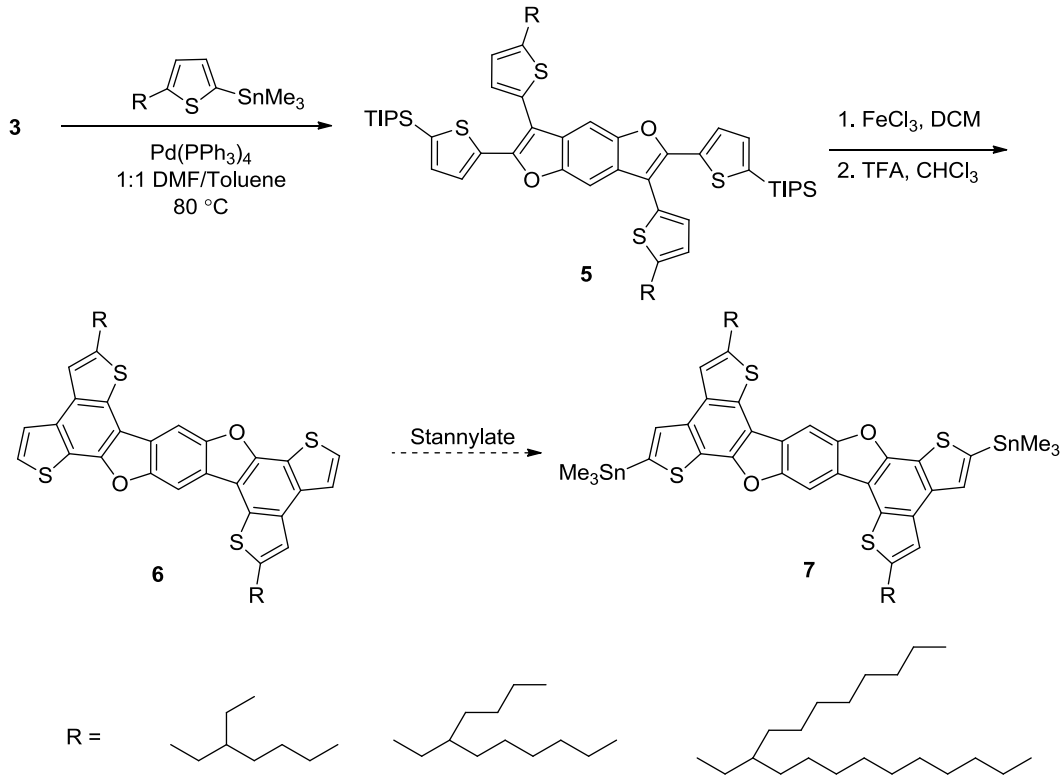

Scheme 6.2. Synthesis of Fused-BDF via an oxidative coupling with varying branched alkyl chains.

Another aspect of design crucial to the success of ladder materials is the judicious selection of alkyl side chains. The increased planarity of these fused systems can cause significant solubility problems in common organic solvents. Expectantly, fused-BDF **6**, which possesses the shorter 2-ethylhexyl side chains, is only soluble in hot chloroform. Compound **6**, bearing the longer 2-butyloctyl chains, exhibits improved solubility, but has limited solubility in the moderate amount of THF required for the subsequent stannylation step. Increasing the alkyl chain length to 2-octyldodecyl chains makes the fused system highly soluble. Although these chains may result in some undesirable properties for organic electronics, they may represent the only option to make this aromatic core into a solution-processable material. Naturally, these fused BDC systems could be evaluated to see how they affect conjugated polymer properties as well as their performance in organic electronics, most specifically, OPVs and OFETs.

Another successful method to fuse aromatic rings together is by a bridging them together with a dialkyl or dialkylphenyl methylene group.[5] Donor-acceptor copolymers comprised of

this class of ladder molecules have been fabricated into devices with PCEs of up to ~7%.[6, 7] Fortunately, this strategy, detailed in Scheme 6.3, can also be applied again to our common precursor, the silylated diiodo-BDF **3**. This can be accomplished by first converting it into either a Grignard reagent or the lithiated dianion species and quenching with dialkyl- or dialkylphenyl-ketone to give the diol **8**. Next, the rings could be closed via acid mediated Friedel-Crafts reaction to give ladder compound **9**. After deprotection of the TIPS group and formation of the bisstannane **10**, this molecule could be ready for polymerization and evaluation as a component in organic electronic devices. With these ladder-type structures in hand, one could evaluate the impact of removing steric hindrance and increasing the planarity on the resulting polymers and devices. Additionally, a variety of chalcogen heteroatoms could be substituted into these ladder molecules to study their effect on the optoelectronic properties and tailor the characteristic of the polymer towards the ideal scenario required for successful, high-efficiency OPVs.

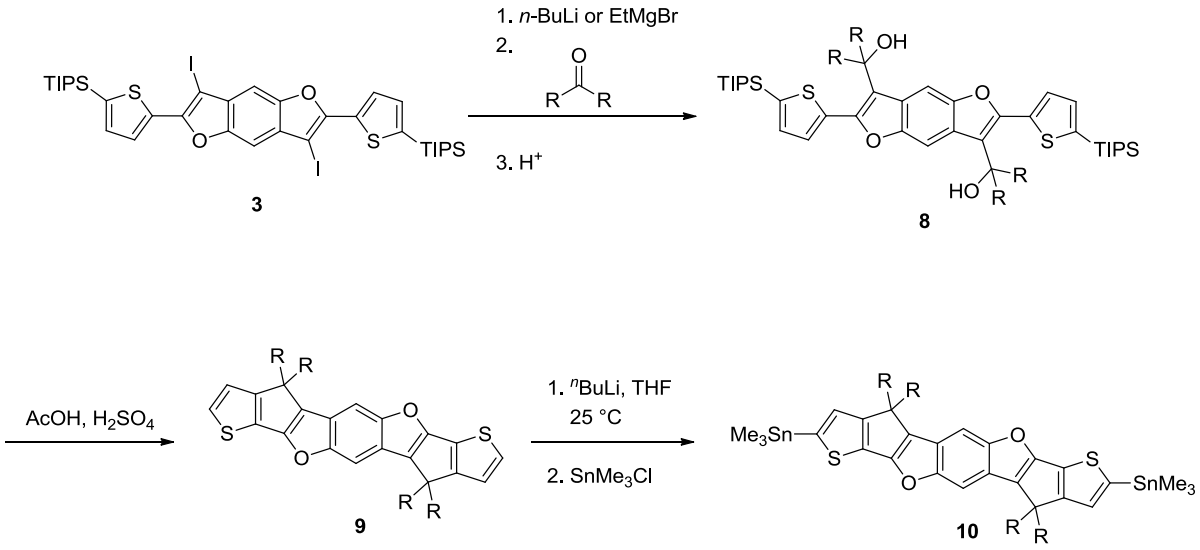

Scheme 6.3. Synthesis of Ladder-BDFs via a Friedel-Crafts cyclization reaction.

6.1.2 Benzodifurans as OLED Components

A potential application of the 3,7-substituted diido-BDF not discussed previously in this dissertation is how they could be used as components in OLED materials. Due to the heavy atom effect, oxygen-based aromatic heterocycles can experience intense fluorescence that

their sulfur- and selenium-based counterparts do not.[8-10] This is certainly true among the BDC compounds reported on this dissertation, as qualitatively observed by the author. Recently, one problem facing OLED research is the development of high efficiency blue OLEDs for red-, green- and blue-based full-color displays.[11, 12] While green and red OLEDs have been fairly well-developed, blue-OLEDs have proven more difficult because the human eye is less sensitive to blue color in general.[13] Interestingly, these diido-BDFs could prove to be useful building-blocks for blue OLEDs as they could be used for a class of materials based on "meta-conjugation." The 3,7-diido BDFs can be polymerized directly via Stille or Suzuki cross-couplings via their two aryliodides and result in a polymerization axis that does not allow extended conjugation or π-electron delocalization along the polymer backbone, resulting in this so-called "meta-conjugation."

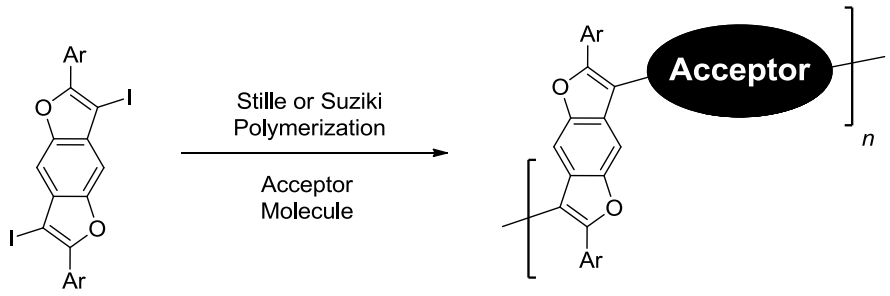

Scheme 6.4. Synthesis of 'meta-conjugated' BDF polymers for OLEDs.

This type of conjugation proves generally useful for the development of blue emissive materials for two main reasons. While meta-conjugation may not be ideal for extended delocalization along the polymer chain that is better suited for successful OPVs, it can be exploited for synthesizing useful materials for OLEDs. Meta-conjugated materials result in decreased quinoid resonance character, which widens the band gap and can be used to achieved blue-light emission.[2] Another reason that these material could be good for the creation of blue OLEDs is that they may prevent the formation of excimers that result in red-shifted emissions in some light-emitting polymers.[14] Meta-conjugation in polyfluorenes and poly(phenylenevinylenes) has been shown to suppress long wavelength emission due to the reduction excimer formation in both photoluminescence and electroluminescence of OLEDs by reducing the conjugation length and introducing kinks into the polymer.[15] Unfortunately,

some wide band gap polymers also suffer from high-lying LUMOs that can cause problems in charge injection and hole transport.[16] Due to this, it would like be necessary to polymerize these "meta-conjugated: BDFs with a weak electron acceptor to help stabilize the LUMO without a significant reduction of the band gap.[17-19]

6.2 DISSERTATION CONCLUSIONS

Over the course of this dissertation, the author has demonstrated how synthetic methodology can be used to design and engineer materials for organic semiconductors at the molecular level. These modifications play an integral role in the tuning of impactful properties for conjugated polymers used in the fabrication of successful OPVs. The adaptation of the iodine-promoted cyclizations reported by Larock, *et al.* offers a new synthetic pathway to a variety of functionalized benzo[1,2-*b*:4,5-*b'*]dichalcogenophene (BDC) molecules. These molecules are functional analogues to the commonly used aromatic heterocycle benzo[1,2-*b*:4,5-*b'*]dithiophene (BDT), which has been incorporated into many high-performing OPVs. One way in which these materials can be modified is through side-chain substitution, including both the position and type of side chains used. The position of the alkyl chains can vary the steric interactions experienced along polymer backbone as well as enhance the solubility and film morphologies of mixed polymer/PCBM blends. These properties can also by modified by varying the side chains between linear and branched, or between aliphatic and alkylarenes. Additionally, the molecular properties can be influenced to through the substitution of different chalcogen heteroatoms within the polymer backbone. The synthesis of analogous oxygen-, sulphur-, and selenium-based heterocyclic arenes can be used to modify the band gap, absorbance profile, HOMO and LUMO levels, solubility, morphologies, and the charge-carrier mobility of any resulting donor-acceptor copolymers.

While some of these materials may not yet be at the levels of their previously published counterparts, they are still in the early stages of development and evaluation. Further structural modification should allow for the improvement of critical properties for this class of materials. One design aspect that could play a crucial role in this is the reduction of detrimental steric effects occurring because of undesirable alkyl side chains interaction with each other, or even with large heteroatoms. Through the careful synthesis of newly functionalized materials with judiciously selected and placed side chains, these problematic

effects could be minimized. Other techniques such as the synthesis of BDC-based ladder-type structures could be used to lock the aromatic rings in place and result in reduced backbone twisting. These modifications provide the next stepping-stone for the continuing evaluation of the structure-function relationships for this class of materials. This ongoing evolution should lead to the fabrication of novel, high-efficiency OPVs. Lastly, by accessing the other polymerization axis of the 3,7-diiodo BDFs, one could synthesize meta-conjugated, blue-emissive materials and study them for OLED applications.

6.3 ACKNOWLEDGEMENTS

The researching, lab work and writing of this thesis have been made possible from the support and graces of my wonderful wife Sara. She has played an enormous role in keeping me sane throughout this entire process. The ability to tolerate a husband who arrives home too late to hardly ever make dinner, work indoors on beautiful weekends, and will go on rants about the pain of organic synthesis has not gone unnoticed these past few years. I also want to thank her for putting her journalistic skills to use in proof-reading the as yet unpublished parts of this dissertation. I would like to thank my parents, Mark and Lyn, for encouraging me to pursue this continuing education and push myself to use the full extent of my abilities. Their advice and support was uplifting in the hardest of times. I also appreciate all of the help they offered to Sara and I with regards to our house.

Of course, I couldn't have made it through this experience without my advisor, Dr. Malika Jeffries-EL. She has instilled in me her ability to merge the pursuit of science and the passion for work and life in general. She has kept me motivated through the darkest of days and the most soul-crushing of failures. When I leave here I will be happy to have her as a future colleague and friend. I must also show my gratitude for the members of the Jeffries-EL group, both past and present: To Robyn Laskowski for being a most splendid friend and lab mate; To Dr. Jared F. Mike for keeping me sane by keeping me insane; To Dr. Jeremy J. Intemann for pushing me to be a more fervent and emotional chemist; To Brian C. Tlach, for showing me the true value and consequences of hard work; To Achala Bhuwalka, for always being there as a true and insanely awesome friend through the best and worst days; To Ben Hale, for being honest, always; To Dana Drochner, for showing me the benefits of lab hygiene; To Monique D. Ewan, for bestowing the ability to feel the rhythm and the rhyme as

well as for making all of my devices; To James Kilmavicz, for also showing me the true value and consequences of hard work; Lastly, to Ramiro Chavez, for being my replacement.

Additionally, I would like to send a huge thank you to Matt "Dilbert" Kobilka for getting my butt out of the lab and into the gym. I don't know what kind of physical and mental shape I would be in today without your motivation and tireless efforts to push me to new heights. During our overlapping time at ISU, I have really enjoyed being able to reconnect with you both as a brother and as a friend. To my In-Laws, Gary and Mary, thank you for your encouragement throughout the years, our "gamping" excursions, and your help with our housework. I would also like to thank Michael Zenner, for making me feel better about myself, whether I liked it or not. I am grateful for the assistance and helpful discussions provided by the ISU chemical instrumentation staff members of Doctors Kamel Harrata, Shu Xu, Dave Scott, and Sarah Cady. Also, to everyone else that I've meet and learned from throughout my time at Iowa State and in the State of Iowa (you know who you are): thank you.

In keeping with the tradition of the Jeffries-EL group members' acknowledgements I would like to thank primarily the Stone, Founder's, Surly, New Glarus, Bells, and New Belgium breweries for their hops and malted-grained-based beverages, the fuel of research excellence. I must also acknowledge the evolving role caffeine (mostly the Caribou Coffee on campus) has played in the creation of this dissertation. From fancy sugar-packed mochas in the early days, to just plain black coffee recently: you have certainly done the trick. Lastly, I would like to thank the Grateful Dead for their song 'Terrapin Station,' without which I could not have written the majority of this dissertation.

6.4 REFERENCES

1. Hertel, D.; Scherf, U.; Bässler, H., *Adv. Mater.* **1998,** *10* (14), 1119-1122.
2. Roncali, J., *Macromol. Rapid Comm.* **2007,** *28* (17), 1761-1775.
3. Schwarz, C.; Bässler, H.; Bauer, I.; Koenen, J.-M.; Preis, E.; Scherf, U.; Köhler, A., *Adv. Mater.* **2012,** *24* (7), 922-925.
4. Dierschke, F.; Grimsdale, A. C.; Muellen, K., *Macromol. Chem. Phys.* **2004,** *205* (9), 1147-1154.
5. Wu, J.-S.; Cheng, Y.-J.; Dubosc, M.; Hsieh, C.-H.; Chang, C.-Y.; Hsu, C.-S., *Chem. Commun.* **2010,** *46* (19), 3259-3261.

6. Chen, Y.-L.; Chang, C.-Y.; Cheng, Y.-J.; Hsu, C.-S., *Chem. Mater.* **2012,** *24* (20), 3964-3971.
7. Intemann, J. J.; Mike, J. F.; Cai, M.; Barnes, C. A.; Xiao, T.; Roggers, R. A.; Shinar, J.; Shinar, R.; Jeffries-El, M., *J. Poly. Sci. A.* **2013,** *51* (4), 916-923.
8. Zander, M. Z.; Kirsch, G. Z., *Naturforsch., A: Phys. Sci.* **1989,** *44*, 205-290.
9. Zander, M. Z., *Naturforsch., A: Phys. Sci.* **1989,** *44* (1116-118).
10. Hayashi, N.; Saito, Y.; Higuchi, H.; Suzuki, K., *J. Phys. Chem. A* **2009,** *113* (18), 5342-5347.
11. Kanno, H.; Hamada, Y.; Takahashi, H., *Selected Topics in Quantum Electronics, IEEE Journal of* **2004,** *10* (1), 30-36.
12. Jarikov, V. V.; Kondakov, D. Y.; Brown, C. T., *J. Appl. Phys.* **2007,** *102* (10), 104908-6.
13. Forrest, S. R.; Bradley, D. D. C.; Thompson, M. E., *Adv. Mater.* **2003,** *15* (13), 1043-1048.
14. Ritchie, J.; Crayston, J. A.; Markham, J. P. J.; Samuel, I. D. W., *J. Mater. Chem.* **2006,** *16* (17), 1651-1656.
15. Pogantsch, A.; Kai Mahler, A.; Hayn, G.; Saf, R.; Stelzer, F.; List, E. J. W.; Brédas, J.-L.; Zojer, E., *Chem. Phys.* **2004,** *297* (1–3), 143-151.
16. Grisorio, R.; Mastrorilli, P.; Nobile, C. F.; Romanazzi, G.; Suranna, G. P.; Gigli, G.; Piliego, C.; Ciccarella, G.; Cosma, P.; Acierno, D.; Amendola, E., *Macromolecules* **2007,** *40* (14), 4865-4873.
17. Mike, J. F.; Intemann, J. J.; Cai, M.; Xiao, T.; Shinar, R.; Shinar, J.; Jeffries-EL, M., *Polym. Chem.* **2011,** *2* (10), 2299-2305.
18. Hancock, J. M.; Gifford, A. P.; Tonzola, C. J.; Jenekhe, S. A., *J. Phys. Chem. C* **2007,** *111* (18), 6875-6882.
19. Lee, Y.-Z.; Chen, X.; Chen, S.-A.; Wei, P.-K.; Fann, W.-S., *J. Am. Chem. Soc.* **2001,** *123* (10), 2296-2307.

APPENDIX

List of Acronyms and Descriptions

Acronym	Description
2D	Two-Dimensional
AFM	Atomic Force Microscopy
APCI	Atmospheric-Pressure Chemical Ionization
BDC	Benzo[1,2-*b*:4,5-*b*′]dichalcogenophene
BDF	Benzo[1,2-*b*:4,5-*b*′]difuran
BDSe	Benzo[1,2-*b*:4,5-*b*′]diselenophene
BDT	Benzo[1,2-*b*:4,5-*b*′]dithiogenophene
BDTe	Benzo[1,2-*b*:4,5-*b*′]ditellurophene
BHJ	Bulk-Heterojunction
BLA	Bond Length Alternation
CN	1-Chloronapthalene
CV	Cyclic Voltammerty
D-A	Donor-Acceptor
DIO	1,8-Diiodooctane
DP	Degree of Polymerization
DPP	Diketopyrrolepyrrole
DSC	Differential Scanning Calorimetry
E_g	Band Gap
ESI	Electron-Spray Ionization
FDPP	3,6-Di(2-furanyl)-1,4-diketopyrrolo[3,4-*c*]pyrrole
FF	Fill Factor
GPC	Gel Permeation Chromatography
HMW	High Molecular Weight

Acronym	Description
HOMO	Highest Occupied Molecular Orbital
HRMS	High Resolution Mass Spectrometry
ITO	Indium Tin Oxide
J_{sc}	Short Circuit Current Density
LMW	Low Molecular Weight
LUMO	Lowest Unoccupied Molecular Orbital
MMW	Medium Molecular Weight
M_n	Number-Averaged Molecular Weight
MO	Molecular Orbital
M_w	Weight-Averaged Molecular Weight
NMR	Nuclear Magnetic Resonance
o-DCB	ortho-Dichlorobenzene
OFET	Organic Field-Effect Transistor
OLED	Organic Light-Emitting Diode
OPV	Organic Photovoltaic Cell
P3HT	poly(3-hexylthiophene)
PCBM	[6,6]-Phenyl-C_{61}-butyric acid methyl ester
$PC_{71}BM$	[6,6]-Phenyl-C_{71}-butyric acid methyl ester
PCE	Power Conversion Efficiency
PDI	Poly Dispersity Index
PEDOT:PSS	Poly(3,4-ethylenedioxythiophene) poly(styrenesulfonate)
PITN	Polyisothianapthene
PPP	Poly(para-phenylenevinylene)
PPV	Poly(phenylenevinylene)
PT	Polythiophene
PV	Photovoltaic

Acronym	Description
PVC	Photovoltaic Cell
SCE	Standard Calomel Electrode
SCLC	Space-Charge-Limited Current
SI	Supplemental Information
T_d	Thermal Decomposition Temperature
TDPP	3,6-di(2-thienyl)-1,4-diketopyrrolo[3,4-*c*]pyrrole
TFA	Trifluoroacetic acid
TIPS	Triisopropylsilyl
TGA	Thermal Gravimetric Analysis
V_{oc}	Open Circuit Voltage